MEDICAL ULTRASONICS:

A COMPUTER ANALYSIS OF ECHOES FROM SOFT TISSUES

DOUGLAS C. MORRISON, M.A.

THESIS PRESENTED FOR THE DEGREE OF DOCTOR OF PHILOSOPHY
OF THE UNIVERSITY OF EDINBURGH, AUGUST 1979.

To my Mother and Father.

What are the wild waves saying ... ?

(J. E. Carpenter)

This thesis describes work done by myself and was composed by myself.

Douglas Morrison. August 1979

CONTENTS

ABSTRACT

To analyse ultrasonic echoes from soft tissues a fast data acquisition system was built. A PDP8/E minicomputer controls a Biomation 8100 transient recorder and an RK8E disk storage unit. The transient recorder can digitise at sample rates up to 100 MHz, with a resolution of up to 8 bits.

The design of the transient recorder interface is described. Single cycle data break transfers are used, and three 8-bit bytes of data can be packed into every two computer words. Maintenance facilities in the interface allow detailed testing.

An assembly language program allows flexible acquisition of echo data. The transient recorder acquisition parameters may be specified by keyboard commands and stored on file.

Approaches to tissue characterisation are briefly reviewed. One fundamental problem is that interference between echoes from closely spaced scatterers introduces a random element in the echo amplitude. The problem of detecting an array of scatterers surrounded by a different array of scatterers is considered.

Simulations based on a discrete scattering model aid the analysis. Signals are synthesised by adding echo pulses with random time delays. Distributions of the average echo amplitude of synthesised data and liver echo data are compared.

The detection of abnormal regions is discussed within the framework of statistical decision theory. The use of moving averages to detect abnormal regions is studied.

Level crossing frequencies of various synthesised waveforms are compared with theoretical predictions.

The random nature of echo amplitudes can limit the achievable resolution in standard B-scan images. Digital scan converter update algorithms are considered from a statistical viewpoint.

CHAPTER 1

INTRODUCTION

1.1 AIMS

Ultrasound offers a safe, non-invasive and convenient means of investigating the internal organs of the body. Pulse echo methods analogous to radar can produce images of the internal organs. Bi-stable displays were in widespread use for a number of years and provided valuable information in the field of obstetrics. The main features of interest were the major interfaces within the body. Low-level echoes caused by scattering from within the organs were rejected as noise. One of the most significant recent advances in diagnostic ultrasound has been the widespread use of grey scale imaging making use of these low-level echoes. These grey scale images have considerably extended the range of applications of ultrasound, which is now routinely used in diagnosis in many clinical areas (Hill et al., 1978; Wells, 1977; White and Lyons, 1978).

Interpretation of the images can be difficult, even for experienced operators (McDicken, 1976). Computer processing of echo information has a number of advantages to offer. Whilst the human brain is good at pattern recognition in images, it has a limited capacity to perform detailed calculations on large amounts of echo data. Phase information in the echo signals is lost in the formation of conventional grey scale images and the displays generally restrict the dynamic range. By processing the raw echo signals we can hope to obtain quantitative information that is not perceivable in the grey

scale images. A review of tissue characterisation methods is given in Chapter 6.

The primary goal of this project is to be able to distinguish between normal and abnormal tissues by analysis of the echo signals. To distinguish between different types of abnormality is a further goal. Hopefully the route to these goals will involve a greater understanding of ultrasonic echoes that can be applied to the design of better imaging devices.

1.2 OVERVIEW

The thesis can be divided into two fairly independent parts: Chapters 2-5 are concerned with the data acquisition system and the associated software; Chapters 6-8 are concerned with echo signals from soft tissues.

1.2.1 The acquisition system

1.2.1.1 Hardware

The requirements of an acquisition system suitable for diagnostic ultrasound applications are discussed (Chapter 2). The system selected uses a PDP8/E minicomputer to control a Biomation 8100 transient recorder (Morrison, 1978). Phase information can be preserved by digitising at a sample rate of up to 100 MHz. The digital to analogue conversions have a resolution of 8 bits, although the accuracy depends on the signal being digitised. The digitised echo signals are transferred to the memory of the PDP8/E minicomputer via a direct memory access interface. The data is then stored on magnetic disk. The disk can be removed and taken to

the departmental PDP12 for subsequent analysis of the data. Although enough data to form images may be stored the main aim of the project does not involve the formation of images with the data.

The design of the interface is described in detail (Chapter 3). To provide the maximum rate of transfer, single cycle data break transfers are used, and three 8-bit bytes of data can be automatically packed into every two 12-bit computer words in memory. The interface allows full digital control of the transient recorder. Maintenance facilities are built into the interface to allow detailed testing.

1.2.1.2 Software

Maintenance programs were written to detect and locate faults in the interface and the transient recorder (Chapter 4).

An acquisition program was written to allow flexible acquisition of echo data (Chapter 5). All the acquisition parameters of the transient recorder can be specified by keyboard commands. These parameters can be stored on file for future use. The program is designed to be used in a clinical environment and can give extensive prompts to the unfamiliar user. The program is written in assembly language for maximum speed and versatility with minimum memory requirements. Suitable background material on assembly language programming may be found in DEC (1972). Background material on operating systems may be found in Donovan (1972), Gear (1969) and Lister (1975).

The acquisition and associated software were designed with long term use in mind. Several short-cuts could have been taken to produce

an operational system with lower speed and less facilities.

1.2.2 Tissue characterisation

Various approaches to tissue characterisation are briefly reviewed (Chapter 6). One fundamental problem is that interference between echoes from closely spaced scatterers introduces a random element in the echo amplitude. To concentrate on this, the problem of detecting an array of discrete scatterers surrounded by another array of scatterers having a different scattering cross section is proposed.

1.2.3 Simulation of scattering from soft tissues

To assist in the analysis, signals were synthesised by adding together echo pulses with random time delays. Amplitude distributions of the average echo amplitude of the synthesised data are compared with theoretical results and with results obtained for liver echo data (Chapter 7). Because the synthesis parameters can be changed in a known way the simulations can lead to a better understanding of echo signals from closely spaced scatterers.

The detection of abnormal regions is discussed within the framework of statistical decision theory (Chapter 8). The use of moving averages to detect these abnormal regions is studied, as a first step towards developing a better detector.

Level crossing frequencies of the envelope of synthesised echo signals were measured to investigate and resolve a discrepancy between the theoretical and experimental results of Atkinson and Berry (1974).

1.2.4 Digital scan converter simulation

The random nature of echo amplitudes can limit the achievable resolution in standard B-scan images. Various scan converter update algorithms are considered from a statistical viewpoint. Preliminary simulations were performed to estimate the relative advantages of the different update algorithms.

.....

The use of simulations allowed many results to be obtained that would have been hard to obtain in any other way. Much work remains to be done to extend the theory, but the work done so far indicates that simulation can provide a useful insight into scattering by soft tissues.

CHAPTER 2

SELECTION OF THE DATA ACQUISITION SYSTEM

2.1 INTRODUCTION

To process echoes with a digital computer the analogue echo signals must be converted into digital form. The computer to be used for the processing was the departmental PDP12. The ultrasound scanners to be used to provide the echo signals were up to two miles away from the PDP12 so the remote location of the scanners was an additional problem.

Although I was involved in the selection of the equipment, Dr. A. K. Boardman, Dr. W. N. McDicken and the Medical Research Council (the grant-giving body), were largely responsible for the choice of the system. I will therefore give a brief account of the factors involved in selecting a data acquisition system for ultrasound signals.

2.2 STORAGE OF THE ECHO SIGNALS

The use of lines to connect the scanners to the computer would not be very practical so some form of echo storage is required. The choice lay between storing the signals in analogue form before digitisation takes place or storing the signals in digital form after the conversion.

Digital storage has the inherent advantage that the data can be stored and recalled with no loss of accuracy. Analogue methods of storage are subject to noise and distortion. Of course conversion into digital form introduces errors, but the signal must be digitised at some point whichever form of storage is used.

The amplitude resolution required and the number of samples required are discussed later in this chapter (sections 2.3.2 and 2.3.1) but if we assume for the moment that we digitise to 8-bits resolution and that we take 2K samples per A-scan and that we digitise up to 100 A-scans per patient then the digital storage requirements are 200K bytes. Although the primary aim of the project does not involve processing entire images it would be an advantage to have the capability to store images to allow image processing in the future. To represent an ultrasound image digitally requires an array of about 512 by 512 elements resulting in a storage requirement of 256K bytes. Because large quantities of data are to be handled the storage must be fairly fast if undue delays are to be avoided. Fast acquisition is also important for dynamic studies: to study the vascularity of tumours by detecting blood-vessel wall motion during the cardiac cycle for example. The requirements for large storage capacity and high transfer rates rule out the use of many digital storage methods.

The PDP12 has a removable magnetic-disk store so if the echoes could be digitised and stored on magnetic disk it would be easy to transfer the disk to the PDP12 and read the data. No additional equipment on the PDP12 would be required. Magnetic disks allow rapid storage of large amounts of data; disk capacity is 1,662,976 formatted 12-bit words, average latency is 20 ms, typical track-to-track access time is 10 ms, and maximum transfer rate is 8.32 μs per word.

The type of disk drive used on the PDP12 can also be controlled by a PDP8/E minicomputer. If a PDP8/E was used to control the disk drive it would be largely software compatible with the PDP12 so the

operating system and many programs used on the PDP12 could run on the PDP8/E. The PDP12 could be used for development of programs to be run on the PDP8/E. To enable the PDP8/E to run the OS/8 operating system and FORTRAN IV a minimum of 8K of core would be required.

The use of a computer to control the acquisition of data allows a very versatile system to be made. Files can contain patient name and other information relating to the scan. Manipulation of files is straightforward using standard system software. Although the PDP8/E has a processing ability the departmental PDP12 would still be preferable since it is well equipped with peripherals (magnetic-tape, line printer/plotter, point plot display oscilloscope, colour TV display), a full 32K of core, and a floating-point processor.

Other digital storage media considered were floppy disks, reel-to-reel magnetic tape, and magnetic tape cartridges and cassettes but all of these were significantly slower and had less storage capacity than the hard-disk cartridge. Furthermore any of the other media would require additional equipment on the PDP12 to read the data.

At the time the system was being selected (early 1975) floppy disks were recently introduced. They had questionable reliability and were not then available for PDP8/E or PDP12 minicomputers. Their use would have required the design and construction of two interfaces and software would have had to be written to support the floppy disks. Now the floppy disk is a low cost alternative to the hard disk that has been used successfully in ultrasonic data acquisition systems.

The form of analogue storage considered was video tape recording.

This offered a cheaper form of storage but not nearly as versatile or as convenient. Furthermore, noise and limited bandwidth would corrupt the signal. Bandwidths of 3-5 MHz are typical for ½ inch tape video recorders. The recorders do not use file-structured storage with directories so finding a particular recording is not very convenient. Serial storage is used so it may take a long time to reach the required recording. In contrast, disk storage uses a file structure and semi-random access.

For the reasons described the removable disk cartridge was selected as the storage medium, storing the signals in digital form under the control of a PDP8/E minicomputer.

2.3 ANALOGUE TO DIGITAL CONVERSION

When selecting a data acquisition system two important factors to consider are the sampling speed and accuracy.

2.3.1 Sampling speed

We wanted to digitise the echo signals fast enough to preserve the phase information. An absolute minimum sampling frequency is set by the sampling theorem which states that to completely recover a continuous bandwidth limited signal from the sampled data the signal must be sampled at a rate of at least twice the maximum frequency component in the signal. This minimum sampling rate is known as the Nyquist frequency. Sampling at lower rates than the Nyquist frequency results in frequency folding: frequency components above half the sampling frequency introduce frequency components of less than half the sampling frequency in the sampled signal. These low frequency

components caused by the presence of high frequency components are known as alias frequencies. Since alias frequencies are indistinguishable from genuine low frequency components their presence makes it impossible to reconstruct the original signal.

In practice the sampling theorem has a number of failings if it is used to determine the minimum sampling frequency. The sampling theorem can be expressed in several ways but it usually assumes that the samples are perfectly accurate, taken at a precisely constant sampling interval, and for an infinite period of time. Clearly none of these assumptions is realised in practice. The necessary sampling rate will also depend on the interpolation algorithm that is used. The very accurate recovery from the samples implies the use of a very high-order interpolation process on the samples, and this in turn requires that the total sample period is long to allow the use of a high-order interpolation process. The sampling theorem does not provide any measure of how close the sampling rate can come to the Nyquist frequency for a given interpolation method and for a specified accuracy.

A further objection is that real signals do not normally have a well-defined upper frequency limit. Wideband noise and errors due to quantisation always lead to aliasing. Even if filters are used the upper frequency limit may still be ill-defined due to the imperfect performance of practical filters. Filters may also introduce errors into the signal before sampling.

The sampling theorem is sometimes restated as "Three (or four, or five)

samples per cycle of the highest significant frequency present is sufficient." However, this statement of the theorem does not give an adequate rule for interpreting "significant" or "sufficient".

Because the B-scan ultrasound transducers emit sharp pulses they have high bandwidths. The width of the frequency spectrum will depend on the design of the transducer, and also on the characteristics of the tissues. To measure the spectrum of ultrasound pulses two diagnostic ultrasound transducers were placed facing each other in a water bath. One transducer was excited by transmitter pulses and the spectrum of the signals from the receiving transducer was measured using a Marconi Instruments model TF2370 spectrum analyser. Frequency components with amplitudes above the wideband noise level could be detected at up to about 1.75 times the centre frequency.

Transducers with a centre frequency of 3.5 MHz are commonly used in abdominal scans. Taking the upper frequency limit to be 1.75 x 3.5 = 6.125 MHz and sampling at only three times this limit requires a sampling rate of 18.375 MHz.

Since the maximum acquisition rate of the PDP8/E is 1.2 μs per word it is clear that a fast buffer memory is required. Transient recorders capture data at high speed and can transfer the data at a lower speed. At the time the equipment was selected the only suitable transient recorder capable of digitising at over 18 MHz was the Biomation 8100. This device can digitise at up to 100 MHz sampling rate. Since that exceeds 18 MHz by a considerable margin it was thought to be quite adequate for the task. Had a wider range of devices been available

it would have been necessary to consider the required sampling rate in more detail. The only other commercial transient recorder that could sample fast enough was the Tektronix R7912 Transient Digitiser. This device uses a scan converter to digitise analogue signals with bandwidths up to 1 GHz. However it was more expensive than the Biomation 8100 and could store only 512 samples. The Biomation 8100 can store up to 2024 samples in its buffer memory. (The buffer memory has a capacity for 2048 bytes but only the first 2024 samples are specified to be valid).

Being able to sample at a higher rate than necessary does have some advantages. The effects of quantisation noise and signal noise can be reduced by increasing the sampling rate. Sampling at a higher rate may allow a lower order of interpolation to be used, or even no interpolation at all. The ability to sample at a higher rate allows the effects of sampling rate to be studied: analysis of data sampled at a high rate may be used to check that it is adequate to sample at a lower rate in the future. The minimum sampling rate will depend on the form of processing used so it is useful to be able to vary it.

A factor influencing the choice of sampling rate is the quantity of data produced. If the quantity of data is fixed the sampling rate will determine the range from which echoes are digitised. If echoes from soft tissues are digitised at 20 MHz then 2K samples correspond to a depth of approximately 78.8 mm. Sampling at a higher rate may well limit the range to an inadequate value so this factor may

ultimately determine the sampling rate.

Although 3.5 MHz transducers are commonly used for abdominal scans 5 MHz transducers are also sometimes used. Eye scans can require 10 MHz transducers. The high digitisation rate of the Biomation 8100 would be useful for analysing echo data from these scans.

2.3.2 Choice of accuracy

Since the constraints imposed by the sampling frequency restricted the number of suitable transient recorders to one, the choice of accuracy was non-existent. The Biomation 8100 digitises with a resolution of 8-bits although it is not claimed to be accurate to within one bit. When digitising high frequencies the principal cause of error is due to its slew rate limitations. The Biomation 8100 uses a folding amplifier (giving the sign bit) and a 7-bit parallel converter using 128 comparators. No sample-hold is used. The input is encoded into a Gray code so that only one bit changes between adjacent levels thus avoiding gross errors when the changing code is latched. The code is converted into signed two's complement form when it is read from the fast buffer memory. Because no sample-hold amplifier is used the least significant bits in the code are unable to change state fast enough to follow very fast changes. This results in missing codes if the slew rate is too high. The error introduced is approximately the same as that produced by an aperture uncertainty of about 3 nanoseconds. The effect of this error on the subsequent processing is not easy to analyse but it was thought that the accuracy would be sufficient for many applications

in diagnostic ultrasonics. Because there are so many undetermined influences on the amplitude of the ultrasound signals (absorption, orientation of reflector, multiple scattering, etc.) the error introduced by the slew-rate errors can be expected to be insignificant in many applications.

Another factor influencing the necessary accuracy apart from the intrinsic accuracy of the signal, is its dynamic range. Consideration of grey-scale images leads one to an approximate estimate of a dynamic range of 40 dB. A more precise estimate would require many parameters to be specified: organs of interest, obesity of patient, transducer design, etc. The noise introduced by quantisation will depend on the amplitude distribution of the input signal. For a bipolar signal with an amplitude distribution uniformly distributed in the sampling range, the signal-to-noise ratio due to quantisation to 8-bits is 42 dB. Thus sampling to 8-bits accuracy would appear to be adequate although it would be preferable to have a wider dynamic range to have greater latitude in the overall gain setting.

2.3.3 Summary of choice of analogue to digital converter (ADC)
There is no simple rule for specifying the necessary sampling rate and accuracy. Simple considerations lead to approximate figures of 20 MHz sampling rate with 8-bits of resolution. At the time the equipment was selected the only transient recorder which could digitise at the required rate was the Biomation 8100.

Since then a number of ADC's capable of digitisation rates of at least

20 MHz have become available, although none of these digitises to a greater resolution than 8-bits. One ADC capable of digitising up to 30 MHz with a resolution of 8-bits has been made on a single monolithic chip (the TDC1007J by TRW). The variety of devices now available makes the choice more difficult. Since different ADC's use different conversion methods a device capable of digitising at a higher rate may give a worse performance than a slower device sampling at a lower rate. For example an ADC using a sample hold and a parallel-series converter is likely to be slower than an all-parallel converter but could have a much smaller aperture uncertainly (a 20 MHz ADC made by DDC has a built-in sample hold with an aperture uncertainty of only 20 picoseconds).

A good discussion of the factors influencing the choice of analogue to digital conversion systems is given by Josiah Macy Jr. (1965).

2.4 THE BIOMATION 8100 TRANSIENT RECORDER

The Biomation 8100 Transient Recorder contains not only a fast ADC and memory but also versatile arming, triggering, and other useful user features. A block diagram of the instrument is shown in Figure 2.1. Input amplifiers have adjustable gain and offsets with a choice of AC or DC coupling. The arm and trigger circuits include adjustable delay periods. The internal timebase can be varied from 10 ns to 10 s sample interval. In one of its modes of operation the trigger signal can be used to stop the recording so that signals occurring before the trigger event can be captured. The trigger event may also be used to change the timebase speed. A digital to

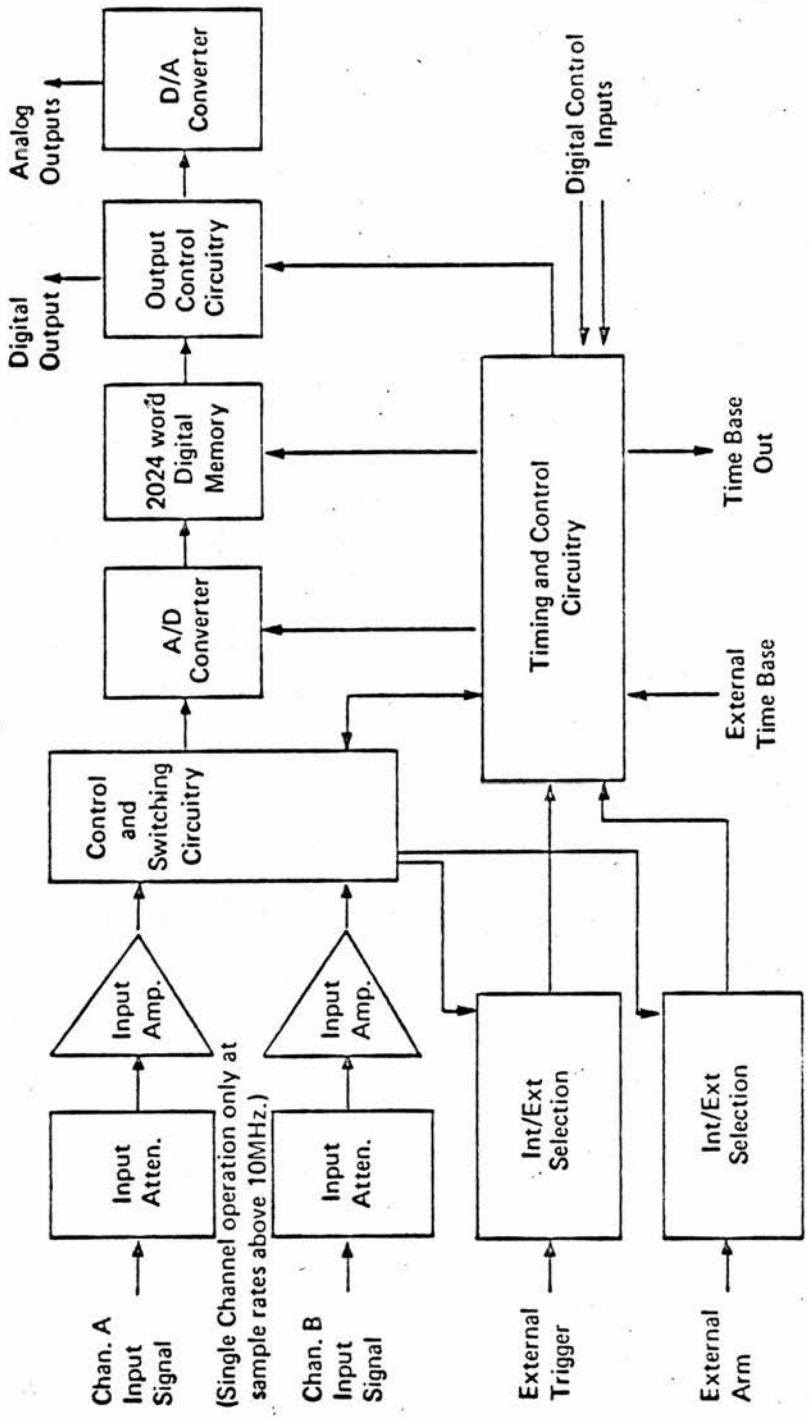

FIGURE 2.1 SIMPLIFIED BLOCK DIAGRAM OF BIOMATION 8100 TRANSIENT RECORDER

analogue converter is included to allow the stored signal to be displayed on an oscilloscope or plotted on a chart recorder. The versatility of the instrument is greatly enhanced by the ability for all the control settings which affect the acquisition of data to be set by external digital control. (The other controls are the on/off switch and the oscilloscope display controls).

By interfacing the transient recorder to the PDP8/E minicomputer a powerful and versatile data acquisition system can be made.

2.5 SUMMARY

A diagram of the chosen system is shown in Figure 2.2. The system uses a PDP8/E minicomputer with 8K of core memory to control the acquisition system. A teletype allows the user to control the PDP8/E. A Biomation 8100 transient recorder is used to digitise the signals with a sample rate of up to 100 MHz and a resolution of 8-bits. An RK05 disk drive is used to store the echo data on removable disk cartridges which are then transferred to the departmental PDP12 for subsequent analysis. A Scopex oscilloscope is used to monitor the signals captured by the transient recorder.

In addition electronic components and an interface foundation module were required to build an interface to allow communication between the PDP8/E and the transient recorder. This interface is described in detail in the next chapter.

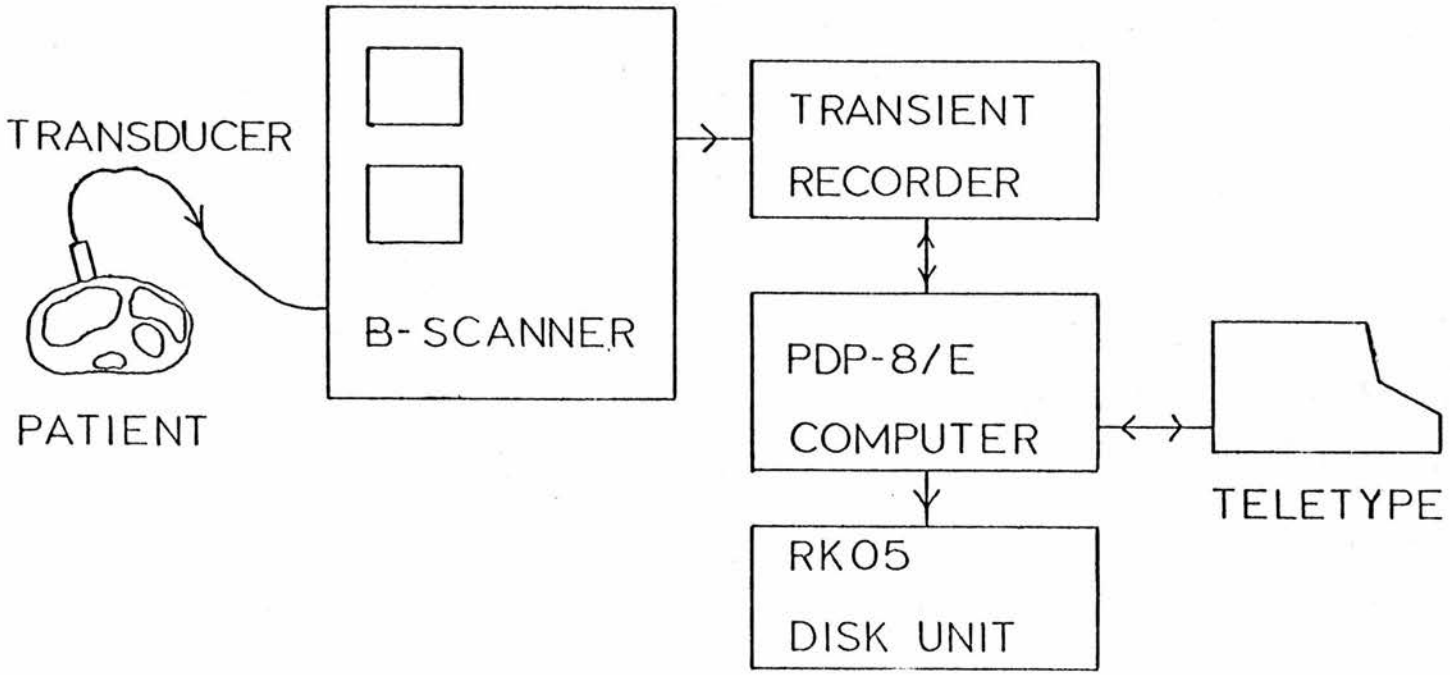

FIGURE 2.2 DATA ACQUISITION SYSTEM

CHAPTER 3

TRANSIENT RECORDER INTERFACE

3.1 INTRODUCTION

To allow the computer to communicate with the transient recorder an interface had to be designed and built. The interface had to allow the fast transfer of the data in the buffer memory of the transient recorder into the memory of the computer. In addition, the interface had to allow full digital control of the transient recorder, enabling the computer to control all the switch settings and give commands to arm, trigger, and reset the transient recorder. The interface must also allow the computer to determine the status of the transient recorder (ready for arm, ready for trigger, recording in progress, etc.).

Several books on digital systems and computer interfacing were valuable when designing the interface (Brignell and Rhodes, 1975; Cluley, 1975; DEC, 1973; Fairchild, 1973; Healey, 1976; Peatman, 1972; Scarlett, 1972; Woollons,1972).

3.2 INTRODUCTION TO PDP8/E INTERFACING

For the benefit of the reader unfamiliar with interfacing to the PDP8/E minicomputer a brief description will now be given. A more detailed account is in the 'Small Computer Handbook' (DEC, 1973).

All communication with the computer takes place via the OMNIBUS. The OMNIBUS is an etched board with rows of connectors soldered onto the board. The pin assignment is the same on all connectors enabling any module to be placed anywhere on the bus, thus eliminating all

random wiring between modules. There are 96 signals available on the OMNIBUS. Interfaces use signals which control transfers, address memory, or contain data to be transferred.

The PDP8/E uses three different types of data transfer: programmed data transfer, program interrupt transfer, and data break transfer.

3.2.1 Programmed data transfer

Each programmed transfer of information is initiated by the execution of an instruction in the program. Generally each input/output transfer (IOT) instruction transfers a maximum of twelve bits of data to or from the accumulator or one bit of status information by means of a skip instruction. The first three bits of an IOT instruction are 110. If the central processor is in executive mode (i.e. not timesharing) it will respond to an operation code of 6 by sending a control signal to every peripheral device. This instructs each peripheral to decode bits 3-8 of the IOT instruction. Bits 3-8 of the IOT contain the device selection code. If the code matches one of the codes for that peripheral device the interface must respond by indicating to the processor whether it is connected to the internal bus (OMNIBUS) or to the external bus (positive I/O). The interface must then decode the operation code bits 9-11 which specify the type of operation to be performed. The type of operation for each operation code is entirely determined by the design of the interface. The interface must activate control signals to indicate to the central processor the type of transfer to be performed (e.g. input data to accumulator, output data from accumulator, clear accumulator, skip next instruction). The interface must latch the data or load the

data onto the appropriate bus at the correct times indicated by timing signals on the OMNIBUS.

The I/O device will normally have one bit of status information used to indicate whether the interface is in the process of performing a transfer or free to commence a new I/O operation. This bit of information is often interrogated by means of a skip on done instruction.

3.2.2 Program interrupt transfer

The PDP8/E interrupt system is activated by asserting the interrupt request line on the OMNIBUS. If the interrupt system is enabled the central processor will execute an effective JMS (jump to subroutine) to location OOOOO. A subroutine will then save the contents of registers (accumulator, multiplier quotient, link, etc.) that may be changed by the interrupt service routine. The subroutine can then test all the peripheral devices in turn to determine which device made the interrupt request. The device may then be serviced, possibly by transferring a word of data. The subroutine must then restore the contents of the registers used by the service routine, turn the interrupt system on, and return back to the mainline program. By using the interrupt system the processor can perform useful processing whilst waiting for interrupts and it can serve several devices concurrently.

3.2.3 Data break transfer

The data break provides the fastest means of transferring blocks of data to or from memory. The data break device can directly access locations in memory without program intervention. The device

automatically modifies the address used and keeps count of the number of transfers made.

The single-cycle data break device has its own self-contained 12-bit current address register and word count register. The three-cycle data break device uses memory locations for these registers. The three-cycle device is slower and less flexible than the single-cycle device and will not be considered further.

When a data break device is ready to make a transfer it must assert control lines to inform the central processor and also assert its own priority line on the DATA bus and determine whether any device of greater priority is also requesting a data break. The device with the highest priority must then provide further control signals and a memory address. Some control signals disable the processor major state register, instruction register and CPMA (central processor memory address) register. Other signals control the direction of transfer and whether or not to add to memory. A device may transfer one word of data in each machine cycle. If no data break requests are made in the following cycle the instruction execution resumes at the point where it was discontinued. The processor major registers are never modified by a data break transfer so no restoration is necessary.

Normally the data break device will be initialised by programmed data transfers to provide it with the starting address and the quantity of data to transfer and any other necessary information. On concluding the transfer of the block of data the device may cause an interrupt to inform the processor that it has finished.

3.3 DIGITAL CONTROL OF THE BIOMATION 8100 TRANSIENT RECORDER

All front panel controls are programmable except display controls and the power switch. It is possible for some of the controls to be under manual control and for others to be under digital control. Control actions such as arm and trigger may be caused by digital commands. Other digital commands are used to read the status of the transient recorder and read the contents of its buffer memory.

The digital control bus of the transient recorder comprises sixteen parallel input data bits plus one input control bit and eight output data bits plus one output control bit. The field specifications of the bus are shown in figure 3.1. Three of the lines specify an address to the device so that up to eight devices with unique addresses may be connected to the same bus. A 5-bit operator is used to specify the function code. Eight bits are used for the input operand and a further eight bits are used for the output operand. No operator which requires an input operand will produce an output operand and so under certain circumstances the input and output operand lines can be connected together on the same 8-bit bus.

Transfer of data to and from the transient recorder is controlled by a flag line (FLG) and a command line (CMD). The flat output indicates the output data status of the transient recorder and acknowledges the acceptance of input data. The command input signal initiates the acceptance of input data. The control signals are used to ensure that data transfers take place only when the data is valid and when both the transient recorder and the controlling device are ready to make the transfer. Such control is often called 'handshake' control.

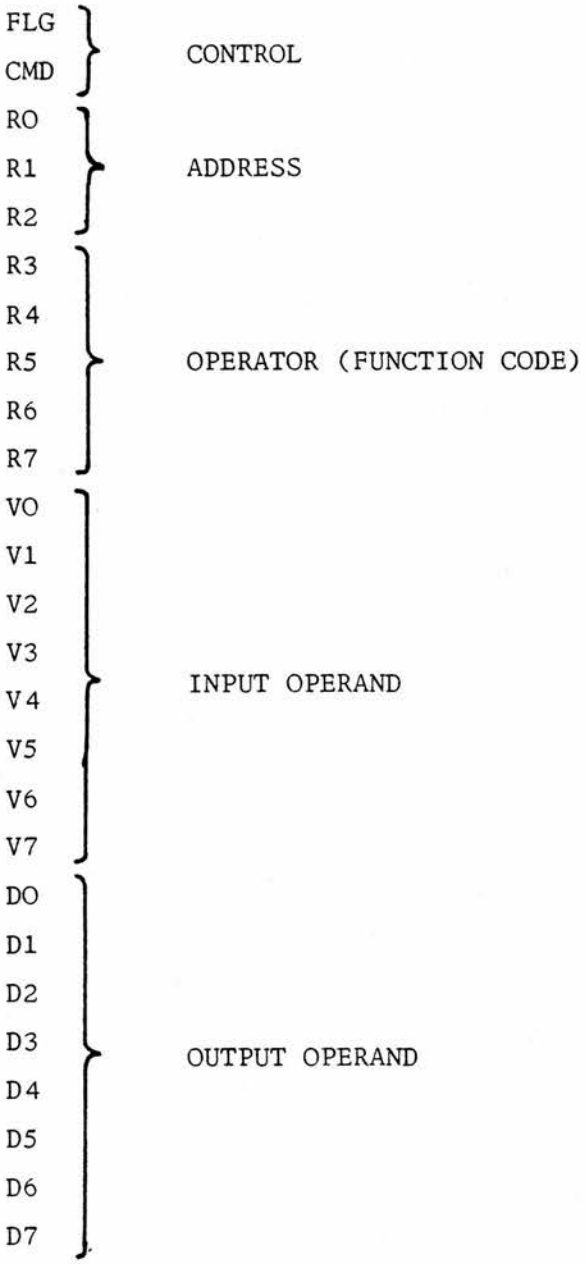

FIGURE 3.1 DIGITAL CONTROL BUS OF TRANSIENT RECORDER

3.3.1 Transient recorder instruction formats

The type of instruction specified by the operator can be divided into six types:

R3	R4	R5	
0	1	0	Control Functions
0	1	1	Output Mode, Timebase & Record Mode
1	0	0	Channel A Functions
1	0	1	Channel B Functions
1	1	0	Arm Functions
1	1	1	Trigger Functions

The control function can be divided into four more functions:

01000 Set Program Mask

01001 Set Function

01010 Read Status

01011 Read Output Data

The set program mask function is used to specify which groups of controls are to be under digital control and which are to be under manual control. Individual bits in the input operand are used to specify the groups.

The set function instruction is used to cause one of the following actions depending on which single bit in the input operand is set:

V

0 Reset

1 Switch to alternate timebase

2 No operation (NOP)

3 Trigger

4 Arm

5 NOP

6 Plot

7 Clear and update status word

The read status instruction yields an output operand with the following structure:

D

0 Offscale Channel B (-)

1 Offscale Channel B (+)

2 Offscale Channel A (-)

3 Offscale Channel A (+)

4 Ready for trigger

5 Ready for arm

6 Output Data Ready

7 Recording in progress

The read output data instruction causes the data in the buffer memory to be gated onto the output operand lines. An 8-bit two's complement code is used to represent the data. Sequential locations in the buffer memory are accessed using the flag and command control lines to synchronise the transfers. When one byte of data has been latched a command pulse is issued to the recorder. The flag line then goes low whilst the data lines change to the next byte of data. When the output operand is valid the flag returns to high and the new datum can then be latched.

The remaining operators are used to define the parameters for the groups under digital control. The operator specifies which controls are to be affected (e.g. 10001 for Channel A input offset magnitude) and the operand is used to specify the actual settings (e.g. 0101 1001 for offset magnitude 0.59).

Further details on the 22 different operators and their corresponding operand structures may be found in the transient recorder handbook.

3.4 THE TRANSIENT RECORDER INTERFACE

The first three sections in this chapter have described some of the requirements to be satisfied by the interface. The design of the interface requires a consideration of both hardware and software aspects, involving a compromise between ease of programming and ease of implementation. Rather than describe the evolution of the design only the final design will be described.

3.4.1 Features of the transient recorder interface

The interface allows full digital control of the transient recorder. Programmed data transfers can be used to give 16-bit instructions to the transient recorder and read the 8-bit output operand. Single-cycle data break transfers are used to transfer the contents of the transient recorder buffer memory into the PDP8/E memory.

Three 8-bit bytes can be packed into every two 12-bit words of PDP8/E memory, thus saving memory and disk storage space and reducing transfer times. If packing is not selected the interface converts from 8-bit two's complement code to 12-bit two's complement code by extending the sign bit into bits 0-3.

Because the transient recorder memory is 2048 bytes long one bit in the command register can be used to select the transferring of 2048 bytes.

The data break transfers can use the add to memory facility and overflows can be detected using a skip instruction.

For efficient programming the interface can make interrupt requests. The interface can detect when the transient recorder has finished recording and automatically start transferring date using data breaks, and make an interrupt request when the transfers are completed. Alternatively the done flag can be set when the end of recording is detected.

A bi-directional external data bus is used which allows other addressable devices to be controlled by the interface.

Extensive maintenance facilities are built into the interface to allow diagnostic programs to detect and locate faults in the interface.

A simplified block diagram of the interface is shown in Figure 3.2. Many of the interconnections have been omitted for clarity.

3.4.2 Operator and operand registers

The transient recorder requires 16-bit words to control it digitally but the PDP8/E computer uses 12-bit words so at least part of the instruction must be stored in the interface. In practice the interface contains an 8-bit operator register and an 8-bit operand register which can be loaded from the accumulator using programmed

data transfers. The operator register includes three address bits and five operator bits. The operand register holds the eight operand bits. Because some instructions require that the operand bits should all be zero the operand register is automatically cleared when the operand register is loaded. If an operand is required the operand register must be loaded after the operator register.

3.4.3 External data busses

The operand register is connected to the operand bus using open-collector gates to allow bi-directional operation. Several addressable devices may use the operand bus for both input and output provided that they use open-collector gates to assert the lines. The operator register is connected to the operator bus using open-collector gates to allow other peripheral devices to drive the bus. A separate operand bus is provided to input data from devices (such as the Biomation 8100 transient recorder) using tri-state outputs. Although the transient recorder never requires an input operand when it provides an output operand it would be possible for a programming error to provide an input operand. Such an error could cause bus conflict and subsequent damage to bus drivers. Clearly software errors must not be allowed to cause hardware errors. By providing a separate input port for devices using tri-state bus drivers this danger is avoided. The two input ports are combined by a bitwise logical OR operation.

3.4.4 Data break control

The interface uses the single-cycle data break transfer because this is the fastest form of transfer on the PDP8/E. One word of data may

be transferred by the interface in every memory cycle.

The timing of data-break requests and disabling of CPU major registers follows the rules laid down in the 'Small Computer Handbook' (DEC, 1973).

3.4.5 Data break priority

Data break interfaces must contain circuitry to prevent more than one device from attempting to make a data break transfer in one memory cycle. Each device is assigned a data line which must be asserted when making the data break request. Each interface must check that no data lines of higher priority (more significant bits) are asserted before proceeding with the data break transfer.

Although the transient recorder interface is capable of making transfers at a higher rate than the disk controller, it was given a lower priority than the disk. This is because the transient recorder interface is capable of making a transfer in every memory cycle and it could thus lock out the disk for 2048 consecutive memory cycles (2048 x 1.2 = 2457.6 microseconds) if it had the highest priority. The disk controller contains a data buffer which holds four words of data and delays of more than 22.5 microseconds will cause data to be lost. In contrast the transient recorder can withstand latency errors of up to 100 microseconds and the disk is incapable of locking out other devices for that length of time. (The average transfer rate for the disk is 8.32 microseconds per word). Even delays of 100 microseconds will not cause transient recorder data to be lost but will only cause an extra delay of up to 1 millisecond whilst buffer memory refresh takes place.

3.4.6 Byte pack control

The byte-packing circuitry can optionally pack three 8-bit bytes into every two 12-bit computer words. Three 8-bit buffer registers are used so that whilst two of the registers are being used to transfer data to the computer memory the third buffer register can accept another byte of data from the peripheral device. This allows a data break to be performed every memory cycle provided the peripheral date is valid within 550 nanoseconds of the last transfer. The Biomation 8100 transient recorder does not always respond fast enough for this: the real advantage of byte packing is the saving in time to transfer to disk and the saving in disk and memory storage space. In fact making transfers in every single cycle would have disadvantages if program instructions had to be executed concurrently.

Multiplexers are used to select the correct bits from the three registers. The format of the packing is shown below:

WORD 1	4 MSB's of BYTE 2	BYTE 1
WORD 2	4 LSB's of BYTE 2	BYTE 3

This differs from the OS/8 (operating system for PDP8's) format for packing bytes of ASCII, which splits the third byte between two words. That is satisfactory for software packing but unsatisfactory for hardware packing at high speed since the interface would have to wait until the third byte was available before the first byte could be transferred.

The byte packing control must work satisfactorily in the presence of delays in transferring data to memory and delays in obtaining data

from the peripheral. In addition the correct number of transfers must be made whether the number of bytes is 3N, 3N+1, or 3N+2.

The loading of the buffer registers is synchronous with computer timing pulses to simplify monitoring the circuitry with an oscilloscope. Three bytes can be transferred in every two memory cycles provided that the peripheral device can give valid data within 550 nanoseconds of the last transfer. It was expected that the Biomation 8100 transient recorder would achieve this, since the data becomes available synchronously with a 2 MHz clock. However, a filter on the CMD line within the transient recorder introduces an additional delay and transfers are not always made on consecutive cycles. At worst this can cause the average transfer rate to drop from 1.5 bytes per memory cycle down to 1 byte per memory cycle, resulting in an increase of 0.4096 milliseconds to transfer 2048 bytes. If the data is subsequently transferred to disk this extra delay is negligible. (The average time to transfer the packed 2048 bytes to disk is about 53 milliseconds.) If the data is to be processed immediately without transferring to disk it will normally be preferable not to pack the data to avoid the delay involved in unpacking the data. If no packing is used, one byte is transferred in every single cycle.

3.4.7 Transient recorder interface instruction set

The operation decode bits of the IOT are used to specify one of the eight operations shown in the table below.

MNEMONIC	CODE	OPERATION
TRCLR	6160	CLEAR. Clears registers within the interface.

MNEMONIC	CODE	OPERATION
TRSKP	6161	SKIP ON DONE. If the done flag is set the program counter is incremented to skip the next sequential instruction.
TRSOV	6162	SKIP ON OVERFLOW. If the overflow flag has been set during an add to memory data break the next sequential instruction will be skipped.
TRRD	6163	READ DATA. The data on the external bus is converted into 12-bit two's complement code and loaded into the accumulator. Clears done flag.
TRRDI	6164	READ DATA and ISSUE CMD. Performs a TRRD and then issues a CMD (command pulse). The done flag is reset when the peripheral flag returns to high.
TRLRG	6165	LOAD REGISTER. Accumulator bits 0-1 determine which register is loaded from the accumulator:

AC0	AC1	Register Loaded
0	0	Command register
0	1	Maintenance register
1	0	Operator register
1	1	Operand register

This instruction is described in more detail later in this section.

TRLBC	6166	LOAD BYTE COUNTER. The contents of the accumulator are loaded into the byte counter. The accumulator must contain the two's complement of the number of bytes to be transferred by the data breaks.

MNEMONIC	CODE	OPERATION
TRLCA	6167	LOAD CURRENT ADDRESS REGISTER. The contents of the accumulator are loaded into the current address register. The accumulator should contain the address of the first data break location.

The instructions TRCLR, TRLRG, TRLBC and TRLCA all clear the accumulator.

The TRLRG instruction requires some further explanation. The accumulator bits 0-1 determine the function of the remaining bits. These functions are shown in tables 3.1 to 3.3.

3.4.8 Further notes on the instruction set

TRCLR CLEAR. The same function is also caused by the CLEAR key on the programmer's console and by the POWER ON RESET pulse.

TRSKP SKIP ON DONE. This instruction provided the means of determining whether the last operation has been completed. The done flag is only set by instructions using a handshake transfer. Loading internal registers such as the byte counter are always accomplished in one memory cycle so there is no need to use the done flag.

TRSOV SKIP ON OVERFLOW. The PDP8/E overflow logic only detects overflows of 12-bit positive numbers. Hence if the signals being added to memory are bi-polar the overflow flag is not a valid indication of overflow. The setting of the overflow flag does not cause an interrupt request. This is to minimise

TABLE 3.1 TRLG accumulator bit functions for AC0=0, AC1=0
(Load command register)

BIT POSITION	FUNCTION
0, 1	Register Select: 00 for command register
2	Clear done flag
3	GO (Start data breaks)
4	GO on end of scan
5	Transfer 2048 bytes
6, 7, 8	Extended Memory Address
9	Add to memory
10	Pack bytes
11	Interrupt on done

TABLE 3.2 TRLG accumulator bit functions for ACO=0, AC1=1

(Load maintenance register)

BIT	FUNCTION
0	Register Select: 01 for maintenance register
1	
2	Clear done flag
3	Clear CMD detector
4	Set done flag on end of scan
5	
6	
7	Flag trap enable
8	Maintenance mode enable
9	Maintenance byte selection
10	
11	

TABLE 3.3 TRLG accumulator bit functions for ACO=1

(Load operator or operand register)

BIT POSITION	FUNCTION
0, 1	Register Select: 10 for Operator register; 11 for Operand register
2	Clear done flag, issue CMD, set done flag when FLG high
3	Set end of scan detector
4, 5, 6, 7, 8, 9, 10, 11	Byte loaded into register

the length of the skip chain testing the cause of the interrupts.

TRRDI READ DATA and ISSUE CMD. Having allotted seven IOT's to all the essential operations, there remained one spare IOT and it was used for this operation. Although it is not essential it is useful for transferring blocks of data without using data breaks.

TRLRG LOAD REGISTER. When the command register is loaded the extended memory address (EMA) is in AC6-8 for compatibility with other instructions using an EMA (RDF, CIF, DLDC, MTLC, etc.).

The multipurpose use of IOT5 has the advantage that the resulting instruction is rather powerful. The main disadvantage of this multipurpose use is that an error in the contents of the accumulator could result in an unintentional series of data breaks.

TRLBC LOAD BYTE COUNTER. The accumulator should contain the two's complement of the number of bytes rather than the actual number of bytes. This is compatible with other data break devices, and it simplifies the circuitry.

TRLCA LOAD CURRENT ADDRESS REGISTER. Although some data break devices require that the current address register should be loaded with the address minus one, this interface follows the more usual practice of loading with the starting address. Also following normal practice, if the address overflows from

7777_8 to 0000_8 the extended memory address is NOT modified. This affords some degree of memory protection in the event of an error.

3.4.9 Automatic detection of end of scan

When the transient recorder has finished recording it indicates the end of scan state by making the FLG line go low for 200 nanoseconds. Alternatively the end of scan state could be detected by using the read status instruction. However, the method of detecting the end of a scan using the status word will depend on the output mode of the transient recorder. Furthermore, if the interface is to be capable of automatically starting data breaks when the end of scan state is detected the read status instruction would have to be changed to a read data instruction before the data breaks commenced. For these reasons it was decided to use the FLG transition to detect the end of scan.

In a typical acquisition program one instruction would be given to arm the transient recorder and then a second instruction would give the enable output data instruction to the transient recorder. On detection of the end of scan the interface would commence performing data breaks. The interface must be capable of detecting the end of scan even if it occurs before the enable output data instruction. However, the data breaks must not occur before the enable output data instruction or faulty data would be transferred. This problem is overcome by using a flag within the command register which inhibits data breaks until it is set to logical 1, and the end of scan is detected. When the arm

instruction is given bit 3 in the accumulator is used to set the end of scan detector. After the enable output data instruction is given the command register is loaded and bit 4 of the accumulator can set the flag which enables the data breaks to commence when the end of scan occurs, e.g.

```
        CLA
        TAD         (4051
        TRLRG                   /SET FUNCTION
        TAD         (7500
        TRLRG                   /ARM, SET EOS DETECTOR
        TAD         (4053
        TRLRG                   /ENABLE OUTPUT DATA
        TAD         (1312
        TRLRG                   /GO ON EOS, TRANSFER 2K TO FIELD 1, PACK
WT,     TRSKP                   /SKIP ON DONE
        JMP          WT         /WAIT
         .
         .
```

It may be thought that the enable output data instruction could always be given before the transient recorder has time to finish recording and that there is no need to use a flag to inhibit the data breaks. Three points should be remembered however:

1. The transient recorder does not always record for 2048 samples. In the pretrigger mode as few as 10 samples may be taken.
2. A program interrupt may occur after the arm instruction but before the enable output data instruction, delaying the latter instruction

until it is too late. Although the interrupt system could be disabled this programming restriction should be avoided.

3. It is desirable to be able to single step the program without causing errors. Single stepping could delay the enable output data instruction too long.

Hence the need to include the safety feature of the enable GO on EOS flag.

3.4.10 Maintenance facilities

It is important to be able to detect errors in an interface and to locate the cause of the error. A common method of repairing digital systems is to locate the fault to the board level and replace the faulty board. This option is not possible in a one-off interface so it is valuable to be able to locate the fault more precisely.

The interface includes a number of features to allow a diagnostic program to detect and locate errors. The status of many registers within the interface can be read by both programmed transfers and data break transfers. Table 3.4 shows which points can be monitored using maintenance mode. Registers can be loaded with every possible combination so rigorous checking is possible.

Since data breaks are under autonomous control of the interface and not under control of the program, faults in the interface are potentially disastrous. Faulty data breaks could corrupt the program and prevent it from printing error messages. If the data breaks continue to occur after the required number of transfers the program

could cease to run at all. By incorporating maintenance facilities into the design much of the logic can be tested without performing data breaks. For example, the byte counter can be clocked under program control. Only when much of the logic has been tested are the potentially disastrous data break transfers performed.

Maintenance circuitry is provided for testing the flag/command handshake circuitry without using a peripheral. Since CMD pulses are too short to be read under program control a CMD detector is included. The CMD detector flag is set when a CMD pulse occurs. Checking the interface handshake circuitry during data breaks is more difficult. It is not adequate to simply use one instruction to hold the FLG line low and use a second instruction to let the flag go high. This is because the interface can perform data breaks every single cycle. Thus once the FLG line was raised the program would not get a chance to hold the FLG low again until all the data breaks were completed. This would give inadequate testing of all transfers after the first one. The problem was overcome by using a FLG TRAP ENABLE flag and the CMD detector. If the flag trap is enabled the FLG line is held low when the CMD detector is set. The FLG line can go high when the CMD detector is cleared by a maintenance instruction. This will allow another byte to be transferred. Another CMD will be issued and this causes the FLG line to be forced low again, preventing further transfers until another maintenance instruction clears the CMD detector.

In addition to testing the handshake control circuitry the flag trap and CMD detector are important for controlling data break transfers

TABLE 3.4

Registers read by maintenance mode

CURRENT ADDRESS

BREAK EXTENDED MEMORY ADDRESS

ADD TO MEMORY

OVERFLOW

INTERRUPT ENABLE

BYTE COUNTER

PACK ENABLE

DATA BREAK ENABLE

SDEOS, GOEOS, PACK COUNTER

CMD DETECTOR, PWT, DONE

OPERATOR

and stopping the transfers if an error is found. This is especially important if the fault caused the interface to continue making data breaks after the appropriate number of transfers. Without the flag trap there would be no way that the program could stop the transfers and print an error message. Although it is still possible that certain types of errors will result in perpetual data breaks they are not so likely to occur.

As an additional aid in detecting and locating faults, a panel of 24 LED's indicate the status of points within the interface. This is also valuable for debugging programs and for monitoring the running of a program. LED's indicate the status of the FLG line, the DONE flag, the GO flag, the maintenance byte selection bits, the +5V and ±15V power lines, and the operator bus and operand bus. Four of the maintenance bytes can be loaded onto the operand bus so the status of these bytes can be seen on the LED's.

Most of the maintenance bits which are not gated onto the external data bus can be indicated by lights on the programmer's console of the PDP8/E. During data breaks the following status information is available on these lights: CURRENT ADDRESS, EXTENDED MEMORY ADDRESS, BREAK IN PROG, BREAK CYCLE, ADD TO MEMORY, and MD DIR.

3.4.11 Implementation of the transient recorder interface

The design was implemented using TTL integrated circuits. These were mounted on two wire wrap modules which plugged into the PDP8/E OMNIBUS, and on seven boards mounted in a VERO rack. An OMNIBUS foundation

module containing IOT decode logic and buffers for a number of OMNIBUS signals was used. The VERO board was used because it was cheaper than using a third OMNIBUS module, left more space on the OMNIBUS, and allowed a panel of LED's to be visible. The rack has room for expansion, with space for plug-in boards and screened modules.

The complete circuit diagram of the interface is given in Figures 3.2 - 3.28. A gate-by-gate account will not be given but the brief notes on parts of the circuit should enable its operation to be understood.

3.4.12 Notes on transient recorder interface circuit diagrams
M1 refers to circuits on the OMNIBUS interface foundation module. M2 refers to circuits on the other OMNIBUS module. M3 refers collectively to the circuits in the VERO rack.

The letter 'L' or 'H' following a signal name indicates the level when the line is asserted, e.g.
INT ENAB L is LOW when interrupts are enabled
OVFLOW H is HIGH when an overflow has occurred.

Figure 3.3 OMNIBUS interface foundation module. Pre-assembled circuitry on this module decodes the device address and function code and buffers various OMNIBUS signals required for programmed transfers.

Figure 3.4 Data buffers. Also on the foundation module are the data buffers. A bi-directional data bus is used to convey data to and from M3 circuitry.

Figure 3.9 C line control logic. The C lines are used to control the loading and clearing of the accumulator during programmed data transfers.

Figure 3.12 Current address register logic. The current address register is loaded at TP3 during IOT7. It is incremented at the end of each data break.

Figure 3.13 Data break control logic. When NEW BK L is LOW a data break request is made. The device's own priority line DATA4 is asserted and all higher priority lines are checked. If no higher priority device is making a data break request the data break proceeds. Various OMNIBUS lines are asserted to prevent the central processor from executing an instruction. The interface loads the address onto the memory address and extended memory address lines on the OMNIBUS and loads the data onto the DATA lines. The signal SUC BK L is generated to indicate to circuitry on M3 that the request was successful. If SUC BK L does not go low another data break request is made in the following memory cycle.

Figure 3.15 Maintenance logic on M2. The maintenance bytes are loaded onto the bi-directional data bus connecting M2 to M3. The multiplexers are disabled during output transfers. If M3 is not connected to M2 eight bits of the current address register are loaded onto the BBDATA lines so that much of the logic on M1 and M2 can be tested without M3.

Figure 3.18 DONE flag logic. A latch is set to cause a CMD pulse

to be issued and another latch is set to cause the DONE flag to be set when the PFLG line goes high. The DONE flag is also set at the end of a series of data breaks (ENDDMA L) or when End of Scan is detected (SCANDUN L).

Figure 3.19 IOT5 decode logic. The two most significant bits in the accumulator during IOT5 are used to generate one of four clock signals to load the appropriate register.

Figure 3.20 Operator and operand register logic. Only one of the eight bistables in each register is shown. The input port for tristate bus drivers is shown (TRIDAT).

Figure 3.21 Byte counter logic. The byte counter is loaded from the accumulator during IOT6 or with a preset value of -2048 (4000_8) during IOT5 if AC0=AC1=0 and AC5=1. It is incremented by BYTCNT L, which occurs when CMD pulses are issued during a series of data breaks.

Figure 3.22 Go/stop logic. The GO bistable is set to allow a series of data breaks to be made. It can be set by program control (LDCMND H and LDATA3 H) or when EOS is detected (DATRDY H and GOEOS H). The GO bistable is cleared when all the data break transfers have been made. The LAST bistable is set when the final byte has been loaded into a register (LASBYT H). Even after LAST is set GO remains set if QUEUE L is LOW or if BLASWD H is HIGH and PACK H is HIGH. QUEUE L is low if another data break request is required due to a data break device of higher priority using the current memory cycle. BLASWD H is HIGH if the last byte was loaded into the B register, thus requiring another data break to transfer the second half of the byte.

Figure 3.23 Flag control of byte packing. This circuitry generates signals used to load the appropriate data register when the peripheral data is valid (PWT L is HIGH). When the NEW BK bistable is loaded a data break request is made. The QUEUE bistable is then loaded but is cleared immediately if the request is successful (SUC BK L). If the QUEUE bistable remains set the operations of the interface are suspended for one memory cycle and another data break request is made in the following memory cycle.

When the final byte has been loaded LAST H goes HIGH and a data break request is made. This allows the transfer of AREG without loading BREG if the final byte was loaded into AREG. It also allows the transfer of the second half of BREG without loading CREG if the final byte was loaded into BREG.

Figure 3.24 CMD pulse logic. This circuitry generates a CMD pulse whenever a data register is loaded during a series of data breaks or when a programmed CMD pulse is required (PROGCMD L). The monostable controls the length of the CMD pulse. The byte counter is clocked every time a CMD is issued whilst GO is set. This arrangement allows programmed clocking of the byte counter to test it. The BYTSEL counter is a modulo 3 counter used to control which data register is loaded next and which word is transferred during data breaks. The BYTSEL counter is clocked when AREG is loaded and when a successful data break request is made (SUC BK L).

Count sequence of BYTSEL:

BYTSELO	BYTSEL1	MEANING
0	0	Load AREG next (at TP1). Clock BYTSEL counter when AREG is loaded.
0	1	Load BREG next (at INT STROBE). Make data break request when BREG is loaded. Clock BYTSEL counter if request is successful.
1	1	Transfer AREG and half of BREG. Load CREG next (at TP2). Make data break request when CREG is loaded. Clock BYTSEL counter if request is successful.
0	0	Transfer CREG and second half of BREG. Sequence repeats.

If PWT L is LOW at the time assigned for loading the next register the register is not loaded until PWT L is HIGH at the same time in some subsequent cycle.

If byte packing is not selected CKAR and CKCR are not generated and CKBR is used to load the AREG.

Figure 3.25 Input multiplexer logic. During the byte pack transfers BYTSELO selects eigher AREG and half of BREG or CREG and the second half of BREG. If byte packing is not selected AREG is transferred and bits 0-3 of the data word are made equal to the sign bit of AREG. During output transfers the multiplexers are disabled.

Figure 3.26 Maintenance logic on M3. Multiplexers load the appropriate maintenance byte onto the POPRND bus. The CMD pulse detector is set when PCMD H goes low. If the flag trap is enabled (FLG CON H) and the external device code is 000_2 the PFLG line will be forced low when the CMD detector is set.

Light emitting diodes indicate the status of 24 test points.

Figure 3.27 and figure 3.28 show the power monitor circuits. The light intensities of the LEDs are sensitive to small variations in power line voltages. The 5V monitor LED becomes dim when the supply drops to 4.75 volts and the ± 15V monitor LED becomes dim when the difference between the positive and negative rails drops to 29.6 volts.

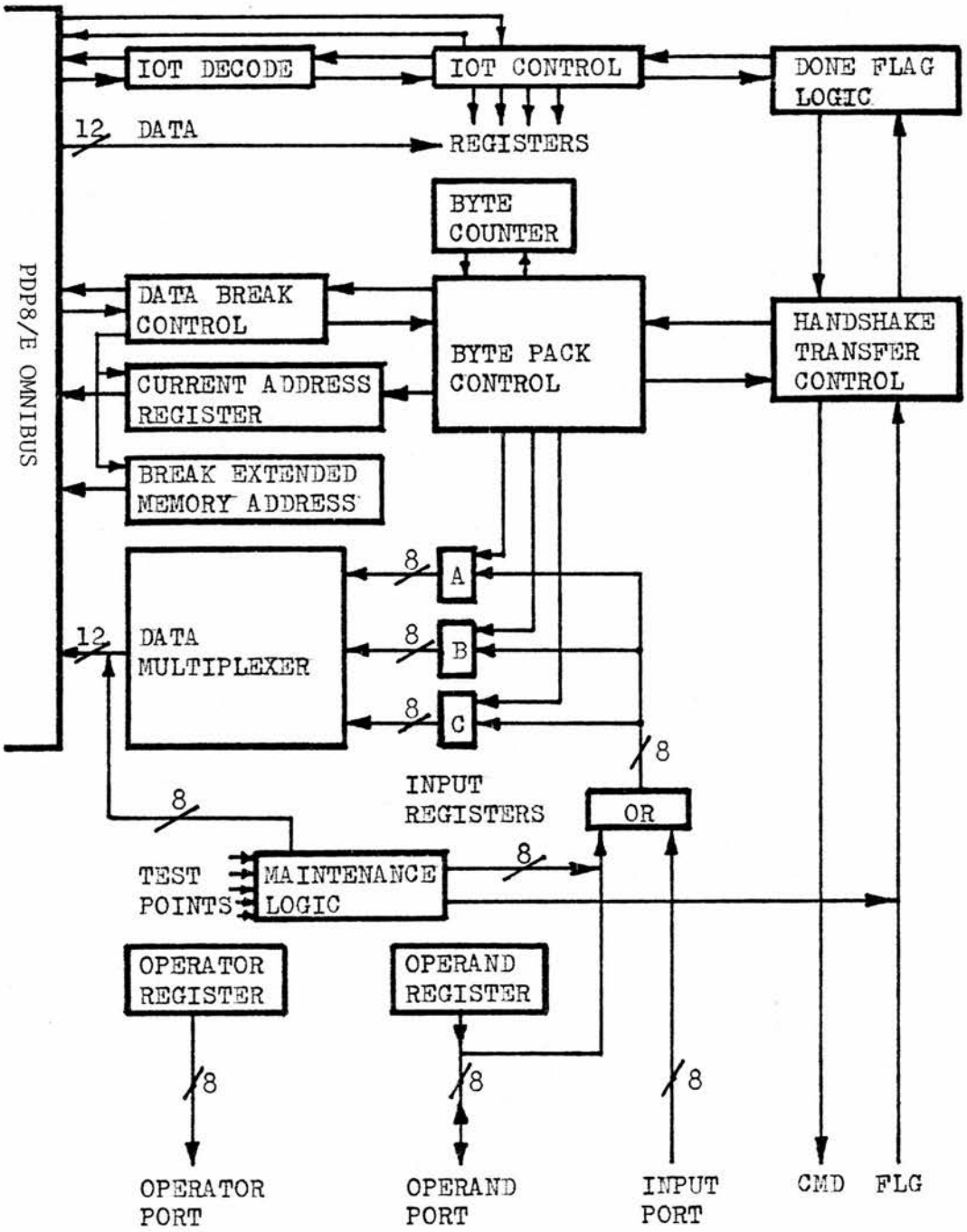

FIGURE 3.2 SIMPLIFIED BLOCK DIAGRAM OF TRANSIENT RECORDER INTERFACE

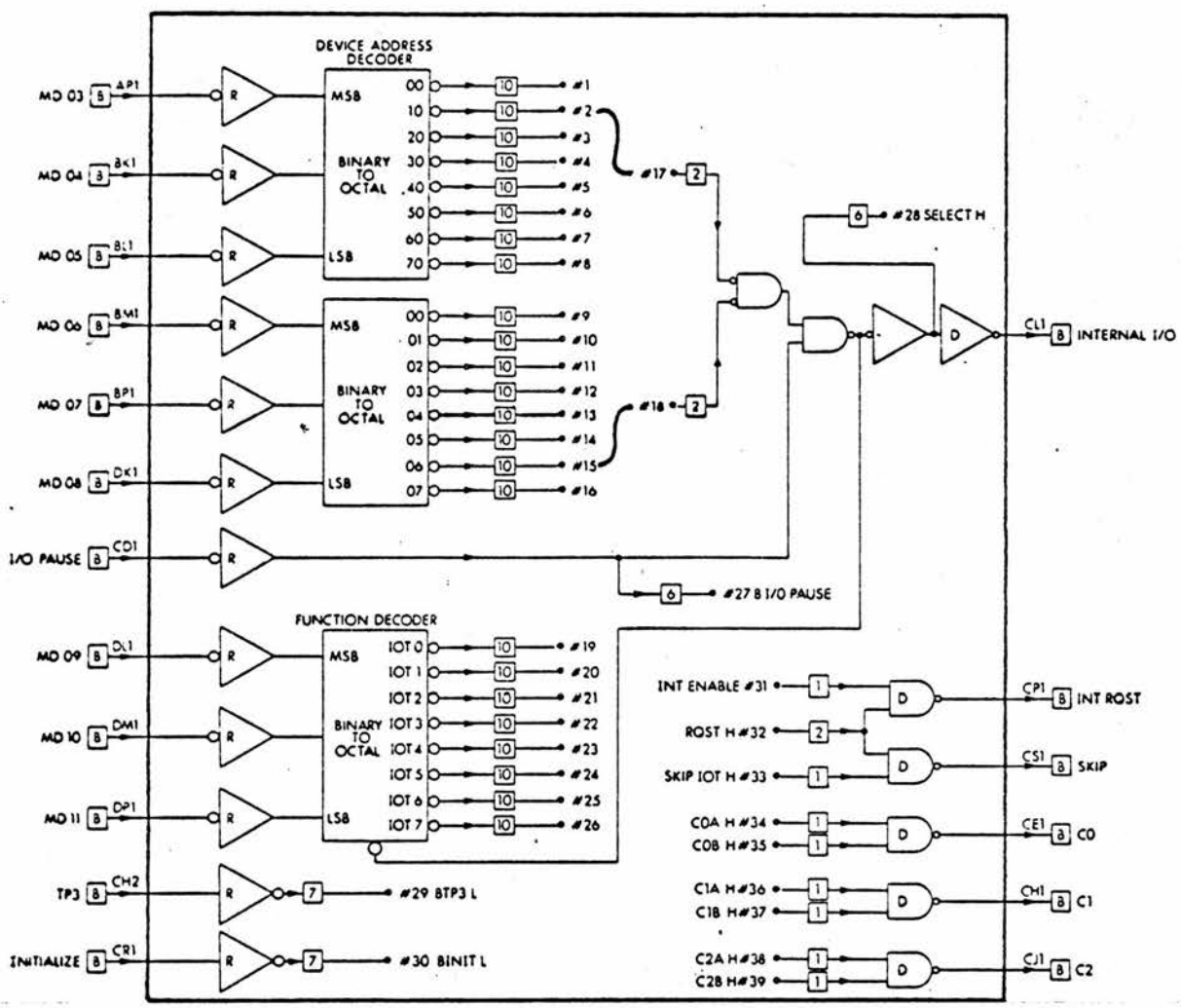

FIGURE 3.3 OMNIBUS INTERFACE FOUNDATION MODULE

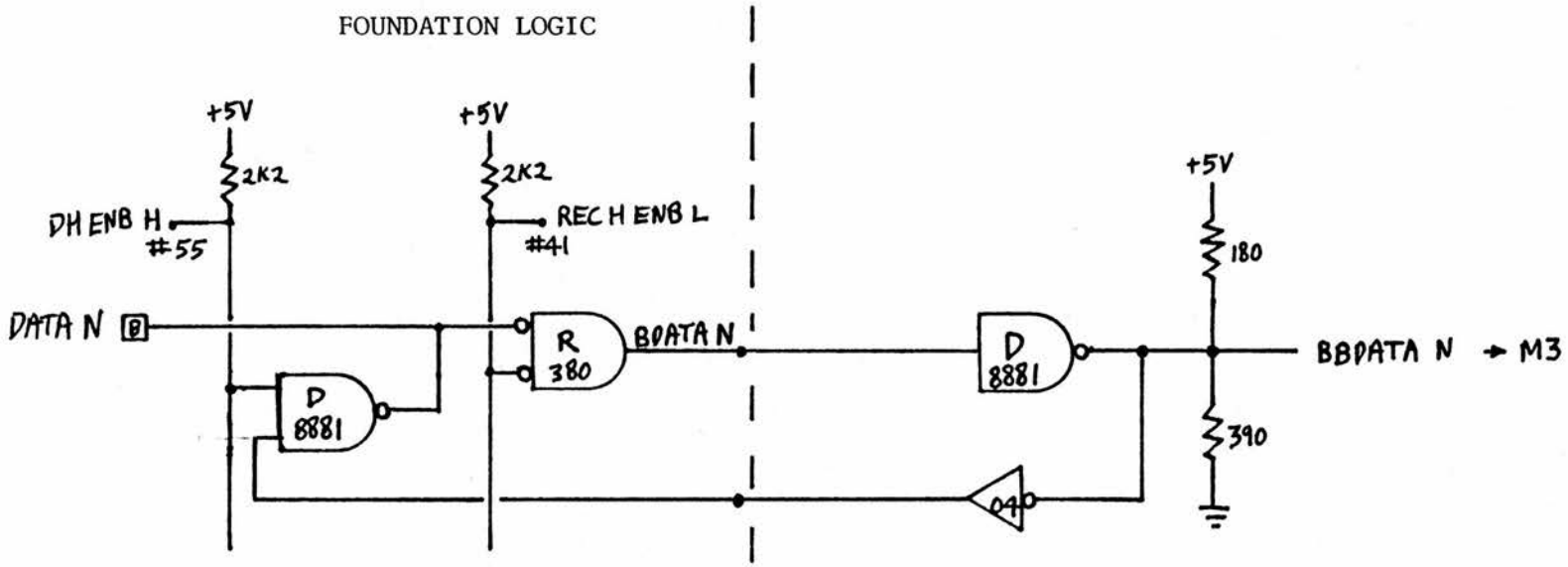

FIGURE 3.4 DATA BUFFERS

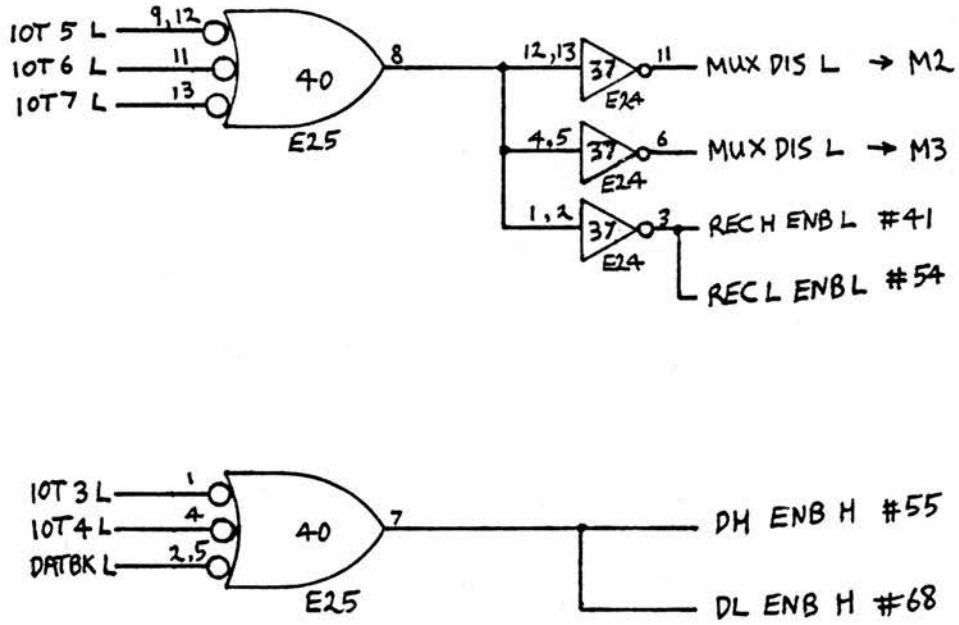

FIGURE 3.5 DATA BUS CONTROL LOGIC

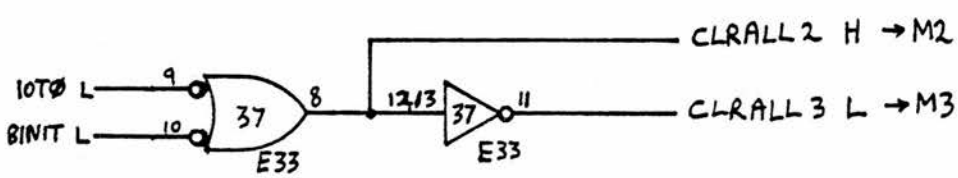

FIGURE 3.6 CLRALL LOGIC

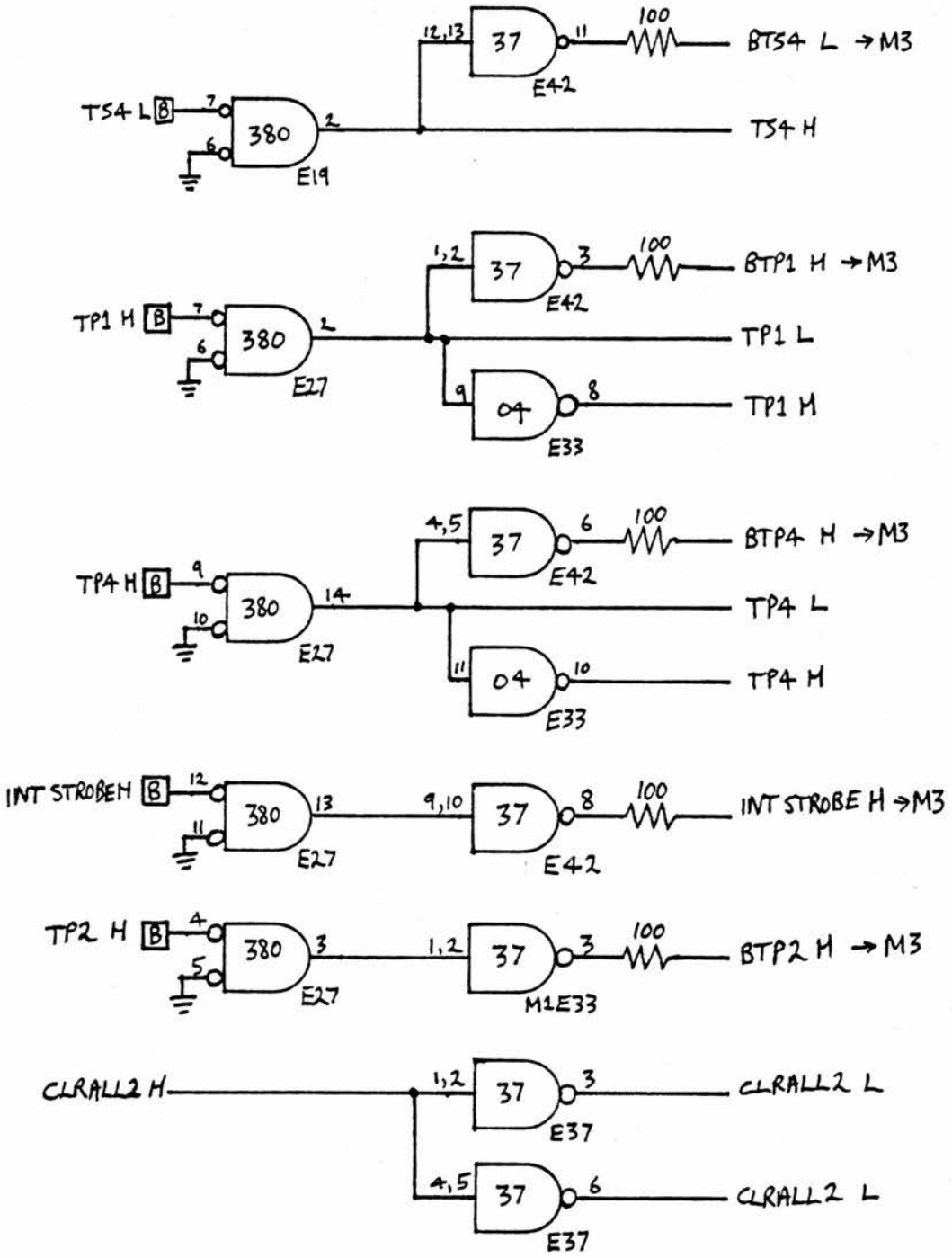

FIGURE 3.7 MISCELLANEOUS BUFFERS

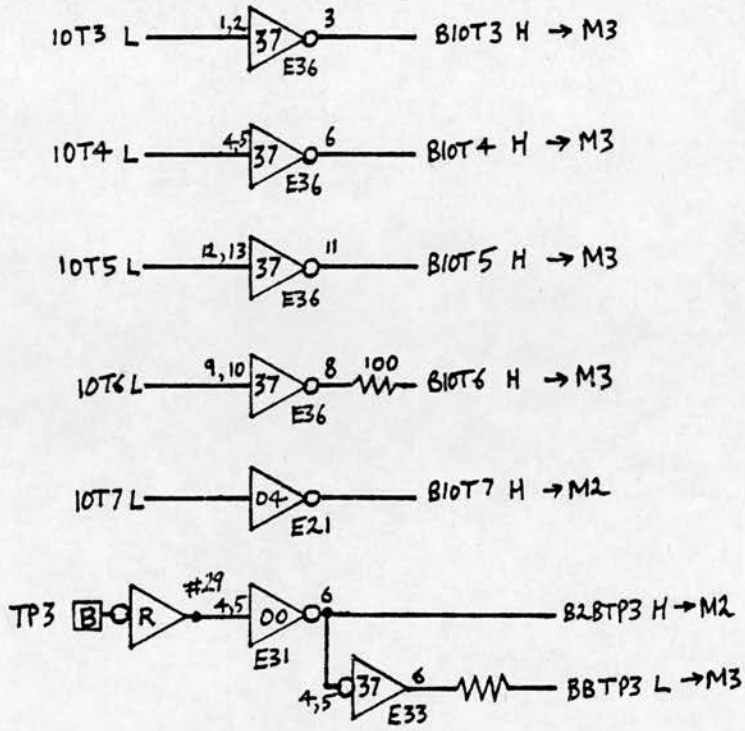

FIGURE 3.8 MISCELLANEOUS BUFFERS

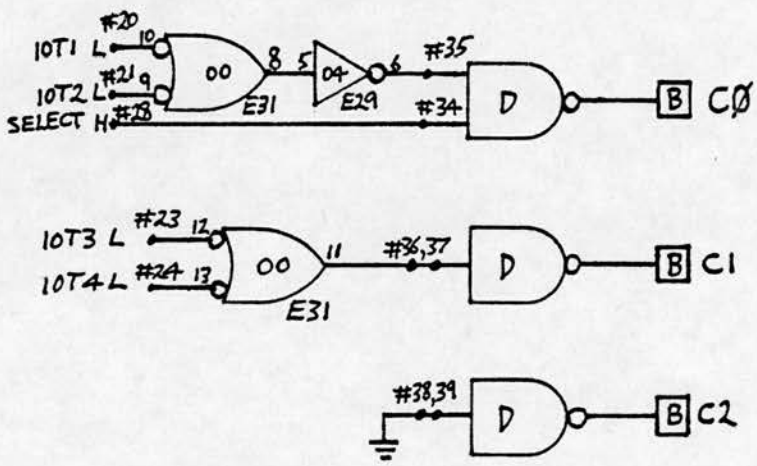

FIGURE 3.9 C LINE CONTROL LOGIC

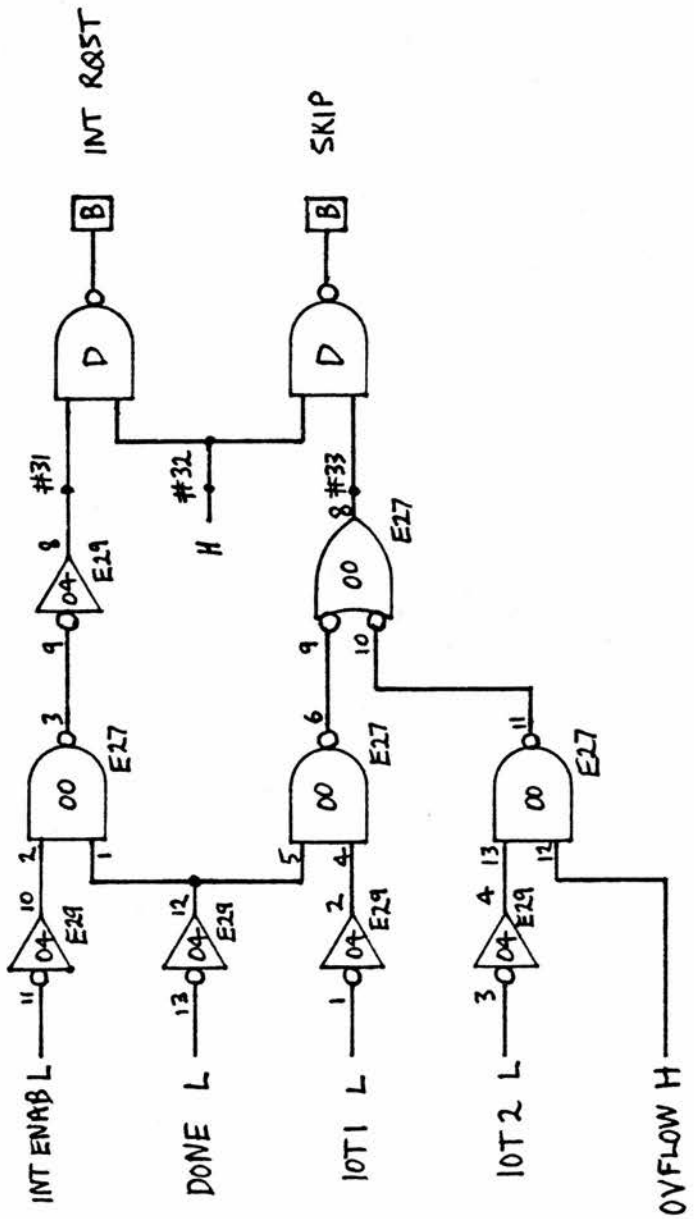

FIGURE 3.10 INTERRUPT AND SKIP LOGIC

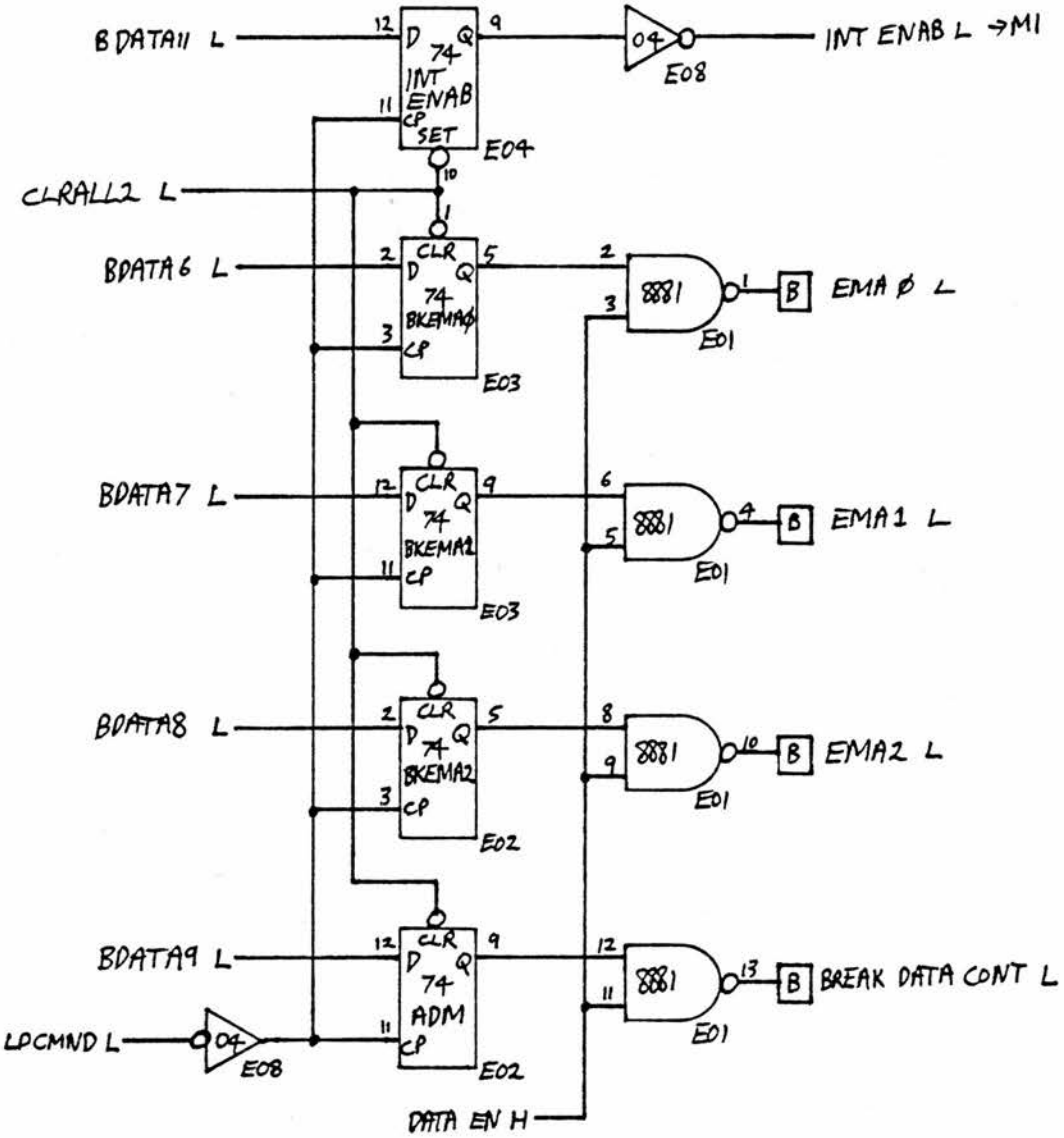

FIGURE 3.11 COMMAND REGISTER LOGIC

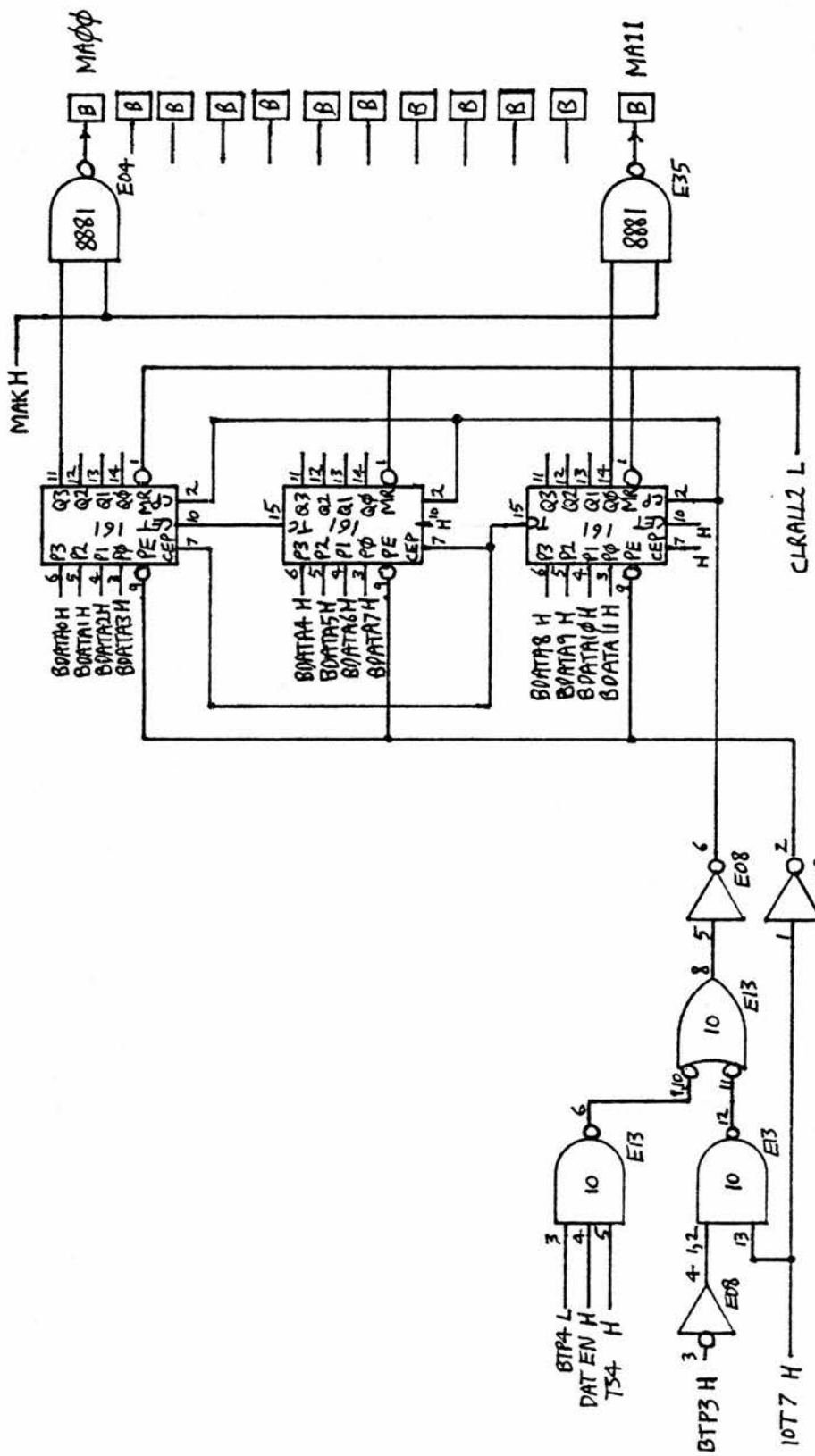

FIGURE 3.12 CURRENT ADDRESS REGISTER LOGIC

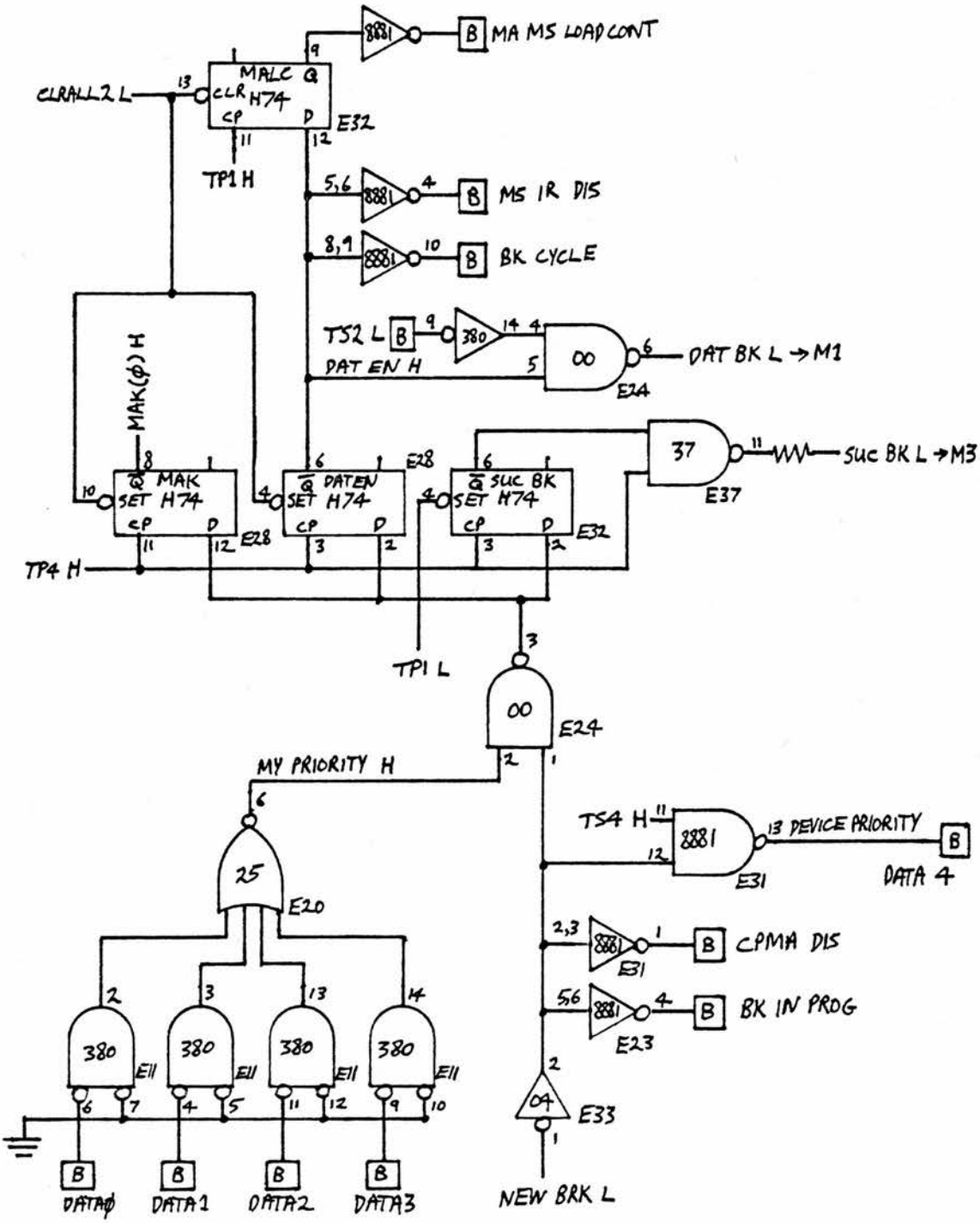

FIGURE 3.13 DATA BREAK CONTROL LOGIC

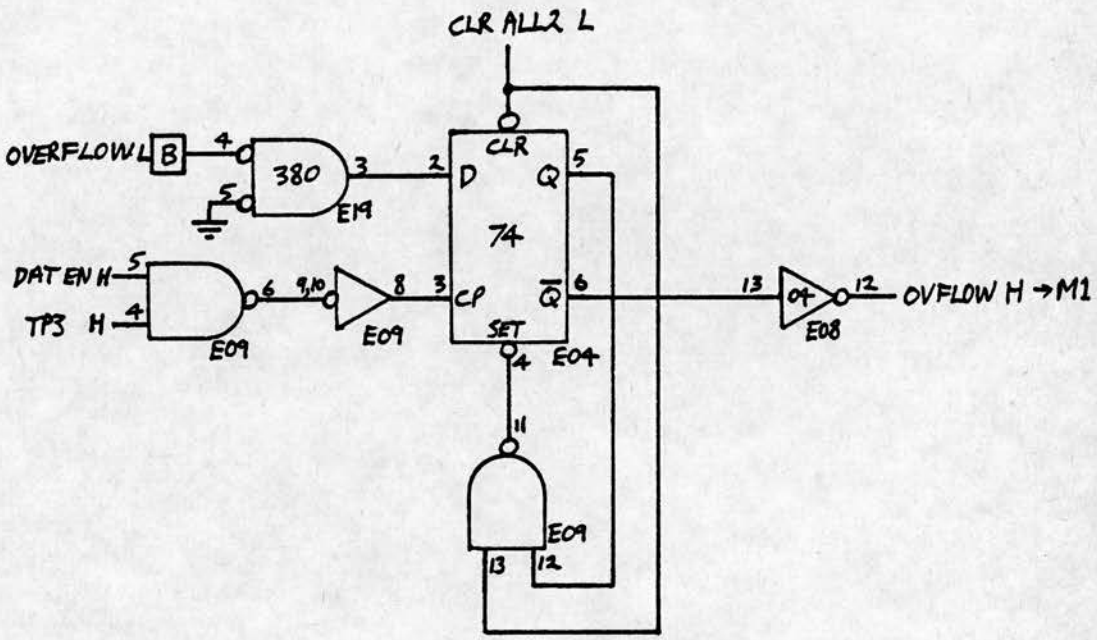

FIGURE 3.14 OVERFLOW LOGIC

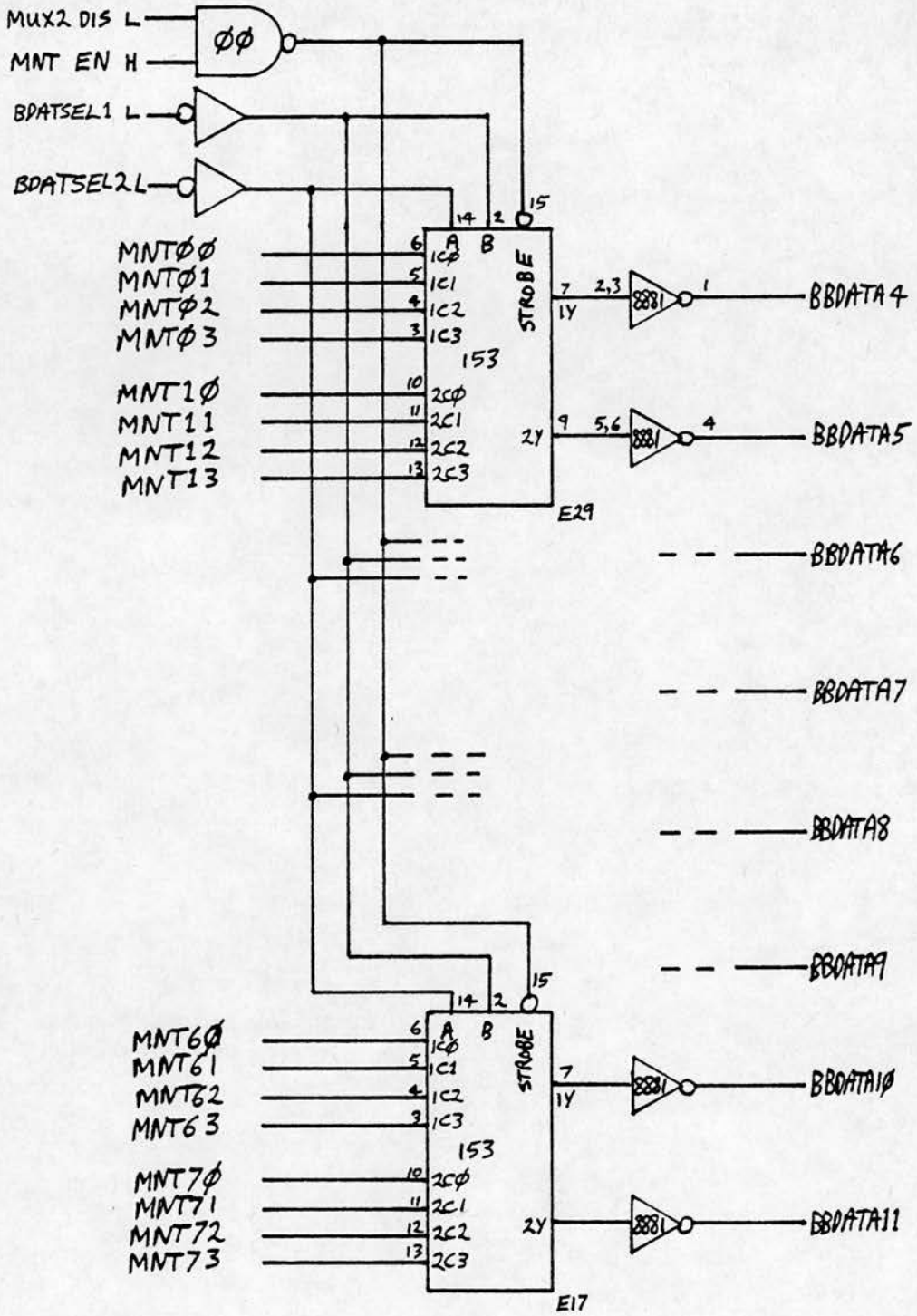

FIGURE 3.15 MAINTENANCE LOGIC ON M2

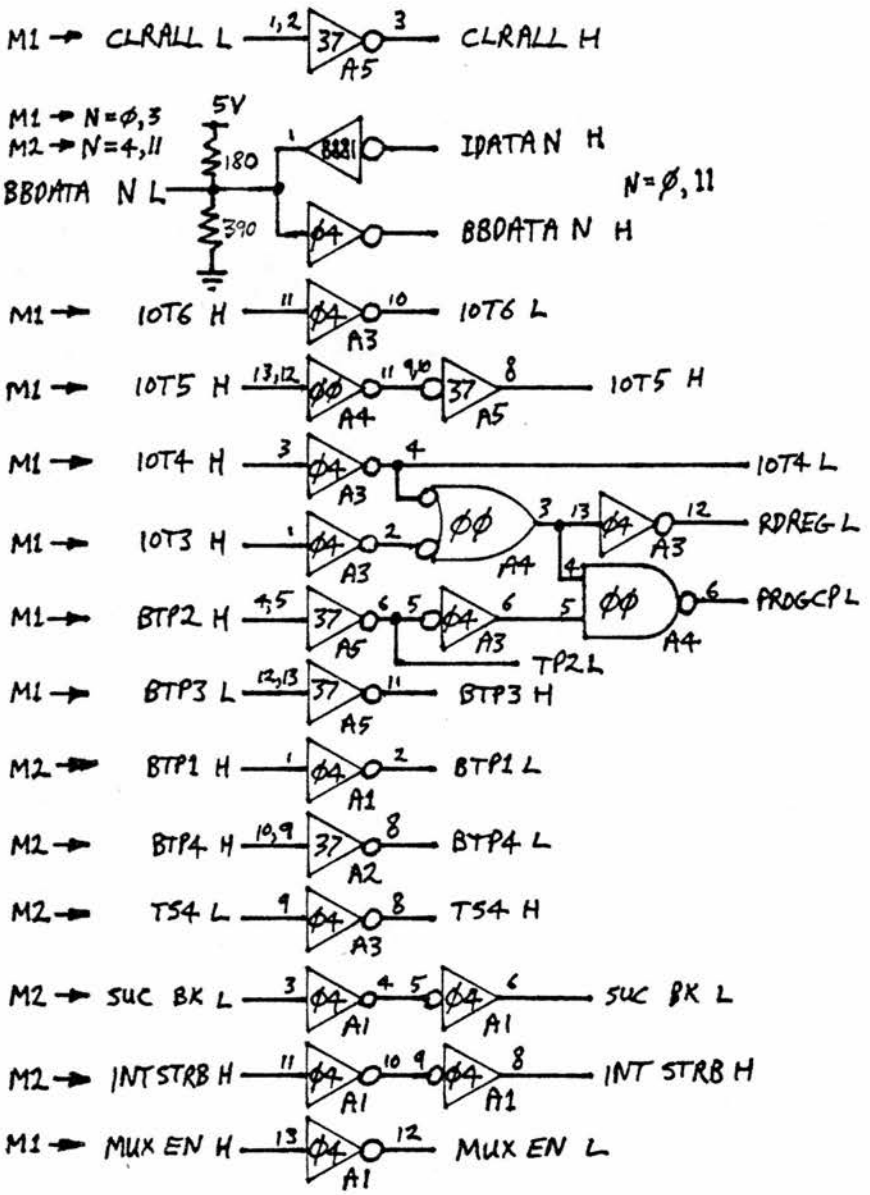

FIGURE 3.16 MISCELLANEOUS BUFFERS ON M3

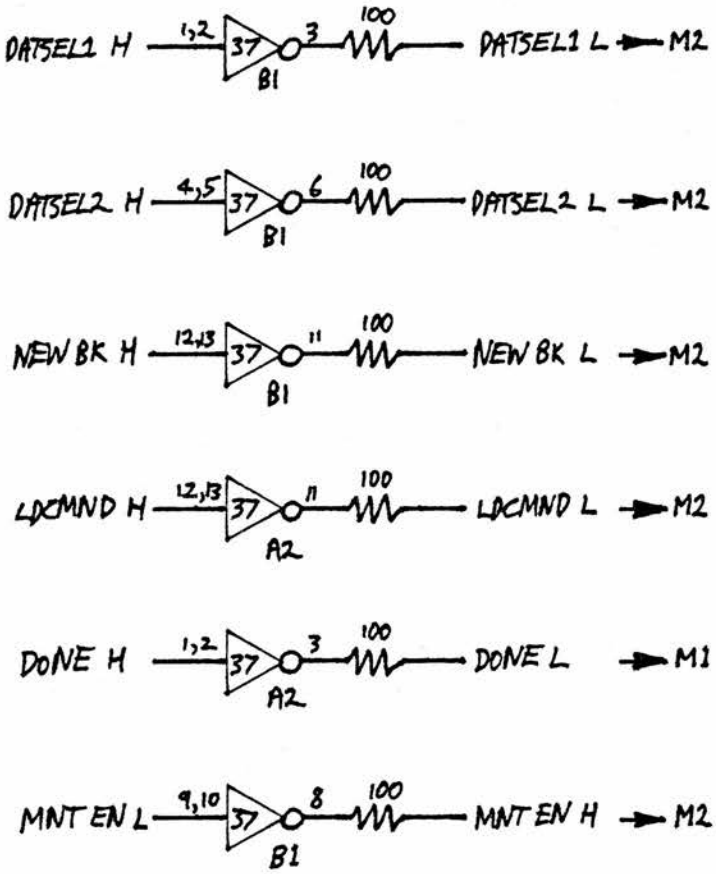

FIGURE 3.17 MISCELLANEOUS DRIVERS ON M3

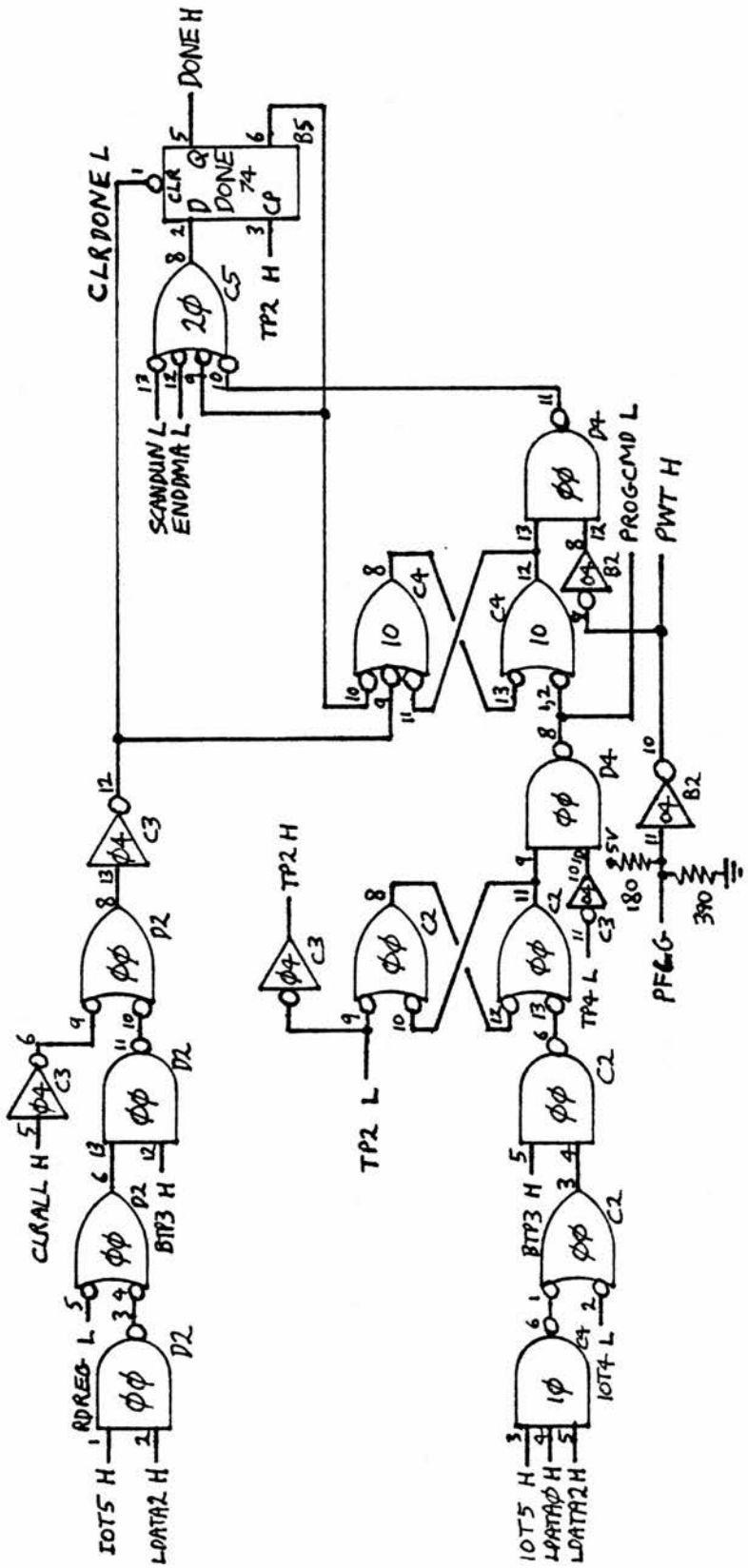

FIGURE 3.18 DONE FLAG LOGIC

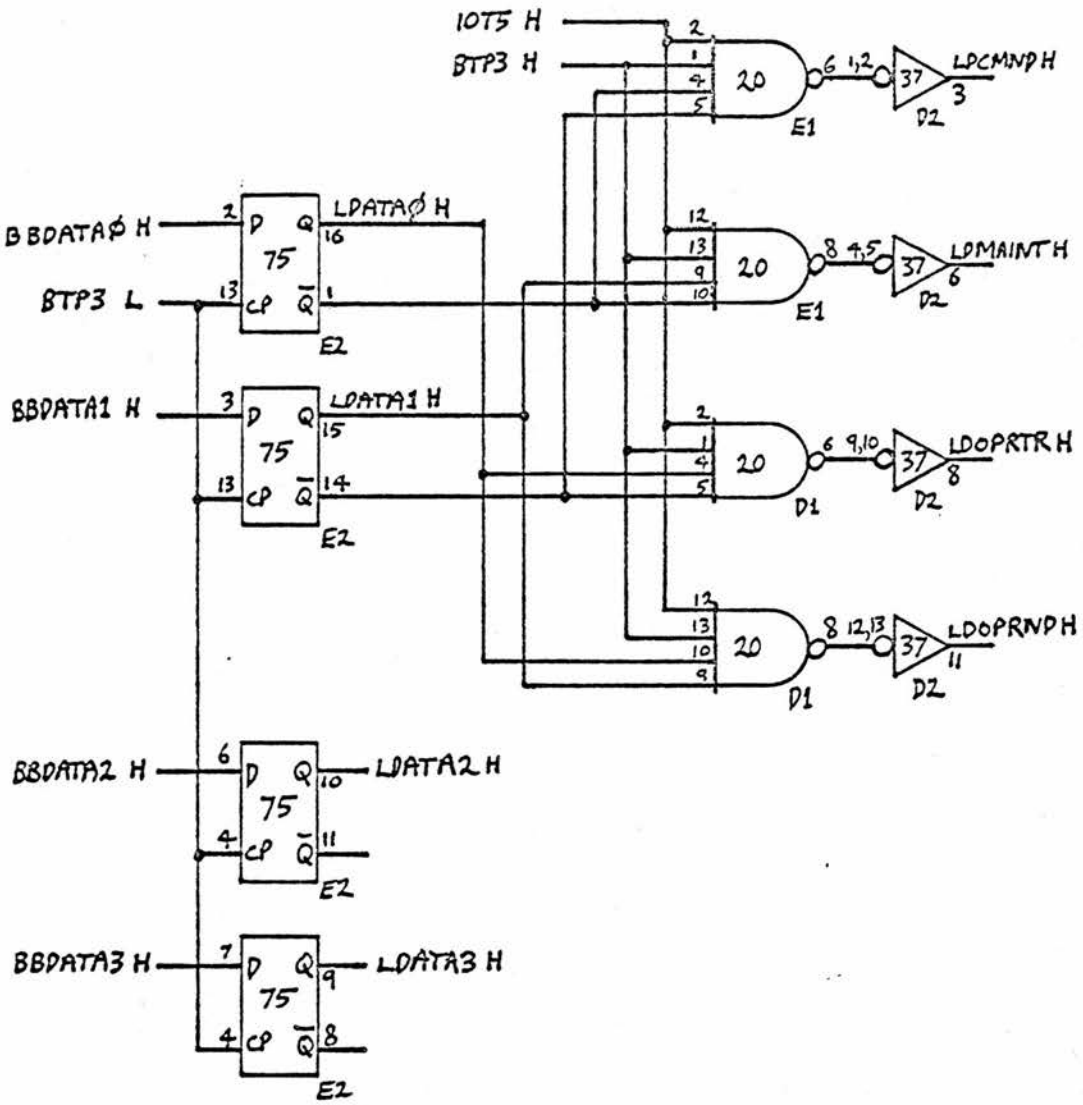

FIGURE 3.19 IOT5 DECODE LOGIC

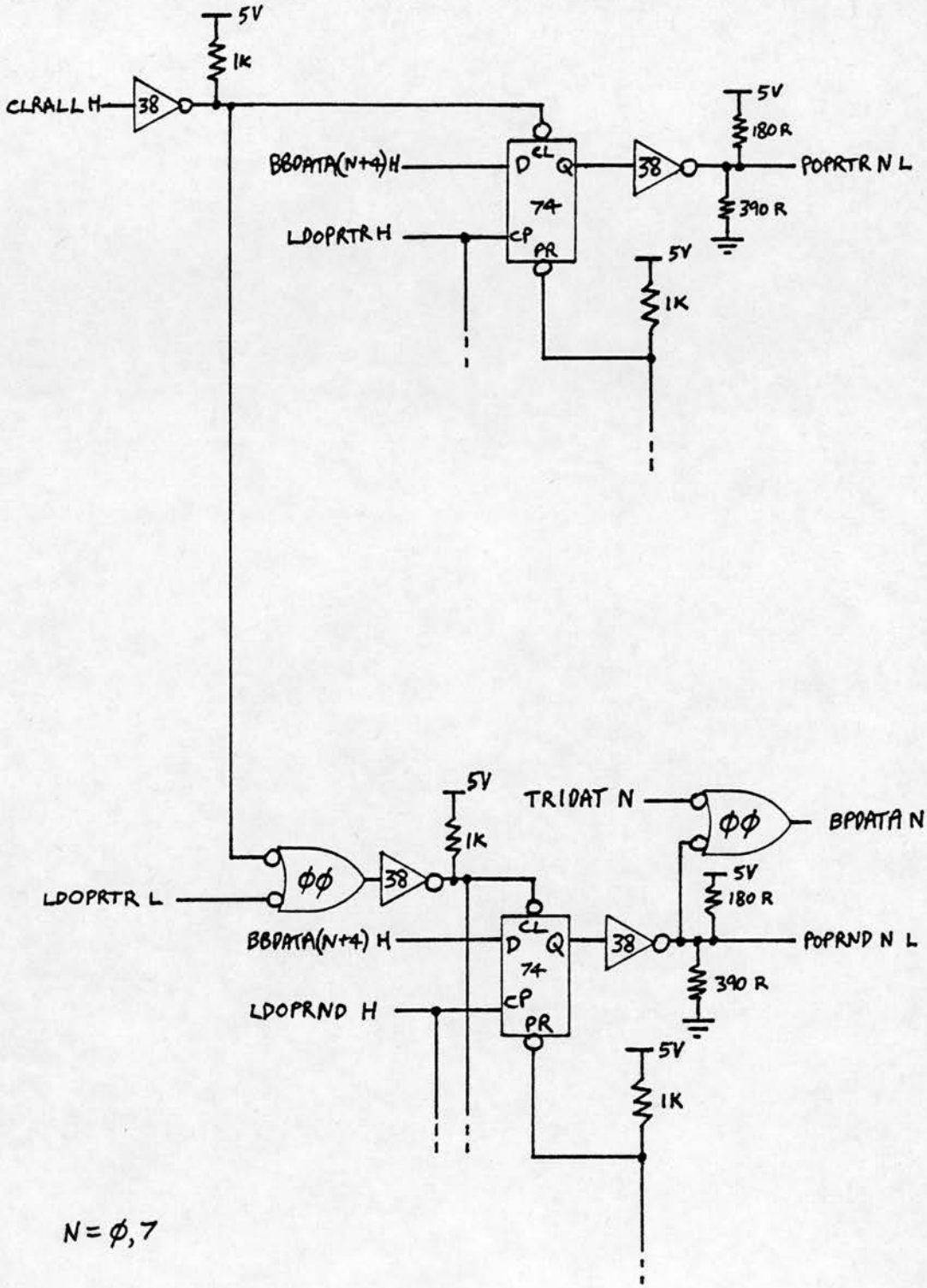

FIGURE 3.20 OPERATOR AND OPERAND LOGIC

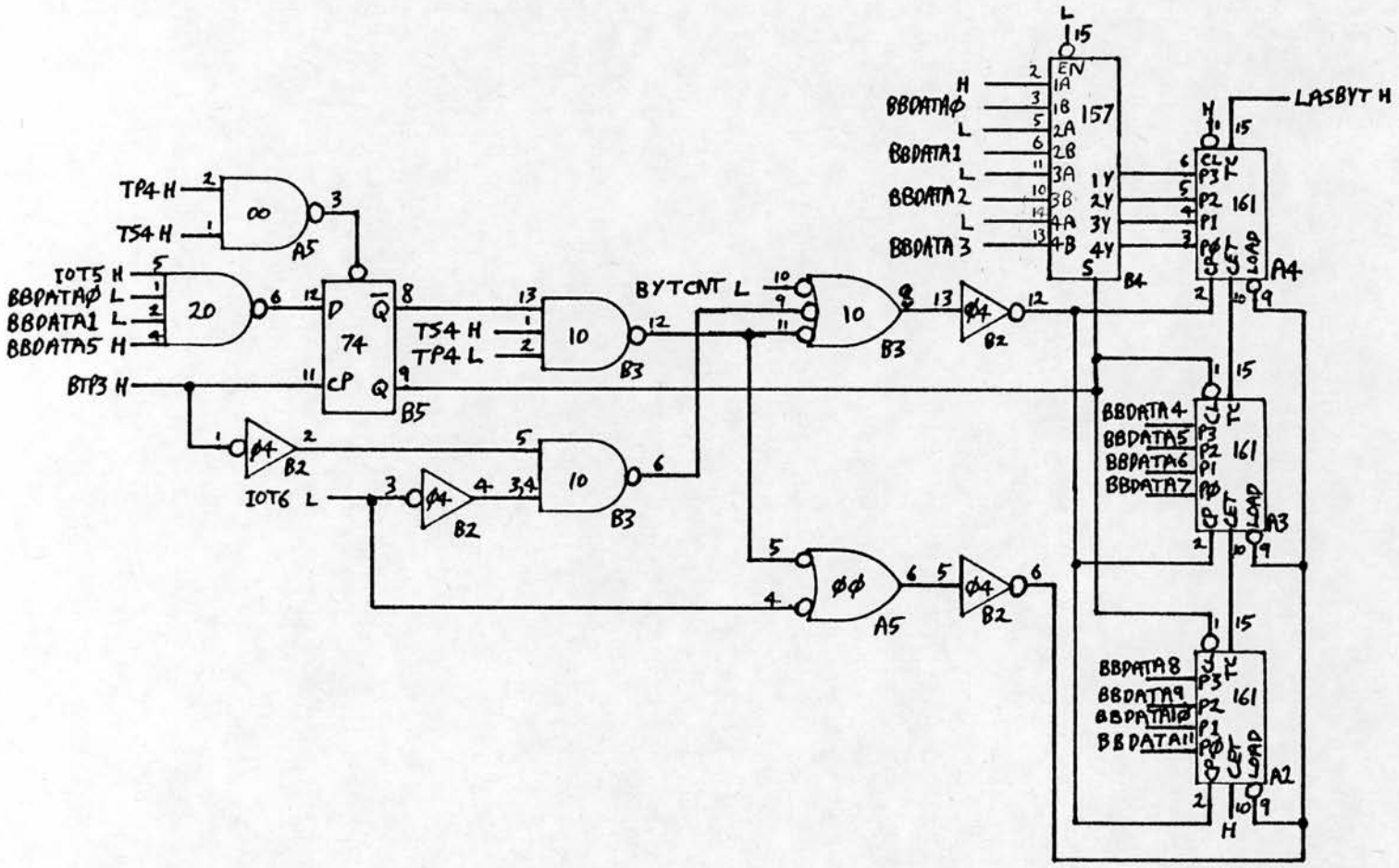

FIGURE 3.21 BYTE COUNTER LOGIC

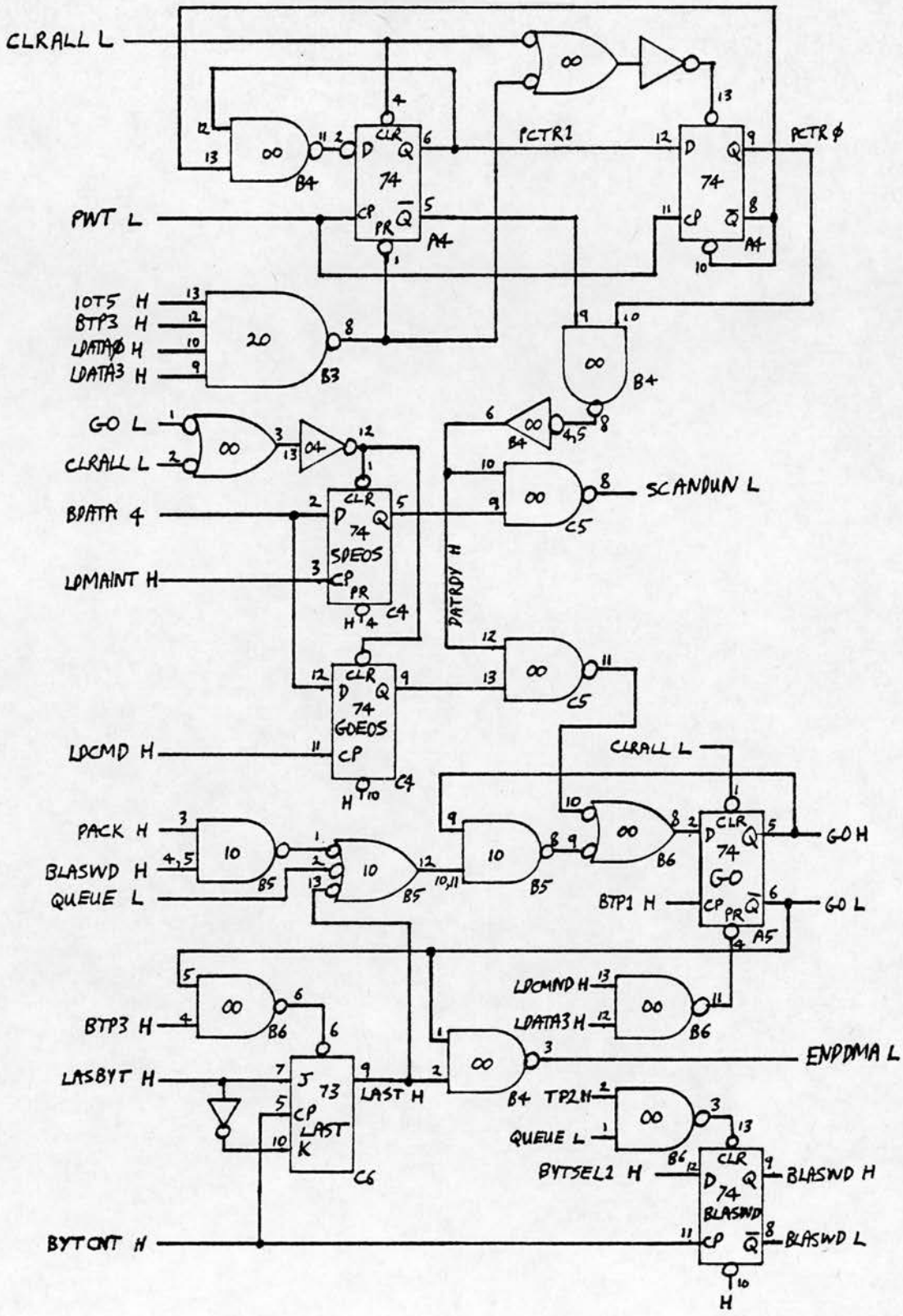

FIGURE 3.22 GO/STOP LOGIC

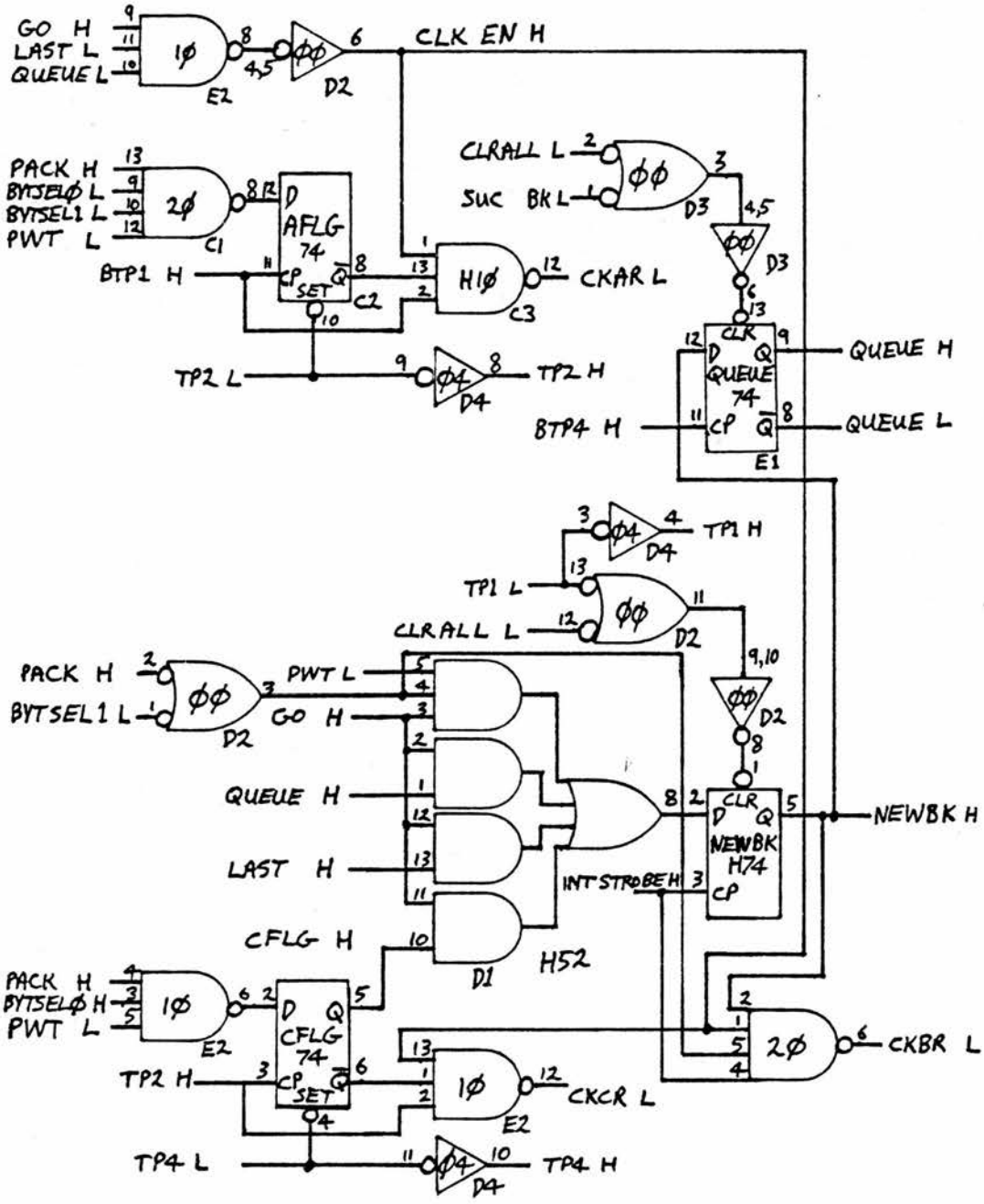

FIGURE 3.23 FLAG CONTROL OF BYTE PACKING

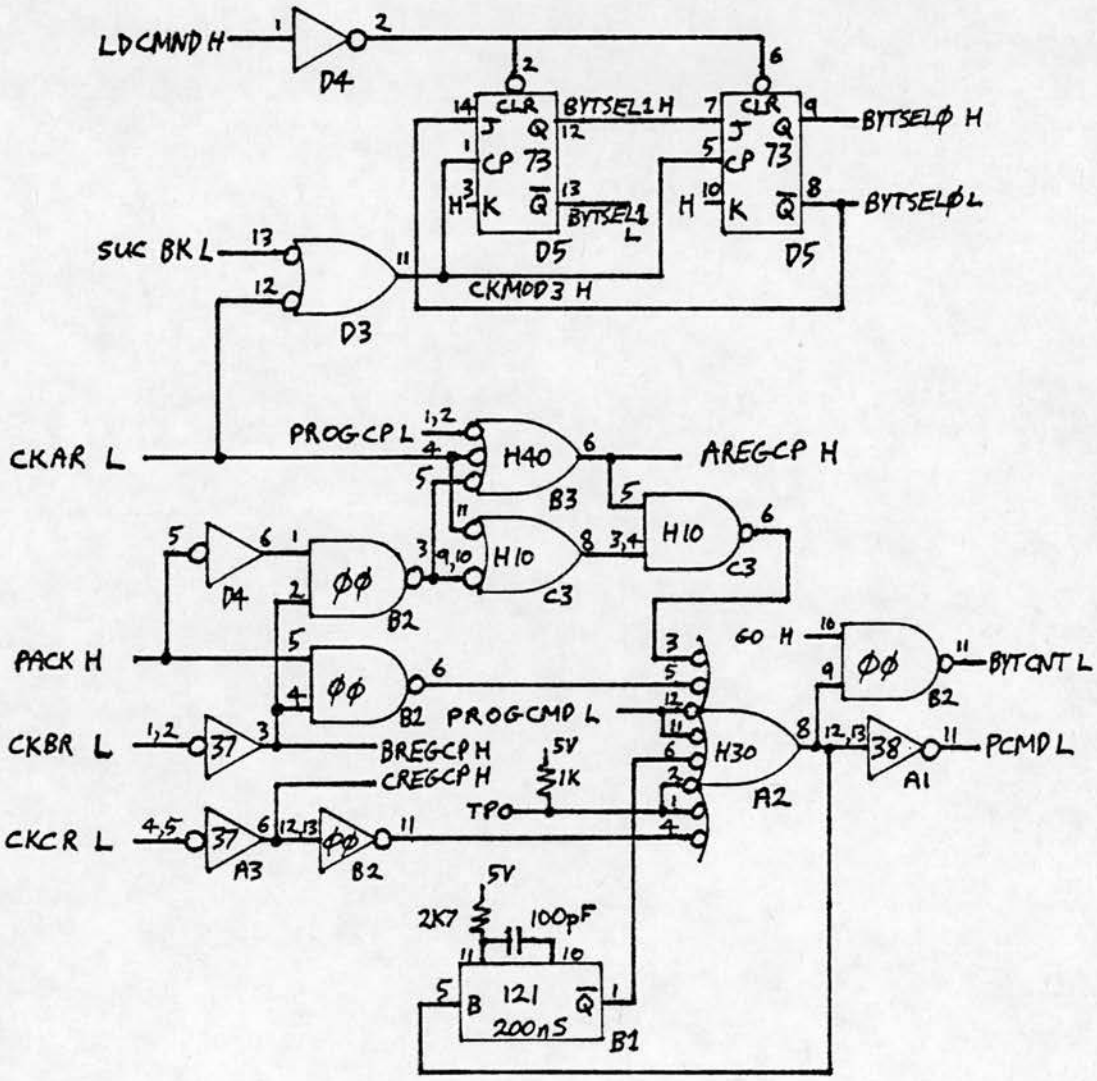

FIGURE 3.24 CMD PULSE LOGIC

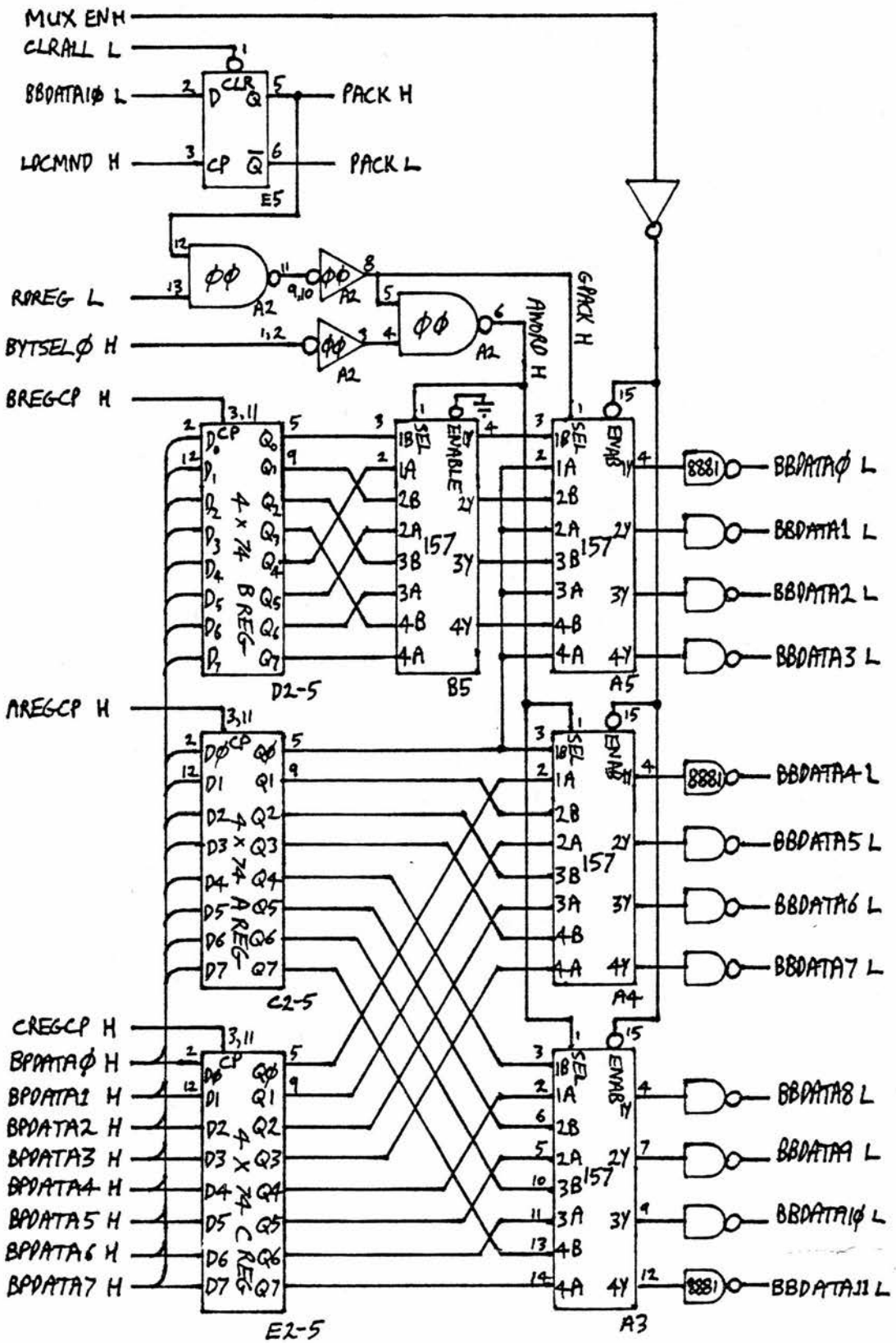

FIGURE 3.25 INPUT MULTIPLEXER LOGIC

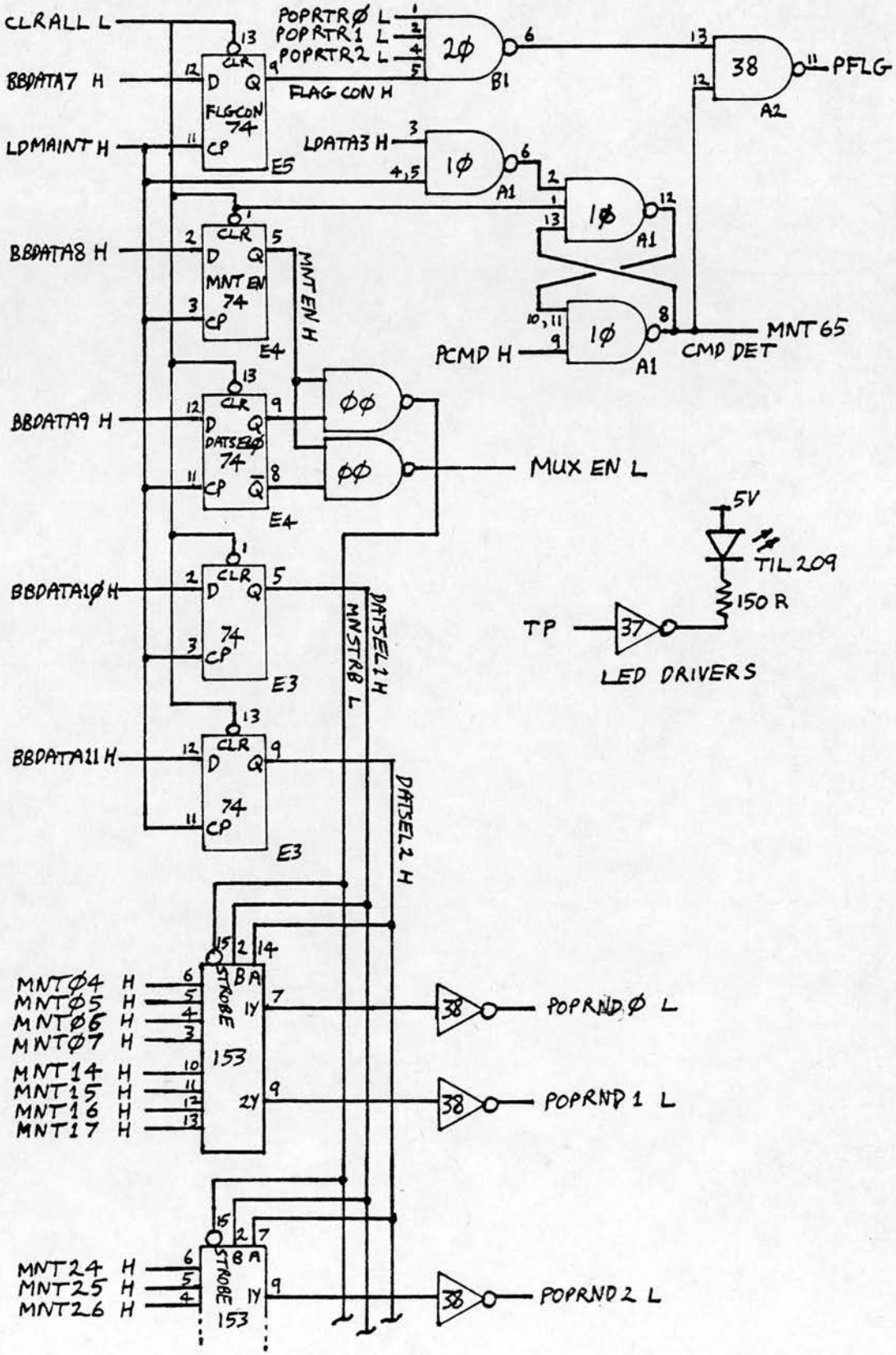

FIGURE 3.26 MAINTENANCE LOGIC ON M3

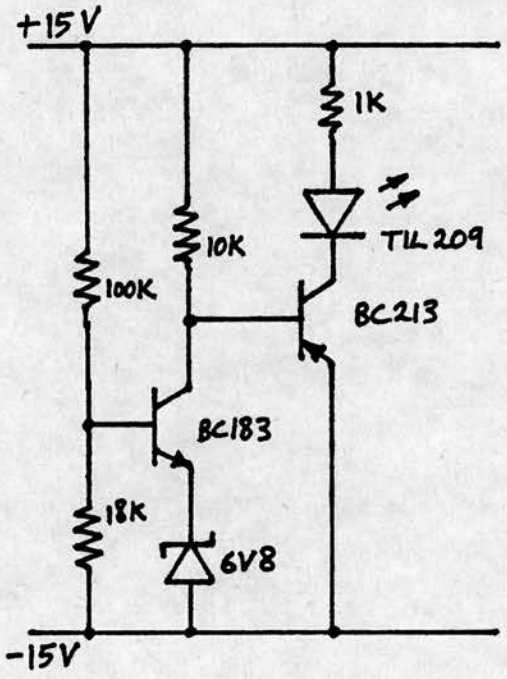

FIGURE 3.27 ± 15V POWER MONITOR

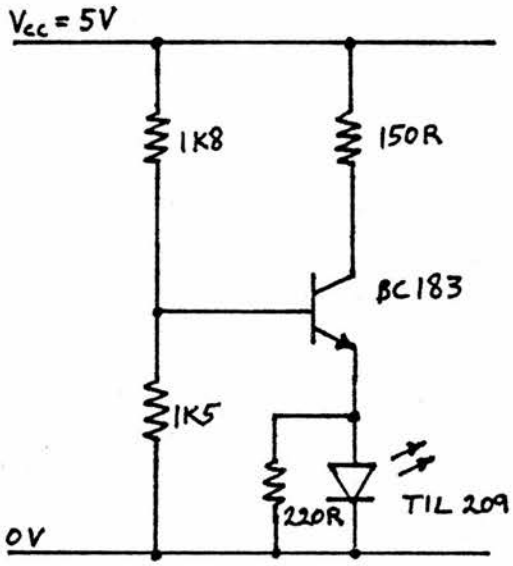

FIGURE 3.28 +5 VOLT POWER MONITOR

CHAPTER 4

MAINTENANCE PROGRAMS

4.1 INTRODUCTION

It is necessary to have some means of testing the operation of the interface. Although oscilloscopes and digital test equipment are available a better way to test the interface is to use a computer program. The computer can be programmed to perform thousands of tests per second and perform a wide variety of rigorous tests.

It is important not only to detect faults but also to locate the source of the fault. In some equipment it is sufficient to trace the fault to the board level and replace the faulty board. Since there are no replacement boards in a one-off system the program should be able to locate the fault fairly precisely.

4.2 GENERAL DESCRIPTION OF THE MAINTENANCE PROGRAMS

Two principal test programs were written. One program (TRID) tests the interface without using the transient recorder. The other program (TRDD) tests the digital control of the transient recorder. This facilitates establishing whether a fault is in the interface or the transient recorder.

The programs are modelled on maintenance programs supplied by Digital Equipment Corporation to test their equipment. This makes it easier for someone familiar with DEC maintenance programs to use TRID and TRDD.

The two test programs include a total of 125 different tests. Normally each test is performed many times (usually 4096) before

the next test is started. In many of the tests some parameter is altered on each pass of the test to make the test more rigorous. For example a test which tests the loading of the current address register will use a different address on each pass of the test.

If an error is detected an appropriate error message is printed along with the status of relevant registers and the expected contents of various registers. Tables 4.1 and 4.2 list all the possible error headings, table 4.3 gives some examples of error printouts and table 4.4 explains the abbreviations.

4.3 SWITCH REGISTER CONTROL OF PROGRAM

The program flow can be controlled by switch register settings. Table 4.5 shows the options available. Typically the program will be run initially with all switches set to zero. With the switches all set to zero each test is repeated a number of times and then the following test is started. When an error is detected an error message is printed and the program halts. After such a halt setting SW08=1 and pressing CONTINUE will result in a printout of the contents of all the interface registers.

Setting SW01=1 prevents the program from proceeding to the next test even if 4096 successful passes are made. This is particularly valuable in detecting intermittent faults. Setting SW00=1 as well as SW01=1 will cause the same test to be repeated continuously without error halts or printouts. A bell rings when an error occurs unless SW02=1. An oscilloscope may be used to display waveforms when the test is repeated in this way. SW10 and SW11 are used to control whether or not REG1 is incremented during scope

loops. REG1 is used to vary parameters on each pass of the test.

If SWOO=O and SWO5=1 the error message is printed but the error halt is inhibited. If SWO1=1 the same test is repeated continuously but if SWO1=O the next test is started when an error occurs.

Thus the various combinations of switch settings allow considerable flexibility in the control of the program.

4.4 DESIGN OF TESTS

Even the simplest operations of the interface must be tested. It is obvious to test that the Skip on Done IOT performs skips correctly. It is less obvious to check that instructions such as Load Current Address never cause skips.

The programs are designed to perform very simple tests initially, followed by more complicated tests which use previously tested logic plus a small amount of untested logic. In this way the point at which a program fails can give a fairly precise indication of where the fault lies.

The maintenance facilities built into the interface facilitate detailed testing of its operation. Without maintenance facilities the first data break would involve a large amount of untested logic.

4.5 ERROR RESISTANT PROGRAMS

The programs are designed to be resistant to errors which might prevent error messages from being printed.

4.5.1 Corruption of the program

If the interface makes data breaks to the wrong address the program

could be corrupted and prevented from printing an error message. To make the program resistant to this error the program checks the loading of the current address register and extended memory address register using the maintenance facilities, without performing the potentially hazardous data breaks. As a further protection the program resides in memory field zero and initially data breaks are performed in higher fields. The program does not use the location 0000 in field zero and the first data breaks use location 0000 in field one so even if the break wrongly occurred in field zero the program would not be corrupted. Only multiple faults would corrupt the program.

4.5.2 Lockout of CPU

If the byte counter fails to count correctly it may never reach the terminal count. This could lead to perpetual data breaks, locking out the CPU and preventing error messages. The maintenance facilities allow programmed clocking of the byte counter and the program tests the byte counter without performing data breaks. Having tested the byte counter in this way other tests using data breaks check that the correct number of breaks are performed. If CPU lockout does occur in spite of the precautions a location in memory containing the starting address of the last successful test should aid in locating the fault.

4.5.3 Change of program flow

If an IOT such as TRLCA (Load Current Address) caused a skip the change in program flow could prevent an error message from being printed. The subroutines used to issue IOT's execute the HLT (HALT) instruction if a skip occurs during an IOT that should

never cause a skip.

Although it is not possible to protect the program against all errors which might prevent error messages it can at least narrow down the number of possible causes so that they are less likely to occur and easier to locate if they do occur.

4.6 PROGRAM DETAILS

In common with other maintenance programs the transient recorder interface maintenance programs are written in assembly language. The general form of the tests is illustrated by the following extract from TRID:

```
/CHECK THAT "TRCLR" CLEARS AC
/WITH ALL COMBINATIONS IN AC
TST9,   TAD     REG1
        CLRALL          /ISSUE "TRCLR"
        DCA     ACREG
        TAD     ACREG
        SNA             /SHOULD CLEAR AC
        NERROR          /OK, 4096 LOOPS
        ERROR
        TST9
        0000
        4000
        4000
/CHECK THAT "TRSKP" DOES NOT ALTER AC
TST10,  TAD     REG1
        DCA     SACRG
        ...
        ...
```

Each test jumps to one of two subroutines depending on whether or not an error is detected. These subroutines handle the switch register options: error printouts, loop on test, etc.

The word following the jump to the error handling subroutine (ERROR) contains the starting address of the test. The following three words specify the form of the printout. Bits 6-11 of the first of these three words select the error heading (Tables 4.1 and 4.2). Bits 0-5 of the first word are a mask to select the printing of certain test parameters: initial byte count, initial current address, break address, final current address. The second word is a mask to select the printing of certain interface registers and the third word is a mask to select the printing of the expected contents of certain registers. Thus considerable control over the form of the printout is achieved. Table 4.3 gives some example error printouts obtained by running the program on a computer without an interface. Table 4.4 explains the meanings of the abbreviations used in the printouts.

The contents of the program counter are printed to allow the failing test to be found in the listing of the program. The program is well annotated to explain the purpose of the test and how it is made.

4.6.1 Software simulation of the interface

A block of locations in memory is used to store the actual contents of interface registers read by maintenance mode. Another block of memory is used as software registers to store the expected contents of interface registers. The subroutines used to perform

TABLE 4.1

Transient Recorder Interface Diagnostic (TRID) error headings.

AC REG ERROR
STATUS ERROR
COMMAND REG ERROR
DATA BREAK ERROR
DATA REG ERROR
SKIP ON DONE ERROR
SKIP ON OVERFLOW ERROR
INTERRUPT ERROR
OPERATOR REG ERROR
OPERAND REG ERROR
BYTE-PACK ERROR
GOEOS ERROR
SDEOS ERROR
CA REG ERROR
BC REG ERROR
FLAG COUNTER ERROR
MOD3 ERROR
TRLRG ERROR
ADD TO MEMORY ERROR

TABLE 4.2

Transient Recorder Digital Diagnostic (TRDD) error headings.

TRANSIENT RECORDER STATUS ERROR
INTERFACE STATUS ERROR
COMMAND REG ERROR
DATA BREAK ERROR
DATA REG ERROR
SKIP ON DONE ERROR
SKIP ON OVERFLOW ERROR
INTERRUPT ERROR
OPERATOR REG ERROR
OPERAND REG ERROR
BYTE-PACK ERROR
GOEOS ERROR
SDEOS ERROR
CA REG ERROR
BC REG ERROR
FLAG COUNTER ERROR
MOD3 ERROR
TRLRG ERROR
ADD TO MEMORY ERROR
TIMING ERROR
PRETRIGGER ERROR
TRIG DELAY ERROR
ARM DELAY ERROR
ARM ERROR
TRIGGER ERROR
DUAL TIMEBASE ERROR

TABLE 4.3

Example error printouts from diagnostic programs.

```
STATUS ERROR
PC:1641 R1:0000

INTERRUPT ERROR
PC:1677 R1:0000

BC REG ERROR
PC:1736 R1:0000
ACTUAL    BC:0014
SOFTWARE BC:0000 CM:0000

BC REG ERROR
PC:1756 R1:0000
ACTUAL    BC:0014
SOFTWARE MP:0000 BC:4000 CM:0000

DATA BREAK ERROR
PC:2043 R1:0000
ACTUAL    BC:0434 CA:0010 ST:0070
SOFTWARE MP:0002 BC:0000 CA:0000 CM:0070 ST:0206

BC REG ERROR
PC:2076 R1:7764
ACTUAL    BC:0434
SOFTWARE BC:0001 CA:0000 CM:0070

DATA REG ERROR
PC:2126 R1:0000 IB:7777 IC:0000 BA:0000
ACTUAL    DT:2421
SOFTWARE DT:0310 CM:0010

DATA REG ERROR
PC:2162 R1:0000 IB:7777 IC:0000 BA:0000
ACTUAL    DT:1020
SOFTWARE DT:7777 PI:0000 CM:0001

CA REG ERROR
PC:2222 R1:0000 IB:0000 IC:0000 FC:7370
ACTUAL    CA:0010
SOFTWARE CA:7370 CM:0010
```

TABLE 4.4 List of abbreviations used in error printouts

PC	Program counter
R1	REG1 (Test pass counter)
IB	Initial byte count
IC	Initial current address
BA	Break address
FC	Final current address
LO	Low limit of expected value; or A REG
HI	High limit of expected value; or B REG
CR	C REG
MP	Multipurpose register
DT	Break data
PD	Peripheral data
PI	Peripheral instruction
BC	Byte counter
CA	Current address
CM	Command register
ST	Status: using maintenance byte 6
TS	Transient recorder status
S2	Status: using maintenance byte 5

TABLE 4.5 Switch register settings for maintenance programs

SW00=1	Scope loop on failing test
SW01=1	Scope loop on good test
SW02=1	Inhibit bell on scope loop error
SW04=1	Stop at end of good test
SW05=1	Inhibit halt on error: go to next test if SW01=0
SW06=1	Inhibit end of pass typout
SW07=1	Halt on end of pass
SW08=1	Print contents of registers after error halt ERHLT9
SW09=1	(TRID only) Clear transient recorder program mask and reset transient recorder before starting tests
SW10=1	Increment REG1 after scope loop on failing test
SW11=1	Increment REG1 after scope loop on good test

IOT's modify the contents of the software registers.

The subroutine that issues TRCLR puts the correct preset values into the software registers. The subroutines that issue TRLBC and TRLCA put the appropriate values into the software byte counter and software current address respectively, in addition to loading registers used in error printouts giving initial conditions of series of data breaks. The subroutine that issues TRLRG decodes AC0 and AC1 to determine which software register is to be loaded. If the operator register is loaded the software operand register is cleared. If the command register is loaded and AC5=1 the software byte counter and initial byte count register are loaded with the preset value of 4000_8.

If TRLRG loads the maintenance register a word is used to store whether or not the flag trap enable was set. This word can be used by other subroutines that use the maintenance mode, so that the status of the flag trap enable bistable can be preserved if necessary. For example, if the flag trap is being used to hold the FLG line low to prevent further data breaks it is essential that the maintenance mode instructions used to read the status of registers between data breaks does not clear the flag trap enable bistable.

The software registers are used for error printouts. By loading them with the subroutines that perform the IOT's they can be kept updated without additional effort on the part of the programmer. Moreover it is a more reliable method since it is easier to test

thoroughly the simulation routines than to test a large number of isolated routines.

The software registers are also used by subroutines which read the contents of particular registers within the interface and compare them with the software register and cause a skip if they differ.

4.6.2 Miscellaneous routines

The programs determine the amount of extended memory available and test data break transfers to all extended memory locations.

The program TRDD includes a manual test routine. The contents of the switch register are loaded into the accumulator, TRLRG is issued, and after a small delay the program halts. After setting the switch register to the next word to be transferred the continue key is pressed and the sequence is repeated. This simple routine can be used to control the transient recorder, initiate data breaks, and read the contents of various interface registers using maintenance mode and the LED display.

One subroutine transfers blocks of data to the interface using TRLRG. A zero location indicates the end of the block. A single call to the subroutine can set the transient recorder program mask, specify settings of the transient recorder, arm and trigger it, and initiate a series of data breaks when the end-of-scan is detected.

4.7 TESTING THE MAINTENANCE PROGRAMS

The programs were tested as new tests were introduced. Errors were

deliberately caused by a variety of methods: grounding pull-up resistors included for that purpose, removing boards and connectors, and using incorrect control settings on the transient recorder.

A genuine fault also allowed the program to be tested. An intermittent fault was discovered and TRID enabled the fault to be quickly located to a single interconnection without the aid of additional test equipment. Each end of the wire making the suspect connection was examined and one end had not been soldered. On soldering the connection the fault was cleared.

CHAPTER 5

DATA ACQUISITION PROGRAM

5.1 INTRODUCTION

Having designed, built, and tested the transient recorder interface it is necessary to write a program to control the acquisition of data. The program was designed to be used in a clinical environment, with a minimum of interruption of the routine scanning of patients. This required that the program should be convenient to use and tolerant of user errors. The program was designed to give considerable assistance to the user who forgets what options are available.

The acquisition program TRCON (Transient Recorder Controller) allows easy keyboard control of the sampling and file storage using single-key commands (the return key is not required in acquisition mode). TRCON also allows all the acquisition parameters of the transient recorder to be specified by keyboard commands. These parameters may be stored on parameter files for future use.

The data files contain header blocks which contain the patient name and code, the name and version number of the acquisition program, the name of the parameter file, a note associated with the parameter file, the parameters used to specify the control settings of the transient recorder, and the status of the transient recorder (offscale etc.) when the data was acquired. Apart from providing information about the settings of the transient recorder, the parameters stored on the data files may be used to specify the

transient recorder settings in the future, or to create a parameter file with the same settings.

The program was written entirely in assembly language to give maximum control over the computer with minimum core requirements, and fast execution.

5.2 PROMPT FACILITY AND HELP OPTION

The program is designed to give help to the user who forgets what options are available. In response to most questions the user can type "?" to obtain a complete list of the options that are available. Questions which require a numerical answer only list all the possible replies if the number of options is small (all input gain options will be listed but not all input offsets will be listed). If a non-numerical symbol is typed when the reply should be numerical the program requests a numerical entry.

Some replies can be abbreviated and the prompting list indicates this by putting a space at the point where the option can be abbreviated. For example an extract from one option list is

RES ET
SAM PLE
STA TUS

indicating that only the first three letters of these commands are necessary.

If the prompting list given by the "?" option is insufficient the

HELP command may be used to solicit more help. The HELP command allows HELP files to be listed. The user is asked to specify the names of the files to be listed. Typing a question mark results in the listing of a HELP file containing a list of the relevant HELP file names and a brief description of their contents (Fig. 5.1).

The HELP files are standard OS/8 ASCII files so they can easily be created and modified by standard text editors.

The program is designed to check for a large variety of user errors and give helpful error messages and a chance to make amends. If the reply given by the user does not appear in the list of possible options the subroutine which searches for a match will type an error message and ask for another attempt. Typing a question mark causes the same subroutine to list all possible options.

5.3 FILE COMMANDS

Input and output files are named using the MAKE command. This calls the OS/8 command decoder, allowing the user to specify input and output files using a standard OS/8 file specification line, e.g.

```
COMMAND: MAKE
*B:LIV27<TO2
```

The output file is a data file called LIV27.DT on device B: and the input file is called TO2.PR on the system device. Data files

```
TRCLST.HL   D.C.M.   17 AUGUST 1977

HELP INFORMATION.
-----------------

THE FOLLOWING LIST DESCRIBES EACH HELP
FILE. TYPE THE NAMES OF THE FILES YOU
WOULD LIKE TO BE LISTED.
THE FILE NAMES (UP TO FIVE) SHOULD
BE SEPARATED BY COMMAS.

TRCCMD - COMMAND MODE
TRCCOP - COMMAND OPTIONS
TRCDM  - CREATING DATA FILES
TRCERR - ERROR MESSAGES
TRCGEN - GENERAL INFORMATION ON PROGRAM
TRCHLP - MAKING HELP FILES
TRCKPR - KEYBOARD ENTRY OF PARAMETERS
TRCLST - (OR "?") PRINT THIS PROMPT FILE
TRCMAK - THE MAKE COMMAND
TRCAC  - ACQUISITION MODE OPTIONS
TRCSUG - SUGGESTIONS AND COMPLAINTS
TRCUP  - USING PARAMETER FILES

FOR MORE COMPLETE INFORMATION REFER TO
THE DOCUMENT ON HOW TO USE THE PROGRAM.
```

FIGURE 5.1 LIST OF TRCON HELP FILES

are given the default extension "DT" and parameter files are given the default extension "PR" when they are created. Input files are assumed to have the default extension "PR".

If either the input file name or output file name are omitted that file will retain the old name (if any).

When a data file is named the program asks for the patient name and code for entry onto the header blocks. When a parameter file is made the program asks for a note which is stored on the parameter file. This note is printed when the parameter file is recalled, and is also stored on the header blocks of data files. The patient name, code and note etc. are converted into a six-bit ASCII code which can be read and printed by FORTRAN programs.

If the file specification line includes a number between square brackets following an output file name the smallest space large enough to hold a file of the specified length will be used. This allows the user to optimise file storage.

The file specification line may include certain options. Single characters preceded by the slash character can select the following options:

Option	Meaning
/D	Type output file directory information
/H	Type output file header text
/O	Write parameter file immediately
/P	Output file is parameter file

/T Type out Transient Recorder Control Block (TRCB). The TRCB contains the settings of the transient recorder controls which are under digital control

If the output file is a parameter file and the /O option is not selected the file may be written with the PSAV command. If an input file is specified it will be read immediately and it can be read again using the PREAD command.

The IDENTIFY (or IDEN) command may be used to alter the patient name or code.

The storage of data on the data file is described later in section 5.12.

The tentative output file can be deleted using the ABORT command. The ERASE command keeps the output file open but subsequent write operations start at the beginning of the file again.

The EXIT command makes the output file a permanent file. The MAKE command may then be used to specify a new output file. The QUIT and BYE commands make the output file permanent before returning to the OS/8 monitor.

Closing an output file with zero length will delete the file from the directory. The combination of MAKE EXIT will delete a specified file from the directory. A single delete command was not included as a safeguard against accidental deletions.

5.4 PRINTING COMMANDS

The TRCB command causes the Transient Recorder Control Block (TRCB) to be printed. The TRCB is used to specify to the transient recorder which control groups should be under digital control and what control settings should be used for these groups.

The STATUS (or STA) command causes the status of the transient recorder to be printed (READY FOR ARM, READY FOR TRIG, RECORDING, DATA READY, OFF A+, OFF A-, OFF B+, OFF B-, NULL).

The DIR command prints the directory information about the output file:

```
COMMAND: DIR

TESDIR.DT-DATA 0234   14/70
   a        b    c     d  e
```

a) File name and extension

b) File type (PARA or DATA)

c) Starting block number in octal

d) Length of file so far (decimal)

e) Total space for file in blocks (decimal)

The same information is obtained with the /D option in the file specification line or with the "D" option in acquisition mode.

The HEAD command can be used to type out the header text that is

stored on the output file. The text has the following format:

TRCON	Acquisition program name
3BV	Version
CRBO7 .DT-DATA	Output file name and type
SMITH JAMES	Patient name
WGH/LIV/23	Patient code
TRCON	Name of program that generated input file
3BV	Version of input file generation program
TO5 .PR-PARA	Input file name and type
CA UP SI .O2 MIC	Input file note

The four letters following the hyphen indicate the type of input file and output file. The three possible types are DATA for a data file, PARA for a parameter file, and MOD if the parameters have been modified since the input was read.

5.5 KEYBOARD CONTROL OF TRANSIENT RECORDER SETTINGS

All the transient recorder settings which affect the acquisition of data can be specified by keyboard commands. Some of the controls may be under digital control and others can be set by the transient recorder front panel controls. To establish which controls are under digital control and which are under manual control the controls are divided into groups, and a bit is set in the program mask of the transient recorder if that group is under digital control. It is not possible to have some controls within one group under digital control and others within the same group under manual control.

Separate commands are used to specify the parameters for the

various groups:

PTRI Program trigger group

PARM Program arm group

PCB Program channel B

PCA Program channel A

PORT Program output mode, record mode, and timebase group

The PORT command must be used initially to program the output mode, record mode, and timebase group. Having used the PORT command the subgroups may be modified independently using the following commands:

PMTB Program main timebase

PATB Program alternate timebase

POM Program output mode

PRM Program record mode

The PALL command can be used to program all groups. Figure 5.2 shows a copy of the printout obtained whilst entering the parameters.

The program asks questions to obtain the parameters. The answers are normally closely based on the legends on the transient recorder front panel to simplify remembering what options are available. The "?" option gives a list of the options if the user does forget.

If the user wishes to leave a parameter unaltered the "=" key can

```
.R TRCON

TRCON  V3BN
FOR HELP TYPE HELP
COMMAND: PALL
IN OM,RM,TB (Y/N) ? Y
MAIN TIMEBASE (Y/N) ? Y
SOURCE: INTERNAL
UNIT: MICRO SEC
RANGE: .Ø2
ALT  TIMEBASE (Y/N) ? Y
SOURCE: INT
UNIT: MIC
RANGE: .Ø1
OUTPUT MODE (Y/N) ? Y
OUTPUT MODE: AUTO
REC MODE (Y/N) ? Y
START: DA
SWITCH TB: T
STOP: DT
A CHAN IN (Y/N) ? Y
MODE: INPUT
+INP COUPLING: DC
-INP COUPLING: DC
RANGE: 5.
OFFSET: Ø
B CHAN IN (Y/N) ? Y
MODE: OFF
ARM GROUP (Y/N) ? Y
DELAY: .2
MODE: INPUT
LEVEL: .99
SOURCE: EXT
SLOPE: -
COUPLING: DC
TRIG GROUP (Y/N) ? Y
DELAY: .Ø5
MODE: INPUT
LEVEL: .1
SOURCE: A
SLOPE: +
COUPLING: DC
```

FIGURE 5.2 KEYBOARD ENTRY OF ACQUISITION PARAMETERS

be pressed provided the parameter was previously under ditital control. This makes it easy to change one parameter within a group without having to re-enter the other parameters.

The questions asked may depend on what parameters have been selected previously. For example, if the AUTO arm mode has been selected the program does not ask for arm level etc.

The keyboard entry of record mode parameters does not follow the transient recorder front panel legends because more options are available when the transient recorder is under digital control. There are two record mode buttons which allow a total of four options (normal or pretrigger, with dual timebase on or off). When the record mode is under digital control the user can specify which events are to start record, switch timebase, and stop record:

Question	Options	Meaning
START:	=	Same as before
	A	Arm
	DA	Delayed arm
	T	Trigger
	DT	Delayed trigger
SWITCH TB:	=	Same as before
	N	No switch
	DA	Delayed arm
	T	Trigger
	DT	Delayed Trigger

STOP:	=	Same as before
	EOS	End of scan
	N	NOP: will not stop!
	T	Trigger
	DT	Delayed trigger

Not all combinations of these options will make sense; selecting a starting event which occurs after the stopping event for example.

The acquisition parameters specified by the keyboard can be stored on parameter files. The parameters may also be stored temporarily in one of two memory buffers using command options XPAR1 and XPAR2. The parameters stored with the XPAR1 and XPAR2 commands may be recalled with the commands YPAR1 and YPAR2 respectively. These facilities make it easy to make some temporary alterations to the parameters and then change the parameters back to the original state.

The MANUAL (or MANU) command puts the transient recorder under temporary manual control. The program asks whether to return to digital control. An answer of "Y" will return the transient recorder to the previously stored settings. An answer of "N" keeps the transient recorder under manual control until the IMPLEMENT (or IMP) command is given to implement the stored parameters, returning the transient recorder to digital control.

The CLPAR command clears the parameters stored in the TRCB and

returns the transient recorder to manual control.

The keyboard commands used to specify the acquisition parameters of the transient recorder may be used to modify the parameters recalled from a parameter file. If this is done the header text will be changed, appending the parameter file name with "MOD" instead of "PARA" to warn users of the data file. The modified TRCB is also stored in the header blocks of the data file so the actual settings may be determined.

5.6 CONTROL COMMANDS

Apart from setting the acquisition parameters it is also possible to give keyboard commands to give control signals to the transient recorder:

Command	Effect
ARM	Arms the TR
TRIG	Triggers the TR
RESET	Resets the TR
SWTB	Switches to the alternate timebase.

These control functions are operational whether or not the transient recorder has any of its control settings under digital control.

It is not normally necessary to use these commands to acquire data but they are useful in some circumstances. The RESET command is useful for error recovery, and the other commands are useful for testing the program's control of the transient recorder.

5.7 HOLD AND BURST COMMANDS

When in the monitor mode the program pauses between taking samples. The length of the pause (or hold-time) can be set with the HOLD command.

When in the acquisition mode a burst of samples may be stored on the output file. The BURST command can be used to specify the number of samples in a burst. (Here a "sample" refers to the full contents of the transient recorder buffer memory).

5.8 ENTRY OF ACQUISITION MODE

The acquisition mode of the program can be entered from the command mode with one of two commands:

Command	Meaning
SAMPLE (or SAM)	Enter the acquisition mode and take one sample
MONITOR (or MON)	Enter the acquisition mode and monitor the signal by taking samples repeatedly.

The acquisition mode is described in section 5.12.

5.9 COMMAND STRINGS

Several commands may be typed on one line and they will be executed sequentially. Command strings may contain up to 65 characters. Text typed between quotation marks will be printed when that part of the command line is reached. Including a slash character in the command line causes a carriage return and line

feed. All characters following the COM command are treated as a comment and are ignored. Errors in the command line terminate execution of the command line, cause error messages, and return the program to the command mode ready to accept a new command line.

The last command line will be repeated if an equals sign is typed in response to "COMMAND: ".

5.10 USER DEFINED COMMANDS

A string of commands may be stored in memory using the XCOM1 or XCOM2 commands. The YCOM1 and YCOM2 commands execute the command strings that followed the XCOM1 and XCOM2 commands respectively. YCOM1 and YCOM2 may appear several times in a command string. Nested definitions are allowed (i.e. YCOM1 may be included in the command line stored with the XCOM2 command or YCOM2 may be included in the command line stored with the XCOM1 command). Circular definitions are not allowed and cause an error message when the command is executed. For example, YCOM1 must not include itself in its definition either directly or indirectly (through a nested definition).

5.11 THE TEST COMMAND

The TEST command is included to aid program testing during development. Because of its specialised nature the TEST option requires the user to supply a password before proceeding with the test. On completing the test the user is asked whether the test should be

repeated. The actual test is modified to test code recently added to the program. By having a TEST command the test can easily be executed at any time, and by reserving one area of memory for the test routines it becomes easy to add, modify, or remove tests when necessary. Tests which are randomly distributed throughout the program are much more awkward to modify with an increased danger of causing errors when modifying tests.

By making it easy to test the program as it is developed its reliability is increased and debugging time is reduced. This is particularly important in an assembly language program since they are harder to debug than high-level language programs.

Conditional assembly pseudo-operators are used to allow the inclusion or exclusion of the TEST option to be determined by a single character in the source code.

5.12 THE ACQUISITION MODE

The acquisition mode of the program performs the primary function of the program. It allows single-key commands to control the sampling of signals and their storage on files. For ease of use the return key need not be pressed: the command is executed immediately the key is pressed. In the following description the word "sample" is a collective term referring to the entire contents of the transient recorder buffer memory rather than individual data values. The options available are:

Key	Meaning
B	Burst. File several samples in a burst
C	Comment. Treat rest of line as a comment
D	Directory. Print output file directory information
F	File. Store current sample on output file, then take another sample
H	Hold. Ask for hold time
M	Monitor. Take samples continuously, without filing
N	Number. Ask for number of samples in a burst
R	Return. Return to command mode
S	Sample. Take sample, without filing
X	Examine. Enter single-sample mode
RETURN KEY	Start new line
CONTROL/C	Return to OS/8 keyboard monitor
CONTROL/R	Immediate return to command mode
CONTROL/T	Toggle echo-control switch. (Used to suppress echoing of characters on teletype).
?	Give prompting list of available options.

The transient recorder is armed by the computer. The transient recorder must then be triggered by some event to synchronise it with the ultrasound scanner (section 5.13). When the record period is over the data is transferred into the computer memory using data breaks.

The acquisition mode is divided into two main modes: the monitor mode and the single-sample mode. The monitor mode allows the input signal to be monitored continuously. In single-sample mode a key has to be pressed to initiate further sampling.

When in monitor mode there is a pause after each sample is taken. The current sample can be stored on the output file by pressing the "F" key. A series of samples are stored on the output file by pressing the "B" key. Another sample can be taken before the end of the hold time by pressing the "S" key. If no key is pressed before the end of the hold time another sample is taken and the cycle repeats itself. Pressing the "X" key prevents another sample from being taken and the single-sample mode is entered.

In single-sample mode the current sample can be examined on the monitor oscilloscope. Pressing the "F" key causes the current sample to be stored on the output file and then another sample is taken. Pressing the "M" key causes a return to the monitor mode.

In either mode the "D" key can be pressed to obtain directory information about the output file, allowing the user to determine how many blocks have been used and how much room remains.

The "C" option is very useful for adding comments to the listing to describe any relevant details about the samples stored on the output file.

5.13 TRIGGERING THE TRANSIENT RECORDER

The program arms the transient recorder but it is left to the user to trigger the transient recorder in some way. One convenient triggering signal that was normally used was derived from the proximal caliper pulse in the EMISONIC 4201 B-scanner. The caliper pips can be made visible on the A-scan display or on the B-scan image. A control on the B-scanner can control the position of these pips. Thus if one of them is used to start the sampling it is easy to select from what depth the samples are taken.

By making the selection of sampling depth so convenient the data can be acquired with a minimum of interruption of the routine scanning.

The transient recorder may also be triggered by the transmitter trigger pulse. The depth can then be determined by the trigger delay period. Whilst this can be used to obtain an accurately known delay it is not as convenient as using the proximal caliper pulse if a variable delay is required.

5.14 CHOICE OF PROGRAMMING LANGUAGE

The choice lay between using a high-level language (FORTRAN IV) or a low level language (PAL). Clearly at least some parts of the program would have to be written in assembly language to control the transient recorder: there are no statements in FORTRAN that can be used to control a transient recorder. In addition, the translation of keyboard commands into control words, used to specify the

acquisition parameters of the transient recorder, requires manipulation of individual bits and FORTRAN IV does not provide such a facility; an assembly language subroutine would be required to do this.

The main disadvantage of using FORTRAN IV for the mainline program is that it takes up too much room in memory. The computer only had 8k of core. The FORTRAN run-time system itself uses over 4k of core. Since the packed data requires over 1.3k of memory there is not much room left for the program itself. Furthermore the output of the compiler uses up more core than a well-written assembly language program. Variables use three 12-bit words instead of one word in assembly language. Although it is possible to use overlays to increase the size of the program that can be run, the PDP8 code assembly language subroutines could not be in overlays. Thus it would be very difficult to include all the desired facilities in the program if it was written in FORTRAN.

Another disadvantage of FORTRAN is that the program takes longer to execute than an equivalent assembly language version. This is especially true if the computer does not have a hardware floating-point processor. In that case floating-point instructions have to be interpreted by software. During execution of a FORTRAN program data which is already in memory and has to be transferred to an output file is first transferred to a buffer area in memory before being transferred to the output file. Thus transfers to files take longer than would be required by an assembly language program and it is

desirable that transfers should be as fast as possible. (The FORTRAN run-time system uses a buffer area because the variables to be transferred may not be contiguous in core in the order specified by the WRITE statement).

Because assembly language can make more efficient use of memory and execute faster than FORTRAN IV it was decided to write the acquisition program entirely in assembly language. Some further advantages of assembly language are discussed in the following section.

5.15 ADVANTAGES OF ASSEMBLY LANGUAGE PROGRAMMING

Assembly language programs are translated directly into machine language instructions. Usually there is a one-to-one relation between assembly language commands and machine instructions giving the assembly language programmer almost complete control over the computer.

Standard OS/8 FORTRAN IV programs require all input and output files to be named before the program starts running, and only one new output file per device can be created. With the flexibility of assembly language TRCON allows files to be named during the running of the program, and any number of output files can be created (consecutively). TRCON can even delete previously existing files.

If a non-numerical character is typed when a numerical reply is required the FORTRAN IV run-time system prints an error message and

aborts the program. This could be rather serious since tentative files that have not yet been made permanent may be lost. That response may be satisfactory if the program is being run in batch mode but it is not satisfactory in an interactive programming environment; especially if routine clinical work is being interrupted. TRCON prints an error message and asks for the number again.

Keyboard entry to a FORTRAN program must be terminated with the return key before any response is made. In acquisition mode TRCON allows flexible control of acquisition by executing single-key commands with no need to press the return key. In all other modes the return key must be pressed.

The poor character-string manipulating facilities of FORTRAN IV would make it difficult to implement the command string and user-defined command features of TRCON.

Furthermore, FORTRAN IV does not enable the user to determine the amount of space available for the output file, which can affect decisions on how to make best use of the available space.

5.16 DISADVANTAGES OF ASSEMBLY LANGUAGE PROGRAMMING

It is much harder to program in assembly language than in a high-level language such as FORTRAN. Usually several lines of assembly language are required to perform the same task as a single line of a high-level language. A detailed knowledge of the computer and its instruction set is required to program in assembly language. For example, the addressing modes of the computer must be understood.

An assembly language program must include its own input and output code conversion routines, and must include its own device handlers or use the operating system handlers to control input and output. Code conversion routines include numerical conversions between decimal ASCII characters and binary numbers with correct handling of leading spaces and zeros. Code conversion between five different ASCII codes were required. (Although the differences between some of the codes were slight special provision for the differences had to be made).

To control file-structured devices the assembly language programmer must learn how to use the OS/8 USR (User Service Routine) to load the device handlers and modify device directories. The use of USR has its own problems that do not concern the FORTRAN programmer since the FORTRAN system automatically loads handlers and interacts with device directories. Problems associated with USR are discussed in section 5.17.

The greater freedom of assembly language over high-level language allows more types of programming errors to be made. If part of an assembly language program overflows past a page boundary or field boundary the program may not run as intended: the FORTRAN system takes care of memory management. Assembly language programs can execute data as though they were instructions which can be disastrous if not intended.

The extra difficulties of assembly language programming make errors more easy to make and correspondingly more difficult to find.

Since each line of program accomplishes less than a high-level statement, on reading the program it is less obvious what the purpose of the code is. This in turn makes it harder to debug or modify. Thus the program must be well documented to explain the purpose of each section.

Nevertheless the advantages of using assembly language (principally the more efficient use of memory) were sufficient to make it the language chosen for the writing of the acquisition program.

5.17 PROBLEMS USING THE USER SERVICE ROUTINE

The User Service Routine (or USR) is a collection of subroutines which perform the operations of loading device handlers, reading and modifying device directories, reading and writing files, and calling the Command Decoder. The USR is used by many system programs and may also be called by assembly language programs. One of the arguments of a call to USR specifies which USR operation is to be performed.

A typical sequence of USR calls to create a new file is:

1. Call Command Decoder. The Command Decoder accepts input from the teletype giving a list of input and output file specifications. The Command Decoder reads the device directories to find the locations of input files and sets up a table in memory giving details of the file specifications.
2. Make a FETCH call to load an appropriate device handler.
3. Make an ENTER call to make a tentative file entry on the

directory of the output device, getting the starting block and length of the space available for the output file.

4. Perform transfers to the output device using the output device handler, keeping track of the number of blocks written and ensuring that the available file space is not exceeded.

5. Make a CLOSE call to make the file entry in the directory permanent with the length calculated. Any previous permanent files of the same name are deleted from the directory.

A problem can occur using TRCON if the input file and the output file have the same name on the same device. The input file will refer to an old permanent file. The output file will be a new tentative file on another part of the storage device. No problems so far: the input file can be read and the output file can be written. However, when the output file is made permanent the input file entry will be deleted from the directory. The input file may still be read satisfactorily. But if a new output file is made on the same device it may be allocated space occupied by the input file. Writing to the output file may then corrupt the input file, and any further reading of the input file could be invalid. TRCON guards against this problem by warning the user if he attempts to read an input file that may have been corrupted in this way.

Another problem can arise if the input file and output file use the same handler. When a FETCH call to USR is made to load a device handler USR refers to the Device Handler Residency Table and only loads the handler if the handler is not already in memory. If the input file uses the same handler as the output file the handler will be loaded for the output file but will not be loaded for the input file. No problem so far: the same handler can be used for both files. But if a new output file is now made requiring a different handler a new handler will overwrite the first handler. Now if any attempt is made to read the input file errors will occur. This can be a problem even if the original input file and output file used different logical devices since single handlers can control several devices (e.g. DSK1, DSK2, etc.). This problem is overcome in TRCON by resetting the Device Handler Residency Table before making any FETCH calls to USR. This forces USR to always load the device handler. When a file is closed it may be necessary to FETCH the handler again since a RESET USR call may have deleted the handler from the Device Handler Residency Table causing an error return from the CLOSE subroutine, since the CLOSE routine would then assume that the handler was no longer in core. Since it is a disk based system the extra loading of the device handler wastes little time. In a floppy-disk based system unnecessary disk transfers should be avoided, both because floppy-disk transfers are fairly slow and because transfers wear out the disk making it less reliable.

USR is loaded into locations 10000 to 11777 and the old contents of these locations are saved on the system device. The USR can be

called in two different ways. With one method the locations are restored to their former state on completion of the USR operation. The second method keeps the USR permanently in core. Subsequent calls to USR can be made without reloading it into core and without saving the old core contents. A special USR call can then be used to restore locations 10000 to 11777 to their former state. Care must be taken that no section of program that has been overwritten with USR is executed before it is restored. Care must also be taken that no USR calls which assume that USR is already in core are made if it is not in core.

The TEST subroutine (section 5.11) was very useful for making detailed checks on the use of USR. Octal dumps of device directories allowed directory modifications to be monitored in detail.

5.18 DATA FILE FORMAT

An essential criterion for the format for the data files was that they must be readable by FORTRAN programs since the processing is performed in FORTRAN. The OS/8 FORTRAN IV Software Support Manual was consulted to determine the precise form of storage used.

Files in OS/8 are divided into blocks, each block containing 256 words. Each FORTRAN IV variable occupies 3 words. Each block can contain up to 85 variables (85 x 3=255). The final word in each block is a block sequence counter and is not available for data storage. Sequential access READ operations check the block sequence counter but direct access READ operations do not. The

TRCON data files are designed to be read by direct access READ operations and the block sequence is not modified.

Each TRCON record has one header block and six blocks of packed transient recorder data. The alphanumeric data in the header block is stored in the same packed six-bit ASCII code as in OS/8 FORTRAN IV. Each FORTRAN alphanumeric variable can store up to six characters. Dummy spaces are included so that separate entities (file names, patient name, etc.) all begin at the start of a FORTRAN variable to facilitate manipulation and printing of the information. The TRCB (Transient Recorder Control Block) is stored in binary form in the header block. A status word recording the status of the transient recorder when the data was captured is also stored in the header block.

Three 8-bit bytes of transient recorder data are packed into every two words. Because the last word in each block is not available for data storage and because it is more convenient to unpack an even number of words, only the first 254 words in each block are used. Thus 381 (=254 x 3/2) bytes are stored in each of the first five data blocks with the remaining 143 bytes stores on the sixth data block.

The use of a header block in each record allows acquisition parameters, patient name, etc. to change from one record to the next within the same file. The penalty for this extra flexibility is the greater file storage space requirements and the greater time to store each record.

A direct-access READ operation in FORTRAN is used to read the header block into one array and the packed data into another array. An assembly language subroutine called UNPK was written to unpack the data and convert it into an array of floating-point variables. The subroutine automatically skips the unused word in every 85th variable. The subroutine was written in RALF (Relocatable Assembly Language, Floating-point) and can be called from FORTRAN programs.

The subroutine must be written in relocatable code so that the absolute address can be assigned by the linking loader which combines the mainline program and the subroutine. The subroutine must follow the OS/8 FORTRAN IV conventions for transfer of program control and transfer of subroutine arguments between routines with different base addresses. This was achieved by writing and compiling a dummy FORTRAN subroutine and editing the resulting RALF code to create UNPK.

One section of UNPK was written in PDP8 code to unpack three bytes from every two words and convert them into three 12-bit signed binary words. FPP (Floating-point Processor) instructions were used to convert the 12-bit words into 36-bit floating-point variables and store them in another array. The linkage between the FPP code and PDP8 code was via the FORTRAN run-time system.

The following two lines of FORTRAN program read one record from a TRCON data file and stores the data in floating-point form in the array FORDAT:

```
READ(9'NREC)  HEADER, PAKDAT
CALL UNPK(FORDAT, PAKDAT, 2048)
```

Thus reading data in FORTRAN is easy using the subroutine UNPK.

5.19 PARAMETER FILE FORMAT

The format of the TRCON parameter files is almost identical to the format of the header blocks in the data files. The only difference is that the input file name is replaced with the parameter file name. The similarity allows data files to be used as parameter files. This is a useful facility since it enables the user to duplicate the parameters used to obtain the data file. Parameter files are only one block long. If the input file of TRCON is more than one block long the user is asked from which block to take the parameters.

5.20 THE TRANSIENT RECORDER CONTROL BLOCK (TRCB)

The TRCB is central to the keyboard control of the transient recorder. The least significant 8 bits of each word in the TRCB contain an operand which can be transferred to the transient recorder to specify control settings. If only some of the parameters are under digital control not all of the operands should be transferred to the transient recorder. If the operand should not be transferred to the transient recorder the word is set to zero. If the operand should be transferred the most significant four bits of the word are set to 1110.

The operator register in the interface is first loaded with the appropriate operator and then the corresponding word from the TRCB is loaded into the accumulator and the TRLRG IOT is issued. If the most significant 4 bits are 1110 the least significant 8 bits will be loaded into the operand register and a CMD pulse

will be issued to transfer the complete 16-bit instruction to the transient recorder. If the TRCB word was zero the TRLRG instruction will simply clear the command register and have no effect on the transient recorder or on the running of the program.

A subroutine called BITSET was written to simplify modifying the TRCB. One of the subroutine arguments specifies which word in the TRCB is to be modified and another argument is a mask word which specifies which bits in the word can be modified. The contents of the accumulator specify the new values of those bits. If the mask word is zero the TRCB word is zeroed. If the mask word is non-zero the most significant four bits in the TRCB word are set to 1110. This is valuable since an incorrect word in the TRCB could initiate a series of data breaks: using a well-tested subroutine to ensure that the control bits of the word are correct prevents this.

To indicate that the parameters have been altered the word specifying the type of input file is changed to "MOD" whenever BITSET is called. Other subroutines which can modify the TRCB make a dummy call to BITSET to change the parameter file designation. (These are the subroutines initiated by the MANUAL, CLPAR, YPAR1, and YPAR2 commands). Thus the parameter file designation is automatically updated without the programmer having to make special provision for it every time the TRCB is modified.

5.21 PROGRAM DOCUMENTATION

Good program documentation facilitates debugging and development of a program. Because an assembly language program is harder to

follow than a high-level program it is especially important that the program is well documented. TRCON contains a large number of comments to give a detailed description of the program flow. Attention is drawn to difficult points (e.g. specifying that a particular subroutine must use re-entrant code). Subroutines are preceded by text describing their purpose and the calling procedure and argument functions. The program documentation is supplemented with a manual specifying the user interface of the program.

5.22 TRCON USER MANUAL

A manual was written to describe in detail how to use TRCON. The use of each command is described and examples are given to show the sequence of commands required to set the acquisition parameters, make and read parameter files, and to control the acquisition of data. Examples of error printouts are also given. All the HELP files about TRCON are listed in the manual.

CHAPTER 6

TISSUE CHARACTERISATION

6.1 INTRODUCTION

The primary aim of the project is to distinguish between different soft tissues by analysis of ultrasonic echoes from the soft tissues. In particular it is hoped that it will be possible to distinguish between normal and abnormal tissue and to differentiate between different types of abnormality.

There are many types of interaction between ultrasound and tissue. This gives rise to the hope that analysis of the echoes can yield information about various physical characteristics of the tissues. However, the multiplicity of complex interactions makes it extremely difficult to separate the factors involved. A number of methods of extracting information from echo data work satisfactorily in ideal laboratory conditions but are quite unsuitable for characterisation of tissues in vivo.

When selecting a suitable approach to analysis of echo data I applied the following criteria:

The approach should:

1) be practical in vivo
2) be clinically useful
3) lead to greater understanding of the problems
4) form a basis for further processing methods

In addition it is beneficial if the greater understanding could be applied to improve the design of B-scanner equipment.

6.2 PHYSICAL FACTORS AFFECTING ULTRASOUND IN SOFT TISSUES

A detailed discussion of the physics of the interactions between ultrasound and soft tissues could fill an entire thesis. The purpose of this section is merely to list some of the factors that affect tissue characterisation methods. Much more detailed accounts may be found in the literature (Chivers, 1973; Hussey, 1975; Nicholas, 1975; Wells, 1977).

The plane disc transducer produces a complex field distribution (Wells, 1977). The pulse shape depends on both the axial distance and the radial distance. Diagnostic ultrasound often uses the part of the beam that is in the transition region from Fresnel diffraction to Fraunhoffer diffraction which is particularly difficult to analyse. The pulse shape also depends on the transducer construction: backing material, quarter wave-plate, lens, parallel electrical impedance, can all alter the pulse shape (Atkinson, 1974). The shape of the excitation pulse from the transmitter and the characteristics of the receiver will also modify the echo signals.

Attenuation in human tissue is large: a typical liver scan using a 3.5 MHz transducer will require a swept gain of approximately 4.6 dB/cm (Wells, 1977). The attenuation is frequency dependent so this adds a further dependence of pulse shape on depth. Attenuation is due to a number of factors: geometrical factors due to the changing beam shape (and echoes from small objects may be strongly divergent), absorption (some of the complex mechanisms involved are described by Hussey, 1975) and scattering and reflection

remove energy from the beam.

A plane wave incident normally on a plane boundary between two homogeneous media will have a proportion of its energy reflected by the boundary:

$$\frac{\text{reflected energy}}{\text{incident energy}} = \left[\frac{\rho_1 c_1 - \rho_2 c_2}{\rho_1 c_1 + \rho_2 c_2} \right]^2$$

where:

ρ_1 is the density of the first medium

ρ_2 is the density of the second medium

c_1 is the velocity of sound in the first medium

c_2 is the velocity of sound in the second medium

Reflection at an oblique boundary is more complex since to prevent the two media from parting at the boundary mode conversions (resulting in shear waves) must occur to some extent (Hussey, 1975).

Echoes from a relatively planar interface (surface radius of curvature $\gg$ dominant wavelength in acoustic pulse) are specular and the echo amplitude received back at the transducer is highly dependent on the orientation of the interface.

Multiple reflection artifacts are produced by sound waves which undergo more than one reflection, giving the appearance of additional interfaces within the tissues.

Soft tissues can act as a dense array of scatterers and interference between echoes from closely spaced discontinuities makes

a major effect on the resultant echo amplitude.

Echoes are often assumed to come from a point on the axis of the transducer and from a depth equal to the time delay from transmission to reception multiplied by half the assumed velocity of propagation of the pulse. Registration errors may be produced by refraction of the beam at interfaces and by errors in the assumed velocity (Wells, 1977). The beam may also be deflected when propagating through media containing many small inhomogeneities (Chivers, 1973; Chernov, 1960). Patient motion also causes registration errors. Registration errors can be particularly serious if the method of characterisation requires the same piece of tissue to be scanned from more than one direction.

Many of the interactions between ultrasound and biological materials are poorly understood, and many of the fundamental parameters, especially on a microscopic scale, have not yet been measured.

Even when considering an incident beam of continuous plane waves in lossless media analytical solutions for the resultant echo amplitudes are only available for a restricted set of relatively simple structures.

In addition to all these difficulties is the fact that we do not simply have to calculate the acoustic field given the properties of the media but have to solve the even more intractable inverse problem: that is, given the echo signals we have to deduce the material properties.

In view of all these problems the prospect of ultrasonic tissue characterisation may look bleak but we can take heart from the undoubted (and somewhat surprising) success of standard B-scanning.

6.3 APPROACHES TO TISSUE CHARACTERISATION

The following subsections briefly review some of the methods that have been used in attempting to characterise tissues by their interactions with ultrasound.

Ultrasonic tissue characterisation methods can be broadly classified into two main types: those methods which attempt to determine some fundamental physical property of the tissue such as the acoustic impedance or absorption, and those methods which measure some complex function of several fundamental properties (e.g. echo amplitude) which can hopefully be correlated with the clinical state of the tissue.

The suitability of the techniques for in vivo characterisation must be assessed. One difficulty which handicaps several techniques is the restricted access to the abdominal organs due to intervening lung and ribs. Gas in the lung effectively blocks the beam. Rib bones seriously degrade the beam by introducing multiple reverberation artifacts, attenuating the beam and distorting the beam due to refraction. This can prevent the use of techniques requiring through transmission in all directions in a plane (e.g. acoustic computer assisted tomography). Bowel gas is also a fundamental limitation to

abdominal scanning but the gas is often absent on repeating the scan on another occasion (Cosgrove, 1978).

6.3.1 Impediography

Deconvolution techniques can be used to determine the impulse response of a linear system if its response to a given stimulus is known. By transmitting sound waves into a multi-layered target and measuring the transmitted waveform and the returning echo waveform the response of the media to an impulse waveform may be determined (Kak and Fry, 1975; Wells and Woodcock, 1977). For plane-parallel layers normal to the beam the integral of the impulse response is simply related to the characteristic impedance of the media as a function of depth, provided that multiple reverberations can be neglected. (The multiple reverberations can be neglected provided that the individual impedance mismatches are small).

Unfortunately the highly idealised model is inappropriate for soft tissues such as liver. If any of the interfaces in the beam are not normal to the beam the method will fail. Since the consequences of the failure of the parallel-planes assumption appear to be very serious a more appropriate method was sought. (The conditions are more nearly satisfied in other body structures such as the skull wall).

6.3.2 Measurement of velocity

Transmission methods may be used to measure the average velocity if it is possible to gain access to the anterior and posterior

boundaries of the tissue, and by placing a reflecting target against the posterior boundary an analogous reflection technique can be used (Kossoff, 1975). (The time-of-flight of an ultrasound pulse can be compared with the time taken for a pulse to travel the same distance through a medium of known velocity). Whilst this can be used for an accessible organ like the breast the requirement of through transmission makes it unsuitable for the human abdomen.

In a technique analogous to X-ray computer assisted tomography velocity profiles may be found using acoustic computer assisted tomography (Greenleaf and Johnson, 1975; Greenleaf, Johnson, and Lent, 1978; Glover, 1977). The time-of-flight through the tissue in many directions in a plane is measured. The requirement of all-round access again makes it unsuitable for abdominal scanning. (Greenleaf and Johnson use a Biomation 8100 transient recorder to acquire their data so the acquisition system described in this thesis should be suitable for acoustic computer assisted tomography if it is required for that purpose).

6.3.3 Measurement of attenuation

Acoustic computer assisted tomography may also be used to obtain images of attenuation in cross sections of tissues (Greenleaf and Johnson, 1975) but again the requirement of all-round access makes it unsuitable for abdominal scanning.

For organs with restricted access a reflection technique is indicated. The attenuation of tissues cannot be determined by

simple comparison of echo amplitudes from the front and back boundaries of an organ because the echo amplitudes depend on the geometries and impedance mismatches at the two boundaries which are generally dissimilar at the two houndaries (Kossoff, 1975). In principle a differential method may be used by measuring the attenuation of different frequency components of a pulse reflected from the two boundaries (Kossoff, 1975).

By assuming that the echo amplitudes from liver might be expected to decay exponentially with range an estimate of the attenuation in liver can be obtained by determining the regression of the logarithm of the mean echo amplitude plotted against depth (Wells et al., 1975; Wells, 1977). By performing this analysis on echoes from thirty normal livers and fifteen cirrhotic livers Wells found that generally the attenuation was lower in cirrhotics than in normals but the individual differences were not significant.

6.3.4 Measurement of scattering amplitudes

Since scattering amplitudes give useful clinical information in B-scan images (Cosgrove, 1978) it might reasonably be expected that quantitative analysis of echo amplitudes could also give useful clinical information.

Pulse-height distributions of echoes from various tissues have been obtained (Mountford et al., 1972a, 1972b, 1973; Wells et al., 1975; Wells, 1977; Taylor and Milan, 1975). Wells found that cirrhotic livers gave rise to echo amplitudes significantly greater than normal livers. Chivers (1973) gives a detailed account of

scattering by soft tissues. Reid (1975) discusses some of the problems associated with measurement of scattering from biological tissues. One problem is that the scattering is difficult to specify because the scattered wave has a wave shape different from the incident wave shape, and the scattered wave depends on frequency and angle as well as on the fundamental elastic properties that give rise to the scattered wave. If the scattering is from within the near field of the transducer the measured scattering will depend on the transducer characteristics as well as the tissue characteristics. Reid suggests that some of these problems can be overcome by the substitution method: scattering amplitudes from tissue are compared with echoes from a standardised target.

Scattering will be discussed at greater length in section 6.5 and in chapters 7 and 8.

6.3.5 Acoustic Bragg scattering

In an acoustic analogue of Bragg diffraction in X-ray crystalography the angular dependence of scattering from soft tissues has been measured (Hill, 1975; Lele et al., 1975; Nicholas, 1975, 1978) using a scanner built so that it is mechanically constrained to direct the axis of the transducer through a fixed point in the tissue. By appropriate time gating of the echo signals the echo amplitude from the same region of tissue may be measured for continuously varying angles. Wells (1977) suggests that uncertainty in the position of the resolution cell when the tissue is examined

from different directions is likely to limit the clinical usefulness of the technique. One answer to this objection is that provided that the position of the resolution cell changes only slowly with angle then the variation in echo amplitude could still be primarily due to the angular change and so the method may well still be able to distinguish between different tissue structures.

6.3.6 Spectral analysis

Spectral analysis has been used in a number of different approaches to tissue characterisation. Absorption, surface scattering, and volume scattering all affect the frequency distribution of the ultrasound waveforms and might reasonably be expected to reveal clinically useful information about the tissues. Consequently considerable effort has been put into spectral analysis techniques (Chivers, 1973; Chivers and Hill, 1975; Hill, 1975; Lele et al., 1975; Waag et al., 1975).

Because a short pulse has a wide frequency spectrum measurements may be made over a range of frequencies with a single transmission pulse waveform (Chivers and Hill, 1975). By comparing spectra obtained from tissue samples with a reference spectrum from a flat reflecting target some of the characteristics of the transducer and receiver can be removed.

Fundamental limitations of the technique are discussed by Chivers and Hill (1975). They suggest that using two transducers to cover a significant range of scattering angles could yield useful information but that it appears that the geometry of the situation

makes exact quantitative analysis of the resulting data very difficult. The simpler geometry and convenience of use of 180° backscattering makes the single transducer arrangement attractive. If a time gate is used to select echoes from a small range of depth the spectrum is modified by the gate and the frequency resolution is limited. The IF filter in the spectrum analyser smooths the displayed spectrum. This affects the convoluted spectra from tissues rather more than the smoother reference spectrum. Thus comparison of spectral analysis results requires a knowledge of the loop spectral response and effective bandwidth of the transducers, the time-gate duration, the gate opening time, and the spectrum analyser IF filter characteristics.

Waag et al. (1975) report the use of swept frequency techniques to measure the frequency dependence of echo amplitude. A computer is used to perform the Fourier inversion of the spectral data to determine structural properties of the scattering media.

Spectral analysis techniques should allow an estimate to be made of the scale of the structures of significance in the scattering process, and thus help to delineate the fundamental limitations of ultrasound diagnosis (Chivers and Hill, 1975).

One of the difficulties of the technique is to find an objective technique for comparing spectra.

A related technique which also seeks to find regularities in the reflecting structure of the tissue is to derive the autocorrelation

function of the reflected waveform. This technique also has the difficulty of objective comparison of results.

6.3.7 Pattern recognition techniques

Two important phases of pattern recognition methods are extraction of features from data, and classification of data by these features (Feucht, 1977). Decker et al. (1973) have used a digital computer to extract the following features from A-scans from the human eye: cross-correlation, 3rd order regression, sine and cosine coefficients, time interval histogram, and amplitude histogram (see reference for details). When these six features are found for an unclassified echogram they are compared with sets of features of various classified echograms. The weighting factors of similar features are added. The ratio of this sum to the sum of all the weighting factors for this class is the deciding figure.

Preston (1975) discusses the use of a variety of statistical measures of the echo waveform and also the use of auditory analysis of frequency shifted echograms.

Lerski (1978) reports encouraging initial results for the classification of alcoholic liver disease.

Wells and Woodcock (1977) briefly describe a number of feature extraction and pattern recognition techniques.

Maus and Enderson (1979) warn that the vast increase in the use of computer statistical packages is leading to the publication of spurious results. The ability to look for many different correlations

is very likely to lead to significant correlations being found purely by chance. The 'significant' findings are selected for publication with little or no mention of the uninteresting tests which showed no correlation. The same danger exists for ultrasonic pattern recognition techniques: by looking for correlations between a large number of echo features and a large number of clinical conditions some spurious results are likely to be generated.

6.4 EXPLORATORY PHASE OF ECHO ANALYSIS

The foregoing review illustrates that although there are several approaches to ultrasonic tissue characterisation many problems have to be overcome to enable the techniques to be practical in vivo. To gain first hand experience of some of these problems I embarked on a preliminary study of echo waveforms.

Before the data acquisition system was built oscilloscope displays of echo waveforms were photographed. Waveforms from spleen, liver, placenta, and bladder tumours were studied. When the acquisition system was built programs were written to calculate the fast Fourier transforms (FFT) and autocorrelation functions of the echo waveforms. Again the resulting waveforms were examined visually.

The visual examination was performed to get an appreciation of the types of signals that would have to be processed, and also to form initial hypotheses about significant features of the waveforms. Although the hypotheses would be subjective they could later be

objectively tested by writing computer programs to measure the proposed features.

The great variability from one echo waveform to another and the consequential variability of the FFT and the autocorrelation function made visual comparison of waveforms very difficult. Since this variability is a fundamental limitation of a variety of tissue characterisation techniques I decided to study the variability in detail.

6.5 RANDOM NOISE IN ECHOES FROM SOFT TISSUES

A fundamental problem in interpreting echoes scattered from soft tissues such as liver is that the scattering arises from structures close enough together for interference effects to have a major effect on the resultant echo amplitude. Very small re-arrangements of the scatterers can result in widely different echo amplitudes being returned. This introduces a random noise element into the echo amplitude. The stochastic nature of the echo amplitudes is evident in the familiar speckled appearance of ultrasound liver images (Chivers and Hill, 1975). Because it is so fundamental to many aspects of medical ultrasonics I decided to concentrate on studying the effects of the interference between echoes from arrays of scatterers.

Whether the scattering is considered to arise from a complex array of interfaces or from discrete scattering centres is largely a conceptual matter (Chivers and Hill, 1975). For convenience I chose to consider the discrete scattering centre model.

Some justification for treating echo signals as random is required. Since the echo signals are mechanistically determined they are not random in the same sense that radioactive decay is random. Rather, they are random in the same sense that coin-tossing is considered to be random. If the conditions of tossing were sufficiently standardised the outcome would be theoretically predictable. In practice, however, the initial conditions are imprecisely known and very slight changes in the initial conditions will change the final (and easily observable) outcome. Similarly, in the ultrasound scattering problem in the absence of knowledge of the precise positions of the scattering interfaces the final echo amplitude is very uncertain. Under these circumstances probability theory seems appropriate.

6.5.1 Automatic detection of abnormal regions

A specific problem posed by the presence of inherent random noise in the ultrasound signal is the automatic detection of an abnormal region producing random signals surrounded by normal tissue producing random signals with a different average amplitude. If a portion of the echo signal is lower than average amplitude how can we tell whether it is from abnormal tissue or is just part of the distribution to be expected from normal tissue?

I decided to concentrate on the detectability of an array of discrete scatterers (abnormal) surrounded by another array of discrete scatterers. The form of the object to be detected is depicted in Figure 6.1. The individual discrete scatterers in

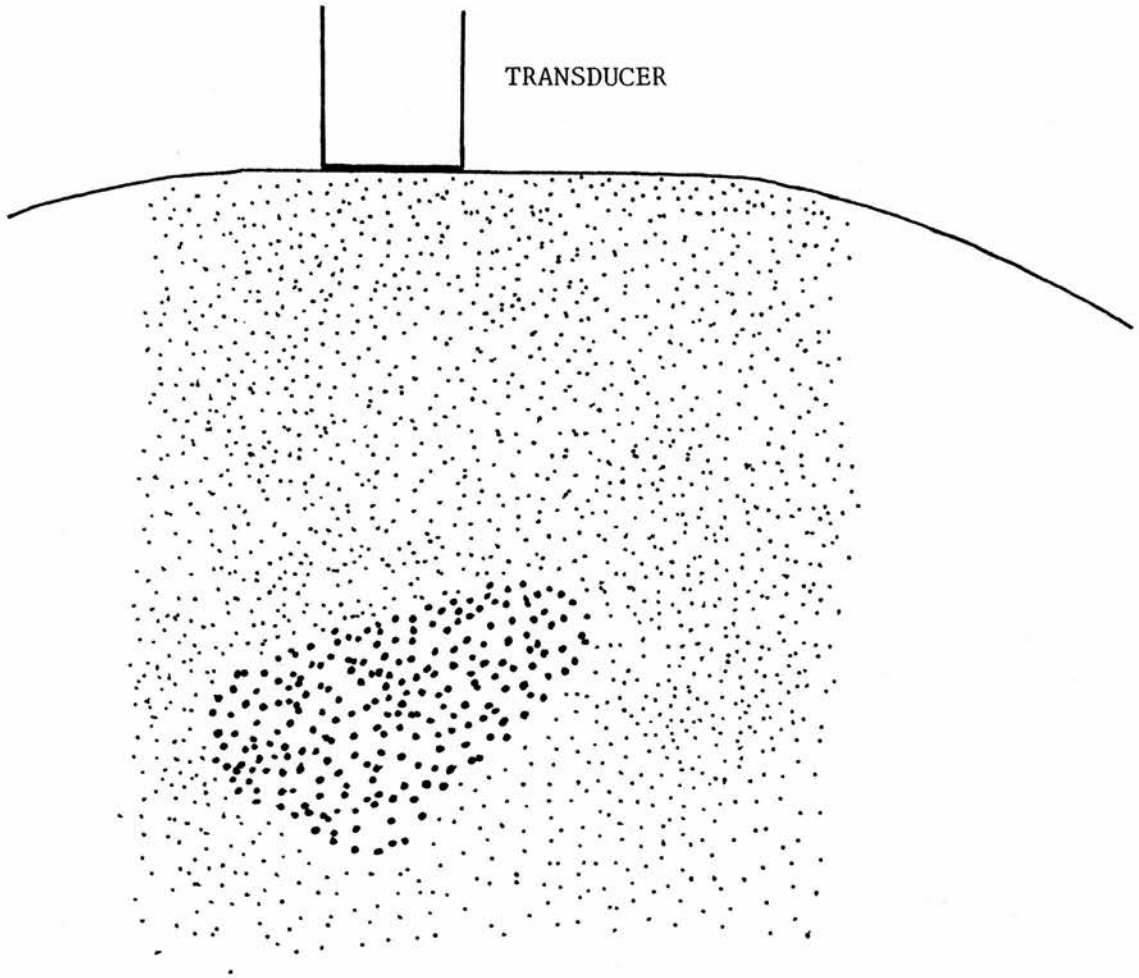

FIGURE 6.1 TUMOUR AND NORMAL TISSUE REPRESENTED AS ARRAYS OF DISCRETE SCATTERING CENTRES

the abnormal region give rise to different scattering amplitudes than the normal scatterers. In the pictorial representation in Figure 6.1 the use of larger dots to represent the abnormal scatterers is not meant to imply that the scatterers are of different sizes.

To further simplify the problem, at least initially, I will assume that the echoes from the interface between the two regions can be ignored. If the interface is oblique to the axis of the transducer this could be a realistic assumption, and we want to be able to detect tumours without having to direct the beam normal to the interfaces. The theory could be modified in the future to allow for echoes from the interface. To include the interface echoes from the start could obscure the problems presented by the scattering problem alone.

A further simplification is to assume that the attenuation can be adequately compensated by swept gain over the region of interest. The effects of attenuation which deviates from the assumed value could be included in a more detailed analysis.

The analysis of problems caused by random variations in echo amplitude should be useful whether or not the random variations are caused by interference effects. Thus the analysis should throw some light on problems caused by other random variations (e.g. spatial variations in attenuation) although some modifications to the theory are likely to be necessary.

6.5.2 Ultrasound B-scan resolution

The interference effects produce the familiar speckle pattern in liver images. The presence of these random variations creates difficulties in interpreting the images. Cosgrove (1978) reports that the smallest metastases that can be detected reliably are an order of magnitude larger than the resolution measured in ideal conditions. The size a tumour has to be before it can be detected reliably will depend on the statistical distributions of echo amplitudes to be expected for normal and abnormal tissues. The larger the region of 'abnormal' echo amplitudes is, the less likely it is to be simply part of the distribution for normal tissue. Thus statistical considerations have a bearing on the achievable resolution.

Resolution is commonly measured by scanning small objects (such as wires) immersed in water. Scanning one or two small objects in a large echo-free region is rather different from scanning soft tissues such as liver or thyroid which contain a dense array of scattering interfaces, and to predict the achievable resolution we will need to take into account the random noise produced by interference effects.

Hopefully a greater understanding of the limitations on achievable resolution could help in the design of scanning equipment.

6.6 SUMMARY

Since it is impractical to try to solve all the problems involved

in tissue characterisation I decided to concentrate on the effects of interference between echoes from closely spaced interfaces. The problem of detecting tumours within normal tissue is represented in idealised form and the problem is reduced to detecting a region of discrete scattering centres (abnormal) within another region of discrete scattering centres (normal). A practical consequence of the random noise caused by interference is that the resolution of standard B-scanners is degraded.

These problems are the subject of the following two chapters.

CHAPTER 7

SIMULATION OF SCATTERING FROM SOFT TISSUES

7.1 INTRODUCTION

The remainder of this thesis is primarily concerned with the significance of scattering amplitudes from soft tissues. Whilst the aim is to detect abnormal regions it is clearly important to determine the range of echo amplitudes to be expected from normal tissue. Hence the present chapter is concerned with scattering from a random array of identical point scatterers, and Chapter 8 is concerned with scattering from an array of point scatterers surrounded by an array of point scatterers of different scattering cross section (Figure 6.1).

7.2 COMPUTER SIMULATION OF SCATTERING

7.2.1 Advantages of simulation

A purely analytical approach to describing the production and processing of echo signals from arrays of scatterers would be very difficult. An alternative is to simulate the scattering and process the resulting data. Programs written to process echo data from tissues could also be used to process simulated data allowing direct comparison of the results.

By simulating the echo signals we have considerable control and precise knowledge of the parameters used in the simulation. In contrast, in the clinical situation we have limited control over the production of the echoes and often have only limited knowledge of the scattering materials. Even using test objects we have limited control

and knowledge of the conditions producing the echoes.

There are dangers in relying on simulations if the model is inappropriate but since we have a data acquisition system we can test our predictions using real echo data from tissues.

The simulations also allow us to test theoretical predictions for simplified situations amenable to analysis. We can simulate situations which could not occur in practice but which nevertheless help our understanding.

Useful introductions to the design of computer simulations have been given by Tocher (1963) and Naylor et al. (1969).

7.2.2 Choice of scattering model

Theoretical models of scattering of ultrasound by human tissues have been reviewed by Chivers (1973, 1977). Many forms of model have been proposed but they may be divided into two main classes: models in which inhomogeneities are discrete and models in which they are continuous. Twersky (1960) reviews approaches to the problem of scattering from arrays of discrete discontinuities and includes over 250 references on the subject. The continuum model has also been discussed in the literature (Chernov, 1960; Chivers, 1973, 1977, 1978; Nicholas, 1975; Gore and Leeman, 1977).

I selected the discrete scattering centre model because it is easier to simulate than the continuum model. Multiple reverberations are assumed to be negligible and the scattering field from all scatterers is assumed to be the sum of the scattering amplitudes of each of the point scatterers in isolation. The assumption that the effect of

multiple reverberation is small can be justified on the grounds that the total scattering cross section is found to be small and also on the grounds that the visualisation of small hepatic ducts would not be possible if multiple reverberation was large.

7.2.3 Synthesis of echo signals

Defining t=0 as the instant at which a pulse is emitted by a disk transducer the reflected waveform P(z,h,t) from a point scatterer at a depth z and transverse displacement h is assumed to be of the form

$$P(z,h,t) = sb(h)F(t-\frac{2z}{v}) \qquad (7.1)$$

where v is the group velocity of the pulse and $s = \pm 1$ to allow for inversion of the pulse. The value of the group velocity v used to convert between time and length measurements is always taken to be 1540 m/s in this thesis. It is assumed that in the region of interest attenuation is compensated for by the swept gain so that pulse amplitude can be taken to be independent of depth. Identifying the parameters associated with the k^{th} scatterer with the subscript k we may write down the formula for the echo waveform from the array of scatterers as

$$P(t) = \sum_k w_k g(t_k) F(t-t_k) \qquad (7.2)$$

where

$$w_k = s_k b(h_k) \qquad (7.3)$$

and

$$t_k = 2z_k/v \qquad (7.4)$$

and $g(t_k)$ is a factor included to represent the presence of abnormal regions with different scattering cross sections. If only one region is being considered $g(t_k)=1$ for all t_k.

The random number w_k is obtained using

$$w_k = s_k u_k \tag{7.5}$$

where

$$s_k = +1 \text{ if constant sign is selected} \tag{7.6}$$

or

$$s_k = \begin{matrix} +1 \text{ with probability } \frac{1}{2} \\ -1 \text{ with probability } \frac{1}{2} \end{matrix} \tag{7.7}$$

and, independent of s_k,

$$u_k = +1 \text{ if constant magnitude is selected} \tag{7.8}$$

or

$$u_k = \text{random number from a specified distribution} \tag{7.9}$$

By allowing s_k to be +1 or -1 we can allow for inversion of the waveform by some of the scatterers. The distribution of u can be selected to give the amplitude distribution expected for a given form of the transverse beam profile b(h), noting that the probability that h_k lies between h and h+dh is $Kh_k\,dh$, where K is a normalisation constant depending on the scatterer density. The distribution of u may also be varied to include the effects of having scatterers with a distribution of scattering cross sections.

In this thesis random distributions of the form $w = \pm 1$ may be taken to mean that the values +1 and -1 are equally likely.

An echo signal obtained using the acquisition system may be used to specify F(t). One echo waveform that was used was obtained from a ball-bearing. F(t) may also be specified using formulae. Following Atkinson and Berry (1974) I used the representation

$$F(t)=a(t)\sin(\omega t-\theta) \qquad (\omega,\theta, \text{ constants}) \qquad (7.10)$$

A realistic form of a(t) is (Gore and Leeman, 1977)

$$a(t)= a_o t \exp(-\alpha t) \qquad (a_o,\alpha, \text{ constants; } t \geqslant 0) \qquad (7.11)$$

An example of such a pulse waveform is shown in Figure 7.1.

One commonly used set of parameters was

$\omega = 2\pi \times 3.5$ MHz $= 21991150$ radian s^{-1}

$\alpha = 2445000\ s^{-1}$ giving a(t) a full width at half maximum = 1 μs

$\theta = 0$

This standard form of F(t) is given the name $F_s(t)$ and is defined by

$$F_s(t) = a_o t \exp(-2445000t)\sin(21991150t) \qquad (7.12)$$

The positions of the scatterers are constrained to keep the numbers within given ranges of depth constant:

$$(n-1)\tau \leqslant t_k < n\tau \quad \text{for} \quad (n-1)N \leqslant k < nN \qquad (7.13)$$

i.e. there are N scatterers in segments of length $v\tau/2$. In physical terms this segmentation prevents very dense packing of scatterers in

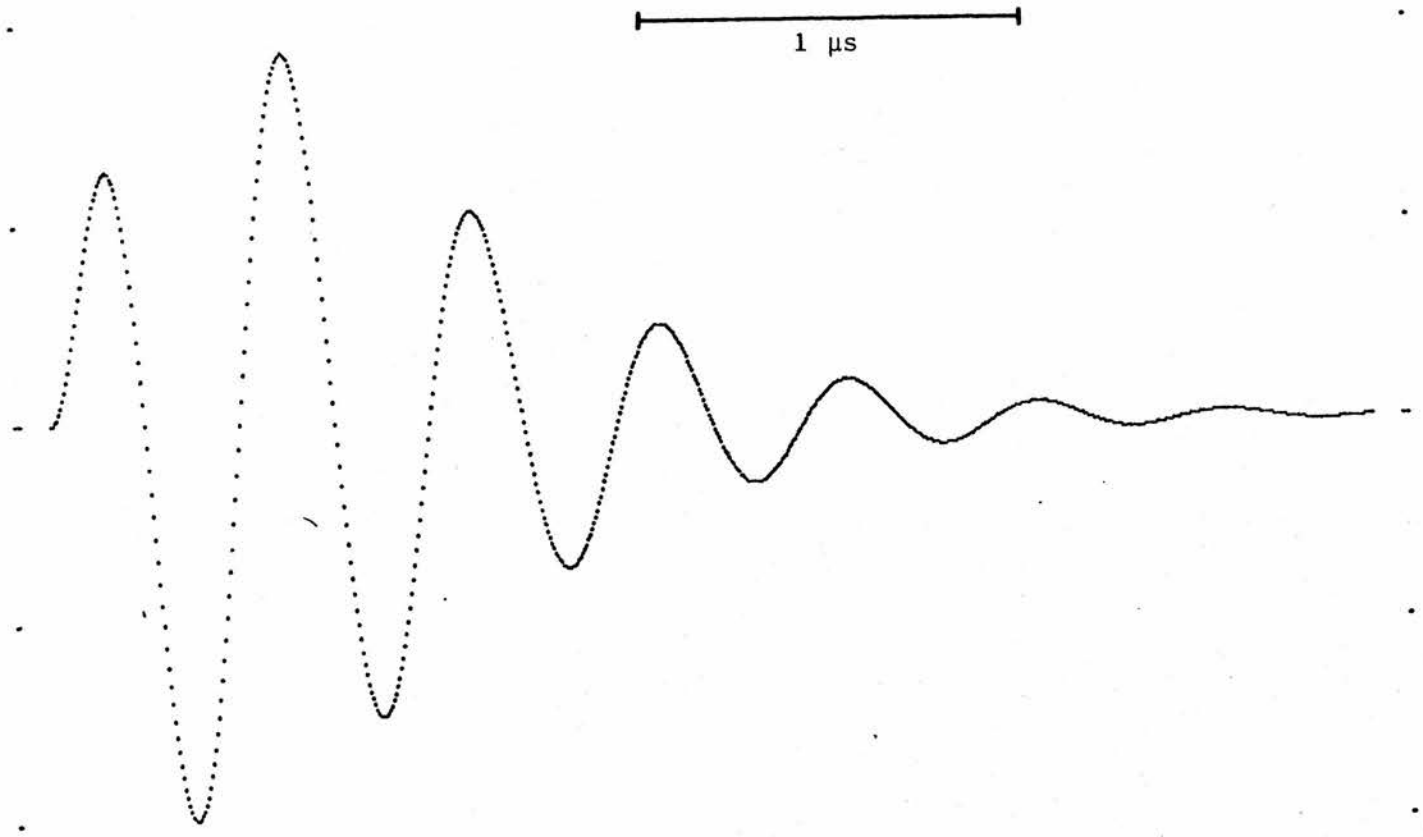

FIGURE 7.1 EXAMPLE OF PULSE WAVEFORM $F(t) = a_o t \exp(-2306604t)\sin(12566370t)$

some regions with very sparse densities in other parts. The positions of individual reflectors can be given sufficient freedom to measure the effects of random phase differences whilst minimising the effects of variations in mean reflector densities. The values of τ and N may be varied to study the effects of segment size and reflector density respectively. The positions of the scatterers within each segment have a uniform random distribution.

The method of constraining the distribution of scatterers was chosen in the interests of simplicity. Other methods of constraint could be introduced in the future (e.g. specifying a minimum possible separation, or introducing an element of short-range order).

An example of a synthesised waveform is shown in Figure 7.2

7.2.3.1 Pseudo random number generator

A pseudo random number generator is used to specify the positions of the scatterers and the echo amplitudes. The subroutine used was obtained from the DECUS program library (Program Number 8-690). The program generates random numbers x_n using the algorithm

$$x_n = (2^{17}+3)\ x_{n-1} \text{ modulo 36 bits} \qquad (7.14)$$

The starting number x_o can be specified to allow repeatable sequences to be generated or it may be randomly selected by a routine that runs as a background job. If the random start is selected variation in the timing of the program (e.g. time taken to enter keyboard commands) will alter the sequence starting point. Once started the sequence will not repeat until it has been called more than 4×10^9 times. The authors of the program found that the random numbers passed tests

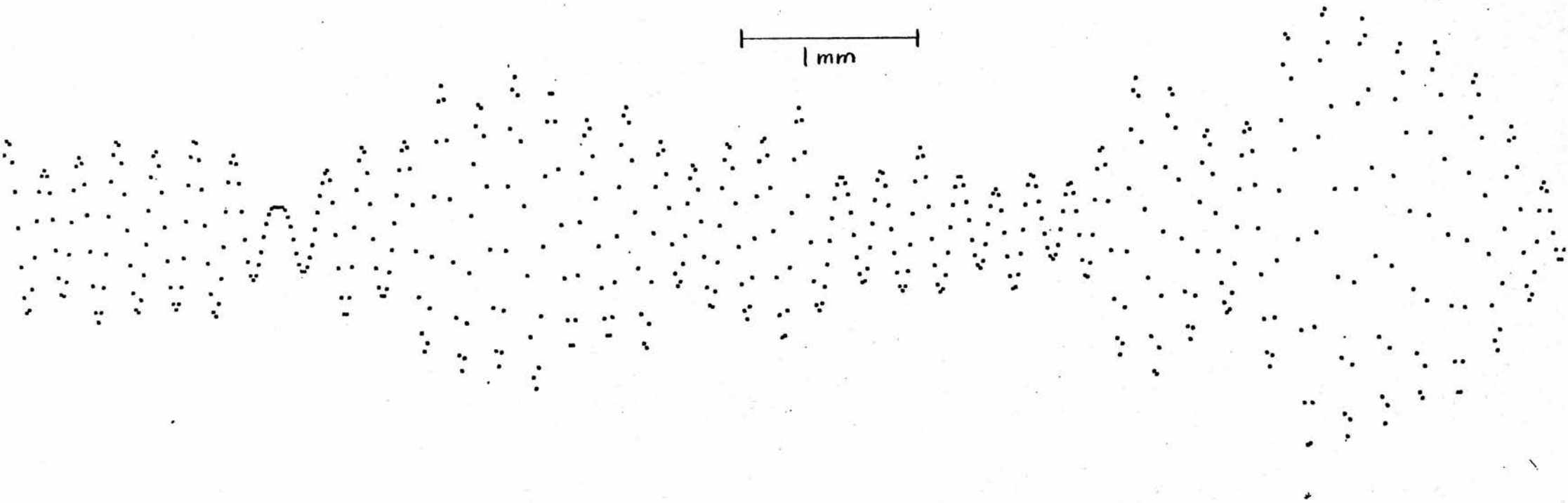

FIGURE 7.2 EXAMPLE OF SYNTHESISED ECHO SIGNAL

Synthesis parameters: pulse waveform = $F_s(t)$ defined in Equation 7.12
number of reflectors per segment, N = 10
segment length, τ = 2 μs
w = $\pm$ 1, g = 1, sample interval = 20 ns

of mean value, variance, frequency of selected numbers, and auto-correlation properties. DECUS program write-up Number 5-25 should be consulted for details.

Rigorous testing of random sequences is difficult since a truly random sequence will not pass all tests that can be devised: the suitability of the sequence is determined by its application. Since the sequence was known to pass several basic tests and various characteristics of the synthesised data were in agreement with the theory I conclude that the random number generator is adequate for the task.

7.3 NOTES ON SYNTHESIS/ANALYSIS PROGRAMS

Since over fifty programs were written in the course of the thesis it would be impractical to describe them all: only the principal programs will be mentioned.

7.3.1 SIGPRO - Signal processor program

Prior to the writing of SIGPRO all the synthesis programs stored the synthesised signals on file. Separate programs could then analyse the data. The original programs received many alterations as new features were added in the light of results obtained. Although altering the original programs allowed fairly rapid development of the programs they became poorly structured and difficult to modify further. Using the experience gained on these earlier programs a new program incorporating many new features was written: SIGPRO.

SIGPRO combined the synthesis and analysis functions in one program so that intermediate file storage was no longer essential. Signals

were synthesised using the methods described in section 7.2.3. To speed up the synthesis, the part of the program that adds together the $F(t-t_k)$ waveforms was written in assembly language. Signals of any length can be synthesised.

Because the start of the signal is different from the rest (since there are no echoes for $t < 0$) a dummy portion of signal is synthesised, and only signals following the dummy portion are analysed.

7.3.1.1 Signal sources

SIGPRO can process signals from four sources:

1) echo data obtained using the data acquisition system
2) data files produced by SIGPRO or other FORTRAN programs
3) data synthesised by SIGPRO itself
4) sequences of independent random variables from specified distributions.

The pulse waveform F(t) used for synthesis can be generated using a formula or can be taken from a file (after processing if required).

The sequence of independent random variables is generated by randomly selecting numbers from an array which can be read in from a file. Section 7.3.2 describes the program used to generate the distributed data file. The same distribution of random numbers can be used to select the values of u_k, the amplitudes of the pulse waveforms added into the signal.

7.3.1.2 Signal processing

The processing is divided into three modular stages: a pre-processing

stage (e.g. rms values of specified sample lengths), a post-processing section (e.g. minimum value of pre-processed signal values in specified sample lengths) and finally a statistics section used to form distributions and statistical measures of the processed data. The statistical measures can be listed on a line printer and the distribution can be stored on a file in the form of a histogram. The signal can be displayed on the VDU before processing, after pre-processing and after post-processing. The processed signal may also be stored on file.

Some of the processing methods would appear to be very obscure without a description of the intended applications so no processing options will be described at this stage. The specific processing options available will be evident from the sections describing the applications. The modular design of the program makes it relatively easy to include additional forms of processing.

Many of the synthesis and processing parameters can be varied automatically in a pre-selected sequence. In this way the program can be left running for hours varying parameters without operator attention.

To allow SIGPRO to run in only 32K of memory it was necessary to use overlays. Care had to be taken to prevent illegal subroutine calls between overlays being necessary. To avoid undue delays it was necessary to ensure that overlays were never swapped during time-critical sections of the program.

7.3.2 DISUTL - Distribution utility program

DISUTL can read distribution files produced by SIGPRO and other programs and calculate statistical features of the distribution. Certain distributions may be formed using formulae (e.g. Gaussian, Rayleigh).

Distributions from several sources may be accumulated into one distribution. The resulting distribution may be stored on file and combined with further distributions later. A histogram of the distribution can be plotted.

DISUTL can also generate sets of data having the specified distribution and store it on a file. This file can then be read by SIGPRO and used to generate random data having that distribution. For example, liver data acquired using TRCON can be processed by SIGPRO to form a distribution of peak values in 0.5 μs periods, and that distribution can be processed by DISUTL to form a set of data having that distribution. This file of distributed data can then be read by SIGPRO and used to generate independent random samples having the same distribution as the processed liver echo data. An application of this process is described in Section 8.15.

7.3.3 PULSYN - Pulse synthesis program

PULSYN uses formulae to generate pulse shapes. Parameters of the pulse waveforms can be altered using control knobs on the PDP12 and the changes observed on the VDU. Such pulses can be added with specified time shifts and scaling factors and again these parameters can be varied continuously as the effects are observed on the VDU.

The resulting waveforms can be stored on file (and used by SIGPRO as the waveform F(t) used for synthesis).

7.3.4 HARDCP - Hard copy program

HARDCP can read TRCON files produced by the acquisition system or data files produced by SIGPRO and other FORTRAN programs, and produce a plot of the signal on the electrostatic printer/plotter. An assembly language subroutine had to be written to control the printer/plotter prior to graphics software being obtained.

7.4 ACQUISITION OF ECHO DATA FROM TISSUES

Echo data from tissues were collected using the data acquisition system under the control of the program TRCON.

The acquisition system was connected to an EMISONIC 4201 B-scanner. Signals were taken from a point in the receiver after all the swept gain stages but before detection. This has the advantage that the swept gain partly compensates for the attenuation and the amplitude of the signals is kept within a relatively small range by the operator of the B-scanner, generally making adjustment of the transient recorder gain controls unnecessary. A further advantage is that we obtain the very signals that are used to form the final B-scan image, which aids analysis of image formation by the scanner.

The use of a separate receiver would be preferable in some circumstances since we could then have control over the receiver characteristics, but at the time of writing such a receiver has not yet been built for the system.

To obtain echo signals a good quality grey-scale image of the region of interest is first formed. The caliper pips are set at the appropriate depth and samples are usually taken as the beam is swept slowly through the region of interest.

To obtain echoes from normal tissue a region free of large ducts would normally be selected. This visual selection could bias the results slightly but it is expected that such samples are more likely to be representative of normal tissue than 'blind' samples which may include large ducts. A plot of a sample of liver echo data is shown in Figure 7.3. A 3.5 MHz transducer was used to obtain all the echo data used in this chapter.

The following sections discuss certain aspects of signal theory and subsequent sections compare theoretical predictions with results obtained by processing echo data and synthesised data.

7.5 STATIONARITY AND ERGODIC SIGNALS

The concepts of stationarity and ergodicity are explained in many text books on signal theory (e.g. Lynn, 1973; Goodyear, 1971; Cramer and Leadbetter, 1967; Schwartz, 1970) and will therefore be dealt with only briefly here.

We can synthesise a set of random signals by synthesising echo waveforms for different random arrays of scatterers. Such a set of random signals is known as an ensemble. An ensemble statistic is a statistic derived from a set of signal values, one value being taken from each member of the ensemble.

A random signal is described as being strictly stationary if its

statistical properties are independent of a shift in the time origin; and is described as weakly stationary if only some of its statistical properties are time invariant.

A random signal is described as ergodic if the time averaged statistics derived from a portion of it are (within the limits imposed by sampling errors) indistinguishable from those derived from an ensemble average. This means that an ergodic signal must take all possible values of the signal with the same probability as those of the ensemble.

The equivalence of the time averaged statistics with the ensemble statistics is useful since the time averaged statistic can be computed more readily.

Due to constraining fixed numbers of scatterers to lie between equally spaced partitions the resulting synthesised signals are not always strictly stationary. Certain statistical functions will have the same periodicity as the partitions. However, in many cases the deviations between the time averaged statistics and the ensemble statistics will be negligible.

Echo signals from tissues will be non-stationary since the echo signals are depth dependent. However, for short ranges of depth the time averaged statistic can be expected to be a good approximation to the ensemble statistic.

7.6 NOISE THEORY

The literature on noise theory is vast. Of particular relevance is

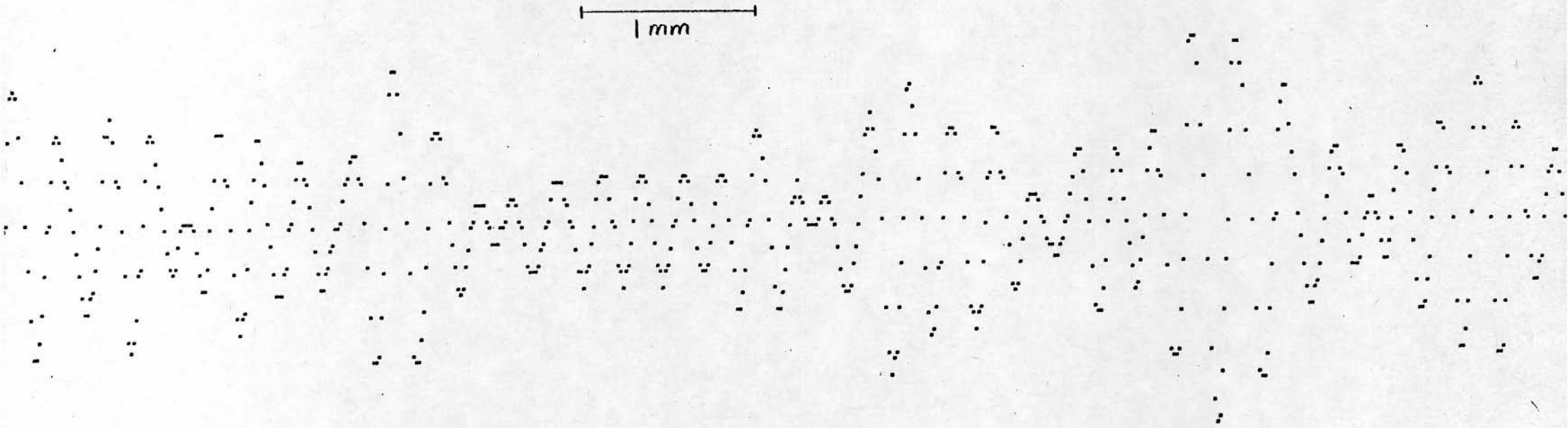

FIGURE 7.3 EXAMPLE PLOT OF LIVER ECHO DATA

Sample interval = 20 ns

the analysis of shot noise. In his classic paper on noise Rice (1944, 1945) represents the shot noise current I(t) by the equation

$$I(t) = \sum_k w_k F(t-t_k) \qquad (7.15)$$
(Rice 1.5-1)

where F(t) is the effect of an electron arriving at time t=0, t_k is the arrival time of the k^{th} electron and w_1, w_2 ... w_k ... are independent random variables all having the same distribution. Since this is analogous to my method of synthesising echo signals (Equation 7.2) the work of Rice is of direct relevance. The principal difference between Rice's model for shot noise and my model for echo signals is that the arrival time of the electrons is assumed to be independent and random (resulting in a Poisson distributed number of arrivals in a fixed time period) whereas the the number of scatterers in certain depth ranges is fixed in my model. However, in the limit of increasing reflector density we would expect the results to converge on those predicted by Rice.

The following sections compare the theoretical predictions with the results obtained for echo data and synthesised signals.

7.7 AMPLITUDE DISTRIBUTION

If the reflector density is large the amplitude of the echo will be the sum of a large number of independent random variables. Hence from the central limit theorem (Hoel, 1971) we would expect the amplitude distribution to be Gaussian.

Adapting Rice's equations, the probability that the echo amplitude

is between the values P and P+dP is given by

$$Pr(P)dP = \frac{1}{\sqrt{2\pi\sigma^2}} \exp(-(P-m)^2/2\sigma^2)\ dP \qquad (7.16)$$

where

$$\sigma^2 = \frac{N}{\tau}\,\overline{w^2} \int_{-\infty}^{+\infty} [F(t)]^2\ dt \qquad (7.17)$$

If $\bar{w} = 0$, then $m = 0$. In this case the rms value of the signal equals σ. For convenience the synthesis program normalises F(t) to make the rms value equal to 100.

If $m = 0$ the distribution is symmetrical about zero and the probability distribution for the modulus of the signal will be given by

$$Pr(|P|)\ dP = 2Pr(P)dP \text{ for } P > 0 \qquad (7.18)$$

Thus the modulus of the signal is expected to have a semi-normal distribution. Figure 7.4 compares the distributions found for the modulus of two synthesised signals and compares them with the theoretical semi-normal distribution. The signals were synthesised by adding pulse waveforms with random sign ($w = \pm 1$).

The standard pulse waveform $F_s(t)$ defined in Equation 7.12 was used for these simulations.

The distribution for the signal synthesised with a high reflector density ($N = 20$, $\tau = 2\ \mu s$) agrees well with the theoretical distribution. The theoretical mean for a semi-normal distribution is $\sigma\sqrt{2/\pi} = 79.7885$ and the mean of the actual distribution was 79.792.

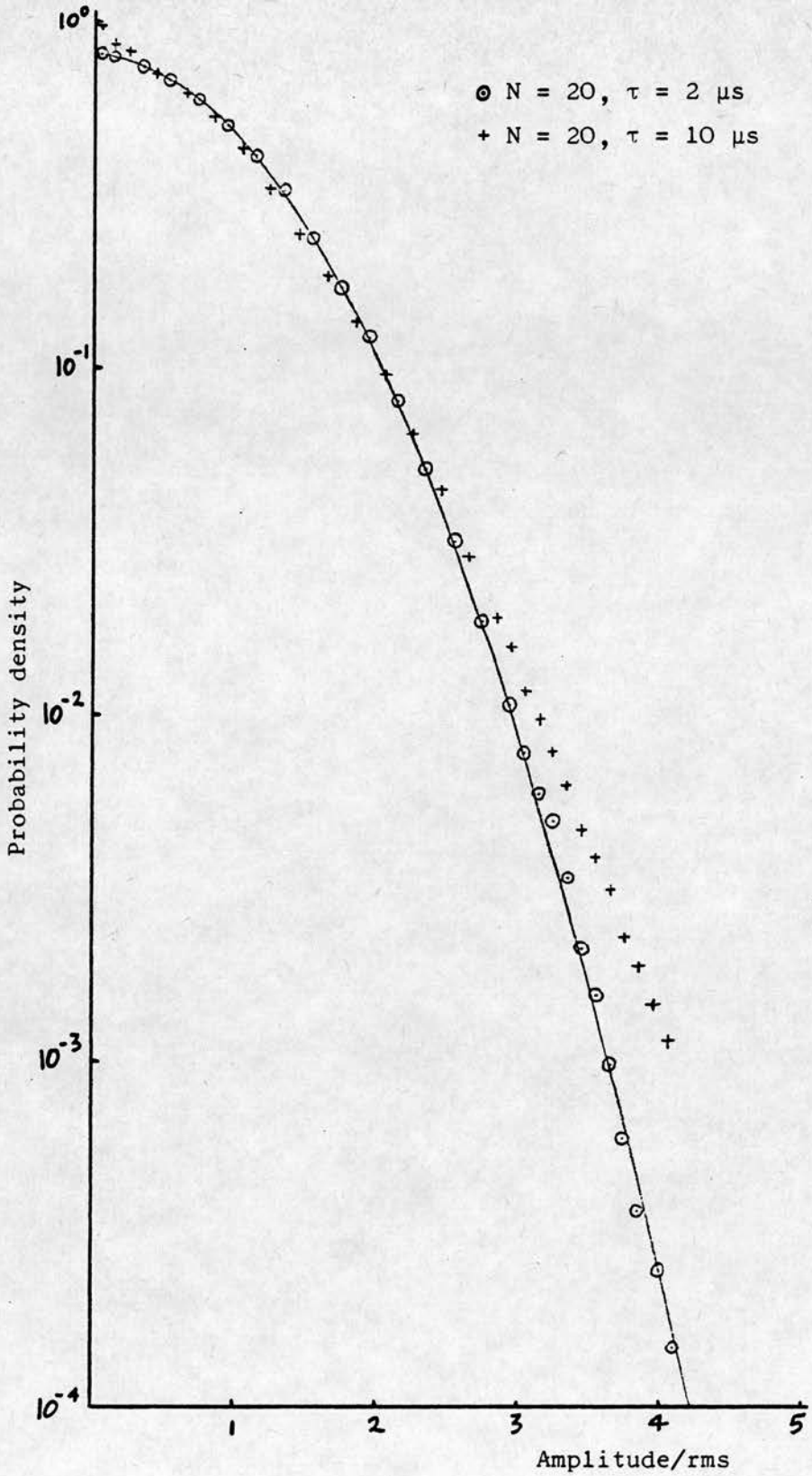

FIGURE 7.4 AMPLITUDE DISTRIBUTION OF MODULUS OF SYNTHESISED SIGNALS COMPARED WITH SEMI-NORMAL DISTRIBUTION

For low densities the probability distribution is not expected to be semi-normal and the distribution for N = 20 and τ = 10 μs can be seen to deviate from the semi-normal distribution (Figure 7.4). The use of Edgeworth's series to represent the approach of the amplitude distribution to the normal law is described in the literature (Rice, 1944, 1945; Cramer and Leadbetter, 1967; Lewis, 1973). Distributions for impulses chosen from a family of shapes F(w,t) depending on the random variable w are discussed by Gilbert and Pollak (1960).

7.7.1 Patient data

The distribution of amplitudes of echo signals from normal liver is compared with a Gaussian distribution with the same standard deviation in Figure 7.5. It can be seen that the distribution approximates to a Gaussian distribution but differences can be seen in the tail regions, high echo amplitudes being more likely in practice than predicted by the Gaussian curve.

7.8 DISTRIBUTION OF AVERAGE ECHO AMPLITUDE

To estimate the echo amplitude we can take some form of average (rms, mean modulus) over a finite time T. It is of considerable interest to know how the distribution of average values will depend on the sample time duration T. The dependence of the distribution on T has direct relevance on the resolution obtainable.

7.8.1 Mean modulus processing

Distributions for the mean modulus of the signal are shown in Figures 7.6-12. The signals were synthesised by adding echoes of the form

$F_s(t)$, (Equation 7.12) with random sign ($w = \pm 1$), N = 10, and τ = 2 μs.

For sample lengths short compared with the wavelength of the pulse the distribution is expected to be semi-normal, and as we have seen in Figure 7.4 this is the case.

The mean value μ will be independent of the sample length and will be expected to be the same as the mean of a semi-normal distribution:

$$\mu = \sigma\sqrt{\frac{2}{\pi}} \tag{7.19}$$

and for signals synthesised with F(t) normalised to make σ (as defined by Equation 7.17) equal to 100 we have

$$\mu = 79.7885 \tag{7.20}$$

For average lengths approximately equal to the wavelength the distribution is expected to approach the distribution of the waveform's envelope and is thus expected to be close to the Rayleigh distribution (Rice, 1944, 1945; Berry, 1973; Goodyear, 1971; Schwartz, 1970). A Rayleigh distribution of the variable x has the form

$$Pr(x) = \frac{x}{\psi^2} \exp(-x^2/2\psi^2) \tag{7.21}$$

The mean of such a distribution is given by

$$\mu = \psi\sqrt{\frac{\pi}{2}} \tag{7.22}$$

Thus to obtain the correct distribution we require that

$$\psi = \mu\sqrt{\frac{2}{\pi}} = \sigma\frac{2}{\pi} = 63.6620 \tag{7.23}$$

The distribution for synthesised data are compared with theoretical

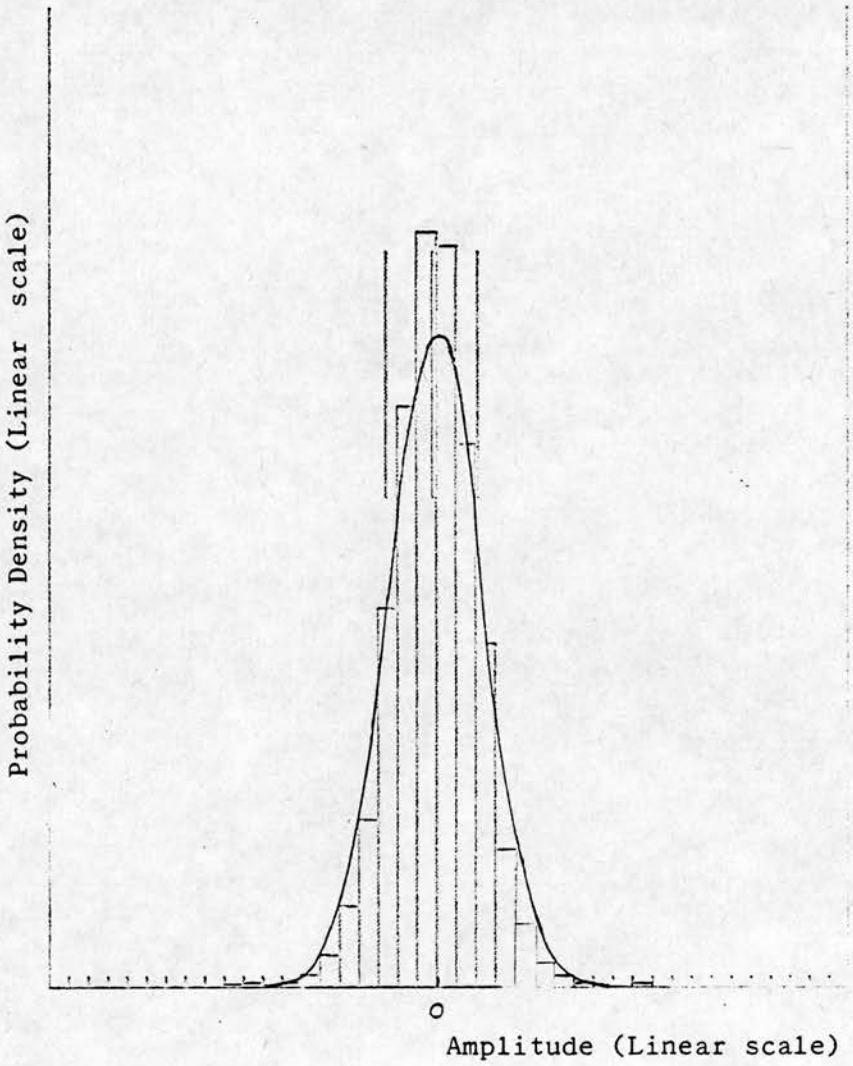

FIGURE 7.5 AMPLITUDE DISTRIBUTION OF LIVER ECHOES COMPARED WITH NORMAL DISTRIBUTION. THE THREE VERTICAL LINES INDICATE THE MEAN AND THE MEAN PLUS OR MINUS ONE STANDARD DEVIATION.

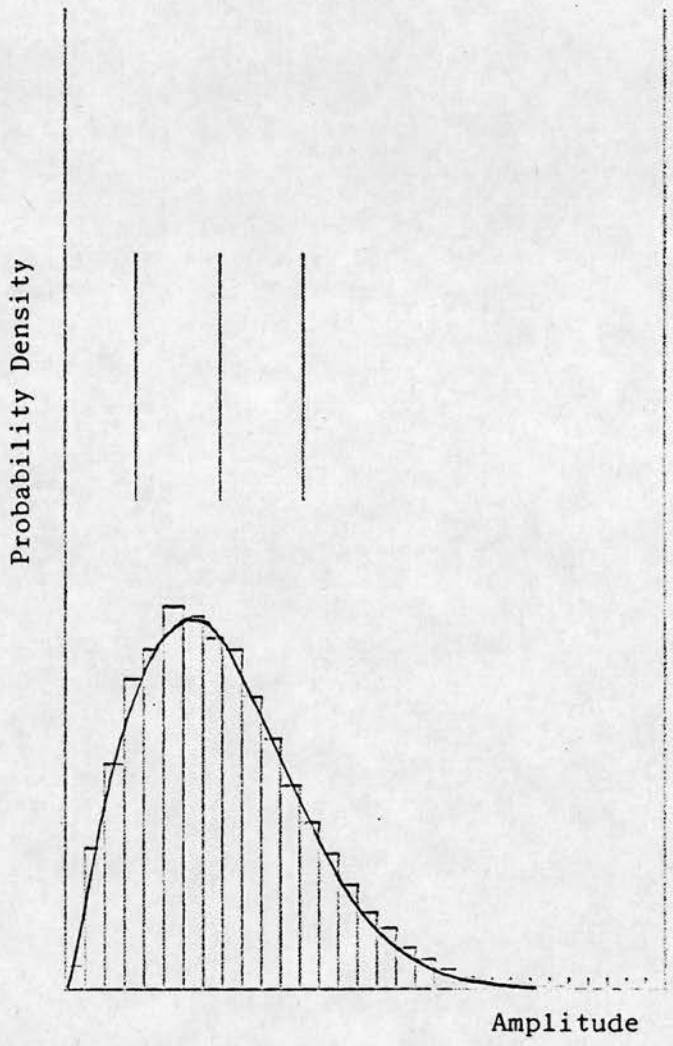

FIGURE 7.6 AMPLITUDE DISTRIBUTION OF MEAN MODULUS OF 0.2 μs SAMPLE OF SYNTHESISED SIGNAL COMPARED WITH RAYLEIGH DISTRIBUTION

Rayleigh distribution in Figures 7.6-9. The distribution is seen to be fairly close to the Rayleigh distribution.

As we increase the sample time T the distribution is expected to get narrower and for samples long compared with the pulse width we would expect the distribution to approach the Gaussian distribution. (This is expected from the central limit theorem, since for large sample lengths the mean will be the sum of several nearly-independent numbers). Figures 7.10-12 compare the distributions obtained for synthesised data with Gaussian distributions with the observed standard deviations and the theoretical mean (= 79.7885). It can be seen that as the sample length is increased the agreement with the Gaussian distribution gets better. Also as expected the distribution gets narrower: in Section 7.9 the dependence of the standard deviation on sample length (and other factors) is determined.

Echo data from human livers were also processed to see how the mean modulus distributions depended on the sample lengths. Figure 7.13 compares a 0.2 μs average with a Rayleigh distribution with the same mean. There is fair agreement over much of the distribution but high amplitudes are more likely to occur than predicted by the Rayleigh distribution. Figures 7.13-15 show how the distribution gets narrower as the sample length is increased. The histograms are compared with Gaussian distributions with the observed mean and standard deviations. As was found for the synthesised data the Gaussian distribution is approached more closely as the sample length is increased. However, the approach is not as close for liver echo data.

7.8.2 RMS processing and peak processing

Histograms were also found for rms values to see how they depended on the sample duration T. Examples of typical histograms for liver and synthesised data are shown in Figures 7.16 and 7.17. A theoretical discussion of fluctuations in noise power (mean square of amplitude) of random signals is given by Slepian (1958).

Also of interest is the distribution of the peak value within a sample of duration T. This is often used as a measure of the signal amplitude in digital scan converters. Typical distributions for peak processing of liver data and synthesised data are shown in Figures 7.18 and 7.19.

An obvious difference between the peak distributions and the rms and mean modulus distributions is that the peak distributions do not reduce in width as much as the other distributions when the sample time T is increased. This observation is discussed more quantitatively in the following section.

7.9 STANDARD DEVIATION OF ECHO AMPLITUDE

A commonly used parameter that gives a measure of the width of a distribution is the standard deviation σ. In our case it is more useful to normalise the values and calculate the coefficient of variation:

$$\text{coefficient of variation} = \frac{\text{standard deviation}}{\text{mean}} \times 100 \qquad (7.24)$$

Although the coefficient of variation does not tell us the shape of the distribution it does allow the effect of various parameters on the width of the distribution to be investigated.

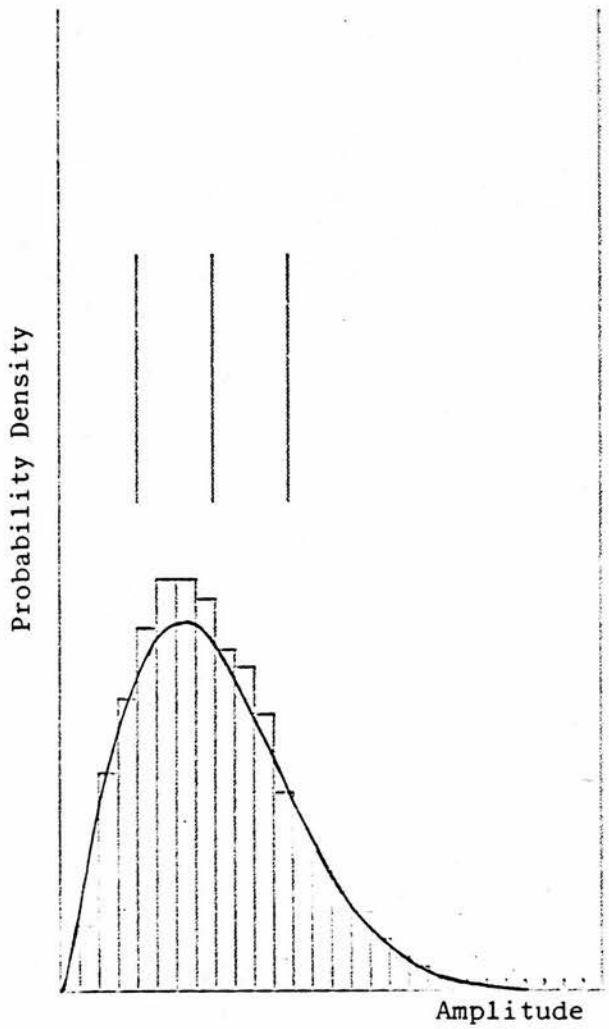

FIGURE 7.7 AMPLITUDE DISTRIBUTION OF MEAN MODULUS OF 0.5 μs SAMPLE OF SYNTHESISED SIGNAL COMPARED WITH RAYLEIGH DISTRIBUTION. SEE FIGURE 7.8 FOR LOGARITHMIC PLOT.

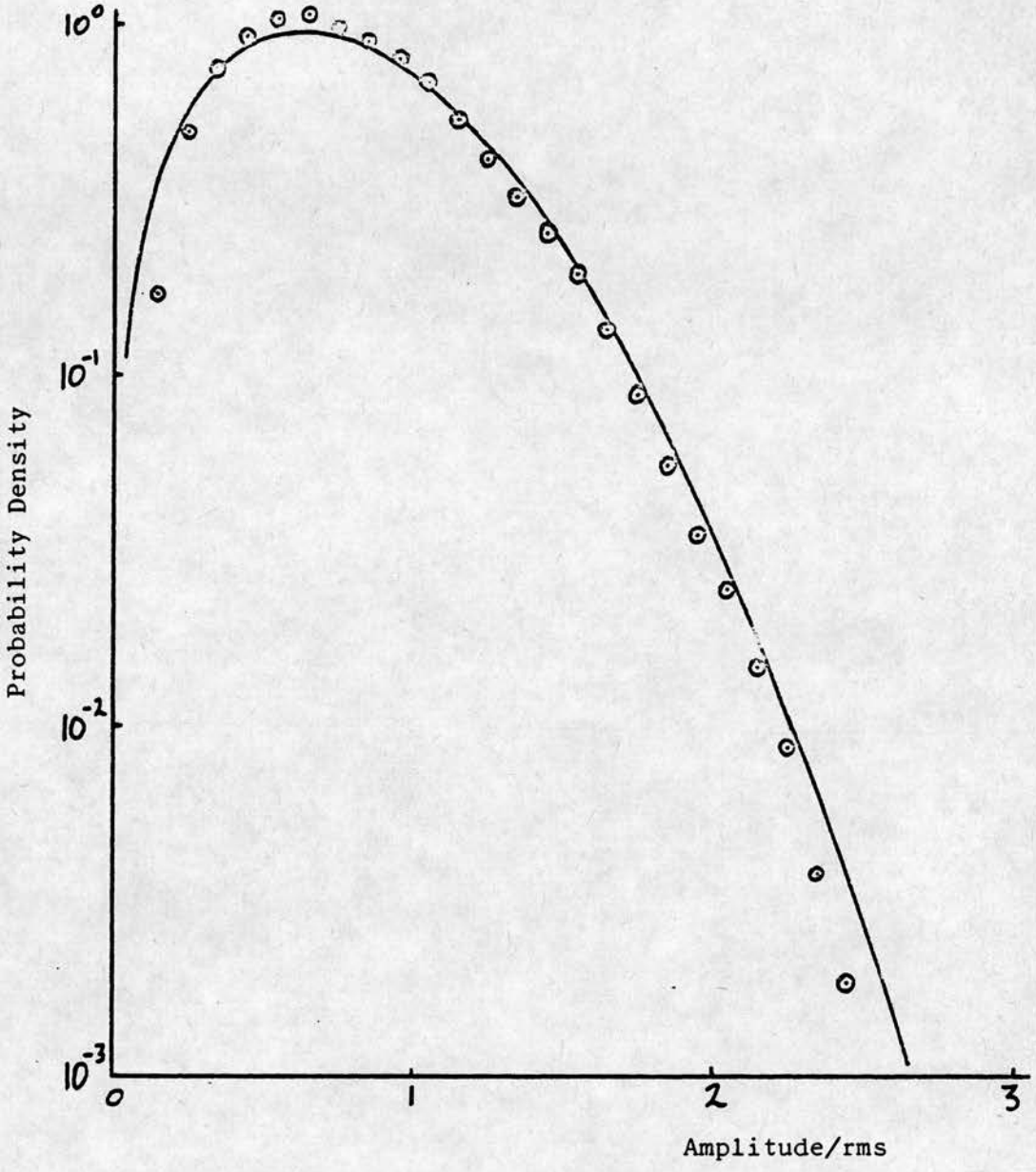

FIGURE 7.8 AMPLITUDE DISTRIBUTION OF MEAN MODULUS OF 0.5 μs SAMPLE OF SYNTHESISED SIGNAL COMPARED WITH RAYLEIGH DISTRIBUTION.

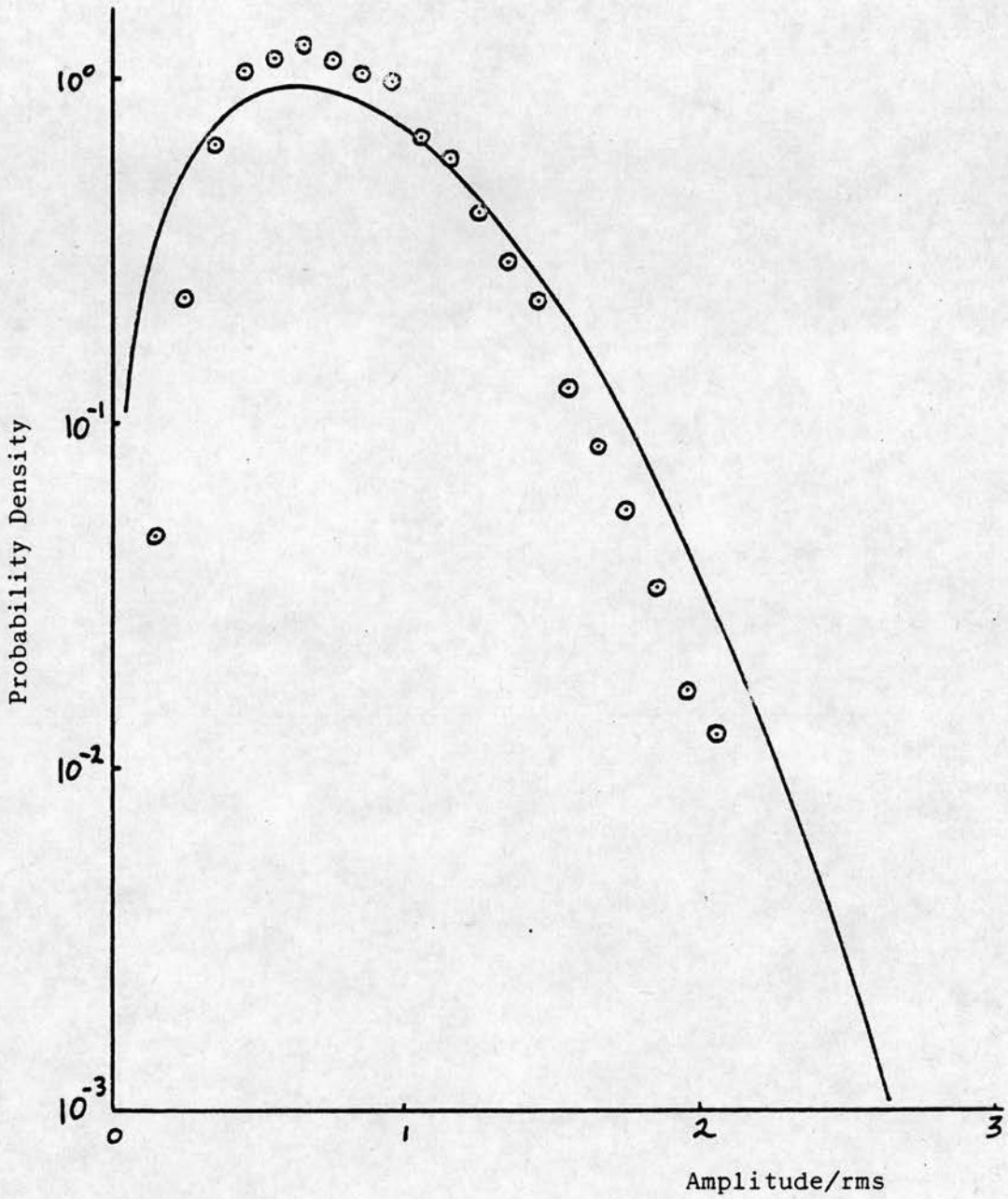

FIGURE 7.9 AMPLITUDE DISTRIBUTION OF MEAN MODULUS OF 1 μs SAMPLE OF SYNTHESISED SIGNAL COMPARED WITH RAYLEIGH DISTRIBUTION.

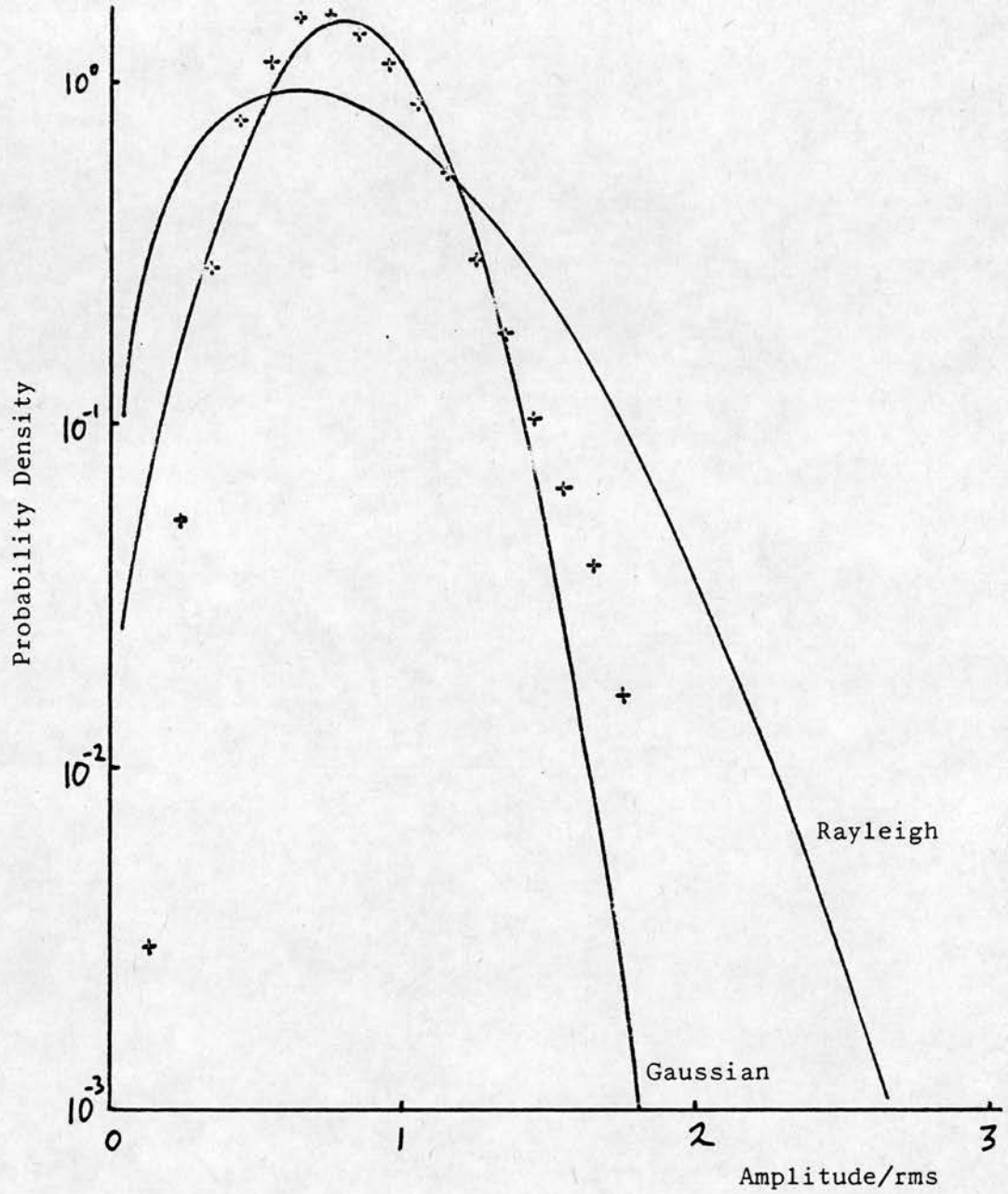

FIGURE 7.10 AMPLITUDE DISTRIBUTION OF MEAN MODULUS OF 2 μs SAMPLE OF SYNTHESISED SIGNAL COMPARED WITH RAYLEIGH DISTRIBUTION AND GAUSSIAN DISTRIBUTION.

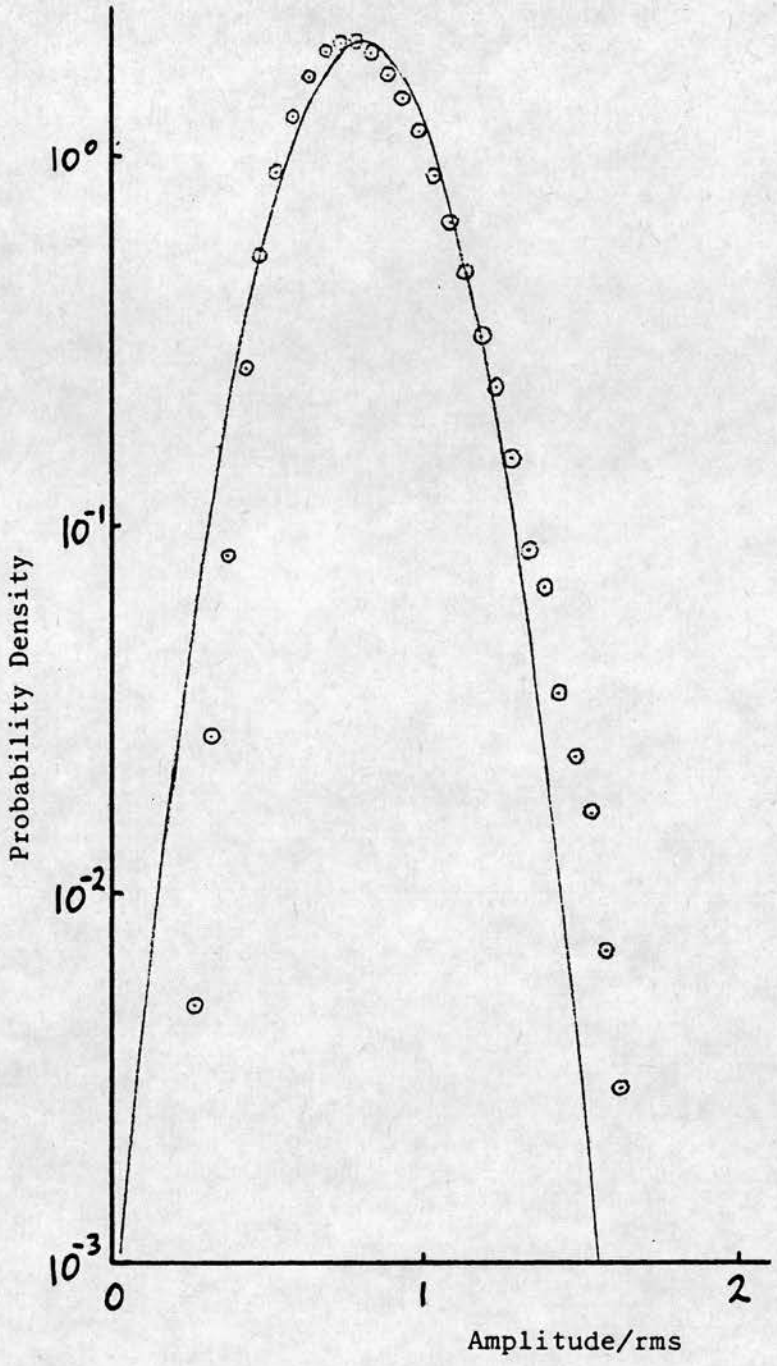

FIGURE 7.11 AMPLITUDE DISTRIBUTION OF MEAN MODULUS OF 4 μs SAMPLE OF SYNTHESISED SIGNAL COMPARED WITH GAUSSIAN DISTRIBUTION.

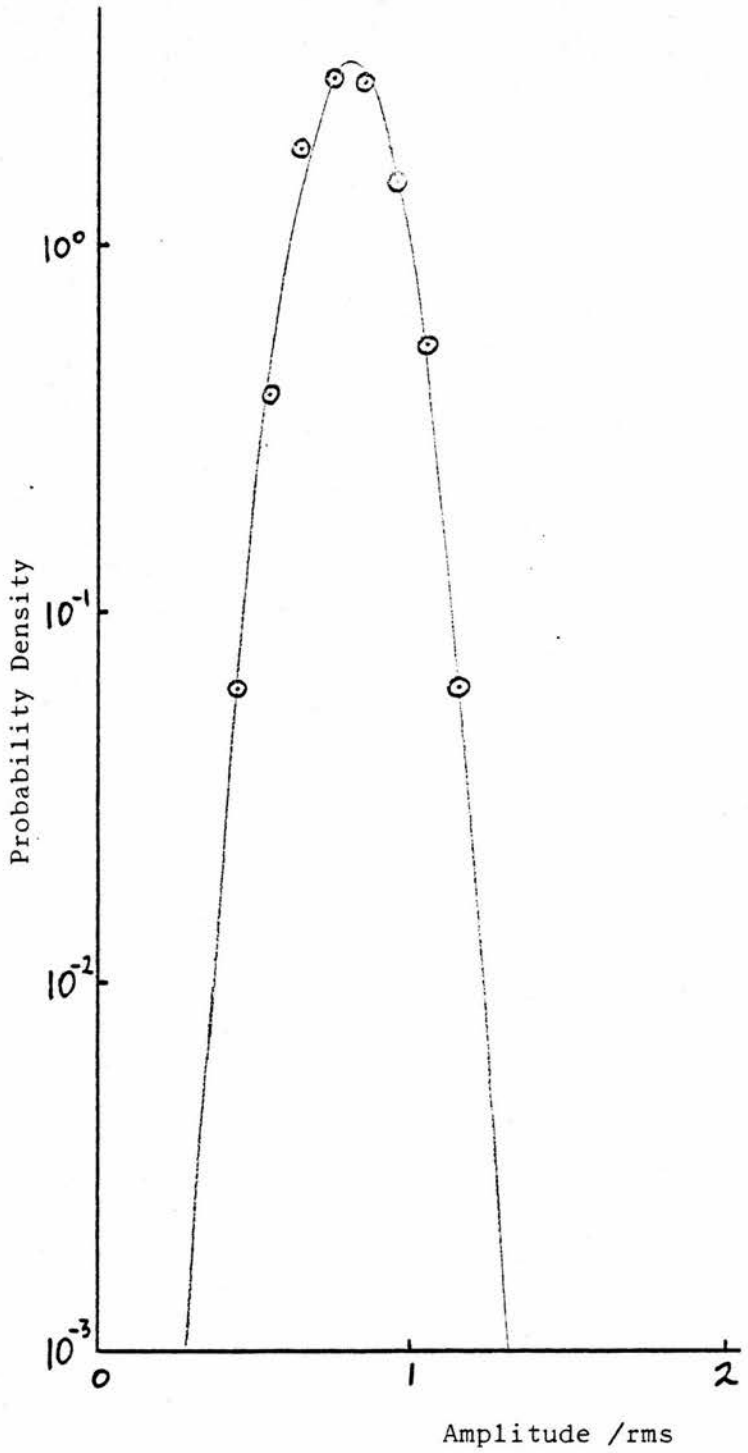

FIGURE 7.12 AMPLITUDE DISTRIBUTION OF MEAN MODULUS OF 10 μs SAMPLE OF SYNTHESISED SIGNAL COMPARED WITH GAUSSIAN DISTRIBUTION.

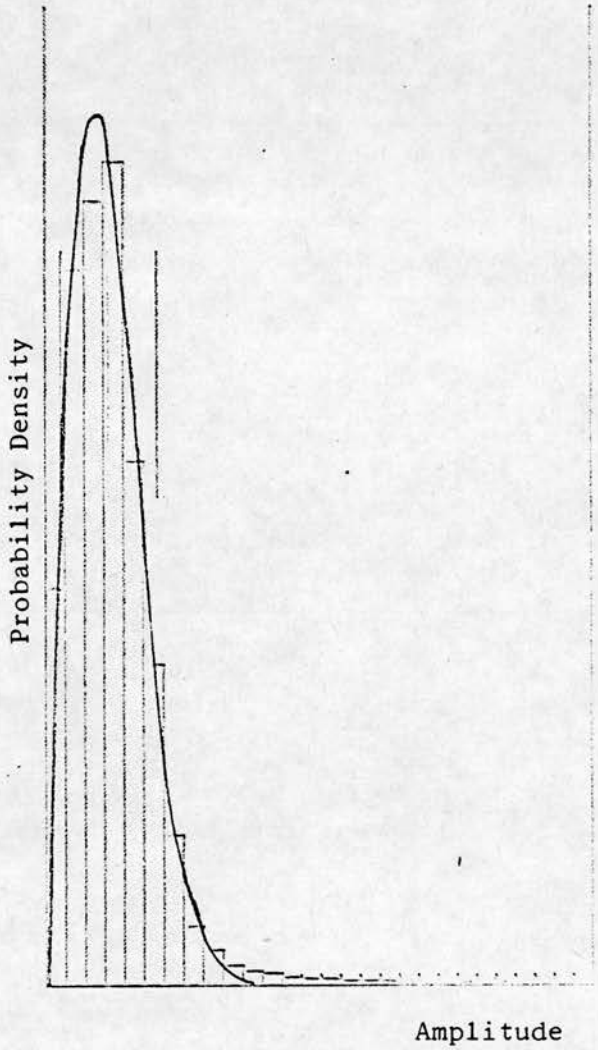

FIGURE 7.13 AMPLITUDE DISTRIBUTION OF MEAN MODULUS OF 0.2 μs SAMPLE OF LIVER ECHO DATA COMPARED WITH RAYLEIGH DISTRIBUTION.

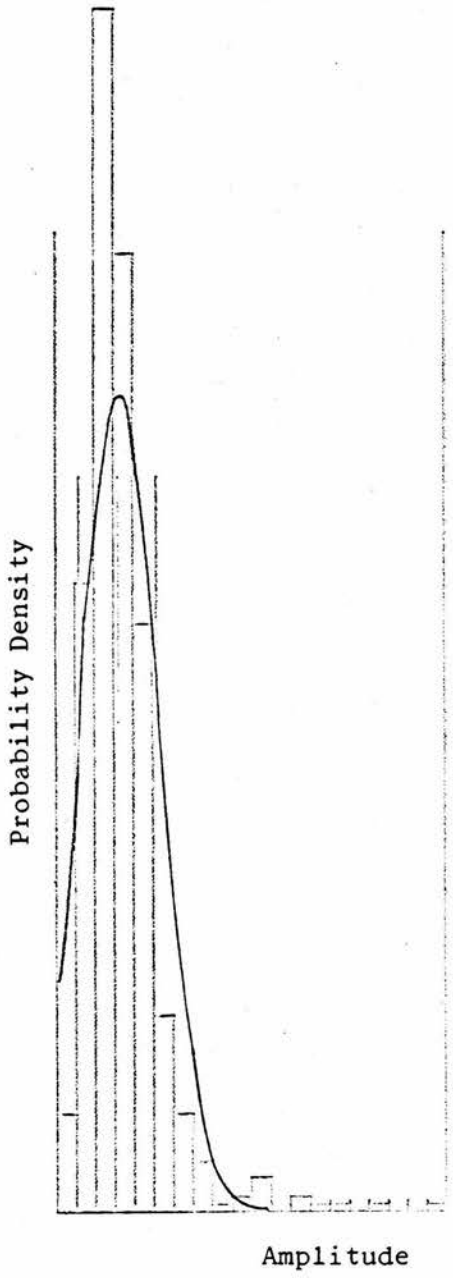

FIGURE 7.14 AMPLITUDE DISTRIBUTION OF MEAN MODULUS OF 2 μs SAMPLE OF LIVER ECHO DATA COMPARED WITH GAUSSIAN DISTRIBUTION.

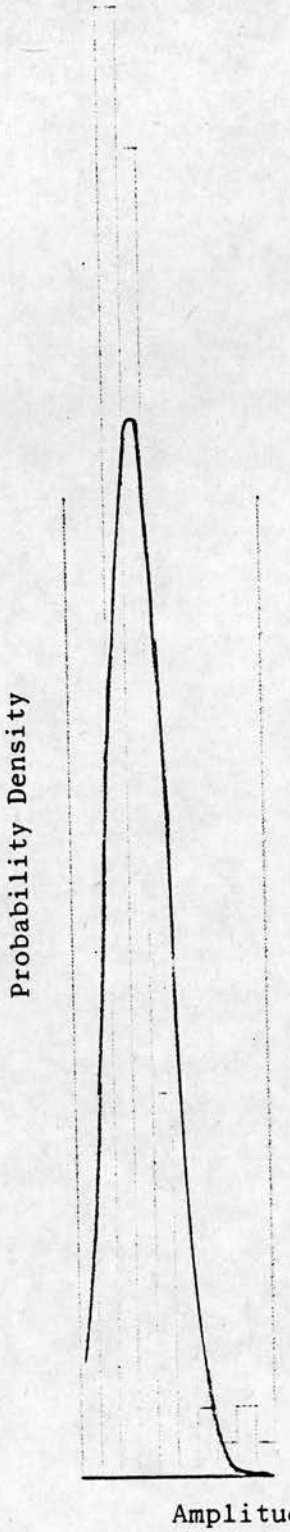

FIGURE 7.15 AMPLITUDE DISTRIBUTION OF MEAN MODULUS OF 10 μs SAMPLE OF LIVER ECHO DATA COMPARED WITH GAUSSIAN DISTRIBUTION.

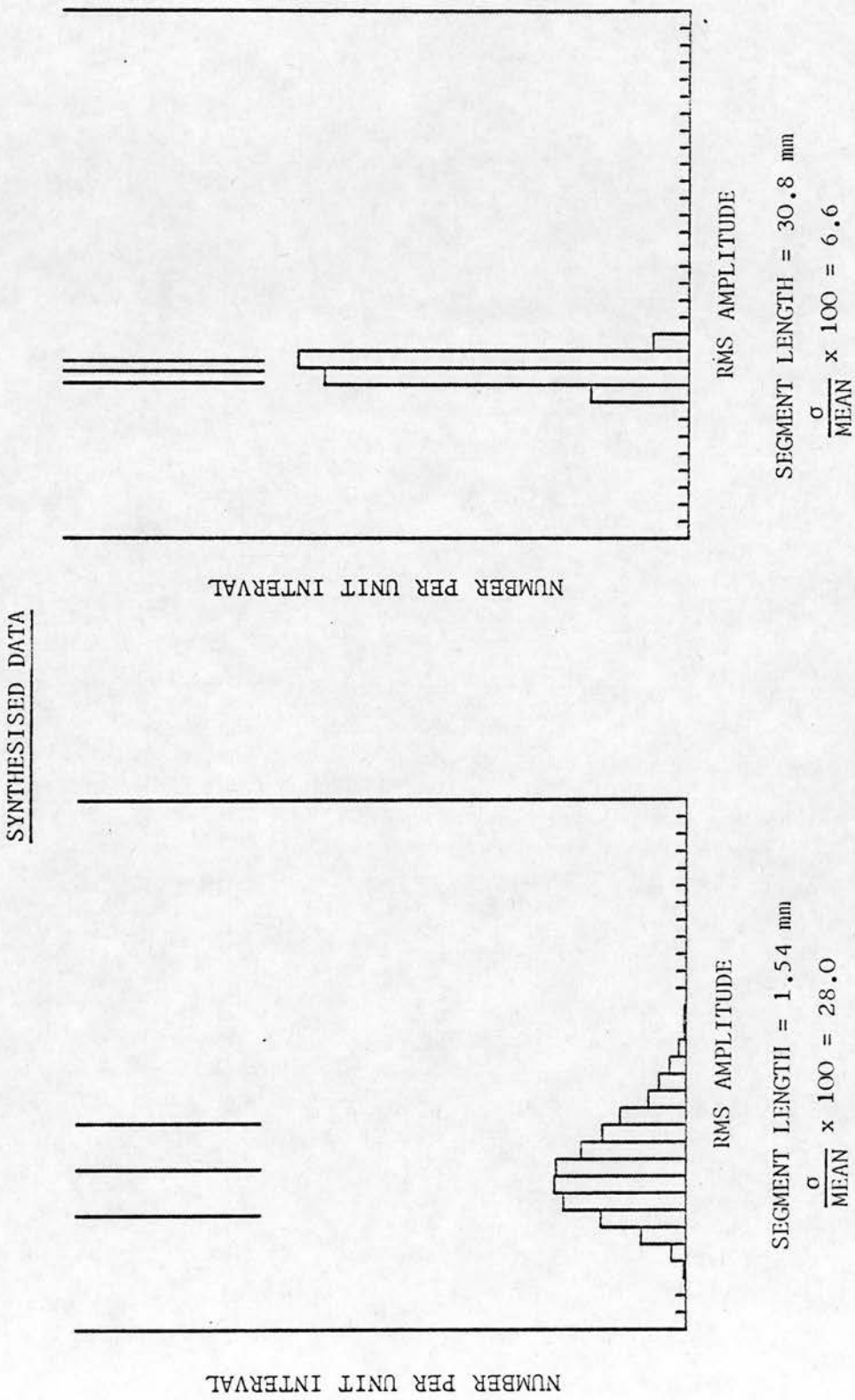

FIGURE 7.16 AMPLITUDE DISTRIBUTIONS FOR RMS OF SAMPLES OF SYNTHESISED DATA.

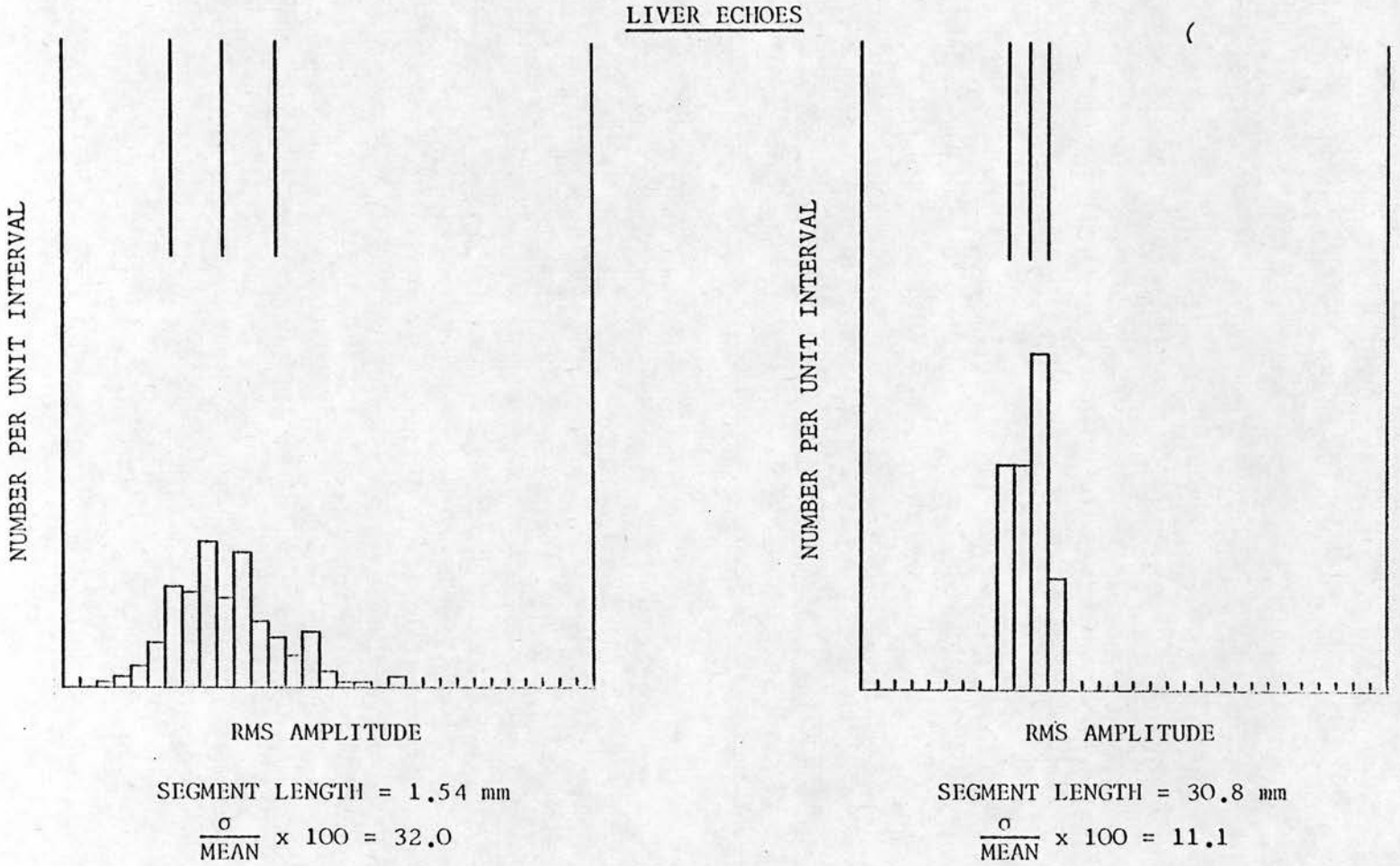

FIGURE 7.17 AMPLITUDE DISTRIBUTIONS FOR RMS OF SAMPLES OF LIVER ECHO DATA.

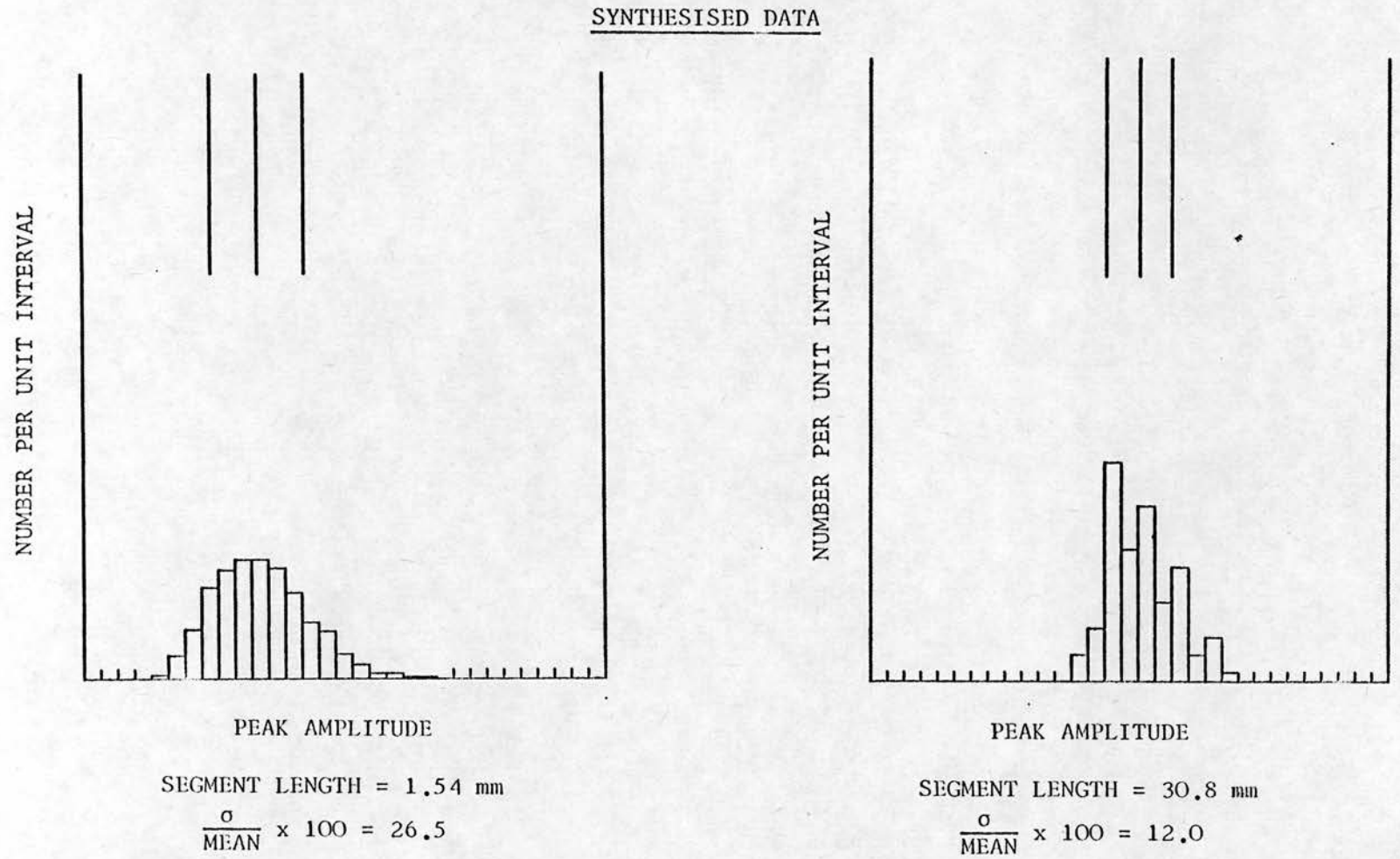

FIGURE 7.18 DISTRIBUTIONS OF PEAK AMPLITUDES WITHIN SAMPLES OF SYNTHESISED DATA.

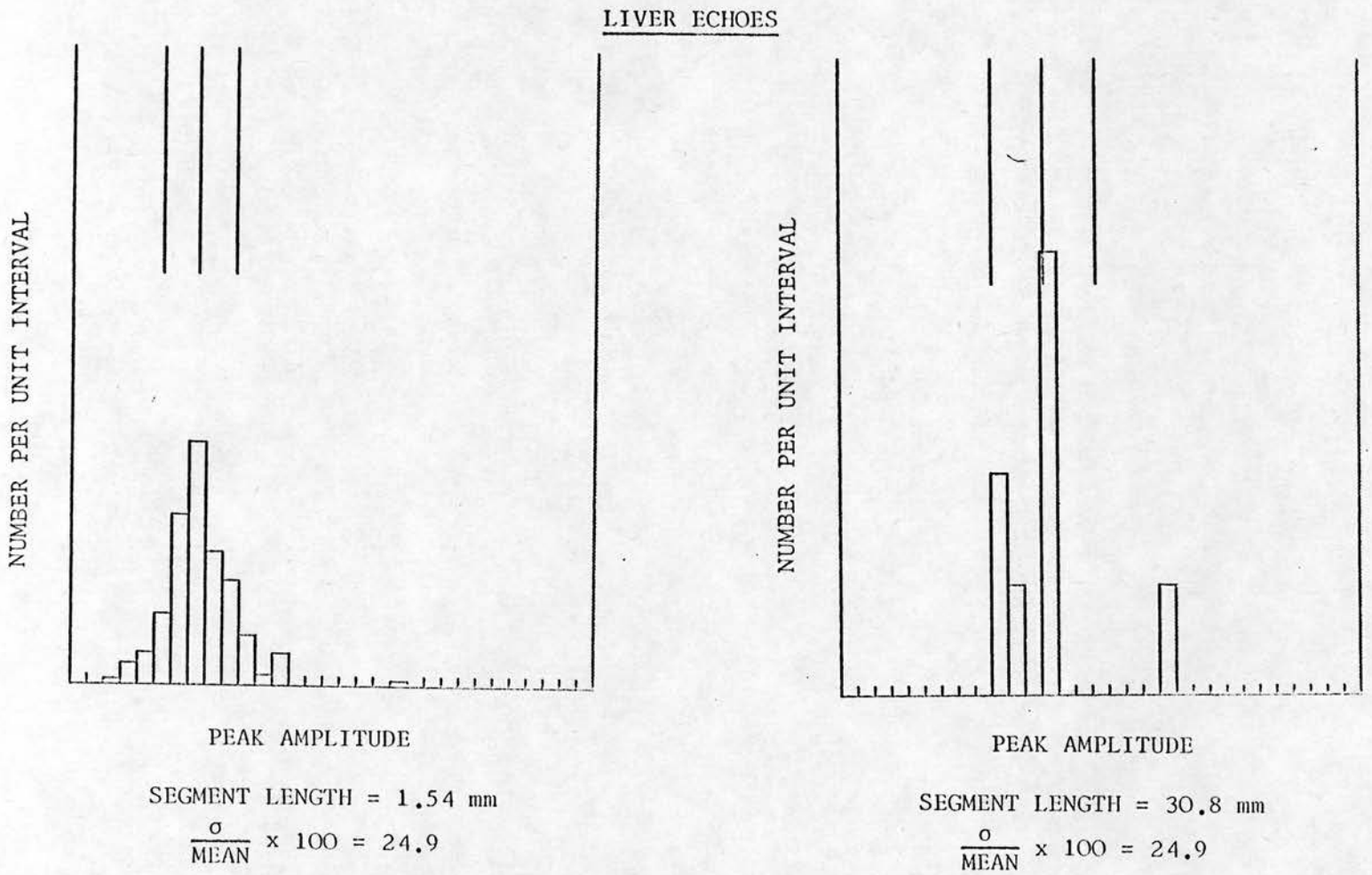

FIGURE 7.19 DISTRIBUTION OF PEAK AMPLITUDES WITHIN SAMPLES OF LIVER ECHO DATA.

7.9.1 RMS processing and peak processing

Synthesised data was processed to find distributions of rms values and peak values. Figure 7.20 shows a graph of the coefficient of variation of the rms value of a sample plotted against the length of the sample. On the same graph is a plot of the coefficient of variation of the peak value within a sample plotted against the sample length. It can be seen that for short segment lengths the coefficients of variation are similar for the two forms of processing. As the sample length is increased the coefficients of variation decrease, and the coefficient of variation decreases more rapidly for the rms processing than for the peak processing. It is to be expected that for long average lengths the peak processing will give a higher coefficient of variation than rms processing. As the sample length is increased the peak value will increase (on average) so a smaller part of the echo amplitude distribution can affect the final peak value. In contrast, for rms processing (and similar averages) all points make a contribution to the final value.

Graphs of the same functions for liver echo data are also plotted in Figure 7.20. Again the values of the coefficients of variation for short sample lengths are similar for rms processing and peak processing, and for longer sample lengths rms processing is seen to be superior to peak processing. However, it can be seen that the coefficient of variation for peak processing does not decrease significantly for longer sample lengths. Only small decreases were found for other livers. The decrease in coefficient of variation with increased sample length for rms processing is also smaller than for synthesised data.

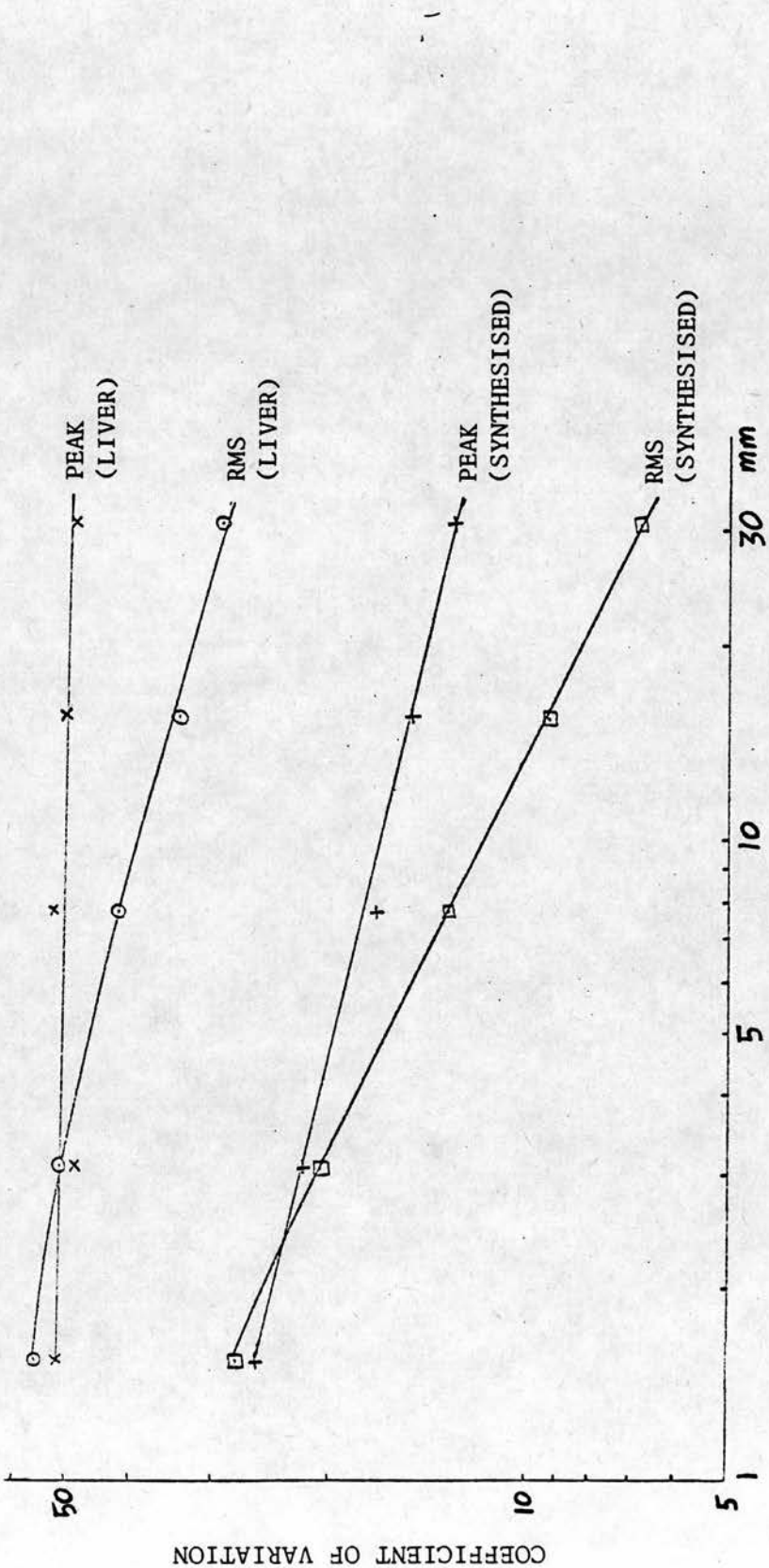

FIGURE 7.20 GRAPH OF COEFFICIENT OF VARIATION AGAINST SAMPLE LENGTH FOR PEAK PROCESSING AND RMS PROCESSING.

The coefficients of variation for both types of processing are larger for liver data than for the synthesised data. This will be discussed in the following sections.

The comparison of different forms of processing is relevant to the design of digital scan converters. A common form of processing is to take the peak value in a small time interval and use that value to assign a value to a pixel (picture element). Figure 7.20 (and similar graphs drawn for other livers) indicate that for sample lengths under about 4 mm the coefficient of variation for peak processing will be as low as for rms processing. Since pixel sizes are typically rather smaller than 4 mm the choice of peak processing would appear to be satisfactory (at least from the point of view of variance of signal values).

If we wish to make more accurate estimates of the echo amplitude longer sample lengths will be required, and for long sample lengths it is expected that rms processing will be superior to peak processing. A form of processing which is easier to implement than rms processing is mean modulus processing; that is, taking the mean of the rectified echo signal within the sample period. Results found for mean modulus processing are discussed in the following sections.

7.9.2 Mean modulus processing

Figure 7.21 shows how the coefficient of variation of the mean modulus of samples of synthesised signal depend on sample length. It is expected that for short sample lengths the width of the

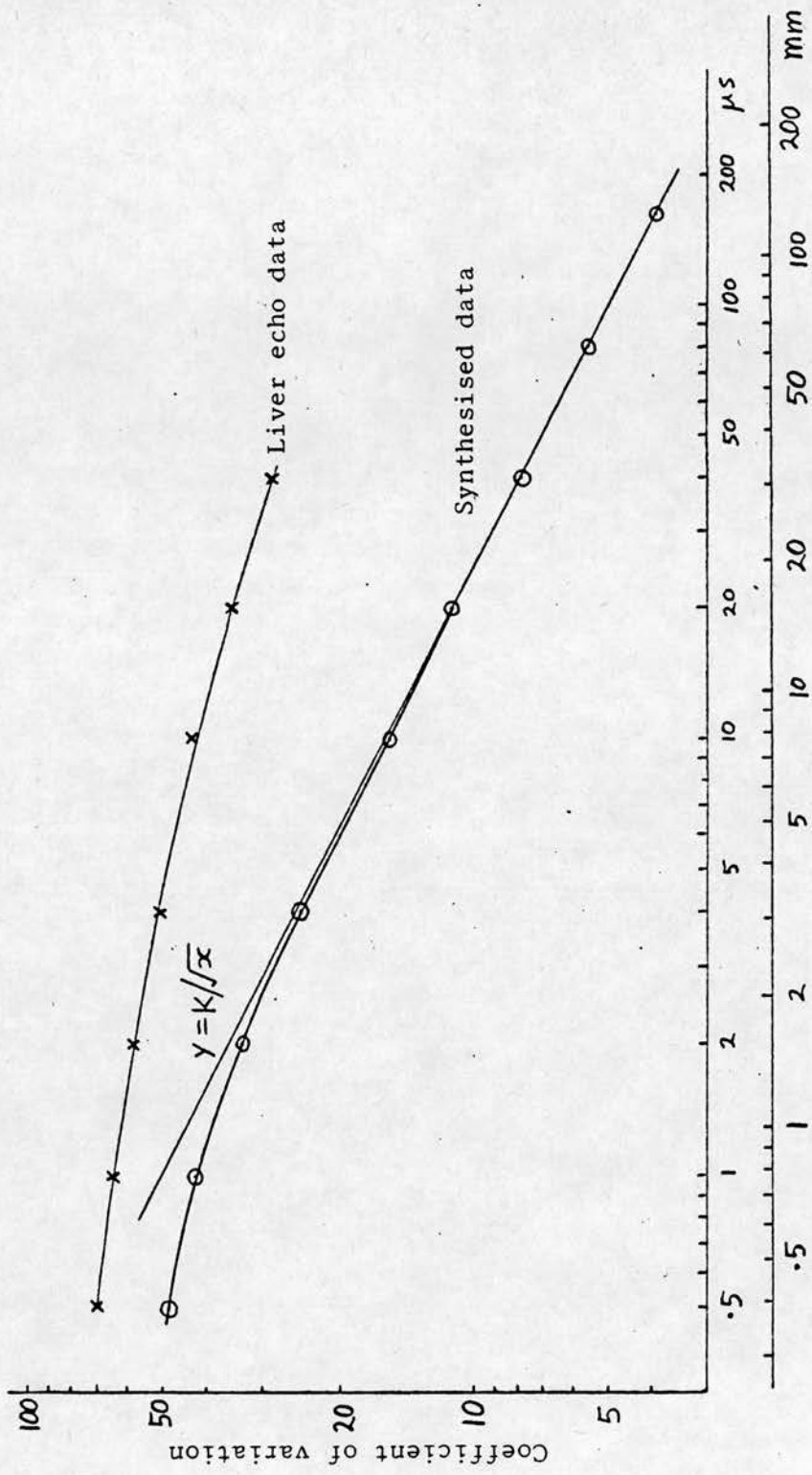

FIGURE 7.21 DEPENDENCE OF COEFFICIENT OF VARIATION OF MEAN MODULUS SAMPLES ON SAMPLE LENGTH

Synthesis parameters: pulse waveform = $F_s(t)$. N = 10, τ = 2 μs, w = $\pm$ 1.

distribution will change only slowly with increased sample length since the closely spaced values of the modulus will be highly correlated. As mentioned in Section 7.8.1 the distribution for mean modulus of samples long compared with the pulse width is expected to approach the Gaussian distribution. The coefficient of variation is expected to be inversely proportional to the square root of the sample length, for large samples. (The mean of n independent random variables, each variable having a standard deviation of σ, is expected to have a standard deviation of $\sigma/\sqrt{n}$).

A line corresponding to the formula $y=K/\sqrt{x}$ has been drawn to allow comparison with the expected asymptotic behaviour of the standard deviation, and it can be seen that the results for the synthesised data do approach that line.

Figure 7.21 also shows how the coefficient of variation of the mean modulus of echo data from a normal liver depends on the sample length. Comparison with the values obtained for synthesised data shows that the echo data from the normal liver has a higher coefficient of variation than the synthesised data and the line has a lower slope than that found for the synthesised data. These two results were found to be typical of all livers analysed in this way.

It is to be expected that the coefficient of variation for liver data is higher than for synthesised data since factors other than interference effects will increase the variation in the signal amplitude. A number of possible explanations for the increased coefficient of variation were investigated. If the tissues overlying

the sample range attenuated the ultrasound by differing amounts for different samples the coefficients of variation would be increased and the slope of log (100 σ/μ) plotted against Log T would be decreased. This possibility is discussed in Section 7.9.3. The effect of errors in the assumed value for the swept gain are discussed in Section 7.9.4. The effect of changing the pulse shape is discussed in Section 7.9.5. The effects of changing the reflector density and form of the distribution of w are discussed in Section 7.9.6. The presence of small ducts and other inhomogeneities are also likely to increase the coefficient of variation (Section 7.9.7).

7.9.3 Effect of overlying tissue

To compensate for differing attenuations in the overlying tissue the echo amplitudes for each 40 μs sample could be normalised to a fixed value before the coefficients of variation were calculated. Instead, for convenience, the coefficient of variation of samples from within one 40 μs sample were calculated, and then the mean of several such coefficients (for several 40 μs samples) was calculated. The dependence of these mean coefficients of variation on sample length are plotted in Figure 7.22. The procedure was performed for liver echo data and for synthesised data. It can be seen that this brings the two plots closer together but there is still a disparity between the two sets of data. It seems likely that variations in attenuation in overlying tissue account for some of the difference between the plots for liver echo data and synthesised data.

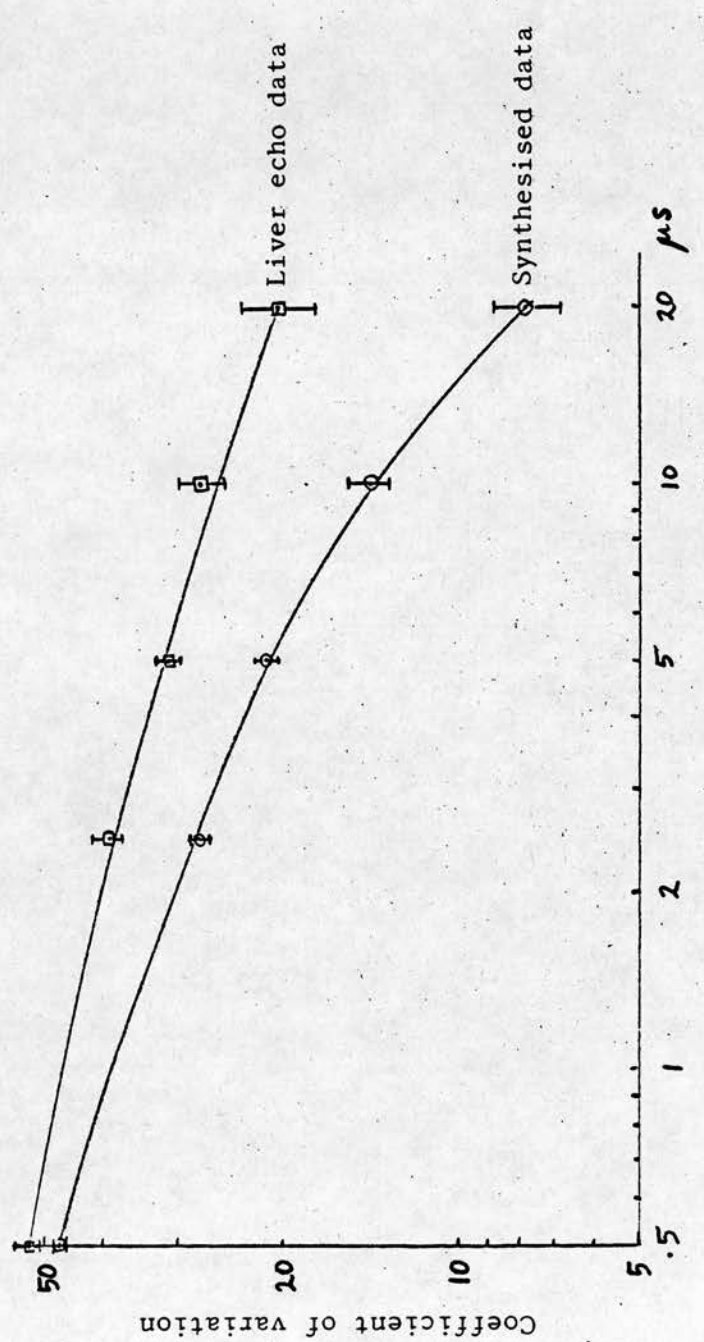

FIGURE 7.22 DEPENDENCE OF MEAN COEFFICIENT OF VARIATION OF MEAN MODULUS SAMPLES ON SAMPLE LENGTH.

Coefficients calculated for samples taken from 40 μs sections of signal.

See text for details.

7.9.4 Effect of error in swept gain

If there was an error in the swept gain the coefficient of variation would be increased. However, using the program SIGPRO to measure the variation of mean echo amplitude with depth shows that the error in the swept gain used to obtain the liver data was under 0.6 dB/cm for the data which was used to produce Figures 7.21-22. A simple estimate indicates that this could only account for a small increase in the coefficient of variation and a simulation including the effects of a swept gain error confirm that an error of 0.6 dB would be insufficient to explain the observed differences. Furthermore, even if the error in the swept gain was high enough to explain the difference in coefficient of variation for small sample lengths it would not account for the high coefficient of variation of the mean modulus of 40 μs samples since all the 40 μs samples start at the same depth, and coefficients of variation are thus little affected by the swept gain.

Although the swept gain error was insufficient to explain the discrepancy in the coefficients of variation of liver echoes and synthesised data its effects should be considered in an accurate comparison.

7.9.5 Effect of pulse shape

The effect of changing the width of the pulse envelope a(t) can be seen in Figure 7.23. As α in equation 7.11 is reduced the pulse width increases and the coefficient of variation of the mean modulus for long sample lengths increases. There is little change in the coefficient of variation for sample lengths comparable with the

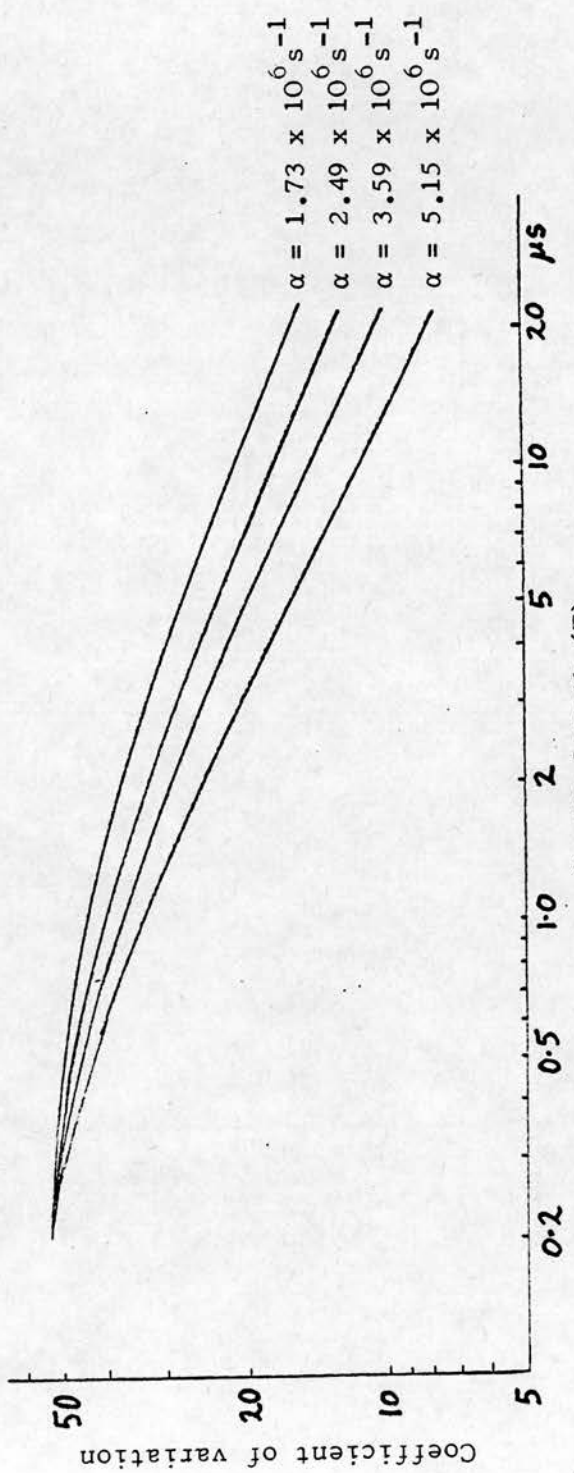

FIGURE 7.23 DEPENDENCE OF COEFFICIENT OF VARIATION ON SAMPLE LENGTH FOR DIFFERENT VALUES OF α. (MEAN MODULUS PROCESSING)

Pulse waveform, $F(t) = a_o t \exp(-\alpha t)\sin(2199150t)$.

$N = 20$, $\tau = 2$ μs, $w = \pm 1$.

wavelength however. This is to be expected, since, for realistic pulse shapes and high reflector densities, the distribution for sample lengths comparable to the wavelength is expected to be a Rayleigh distribution and thus has a fixed coefficient of variation (= $100\sqrt{(4-\pi)/\pi}$ = 52.2723. Thus the discrepancy between liver data and synthesised data remains unexplained. However, for lower reflector densities deviations from the Rayleigh distribution can be expected, resulting in different values for the coefficient of variation. This is discussed in the following section.

7.9.6 Effect of reflector density and amplitude distribution

The synthesised signals used to obtain the results presented so far in this section were all synthesised with high reflector densities and each echo added in with amplitude w = $\pm$ 1. (Here 'high density' refers to densities that are high enough for further increases in reflector density to make little difference to the statistical properties being measured). The distribution of w = $\pm$ 1 was chosen for simplicity after establishing that using any distribution will give similar results at high reflector densities provided all individual echoes are small compared with the rms signal amplitude. The effects of varying the reflector density and the distribution of w are discussed in the following sections.

7.9.6.1 Varying reflector density with w = $\pm$ 1

Signals were synthesised by adding echo pulses of the form $F_s(t)$ defined in Equation 7.12 with w = $\pm$ 1. Figure 7.24 shows the effect of varying the reflector density. It can be seen that the coefficient of variation is highest for low reflector densities and

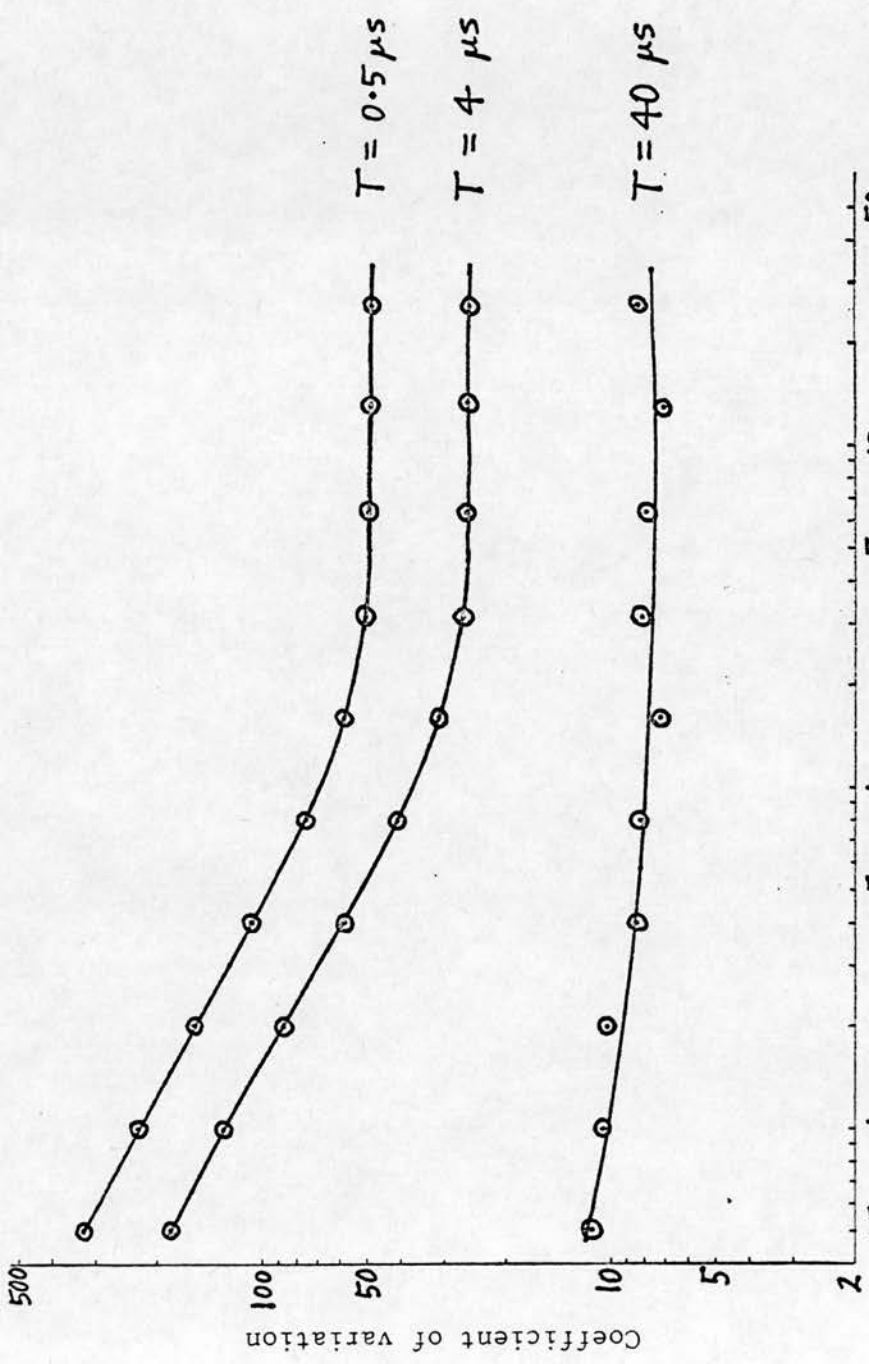

FIGURE 7.24 DEPENDENCE OF COEFFICIENT OF VARIATION OF MEAN MODUS SAMPLES ON REFLECTOR DENSITY.

There are N reflectors in segments of length τ = 20 μs.

Pulse waveform = $F_s(t)$. $w = \pm 1$.

decreases as the reflector density is increased approaching a limiting value with further increases in reflector density making little difference to the coefficient of variation. Under some conditions the coefficient of variation may reach a minimum before rising to a limiting value.

As described in Section 7.2.3 the positions of the scatterers are constrained to keep N scatterers in ranges of length $v\tau/2$. The signals used to obtain Figure 7.24 were synthesised with $\tau = 20\mu s$. The same lines are plotted in Figure 7.25 and compared with values obtained for signals synthesised with $\tau = 2\ \mu s$. Using shorter segment lengths reduces the coefficients of variation for low reflector densities, but at high reflector densities changing τ has little effect.

Due to the method of synthesis, the possible values of t_k in Equation 7.2 are quantised. The amplitude of the pulse waveform which will be added in starting at a time t_d will be the sum of all w_k such that $t_k = t_d$. In the limit of high reflector densities the effective amplitude added in for each possible delay will have a Gaussian distribution (according to the central limit theorem). Similarly, for other distributions of w we will again be able to apply the central limit theorem, provided no single w_k makes a significant contribution to the resultant contribution for that time delay, and again obtain a Gaussian distribution for the contribution for each possible time delay. (The possible individual contributions must come from the distribution of w or be equal to zero for echoes that start at some other time). It seems plausible

that this argument could be extended to the case where the possible values of t_k are continuous by subdividing the total time into small subdivisions, considering the contribution from each subdivision, and taking the limit for the length of subdivision approaching zero. However, I have not attempted to make a rigorous proof along these lines.

Echo signals were synthesised with one echo being added for each possible time delay, and with the echo amplitude w_k having a Gaussian distribution. The values obtained for the coefficients of variation for different sample lengths were found to be the same as the limiting values for high densities (within the limits of statistical error). The values obtained are plotted on the graph in Figure 7.25.

For low reflector densities the main contribution to the coefficient of variation is expected to be due to the random fluctuations in mean echo density. At low reflector densities echo pulses will overlap only rarely and the effects of interference will be negligible. To see what would happen in the absence of any interference, signals were synthesised by adding together waveforms of the form $F(t) = F_s(t)$ with constant sign ($w = +1$). Now the contribution that each pulse waveform makes to a sample value of the mean modulus is independent of the contribution made by the other reflectors. Although the constraint that equal numbers of reflectors exist in consecutive segments complicates the argument, we can predict that the coefficient of variation will be proportional to the $1/\sqrt{n}$ where n is the reflector density. (The mean of n independent random variables, the i^{th} random variable having a

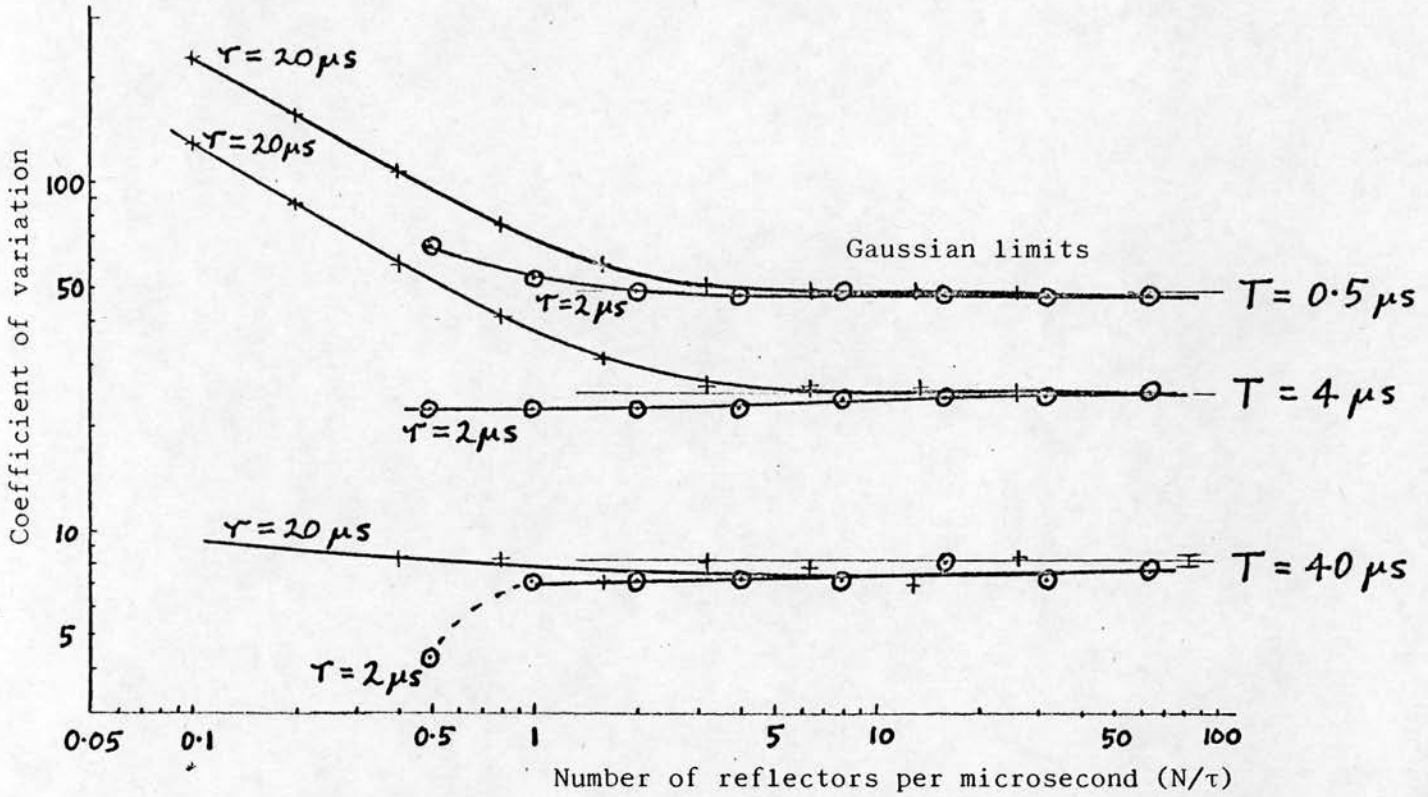

FIGURE 7.25 DEPENDENCE OF COEFFICIENT OF VARIATION OF MEAN MODULUS SAMPLES ON REFLECTOR DENSITY.

There are N reflectors in segments of length τ. The mean modulus samples are of length T.

Pulse waveform = $F_s(t)$. $w = \pm 1$.

Horizontal lines show limits obtained for N = 1, τ = 20 ns, and w having a Gaussian distribution.

standard deviation of σ_i, will have a standard deviation of $(\sum_i \sigma_i^2/n)^{\frac{1}{2}}$).

The effect of varying the 'reflector' density can be seen in Figure 7.26. A straight line of the form $y = K/\sqrt{x}$ has been fitted to the data and a good fit is achieved.

The plots of coefficient of variation against reflector density for synthesised echo data shown in Figure 7.24 are also shown in Figure 7.26 to allow a comparison to be made. This comparison confirms that the variation in mean modulus echo amplitude is mainly due to the variation in mean reflector density for low reflector densities, but for high reflector densities the interference effects make the major contribution.

Comparison with the coefficients of variation for liver echo data shows that whilst agreement can be achieved for short sample lengths the coefficients of variation for long sample lengths will still be higher for liver data than for synthesised data. The low values of coefficient of variation for long sample lengths of synthesised data using low reflector densities is due to adding constant numbers of reflectors in long sample lengths. The use of different forms of constraint on the distribution of t_k could be investigated: the method used was selected for simplicity, as a first step towards studying the effects of constraints on t_k.

The effect of reflector density on signal amplitude is shown in Figure 7.27. The signals were synthesised with $F(t) = F_s(t)$, $\tau = 20$ μs and $w = \pm 1$. The rms value of the signal is proportional to the square root of the reflector density. For low reflector

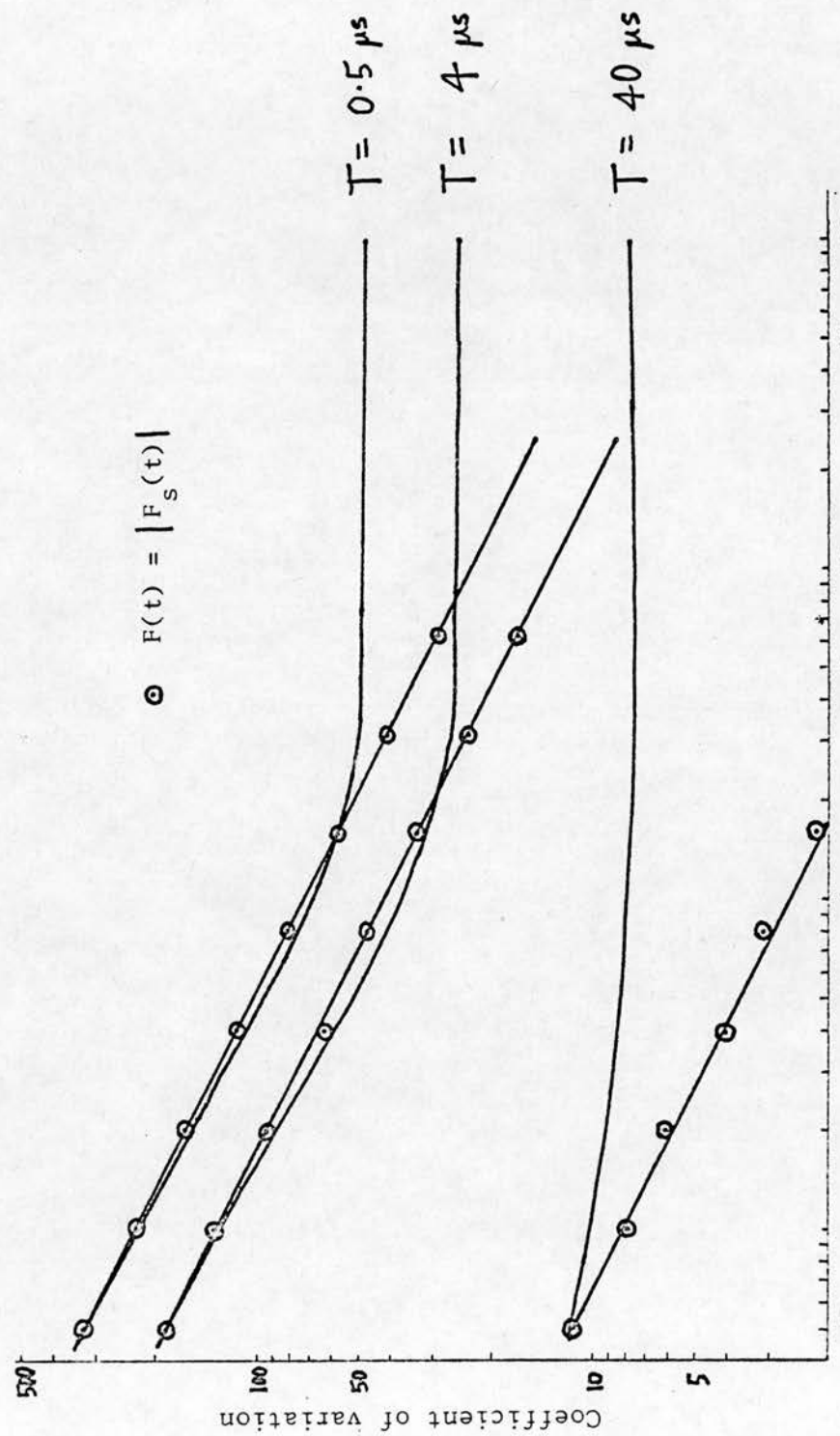

FIGURE 7.26 EFFECT OF ADDING $|F_s(t)|$ WITH CONSTANT SIGN (w = +1).

Data plotted in Figure 7.24 is compared here with data obtained from signals synthesised with $F(t) = |F_s(t)|$ and w = 1. (τ = 20 μs as before).

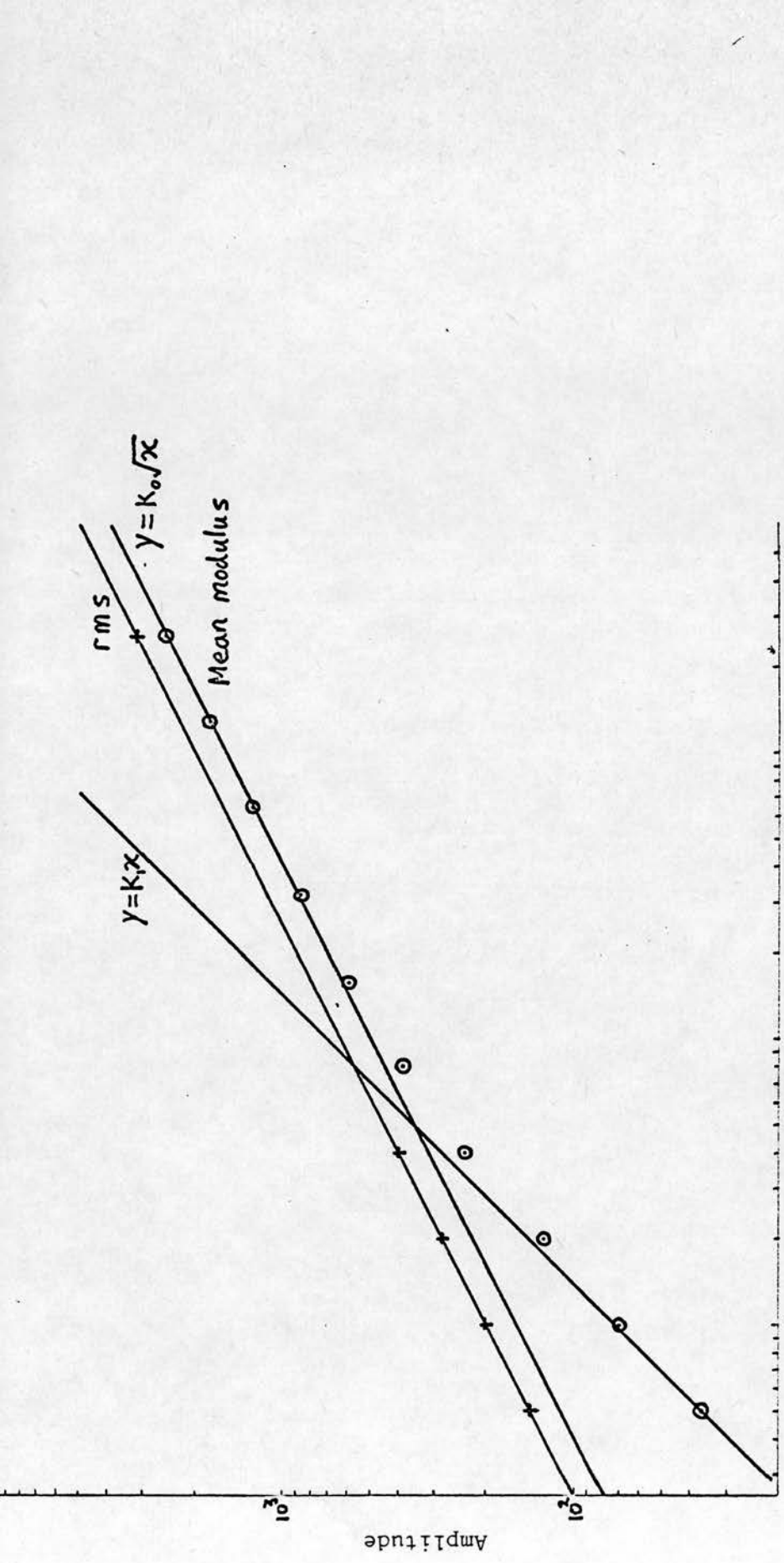

FIGURE 7.27 DEPENDENCE OF ECHO AMPLITUDE (RMS AND MEAN MODULUS) ON REFLECTOR DENSITY.

$F(t) = F_s(t)$, τ = 20 μs, w = ± 1.

densities (and hence negligible interference) the mean modulus amplitude is proportional to the reflector density. For higher reflector densities the mean modulus amplitude is proportional to the square root of the reflector density. This is to be expected since at high reflector densities the probability distribution of the modulus will be semi-normal (Section 7.7) and will thus have a mean value $\sqrt{2/\pi}$ (=.797885) times the rms value.

7.9.6.2 Effect of different distributions of w

The distribution of u can be chosen to give the same amplitude distribution expected for a given form of the transverse beam profile b(h). The form of b(h) used by Atkinson (1974) and Atkinson and Berry (1974) is given by

$$b(h) = \exp(-h/h_B) \qquad (h_b \text{ constant}) \tag{7.25}$$

From Equation 7.3 and 7.5 we have

$$u = b(h) \tag{7.26}$$

giving

$$u = \exp(-h/h_B) \tag{7.27}$$

hence

$$h = h_B \ln(u) \tag{7.28}$$

and

$$du = -u\, dh/h_B \tag{7.29}$$

The probability that the radial displacement is between h and h+dh is Pr(h)dh given by

$$Pr(h)\,dh = Kh\,dh \qquad (7.30)$$

where K is a normalisation constant. Thus the probability that u_k lies between u and u+du is given by $Pr(u_k)du$ obtained by combining Equations 7.28 - 30 :

$$Pr(u)du = Pr(h)dh$$
$$= K_o(\ln(u)/u)\,du \qquad (K_o \text{ constant}) \qquad (7.31)$$

If w = su and s = ± 1 then the probability distribution of w is

$$Pr(w)dw = K_1(\ln(w)/w)\,dw \qquad (K_1 = K_o/2 = \text{constant}) \quad (7.32)$$

Echo signals were synthesised using the distribution of w defined in Equation 7.32. The effect of changing the reflector density is shown in Figure 7.28. It is seen that for high reflector densities the coefficients of variation obtained are close to the values obtained for the distribution w = ± 1 and for w having a Gaussian distribution.

For lower reflector densities the coefficients of variation are higher. The dependence of coefficient of variation on sample length is plotted in Figure 7.29 and compared with the values obtained for liver. The value of reflector density was selected to give the same coefficient of variation for short sample lengths. Again we see that the coefficient of variation for long sample lengths is lower for synthesised data than for the liver data.

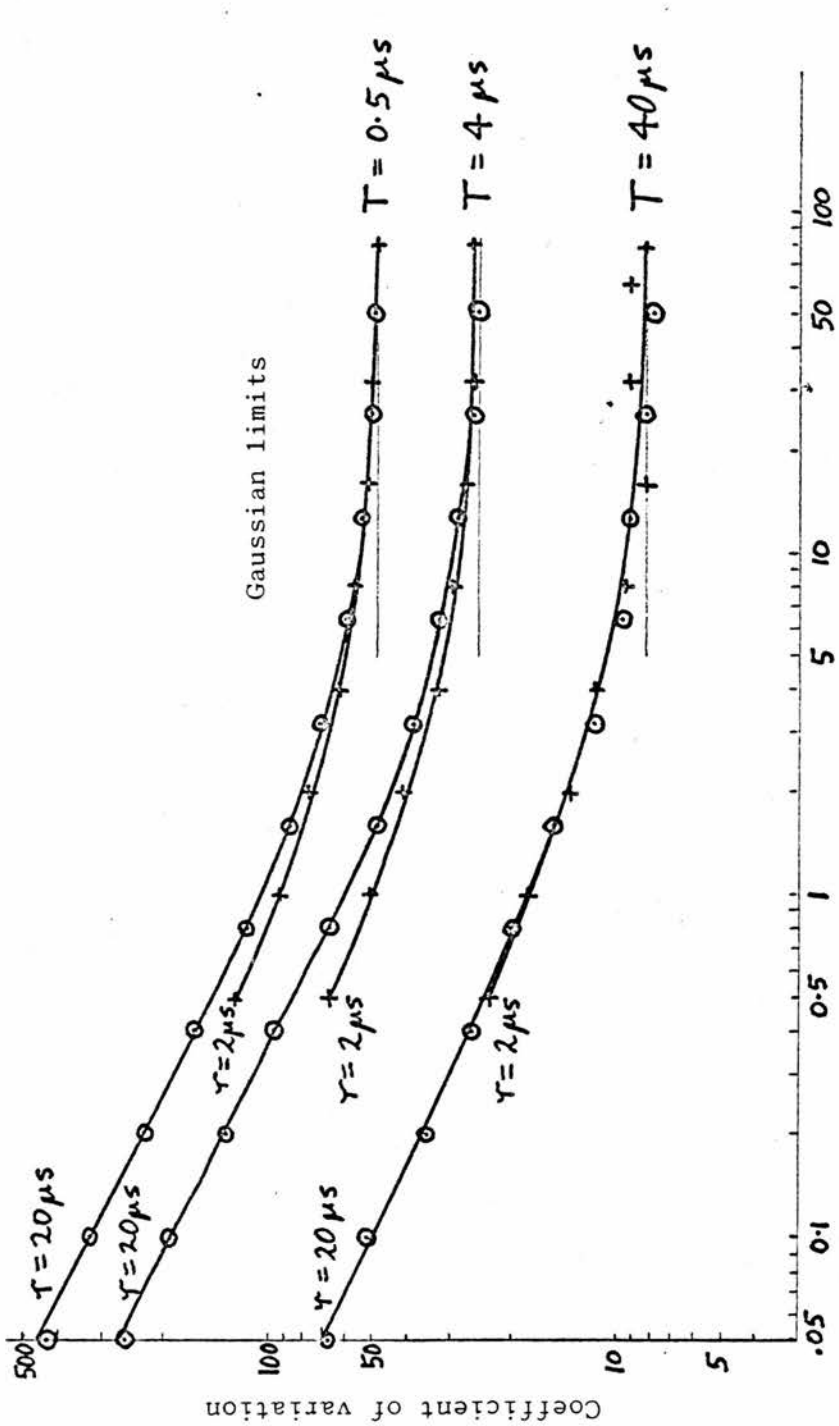

FIGURE 7.28 DEPENDENCE OF COEFFICIENT OF VARIATION OF MEAN MODULUS SAMPLES ON REFLECTOR DENSITY FOR SIGNAL SYNTHESISED WITH DISTRIBUTION OF w APPROPRIATE FOR TRANSVERSE BEAM PROFILE $b(h) = \exp(-h/h_B)$.

(See Equation 7.32). $F(t) = F_s(t)$.

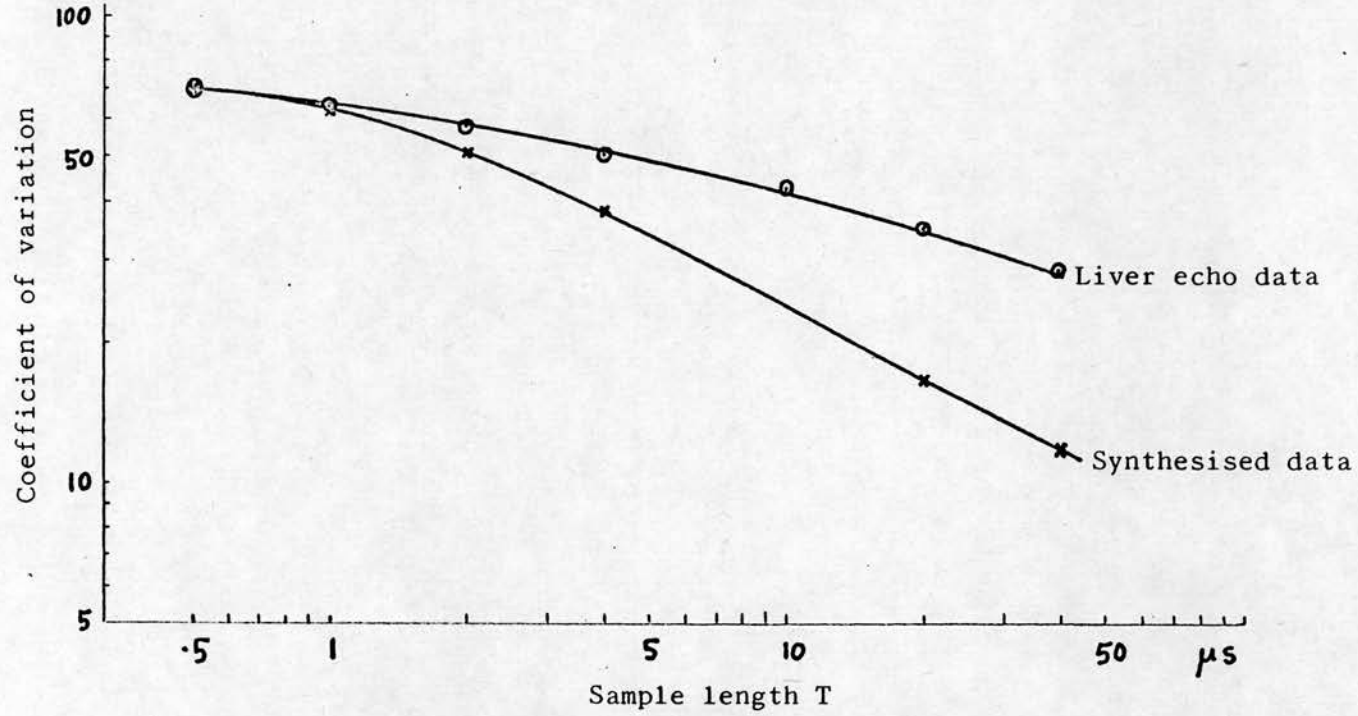

FIGURE 7.29 DEPENDENCE OF COEFFICIENT OF VARIATION OF MEAN MODULUS SAMPLES ON SAMPLE LENGTH.

The reflector density used in the synthesis is selected to give the same coefficient of variation as the liver echo data for short samples. Data synthesised with $F(t) = F_s(t)$, $N = 64$, $\tau = 20$ μs and w has the 'radial' distribution defined in Equation 7.32.

The form of distribution for w will also depend on the distribution of scattering cross sections of the scatterers. To investigate the effect of having a wide distribution for w the following (somewhat unlikely) distribution was used:

$$w = \begin{cases} -9 \text{ with probability } 0.05 \\ -1 \text{ with probability } 0.45 \\ +1 \text{ with probability } 0.45 \\ +9 \text{ with probability } 0.05 \end{cases} \qquad (7.33)$$

Figure 7.30 shows how the coefficients of variation for various sample lengths depend on the reflector density. Again the sample length dependence of the coefficient of variation will not match that found for the liver data.

7.9.7 Effect of ducts and other inhomogeneities

Although the B-scan images can be used to avoid collecting data from regions with large ducts it is not possible to avoid regions of liver containing small ducts.

One method of simulating the effect of inhomogeneities would be to change the distribution of w used to synthesise the data. The effect of this was discussed in the previous section; although the distribution of w can affect the coefficients of variation it seems unlikely that it could result in the sample length dependence observed for liver echo data.

A further method of simulating the effect of inhomogeneities would be to make $g(t_k)$ in Equation 7.2 a random function of t_k. The

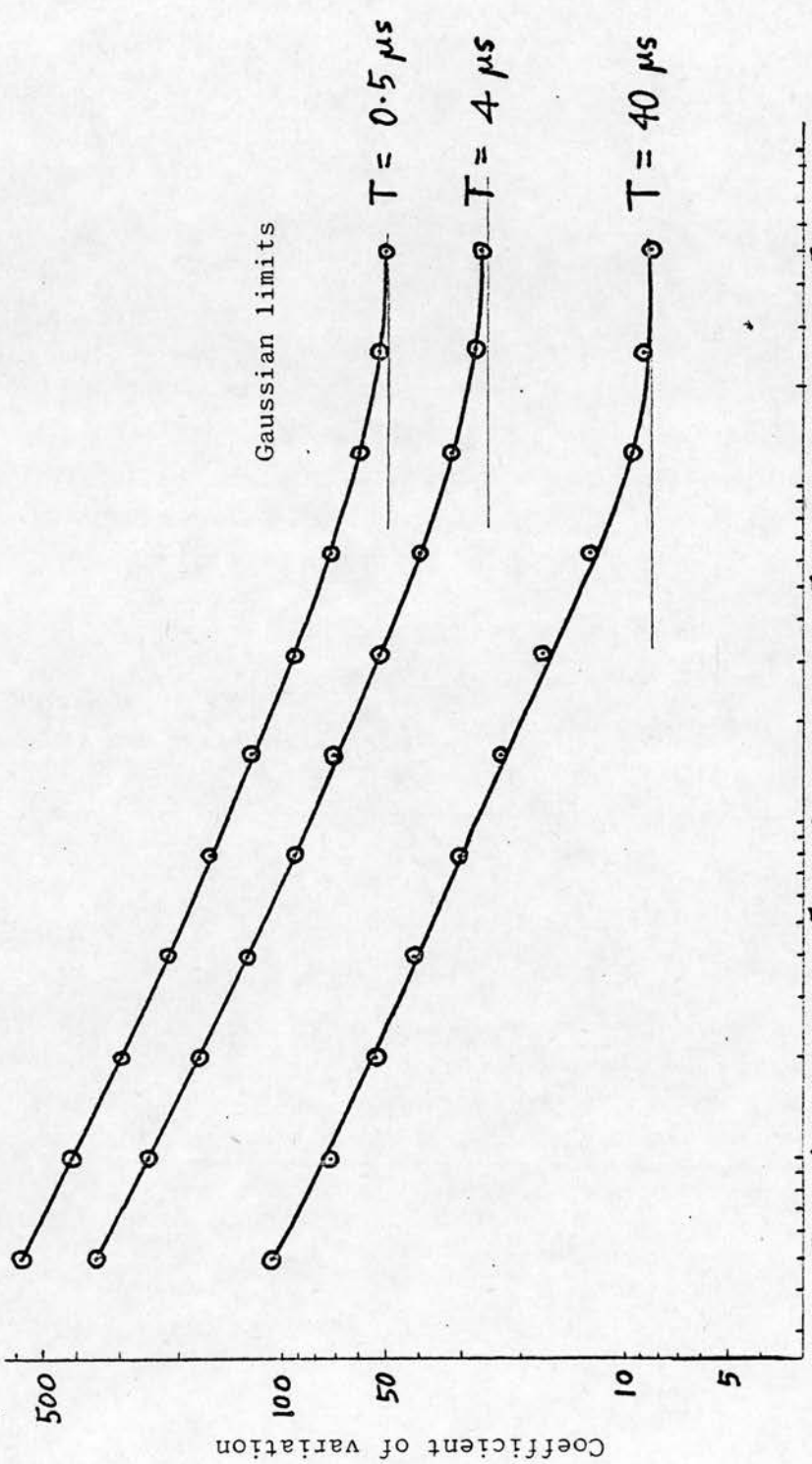

FIGURE 7.30 DEPENDENCE OF COEFFICIENT OF VARIATION OF MEAN MODULUS SAMPLES ON REFLECTOR DENSITY FOR SIGNAL SYNTHESISED WITH DISTRIBUTION OF w DEFINED IN EQUATION 7.33 (wide distribution).

value of g(t) could be constant for small ranges of t and take sudden changes in value at random values of t. At present the function g(t) is specified by keyboard commands and there is no facility included for making it change at random intervals, so this approach remains to be investigated.

7.10 SUMMARY

A program was written to synthesise echo data by adding together pulse waveforms with random time delays. The same program could process the synthesised data and echo data from tissues obtained using the data acquisition system.

Amplitude distribution for samples of the signals were obtained for a range of sample durations. The coefficients of variation of these distributions were obtained. It was found that the liver echo data had higher coefficients of variation than the data synthesised with high reflector densities. This was to be expected since a number of factors which can contribute to the variations in liver echo amplitude are absent in the synthesis process: variable attenuation in overlying tissue, swept gain errors, the presence of ducts and other inhomogeneities. These factors were considered in turn, and no single factor could explain the observed dependence of coefficient of variation on sample length. However, it seems likely that a combination of the factors considered could be responsible for the observed dependence. This could be investigated further by modifying the simulation program to include the effects of random variations in attenuation and mean scattering cross sections.

However, rather than pursue this approach immediately I decided to investigate the properties of the synthesised data further. The detectability of an abnormal region of scatterers surrounded by an array of normal scatterers is discussed in the following chapter. Although the synthesised data does not have the same statistical properties as liver echo data it should be sufficiently realistic to gain an insight into the problems of detecting abnormal regions of the type described.

CHAPTER 8

DETECTION OF ABNORMAL REGIONS

8.1 INTRODUCTION

This chapter is concerned with the detectability of an array of discrete scattering centres surrounded by another array of scattering centres as depicted in Figure 6.1. Interference between echoes from closely spaced scatterers introduces a random element to the echo amplitude. This leads to the problem of deciding whether the observed amplitudes are from an abnormal region or from the distribution to be expected from normal tissue. The problem to be solved was described in more detail in Section 6.5.

8.2 STATISTICAL DECISION THEORY

Statistical decision theory is concerned with deciding between alternative hypotheses when the observations are subject to statistical error (Skolnik, 1962; Hoel, 1971; Goodenough, 1976). This section gives a brief introduction to some of the concepts involved.

Figure 8.1 shows the probability distribution of a random variable y for two alternative hypotheses, H_o and H_1. The hypotheses might be defined as follows:

H_o is the hypothesis that the tissue is normal
H_1 is the hypothesis that the tissue is abnormal

The random variable y will be some function of the received echo waveform. In general there will be more than two hypotheses under

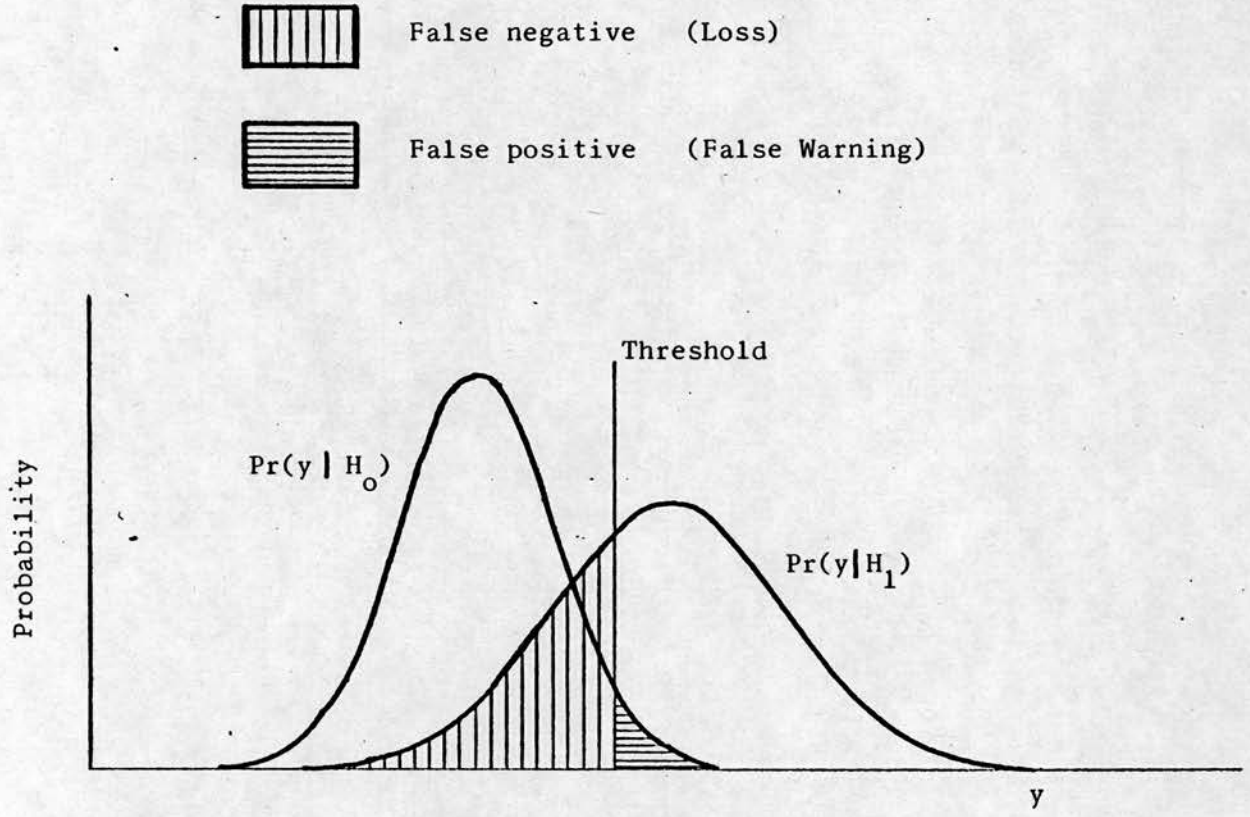

FIGURE 8.1 OVERLAPPING PROBABILITY DISTRIBUTIONS.

consideration but for simplicity only two will be considered in this introduction. Given the above definitions of the hypotheses

$Pr(y|H_o)$ is the probability of the value y occurring given that the tissue is normal

$Pr(y|H_1)$ is the probability of the value y occurring given that the tissue is abnormal

Generally the decision of which hypothesis to accept as true will depend on whether y is greater than or less than some threshold value. Occurrences of y greater than the threshold value when H_o is true will cause the wrong decision to be made (termed 'false alarm' or 'false positive'). Occurrences of y less than the threshold when H_1 is true will also lead to errors (termed 'loss' or 'false negative'). For the distributions shown in Figure 8.1 moving the threshold to reduce one type of error will increase the probability of the other kind of error; hence the choice of threshold level involves a compromise.

One of the tasks of statistical decision theory is to select an appropriate threshold level. Another task is to select the optimum form of signal processing used to obtain y from the signal waveform. In a typical diagnostic ultrasound application y will be a function of echo delay time and will give some measure of the probabilities for the hypotheses H_o and H_1 for the depth corresponding to that delay.

8.2.1 The likelihood ratio

The likelihood ratio is defined as

$$L_r = \frac{Pr(y|H_1)}{Pr(y|H_o)} \qquad (8.1)$$

If the ratio is sufficiently large it is reasonable to suppose that the tissue is abnormal. Various criteria which may be used to select the threshold value of L_r are considered in the following sections.

8.2.2 Baye's rule

The probabilities $Pr(y|H_o)$ and $Pr(y|H_1)$ are known as direct probabilities: $Pr(y|H_o)$ is the probability of y occurring given that H_o is true. Determining which hypothesis is appropriate given that a particular value of y has occurred is a problem of inverse probability. The probabilities of H_o or H_1 being true without knowing the value of y are the a priori probabilities. The probabilities of H_o or H_1 being true for a given value of y are the a posteriori probabilities. The joint probability of y and H_1 may be written

$$Pr(H_1,y) = Pr(H_1)Pr(y|H_1) = Pr(y)Pr(H_1|y) \tag{8.2}$$

Re-writing Equation 8.2 we obtain Baye's rule:

$$Pr(H_1|y) = \frac{Pr(H_1)Pr(y|H_1)}{Pr(y)} \tag{8.3}$$

Since H_o and H_1 are mutually exclusive we may write

$$Pr(y) = Pr(y|H_o)Pr(H_o) + Pr(y|H_1)Pr(H_1) \tag{8.4}$$

and

$$Pr(H_o) = 1 - Pr(H_1) \tag{8.5}$$

Combining Equation 8.3 and 8.4 we obtain

$$Pr(H_1|y) = \frac{Pr(H_1)Pr(y|H_1)}{Pr(y|H_o)Pr(H_o) + Pr(y|H_1)Pr(H_1)} \qquad (8.6)$$

Combining Equations 8.1, 8.5 and 8.6 we obtain

$$Pr(H_1|y) = \frac{L_r(y)Pr(H_1)}{L_r(y)Pr(H_1) + 1 - Pr(H_1)} \qquad (8.7)$$

Thus a system which computes the likelihood ratio L_r may be calibrated in terms of the a posteriori probability $Pr(H_1|y)$ if the a priori probabilities are known. A separate a posteriori probability may be computed for each hypothesis, and the hypothesis with the greatest a posteriori probability is selected as the most likely to explain the event. The method may be modified by ascribing a cost function to errors of different types (Hoel, 1971). The use of Baye's rule in radar applications is described by Woodward (1953).

The requirement that the a priori probabilities $Pr(H_o)$ and $Pr(H_1)$ be known may be a fundamental limitation to the use of Baye's rule. It may be hard to obtain realistic estimates of the a priori probabilities for diagnostic ultrasound problems. The 'a priori' problem is discussed further in Section 8.2.6.

8.2.3 Neyman-Pearson Observer

Named after a statistical test (Hoel, 1971) the Neyman-Pearson Observer sets the threshold level to maximise the probability of detection for a fixed (direct) probability of a false positive decision. It is equivalent to specifying a threshold level K for the likelihood ratio, and determining if $L_r(y) \geqslant K$ where K depends

on the probability of false positives selected.

The Neyman-Pearson criterion does not require a knowledge of the a priori probabilities and could be well suited to diagnostic ultrasound applications.

8.2.4 The 'Ideal' Observer

The Ideal Observer maximises the total probability of making a correct decision. (The term 'ideal' does not imply that it is the ideal criterion). The probability of error is

$$Pr(Error) = Pr(H_o)Pr(False\ negative) + Pr(H_1)Pr(False\ positive) \quad (8.8)$$

Unlike the Neyman-Pearson Observer, the Ideal Observer requires a knowledge of the a priori probabilities, which may be very hard to specify in the case of diagnostic ultrasound.

It is equivalent to examining the likelihood ratio and determining if

$$L_r(y) \gtrless \frac{Pr(H_o)}{Pr(H_1)} \quad (8.9)$$

The Ideal Observer may be modified to allow for the cost of error being different for the two types of error.

8.2.5 Sequential Observer

If the first test yields an inconclusive result the Sequential Observer repeats the test until a specified certainty is achieved. This procedure is frequently applied informally in routine ultrasound B-scanning.

It is equivalent to comparing the likelihood ratio for the n'th test,

$L_r(y_n)$, with two thresholds, $K_{o,n}$ and $K_{1,n}$, whose values may depend on the previous tests. If $L_r(y_n) \ll K_{o,n}$ the hypothesis H_o is accepted. If $L_r(y_n) \gg K_{1,n}$ the hypothesis H_1 is accepted. If $L_r(y_n)$ lies between the two thresholds a further test is made.

In radar applications it can lead to considerable reductions in the number of observations required to achieve given error rates and it can be shown to be superior to both the Neyman-Pearson Observer and the Ideal Observer. It seems likely that it will also have advantages for tissue characterisation methods.

8.2.6 Further comments on the a priori problem

The difficulty of supplying the a priori information is one of the fundamental problems in radar. A similar lack of a priori information exists in the diagnostic ultrasound application.

Since the probability of detection will generally depend on the size of the lesion the a priori probability for different sizes of lesion will be required. If differential diagnosis is required then a priori probabilities for all the possibilities will be required. The a priori probabilities will depend not only on the incidence of the various lesions but also on how early patients present with the case and on the referral system in use in the hospital. A further factor is that the result of the ultrasound scan will often be compared with the results of other tests and may indicate that further tests should be undertaken.

Thus the rigorous applications of statistical decision theory presents many difficulties. However, we can expect the concepts to be useful

for the design of detection systems. The lack of a priori information suggests that a realistic approach would be to use the Neyman-Pearson criterion (Section 8.2.3), which does not require a priori probabilities. The performance of a practical detector could be determined by clinical trials.

8.3 FIELDS USING STATISTICAL DECISION THEORY

It would be quite impractical to give an exhaustive list of the many fields which contribute to statistical decision theory. The following subsections comment on some of the fields which could be of assistance in developing ultrasound detection theory.

8.3.1 Radar

Most of the concepts briefly described in Section 8.2 were taken directly from radar detection theory. Many of the radar detection problems are concerned with distinguishing between noise alone and an echo signal plus noise, and generally the echo signals are widely separated. In the ultrasound detection problem we are considering the noise is essentially multiplicative rather than additive, and we wish to detect extended regions of abnormality rather than isolated targets. Thus we may expect the solutions to the problems to be different. However, many of the concepts involved are relevant and there is clearly much to be learnt from a field which has had such vast resources devoted to it.

References: Berkowitz, 1965; Lawson and UHlenbeck, 1950; Price, 1960; Schwartz, 1970; Skolnik, 1962.

8.3.2 Telecommunications

The detection of signals in the presence of noise presents similar problems in radar and telecommunications. Although many of the techniques (such as error correcting codes) cannot be directly applied to diagnostic ultrasound there is still much relevant material in the field of telecommunications. Of particular relevance is the problem of transmission through fading channels. An example of a fading channel is the ionosphere, from which shortwave radio signals are reflected back to earth. In fading channels the transmitted beam is scattered into multiple paths by random media (Schwartz, 1970). The resulting amplitude at the receiver will depend on the relative phases and attenuation of the separate beams. Changes in the random media result in changes in the amplitude of the received signal. This amounts to multiplicative noise and the cause of the noise is clearly analogous to the interference effects which results in multiplicative noise in scattering from soft tissues. Fading channels are also of importance in underwater acoustic communication and propagation of seismic signals through the earth.

References: Goodyear, 1971; Halliwell, 1974; Schwartz, 1970.

8.3.3 Information theory

Information theory has made major contributions to radar and telecommunications. Detection systems can be assessed in terms of the amount of information they preserve from the received signal (Woodward, 1953).

References: Goodyear, 1971; Pierce, 1973: Schwartz, 1970; Shannon and Weaver, 1949; Woodward, 1953.

8.3.4 Pattern recognition

Statistical decision theory is fundamental to many aspects of pattern recognition (Feucht, 1977). Pattern recognition in medical images by humans has been discussed by Goodenough (1976), Hay and Chesters(1976) and Metz et al. (1976).

8.3.5 Optimisation, system identification, filter theory and control theory

Optimisation theory has been applied to making decisions on the basis of observations subject to statistical errors. A comprehensive treatment of optimisation theory is given by Wilde and Beightler (1976).

System identification is the process of determining the differential equations that can be used to describe a physical process (Sage and Melsa, 1971). The equations are to be determined by measuring the response of the system to a known input. In addition to the known input there is also an unknown noise input and the measurements are also subject to noise. Since system identification involves the estimation of parameters in the presence of noise it is relevant to the ultrasound detection problem.

Closely related to system identification are filter theory and control theory. One of the concerns of filter theory is the optimal separation of signals and noise. A number of control problems are mathematically equivalent to filter theory problems (Zadeh, 1960).

References: Barham and Humphries, 1969; Davenport and Root, 1958; Kailath, 1974; Kuk, 1979; Zadeh, 1960.

8.4 DETECTION OF A CHANGE IN MEAN

In a typical radar application the aim is to detect one or more isolated objects. In our ultrasound problem the target may be extended over a considerable range and we should try to make optimum use of the extended nature of the target.

We wish to detect a change in mean value of the echo amplitude over the range of depth corresponding to the abnormality. A simplification is to treat it as the problem of detecting changes in mean in a sequence of random variables. For example Chernoff and Zacks (1964) consider successive observations of n independently and normally distributed random variables $X_1, X_2, \ldots, X_n$ with means $\mu_1, \mu_2, \ldots, \mu_n$ and variance 1. Each mean μ_i is equal to the preceding mean μ_{i-1} except when an occasional change takes place. The problem is to estimate the current mean μ_n. The problem is discussed within a Baysian framework. Similar statistics problems are discussed by Hinkley (1970), Sen and Srivastava (1975), and Hines (1976).

The a priori assumptions about the distributions and the changes in the distributions are not strictly appropriate for the ultrasound detection problem and it would be hard to predict the effect of the differences. The problems considered in the above references are far from trivial and it seems that a purely analytic approach to the ultrasound detection problem would be very difficult. Hence, I decided to investigate the problem using simulations.

8.5 USE OF A MOVING AVERAGE AS AN ESTIMATOR

Due to the difficulty of deriving the ideal estimator analytically

I decided to study the use of a moving average of the rectified echo signal as a simple estimate of the current mean value of echogenicity. The moving mean modulus M(t,T) is defined as

$$M(t,T) = \frac{1}{T}\int_{t}^{t+T} \left|P(t')\right| dt' \qquad (8.10)$$

The moving mean modulus could be compared with a threshold to decide whether the tissue should be taken to be normal or abnormal. To detect small abnormalities a short moving average (small T) would be required, but for large abnormalities a longer moving average would be expected to give better performance. It is hoped that the experience gained in studying the simple moving average will be of use in designing better estimators in the future.

By taking the moving average of the modulus of the echo waveform we are not making use of phase information. However, since it is possible to diagnose some liver metastases from grey scale images of the liver it must be possible to detect metastases by analysis of echo amplitudes. Methods using phase information could be investigated at a later stage.

To study the detection of abnormal region signals were synthesised using a depth dependent $g(t_k)$ in Equation 7.2. This is described in later sections. First we consider the number of false warnings that will occur if the moving average and threshold detector are used to test normal signals (synthesised with $g(t_k) = 1$).

8.6 LEVEL CROSSING THEORY

The amplitude distributions of moving averages of the type defined

in Equation 8.10 were obtained in the last chapter. The moving average of the modulus of the signal has the same distribution as independent samples of the mean modulus of the signal due to its ergodicity (Section 7.5). From these distributions we can obtain the fraction of time spent above or below a threshold level. However, knowledge of the distributions alone tells us nothing about how often a threshold level is crossed. Since the frequency of level crossings gives a measure of how often there will be a false warning it is a useful factor to determine.

Level crossing theory has been applied in many fields: a review paper on the subject (Blake and Lindsey, 1973) contains 133 references. One of the early papers in the field was by Rice (1944, 1945). A more general treatment of the subject is given by Cramer and Leadbetter (1967).

Consider the number of times, $N_t(\Phi)$, that an ergodic random process $x(t)$ crosses a level Φ in unit time. Let the joint distribution of x and $\dot{x}$ $(=\frac{dx}{dt})$ be given by $p(\Phi,\beta)$ defined by

$$p(\Phi,\beta)\, d\Phi d\beta = \Pr(\Phi \leqslant x < \Phi + d\Phi,\ \beta \leqslant \dot{x} < \beta + d\beta) \qquad (8.11)$$

If the process crosses the threshold level Φ with velocity β, then, neglecting second order effects, it will take $(d\Phi/|\beta|)$ time units to cross $(\Phi,\Phi + d\Phi)$. Hence the expected number of crossings of level Φ per unit time with velocity in the range $(\beta,\beta + d\beta)$ is

$$\frac{p(\Phi,\beta)\, d\Phi d\beta}{d\Phi/|\beta|} = |\beta| p(\Phi,\beta)\, d\beta \qquad (8.12)$$

and the expected number of crossings (up or down) of level Φ per unit

time is

$$N_t(\Phi) = \int_{-\infty}^{\infty} |\beta|\ p(\Phi,\beta)\ d\beta \qquad (8.13)$$

The level crossing frequency of a moving mean modulus of synthesised echo signals is determined in Section 8.8. First we consider the related problem of level crossings of the signal envelope.

8.7 LEVEL CROSSINGS OF THE ECHO SIGNAL ENVELOPE

8.7.1 Random echoes from blood

Atkinson (1974) and Atkinson and Berry (1974) represent echo signals from blood as a summation of pulses from the individual blood corpuscules. The blood corpuscules are assumed to be randomly distributed in space although their centres have a minimum separation due to their physical size. The random distribution leads to the echo amplitudes having a Gaussian distribution and the envelope has a Rayleigh distribution. The fluctuations in the envelope will change if the blood moves. This variation in echo amplitude with time has been used as the basis of a novel form of blood flow meter.

The theoretical level crossing frequency of the signal envelope was found to disagree with the measured value. Since the theory should apply to the signals synthesised by the method described in Chapter 7 I decided to try to resolve the discrepancy by determining the level crossing frequency of the envelope of the synthesised echo waveform. It would be a useful check of the theory and since it is the basis of a blood flow meter the result could be of practical value.

8.7.2 Comparison between theory, experiment and simulation

The theory of Atkinson and Berry (1974) is based on the theory of scattering of radar signals by rough surfaces (Berry, 1973; Beckmann and Spizzichino, 1963). Following Berry (1973) the probability distribution $Pr(\Phi)$ of the envelope is given by the Rayleigh distribution:

$$Pr(\Phi) = \frac{\Phi}{\sigma^2} \exp\left\{-\frac{\Phi^2}{2\sigma^2}\right\} \qquad (8.14)$$

where σ gives the rms amplitude of the echo amplitude. If $C(t)$ is the autocorrelation function of the echo signal then the level crossing frequency (fading factor), $N_t(\Phi)$, of the level Φ is given by

$$N_t(\Phi) = Pr(\Phi) \left[\frac{-2\sigma^2}{\pi} \frac{\delta^2 C(o)}{\delta t^2}\right]^{\frac{1}{2}} \qquad (8.15)$$
(Berry, 4.38)

The level crossing frequency for the mean level $\mu = \sigma\sqrt{\pi/2}$ will therefore be

$$N_t(\mu) = \exp(-\pi/4) \left[\frac{-\delta^2 C(o)}{\delta t^2}\right]^{\frac{1}{2}} \qquad (8.16)$$

The pulse envelope $a(t)$ used in Atkinson's theory was the Gaussian form

$$a(t) = a_o \exp(-t^2/2T_p^2) \qquad (a_o, T_p \text{ constant}) \qquad (8.17)$$

Using the relation

$$\frac{\delta^2 C(o)}{\delta t^2} = \frac{-\int_{-\infty}^{\infty} [da(t)/dt]^2 \, dt}{\int_{-\infty}^{\infty} [a(t)]^2 \, dt} \qquad (8.18)$$

and combining with Equations 8.16 and 8.17 they obtain

$$N_t(\mu) = \frac{\exp(-\pi/4)}{T_p\sqrt{2}} = \frac{0.322}{T_p} \qquad (8.19)$$

The pulse shape used by Atkinson to obtain the experimental level crossing frequency was not Gaussian. To apply the above formula Atkinson selected a value of T_p to give the same full width at half maximum as the experimental pulse, assuming that this would not lead to any serious error (but see below). Using a value of $T_p = 0.45 \pm 0.03$ μs (to give a full width at half maximum of $T_p(8 \ln 2)^{\frac{1}{2}} = 1.06 \pm 0.07$ μs) they obtain

$$N_t(\mu) = \begin{matrix} (0.72 \pm 0.05) \text{ MHz} & \text{(theory, Atkinson)} \\ (0.53 \pm 0.05) \text{ MHz} & \text{(experiment, Atkinson)} \end{matrix} \qquad (8.20)$$

It seemed possible that this disagreement could be due to using a different pulse envelope so I synthesised signals using a Gaussian envelope and a gamma envelope (named after the statistical distribution). The gamma envelope is of the form defined previously in Equation 7.11

$$a(t) = a_o t \exp(-\alpha t)$$

The width of the gamma pulse envelope was obtained numerically and found to be $(2.445/\alpha)$. To give the same full width at half maximum as Atkinson's pulse a value of $\alpha = 2306604\ s^{-1}$ was used.

The experimental arrangement used by Atkinson smooths the rectified echo waveform with a filter having a time constant of approximately one wave period (0.5 μs). To approximate this the modulus of the synthesised envelope was averaged over 0.5 μs periods. The resulting sequence of samples (with an interval also of 0.5 μs) was then processed to determine the mean-level crossing frequency. The results obtained for the two pulse envelopes were

$$N_t(\mu) = \begin{cases} (0.62 \pm 0.01)\ \text{MHz} & \text{(synthesised with Gaussian pulse)} \\ (0.64 \pm 0.01)\ \text{MHz} & \text{(synthesised with gamma pulse)} \end{cases} \quad (8.21)$$

The simulation results lay tantalisingly between Atkinson's theoretical and experimental results (Equation 8.20) and out of agreement with both. The errors quoted in Equation 8.21 were obtained from the statistical distribution of several determinations of N_t.

To investigate the discrepancies various simulation parameters were changed. By synthesising signals for different values of α the key to the explanation was found. The value of N_t was expected to be inversely proportional to the width of the pulse envelope (Equation 8.19) and hence proportional to α. Figure 8.2 shows a plot of $N_t(\mu)$ against α and instead of a straight line a curve is obtained. Because the mean modulus samples are 0.5 μs apart there is an absolute maximum level crossing rate of 2 MHz. The averaging and the finite sample interval acts like a filter and reduces the measured level crossing rate.

Evaluation of the integrals in Equation 8.18 for the gamma envelope (Equation 7.11) and substituting in Equation 8.16 we obtain

$$N_t(\mu) = \alpha \exp(-\pi/4) = 0.455938\alpha \quad \text{(theory, gamma pulse envelope)} \quad (8.22)$$

and for $\alpha = 2306604$ we obtain

$$N_t(\mu) = 1.051669\ \text{MHz} \quad \text{(theory, gamma pulse)} \quad (8.23)$$

Thus there is an even greater discrepancy between the simulation result and the theoretical result for the gamma pulse. It also

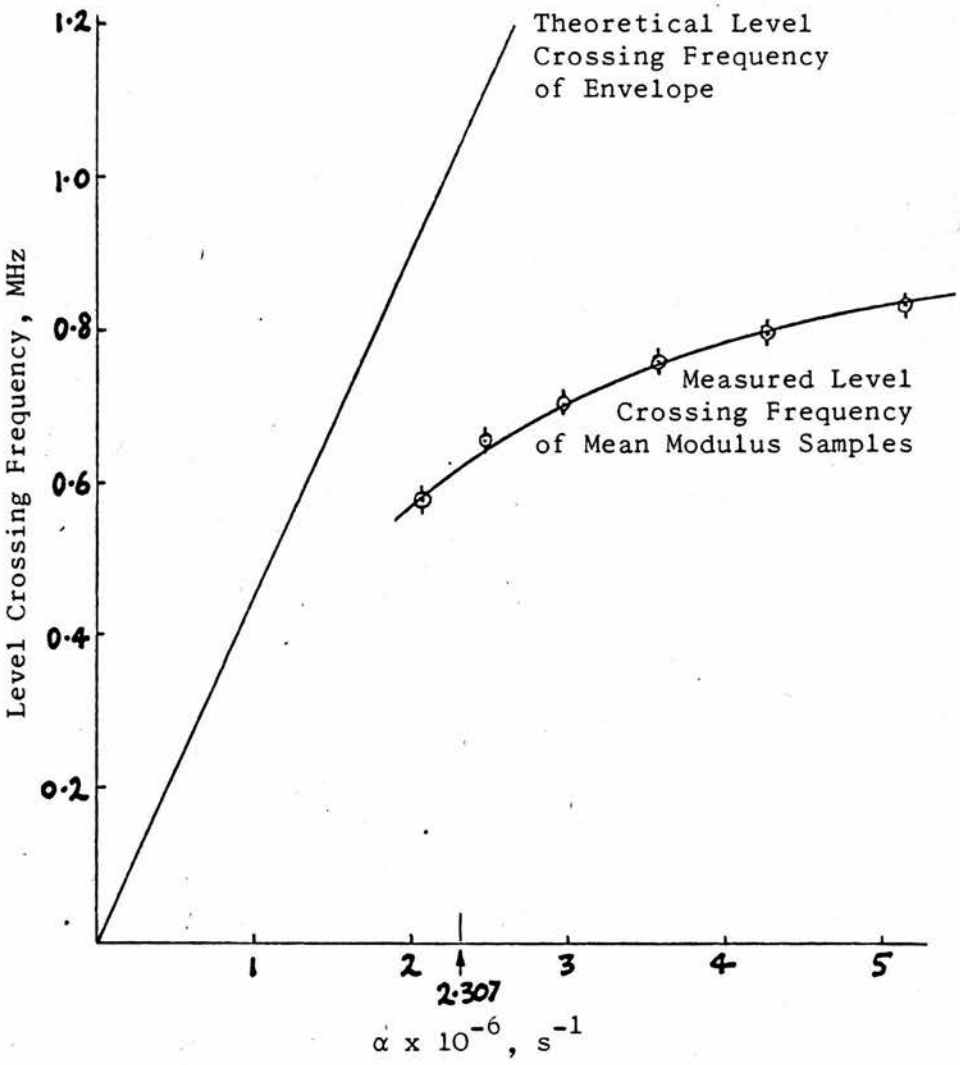

FIGURE 8.2 DEPENDENCE OF LEVEL CROSSING FREQUENCY ON α

$F(t) = a_o t \exp(-\alpha t)\sin\omega t$

demonstrates that the theoretical result depends on the shape of the pulse envelope and not just on the full width at half maximum.

To reduce the effect of filtering, shorter average lengths with shorter sample intervals can be used; however, the high frequency component is no longer adequately filtered and ripple appears on the envelope. This ripple contributes to the level crossing frequency and it is not possible to check the theoretical prediction. In an attempt to overcome this problem the program was modified to allow moving averages of the modulus of the synthesised waveform to be obtained. This allowed the sample interval and the length of the averaging period to be changed independently. However, similar problems occurred using the moving average and it was not possible to adequately filter the high frequency components of the modulus of the signal whilst preserving the high frequency components of the envelope. By increasing the carrier frequency the ripple could be filtered more effectively but the problem was still significant.

8.7.3 Qualitative explanation for the level crossing frequency discrepancy

It seemed likely at this stage that the discrepancies between the theoretical, experimental and simulated values for the mean-level crossing frequency could be explained in terms of filtering. In the absence of further details about the filter and the shape of the pulse used in Atkinson's experimental arrangement it would not be possible to give a quantitative prediction for the level crossing frequency. From a practical point of view it is evident that the pulse shape and method of filtering the rectified echo waveform are

important characteristics of a flow meter based on this principle, although calibration by experiment reduces the problem.

Because the explanation of the discrepancies was only qualitative there remained the doubt whether the theory was appropriate for the simulated waveforms. How could the value of N_t be measured more precisely given that any filter (even an ideal filter) which adequately filters the high frequency component of the rectified signal will also remove some of the high frequency components of the envelope? One approach considered was to measure the level crossing frequencies for a set of filters and use extrapolation to predict the value of N_t in the absence of any filtering of the envelope. However, this was rather inelegant and would be likely to require a theory rather more doubtful than that being tested. In the event it was not necessary to use extrapolation because an alternative method was devised.

8.7.4 Generation of ideal envelope

Atkinson and Berry (1974) developed their theory using complex pulse waveforms to generate complex echo signals. In a similar way we can generate complex signals $P_c(t)$ by adding together complex pulses of the form

$$F_c(t) = a(t) \exp\left[j(\omega t - \theta)\right] \qquad (8.24)$$

But this can be separated into real and imaginary parts, $F_r(t)$ and $F_i(t)$ given by

$$\begin{aligned} F_r(t) &= a(t)\cos(\omega t - \theta) \\ &= a(t)\sin(\omega t - \theta - \pi/2) \end{aligned} \qquad (8.25)$$

and

$$F_i(t) = ja(t)\sin(\omega t - \theta) \qquad (8.26)$$

We can generate the real part and the imaginary parts of the signal separately by synthesising the real signal $P_r(t)$ by adding pulse waveforms defined in Equation 8.25 and the imaginary waveform $P_i(t)$ by adding pulse waveforms defined in Equation 8.26. The same sequence of random numbers is used for the real and imaginary parts of the signal.

The envelope of the complex signal is defined to be

$$P_{env}(t) = \sqrt{P_r^2(t) + P_i^2(t)} \qquad (8.27)$$

A program was written to read files containing the complex components of the waveform and produce a file containing the ideal envelope as defined above. This is the envelope to which the level crossing theory of Atkinson and Berry refers. We can thus obtain the ideal envelope without recourse to filtering. Complex signals and their envelopes were synthesised using a Gaussian pulse envelope and a gamma pulse envelope. An example of an envelope obtained in this way is shown in Figure 8.3.

8.7.5 Level crossing frequency of synthesised envelope

The level crossing frequencies for the synthesised envelopes were measured and compared with the theoretical predictions

Gaussian pulse

$$N_t(\mu) = \begin{matrix} 0.716 & \text{MHz} & \text{(theory)} \\ (0.71 \pm 0.01) & \text{MHz} & \text{(simulation)} \end{matrix} \qquad (8.28)$$

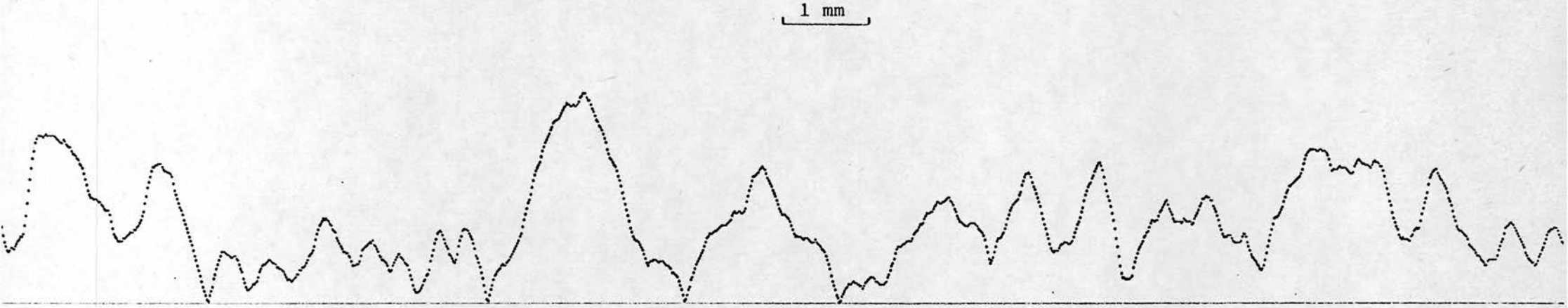

FIGURE 8.3 ENVELOPE WAVEFORM DERIVED FROM COMPLEX SIGNAL.

COMPLEX SIGNAL SYNTHESISED WITH COMPLEX PULSE:

$F_r(t) = a_o t \exp(-\alpha t)\sin(\omega t)$

$F_i(t) = a_o t \exp(-\alpha t)\cos(\omega t)$

$\alpha = 2445000\ s^{-1}$

$\omega = 21991150$ radian s^{-1}

Gamma pulse

$$N_t(\mu) = \begin{matrix} 1.052 & \text{MHz} & \text{(theory)} \\ (1.03 \pm 0.02) & \text{MHz} & \text{(simulation)} \end{matrix} \qquad (8.29)$$

Hence we now find that the theoretical values and simulation values are much closer and can be taken to be a confirmation of the theory. The quoted errors were again determined statistically.

As a check on the theory that the reduced value of $N_t(\mu)$ for mean modulus samples of the echo waveform was due to filtering, the ideal envelope was processed in the same way to obtain the following result:

$$N_t(\mu) \begin{matrix} (0.64 \pm 0.01) \text{ MHz} & \text{(mean modulus samples of signal)} \\ (0.63 \pm 0.01) \text{ MHz} & \text{(mean modulus samples of envelope)} \end{matrix} \qquad (8.30)$$

The similarity of these values lends support to the idea that the reduction is due to filtering.

As a further check of the theory for the level crossing frequency of the envelope the dependence of $N_t(\Phi)$ on the threshold level Φ was determined and compared with the theoretical prediction (Figure 8.4). The solid curve is the theoretical curve obtained by combining Equations 8.14, 8.15, 8.18, and 7.11 to give

$$N_t(\Phi) = \frac{\Phi}{\sigma^2} \exp\left\{\frac{-\Phi^2}{2\sigma^2}\right\}\left[\frac{2\sigma^2}{\pi}\right]^{\frac{1}{2}} \alpha \qquad (8.31)$$

where σ is the rms value (= 100) of the echo waveform.

The good agreement between the theoretical prediction (which contains no free variables) and the simulation values allows us to

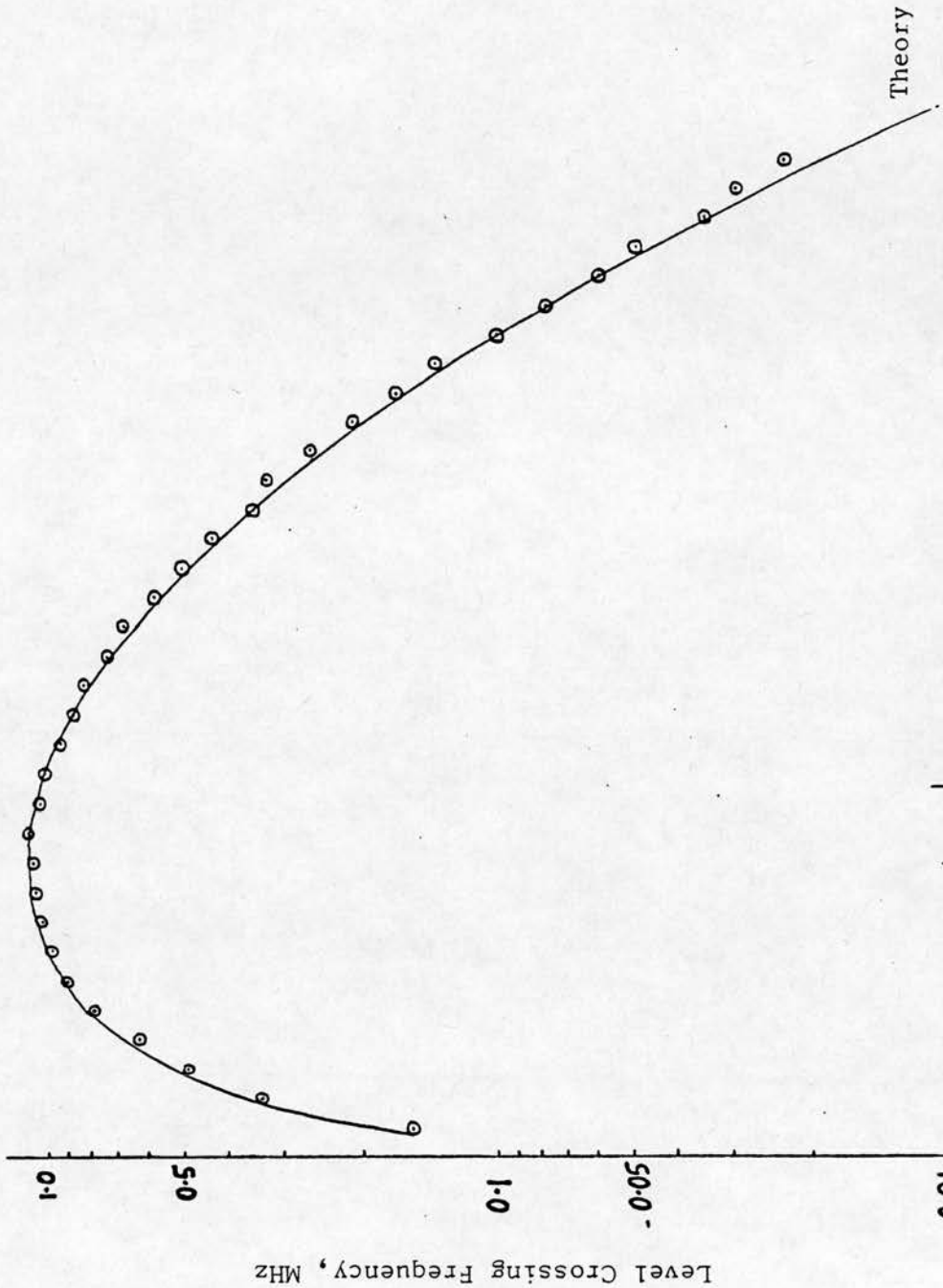

FIGURE 8.4 LEVEL CROSSING FREQUENCY FOR ENVELOPE OF SYNTHESISED COMPLEX SIGNAL.

to have some confidence in the theory and in the program used to synthesise the echo signals.

8.7.6 Possible further simulations

Atkinson and Berry (1974) also calculated and measured the level crossing rate for the envelope of the echo waveform from blood moving perpendicular to the axis of the ultrasound beam. The theoretical and experimental values were in agreement. No simulations were performed to check these results although the program could be modified to do so in the future. Simulation of scattering from moving blood could also be of value in developing the theory of standard Doppler blood flow measuring devices.

A further simulation of interest would be to simulate the effect of moving the probe in an arc, always pointing at a fixed point. The program could measure the fluctuations in echo amplitude corresponding to the depth of that point. The results could be compared with the results of acoustic Bragg scattering work (Section 6.3.5).

8.8 LEVEL CROSSING FREQUENCY OF LONG MOVING AVERAGES

As described in Section 8.6 the purpose of measuring the level crossing frequency is to determine how often a moving average will reach a certain level, since this will give us a measure of the false warning rate for a moving average and threshold detector.

8.8.1 Clustering of level crossings

When there has been an upward crossing of a high level there is a greater chance of another upward crossing in the near future than there is if there has not been an upward crossing recently. A

small ripple of the moving average can produce an extra upcrossing. This results in a tendency for level crossings to occur in clusters.

In a realistic detection system the cluster of level crossings would be considered to be the manifestation of a single abnormality. To be relevant to the abnormality detection problem it is more realistic to measure the average distance between clusters, than between all upward (or downward) level crossings.

To minimise the effects of ripple, the level crossing frequency of a moving average of the synthesised envelope was determined (thus removing the high frequency ripple), and the samples were spaced by intervals of 0.2 μs rather than using the 0.02 μs sample interval of the generated data. Any ripple that causes an even number of level crossings within the sample interval of 0.2 μs will not increase the measured level crossing rate. Because the measured average interval between level crossings of a 4 μs moving average is greater than 4 μs we can anticipate that using a sample interval of 0.2 μs will not cause many of the 'genuine' level crossings to be missed. Simulations using smaller sample intervals indicate that the change is only slight. If the time spent above the threshold is much smaller than the time spent below the threshold it is the average time spent between the upcrossing and the following downcrossing that should be compared with the sample interval to estimate how many level crossings will be missed (and conversely for more time being spent above the threshold than below).

The level crossing frequency of the moving average of the modulus

of the synthesised echo waveform was also measured to see whether the ripple had a significant effect. It was found that the level crossing frequencies were very similar to the values found for the moving average of the synthesised envelope.

The effect of clusters has been considered by Barbé (1976). Barbé was concerned with level crossings of processes modelled by nondifferentiable processes. These processes have clusters of level crossings with an infinite number of crossings in each cluster. Simple filtering does not remove the problem because the number of level crossings then depends very strongly on the filter time constants. To estimate the separation of the clusters Barbé considers the level crossing frequency of a related process which is a linear interpolation between samples of the process. This is identical in principle to the method I used to avoid multiple crossings in a cluster, with the exception that I do not estimate the time of crossing by using a linear interpolation. The error involved in assuming that the level crossing occurs midway between the samples will be negligible if we measure the number of crossings in a long interval. The problem of clustering is not as severe for the synthesised echo signals as for the processes considered by Barbé; taking samples at shorter intervals produces only a small increase in the measured level crossing frequency of the synthesised signals.

8.8.2 Theory of level crossings of moving averages

Let x be the moving average of an ergodic random variable y

$$x(t,T) = \frac{1}{T}\int_{t}^{t+T} y(t')\, dt' \qquad (8.32)$$

The variable y may be the envelope or the modulus of the echo waveform. From Equation 8.32 we have

$$\dot{x}(t,T) = \left[y(t+T) - y(t) \right] / T \tag{8.33}$$

Let q be defined as

$$q = T\dot{x} = y(t+T) - y(t) \tag{8.34}$$

and let G(q) be the probability function of q. For long moving averages y(t+T) will be independent of y(t) and so the probability distribution G(q) will be independent of T for large T.

For large values of T the values of y(t+T) and y(t) will be almost independent of x(t,T). If x and $\dot{x}$ are independent the joint distribution of x and $\dot{x}$ given by $p(\Phi,\beta)$ defined in Equation 8.11 can be written as the product of the distribution function of x and the distribution function of $\dot{x}$. Thus we obtain

$$p(\Phi,\beta)\, d\Phi,d\beta = \Pr(\Phi \leqslant x < \Phi + d\Phi)\Pr(\beta \leqslant \dot{x} < \beta + d\beta) \tag{8.35}$$

which leads to

$$p(\Phi,\beta)\, d\Phi d\beta = \Pr(\Phi) G(q) d\Phi dq \tag{8.36}$$

substituting this in equation 8.13 we obtain for the level crossing frequency

$$N_t(\Phi) = \int_{-\infty}^{\infty} |\beta| \Pr(\Phi) G(q) dq \tag{8.37}$$

Substituting $\beta = q/T$ we obtain

$$N_t(\Phi) = \frac{\Pr(\Phi)}{T} \int_{-\infty}^{\infty} |q| \, G(q) \, dq \tag{8.38}$$

Since the distribution of q is independent of T for long T we can replace the integral by a constant and obtain

$$N_t(\Phi) = \frac{Q}{T} \Pr(\Phi) \qquad (Q \text{ constant}) \tag{8.39}$$

For very long moving averages the probability distribution $\Pr(\Phi)$ approaches a Gaussian distribution with mean μ and standard deviation $\psi' = \psi_o/\sqrt{T}$ where ψ_o is a constant. Using such a distribution for $\Pr(\Phi)$ in Equation 8.39 we obtain

$$N_t(\Phi) = \frac{Q}{\psi_o\sqrt{2\pi T}} \exp\left[-T(\Phi-\mu)^2/2\psi_o^2\right] \tag{8.40}$$

If we substitute $\Phi = \mu$ we obtain for the mean-level crossing frequency

$$N_t(\mu,T) = \frac{Q}{\psi_o\sqrt{2\pi T}}$$

$$= \frac{K_N}{\sqrt{T}} \qquad (K_N \text{ constant}) \tag{8.41}$$

Thus for very long moving averages we predict that the mean-level crossing frequency will be inversely proportional to the square root of the length of the moving average.

8.8.3 Simulation results for level crossing frequency of moving average

A graph of the mean-level crossing frequency of the moving average of a synthesised envelope waveform plotted against the length of the moving average is shown in Figure 8.5. Comparison with a line drawn for $y = K/\sqrt{T}$ shows that for large T Equation 8.41 is in fair agreement with the measurements on the simulated waveform. For smaller values of T the distribution of the moving average is not expected

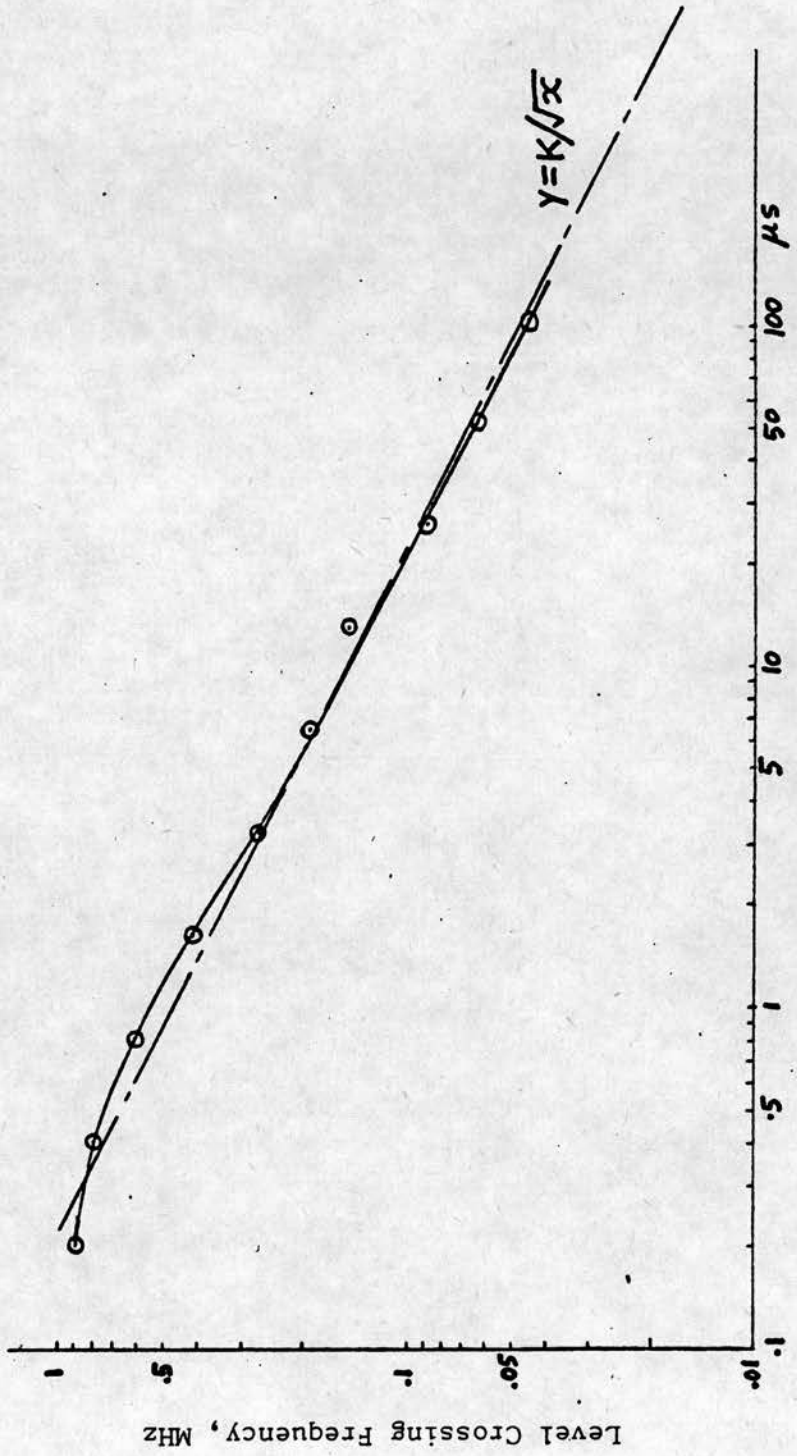

FIGURE 8.5 DEPENDENCE OF LEVEL CROSSING FREQUENCY ON DURATION OF MOVING AVERAGE.

Datum level = theoretical mean of envelope. See also Figure 8.6.

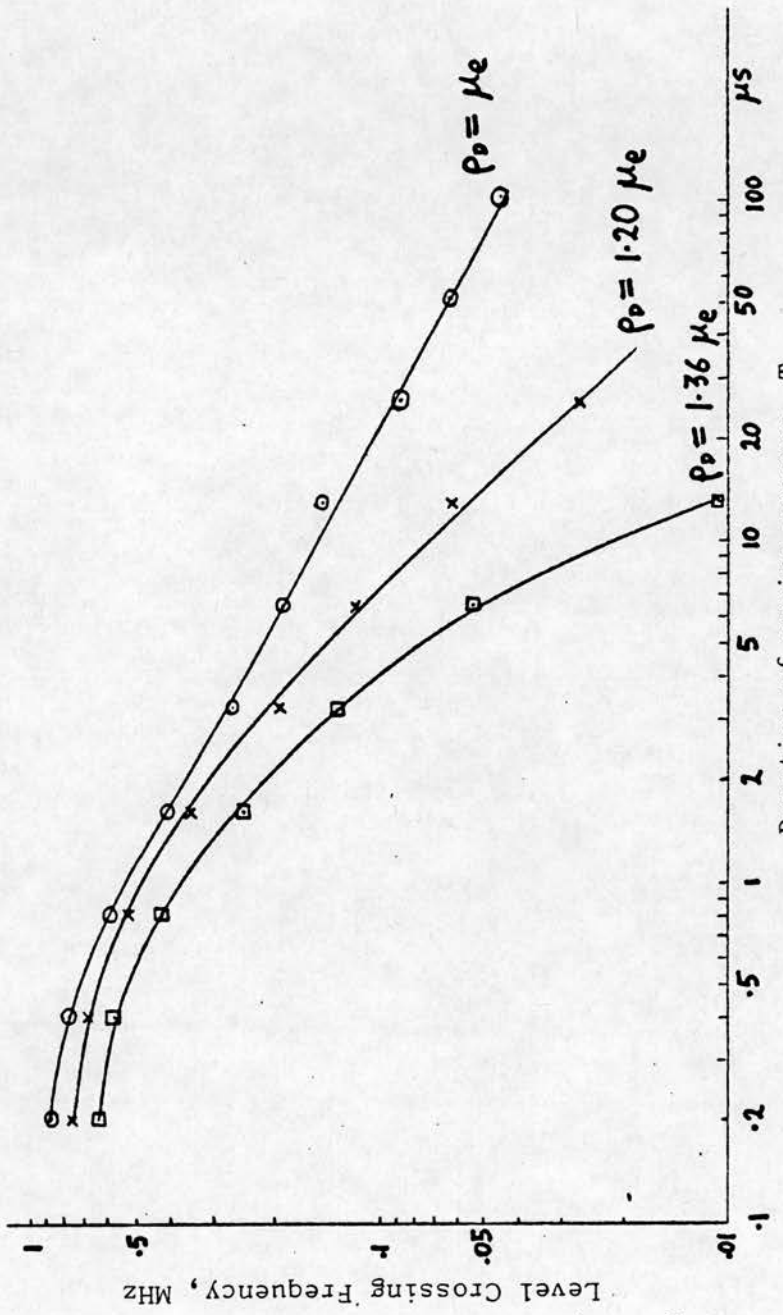

FIGURE 8.6 DEPENDENCE OF LEVEL CROSSING FREQUENCY ON DURATION OF MOVING AVERAGE.

The datum level ρ_D is expressed in terms of the mean of the envelope μ_e

to be Gaussian and so the $y = K/\sqrt{T}$ line is not expected to fit for low values of T.

The dependence of level crossing frequency on length of moving average is shown for three different threshold levels in Figure 8.6. The rapid fall off with increasing T for thresholds above the mean level can be attributed to the amplitude distributions being narrower for increasing T (see Equations 8.39 and 8.40)

The dependence of the level crossing frequency on threshold level is shown for three values of T in Figures 8.7-9. The results are compared with the amplitude distributions scaled to match the mean-level crossing frequency. Since the probability distribution in Equation 8.39 is only expected to be Gaussian for vary large values of T the distributions were determined using synthesised data. It can be seen that there is fair agreement between the measured level crossing frequencies and the scaled amplitude distributions although there is some deviation, especially for the lower values of T (Figure 8.7).

For values of T as low as 4 μs the values of y(t+T) and y(t) will not be expected to be entirely independent of x, the value of the moving average (see Equations 8.32 and 8.33). If x is low then the difference between y(t+T) and y(t) will be lower on average than for entirely uncorrelated variables; for high mean values there is less of a constraint on the average difference between y(t+T) and y(t) and so the average difference will be greater. Thus the average value of $\dot{x}$ will be higher for high values of x than for low values of x. Since Equation 8.39 assumed that x and $\dot{x}$ were uncorrelated

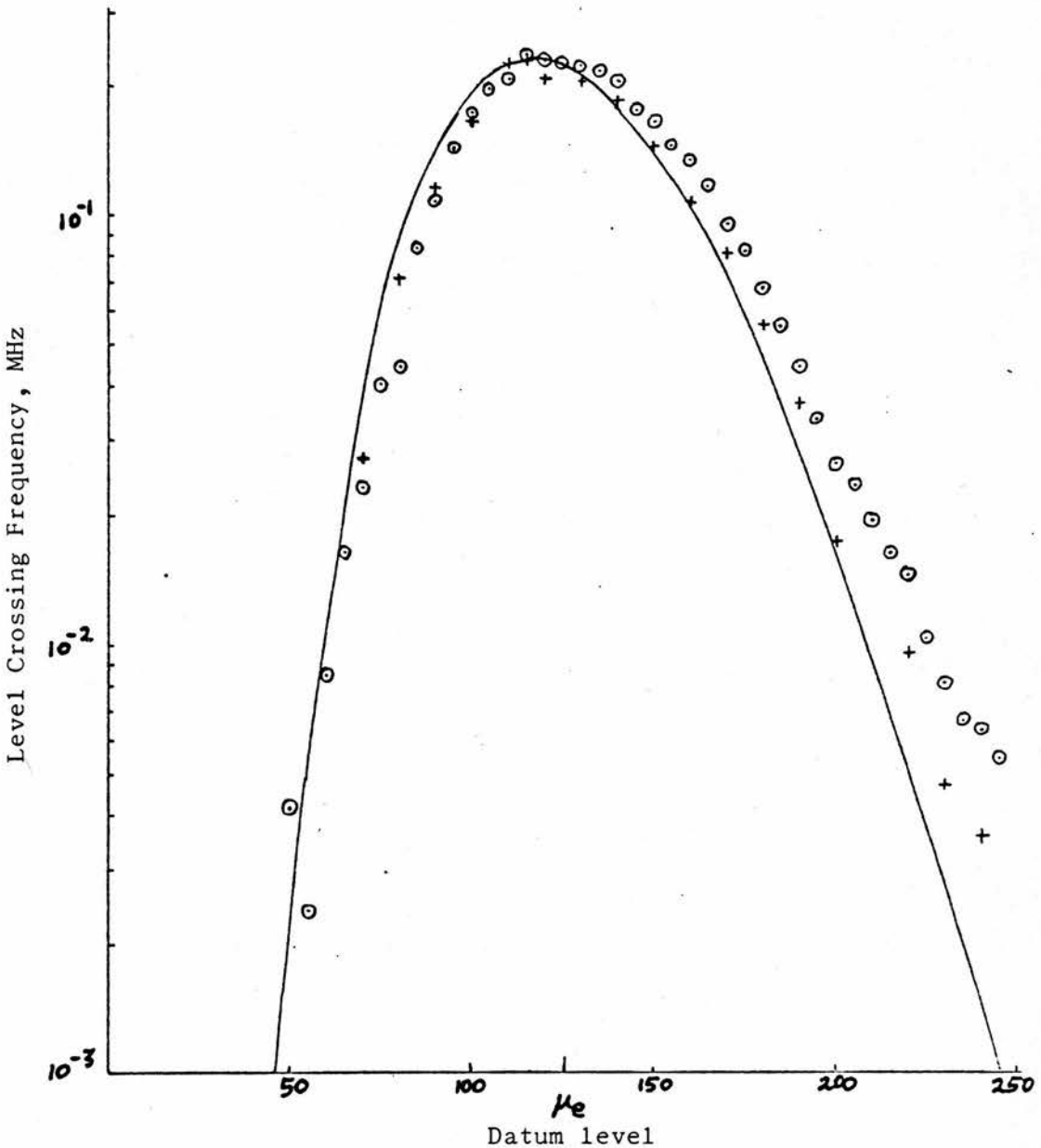

FIGURE 8.7 LEVEL CROSSING FREQUENCY OF MOVING AVERAGE OF LENGTH 4 μs

⊙ Level crossing frequency

\+ Scaled amplitude distribution of moving average of envelope

—— Scaled amplitude distribution of mean modulus of signal

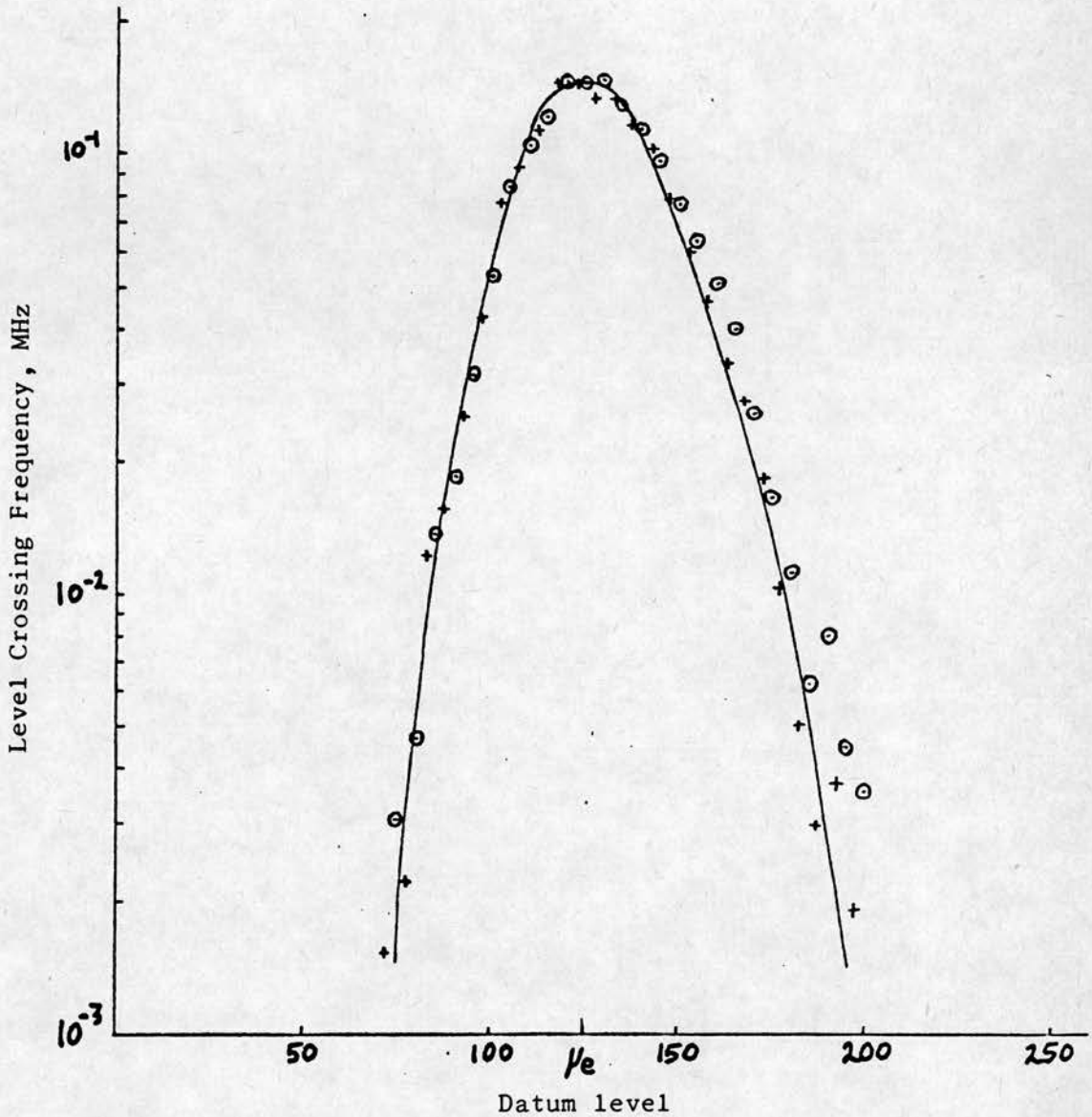

FIGURE 8.8 LEVEL CROSSING FREQUENCY OF MOVING AVERAGE OF LENGTH 10 μs

⊙ Level crossing frequency

\+ Scaled amplitude distribution of moving average of envelope

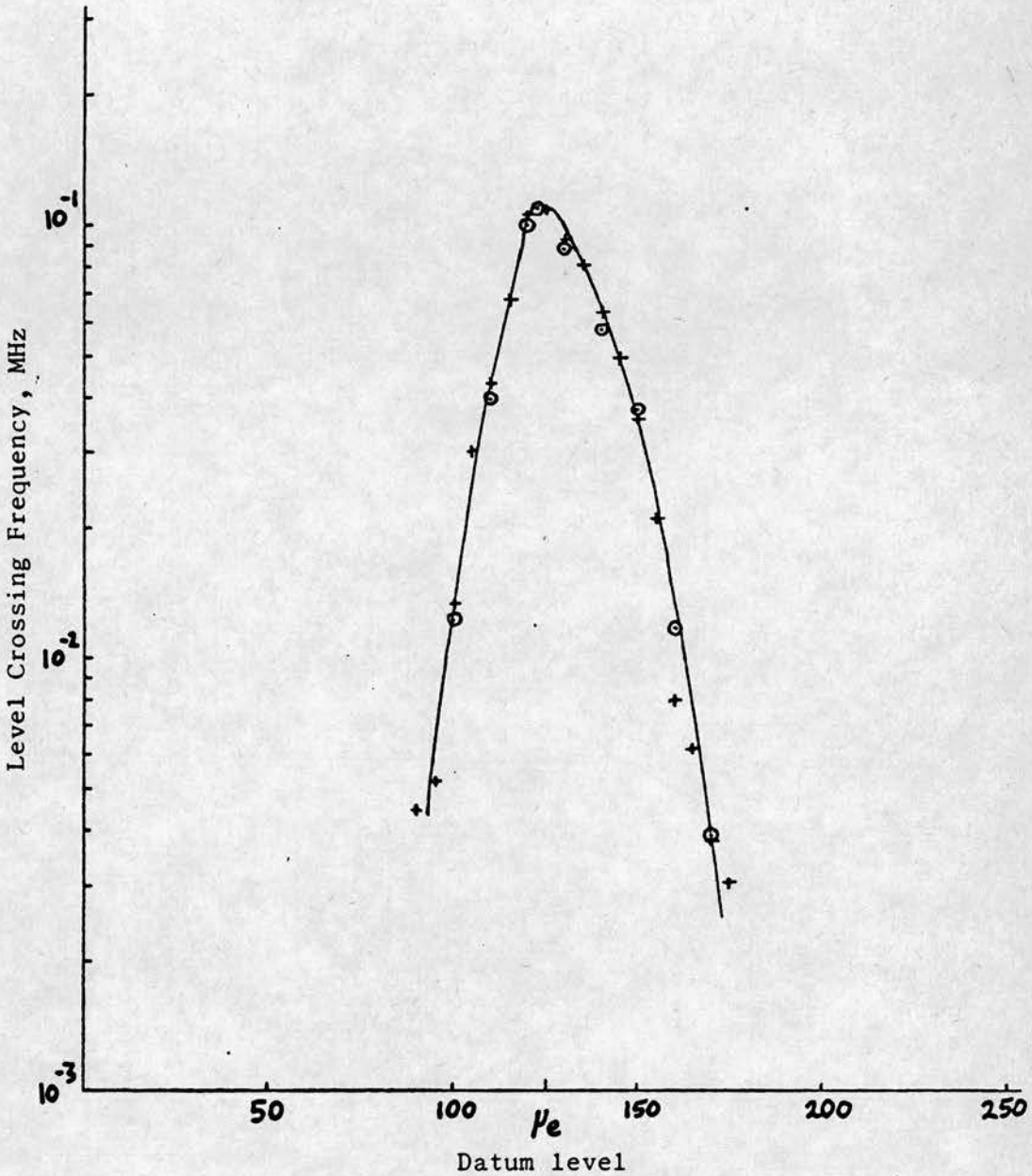

FIGURE 8.9 LEVEL CROSSING FREQUENCY FOR MOVING AVERAGE OF LENGTH 20 μs

⊙ Level crossing frequency

\+ Scaled amplitude distribution of moving average of envelope

it will overestimate the level crossing frequency for low values of x. Since the amplitude distribution was scaled to fit for the mean-level crossing frequency it will be expected to fall below the measured level crossing frequency for higher levels. Thus we can qualitatively explain the observed deviation at high threshold levels. For higher values of T we expect x and $\dot{x}$ to be more independent and better agreement between the scaled amplitude distribution and measured level crossing frequency is found.

8.8.4 Bias in level crossing frequency determinations

The level crossing frequency is found by determining the position of the first crossing of the level and counting all the crossings in the same direction as the first crossing. The crossing frequency was taken to be double the number of crossings following the first crossing divided by the time between the first and last crossing in the same direction. If all crossings (in either direction) were counted there would be a slight bias in the results because the interval spent on one side of the threshold could be much greater than that spent on the other side. This makes it more likely for the first and last crossing interval to be shorter than average, thus producing a bias towards high level crossing frequencies. By measuring level crossings in the same direction this bias is reduced.

Another bias similar to the one described above is caused by the random nature of the crossing intervals. A long interval is more likely to contain the start (or end) of the signal than a short interval is. Since the intervals containing the start and end of the signal are not used this results in a bias towards high values of level

crossing frequency. If there are a large number of crossings this bias will make only a small difference in the final value. However, if the signal length includes only a few crossings the bias can be very significant. Figure 8.10 illustrates this dramatically. Estimates taken from 15 sections of length 200 μs are compared with estimates based on 1 section of length 15 x 200 = 3000 μs. The average for the 15 sections was obtained using the formula

$$N_t = \frac{2\sum_i N_i}{\sum_i T_i'} \qquad (8.42)$$

where T_i' is the total time for the N_i intervals in the i^{th} section of signal. A signal of length 200 μs corresponds to a tissue range of 154 mm so this bias could be significant for practical sample lengths from tissue. The signal used to produce Figures 8.7-9 was a single length of 3000 μs duration.

Since the effect is greatest for low level crossing frequencies one might expect that it is only necessary to be wary when the measured level crossing frequency is low; Figure 8.10 indicates the gross error of this assumption - a measured level crossing frequency of 0.155 MHz is accurate to within 1% for $\Phi = 125$ and out by a factor of about 17 for $\Phi = 185$. To give warning of this bias the computer printout includes not only the level crossing frequency but also the total number of crossings and the total time between crossings.

The relationship between the level crossing frequencies and the error rate for a moving-average threshold detector is discussed in Section 8.12.

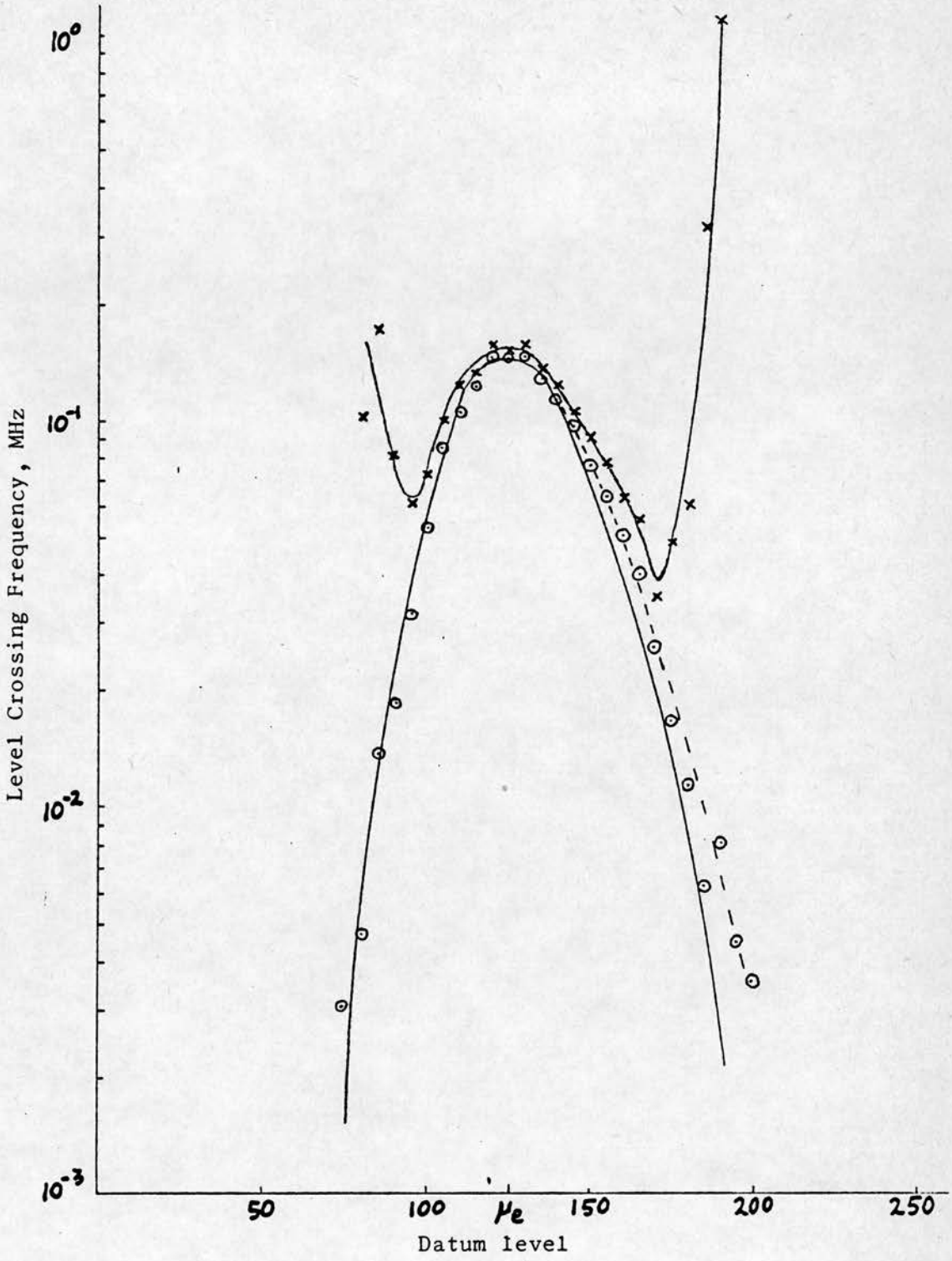

FIGURE 8.10 EFFECT OF USING SHORT SECTIONS OF SIGNAL TO ESTIMATE THE LEVEL CROSSING FREQUENCY. MOVING AVERAGE

T = 10 us

× Estimate from 15 sections of length 200 μs

⊙ Estimate from 1 section of length 3000 μs

8.9 SYNTHESIS OF ECHO SIGNALS FROM ABNORMAL REGIONS

Echo signals were synthesised using Equation 7.2 with values of $g(t_k)$ dependent on t_k. This was done to investigate the detectability of regions with different scattering cross sections. The program allows the dependence of $g(t_k)$ on t_k to be defined in terms of several linear segments. However, for the simulations referred to in this thesis it is assumed that the transitions between the regions are rapid; $g(t_k)$ takes on one of two values depending on t_k

$$g(t_k) = \begin{cases} 1 & (t_o > t_k, \text{ or } t_k \geq t_o+t_r) \\ g_r & (t_o \leq t_k < t_o+t_r) \end{cases} \qquad (8.43)$$

where t_o, t_r and g_r are constants. That is, the value of $g(t_k)$ is unity except for the abnormal region of length t_r, when it takes the value g_r. The echo signals were synthesised using the pulse waveform $F_s(t)$ defined in Equation 7.12. The values of w_k come from a normal distribution and N = 1, τ = 0.02 μs to obtain the high density limit. An example of such a synthesised waveform is shown in Figure 8.11.

8.9.1 Moving mean modulus of signal from abnormal regions

Signals synthesised by the method described above were processed to determine how many of the abnormalities would be detected by a moving average of the modulus of the signal followed by a threshold detector. For a signal synthesised with $g_r < 1$ the minimum value of the moving average was determined

$$\Omega_- = \min_{t_s \leq t < t_s+t_w} \left[M(t,T) \right] \qquad (8.44)$$

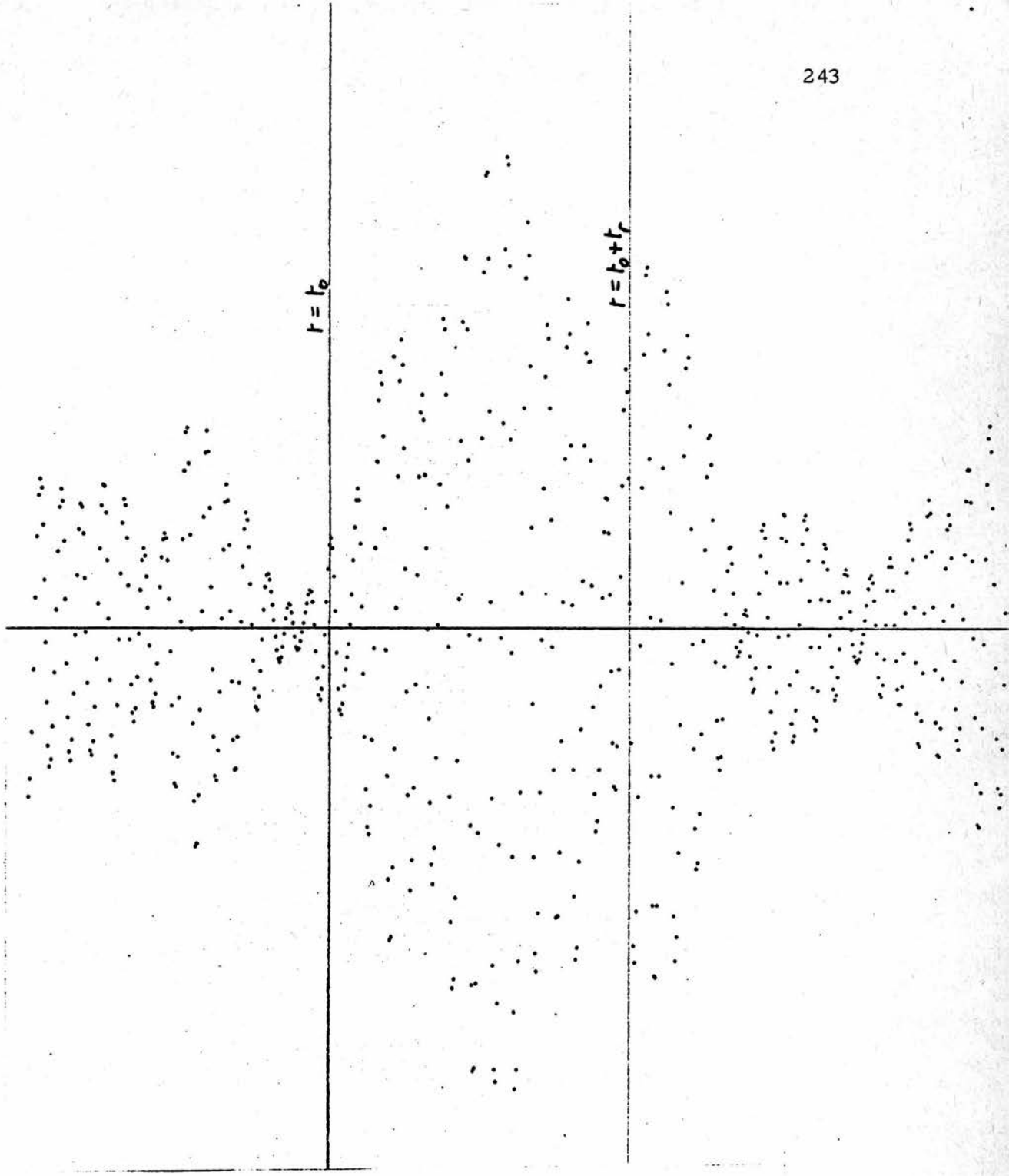

FIGURE 8.11 SYNTHESISED ECHO DATA FOR ABNORMAL REGION.

$g_r = 3$, $t_r = 4$ μs (See Equation 8.43)

The Moving average M(t,T) was defined in Equation 8.10. For a signal synthesised with $g_r > 1$ the maximum value of the moving average was found

$$\Omega_+ = \max_{t_s \leq t < t_s + t_w} \left[M(t,T) \right] \qquad (8.45)$$

In the following discussions Ω refers to either Ω_- or Ω_+. The distribution of Ω was determined by evaluating Ω for each member of an ensemble of 100 synthesised signals. This was repeated for various lengths of moving average T, and also for different sizes of abnormality.

The selection of t_s and t_w in Equations 8.44 and 8.45 involves a compromise. If the time window t_w is too large the normal signal on either side of the abnormality could make a significant difference to the distribution of Ω. If the time window t_w is too short minima (or maxima) caused by the abnormal region may be missed. For regions of length t_r = 4 μs, a time window of 12 μs was used. Normal signals synthesised with g_r = 1 were also processed to find the distribution of Ω for various values of t_w and T.

8.9.1.1 Cumulative distribution of Ω_-

The cumulative distribution of Ω_- for normal signals (g_r = 1) are shown for various values of T in Figure 8.12. A value of t_w = 12 μs was used for the length of time window. (For ergodic signals the starting time t_s should not affect the distribution). The cumulative distribution gives the fraction of values of Ω_- that would be lower than the threshold level. As one would expect, the detection rate for a given threshold level is higher for shorter moving averages.

Since the signal is normal this corresponds to a larger number of false positives for shorter moving averages.

The cumulative distributions of Ω_- for signals synthesised with abnormal regions with g_r = 0.376 and t_r = 4, 10 and 20 μs are shown in Figures 8.13-15. The distribution of Ω_- for a normal signal are shown in Figures 8.13 and 8.15 for comparison. The mean value and standard deviation of Ω_- were also determined for normal and abnormal signals. Figure 8.14 compares the cumulative distribution of Ω_- for an abnormal signal with the cumulative Gaussian distribution (straight line on probability graph paper) having the same mean and standard deviation.

It can be seen that there are significant deviations from the Gaussian distribution but nevertheless the two distributions are fairly close,apart from at the tails. (For a Gaussian distribution 68.26% of the distribution lies within one standard deviation of the mean, and 84.13% of the distribution lies below the mean plus one standard deviation).

Since the Gaussian distribution is a reasonable approximation to the actual distribution a knowledge of the mean value and standard deviation will give us a reasonable indication of the actual distribution.

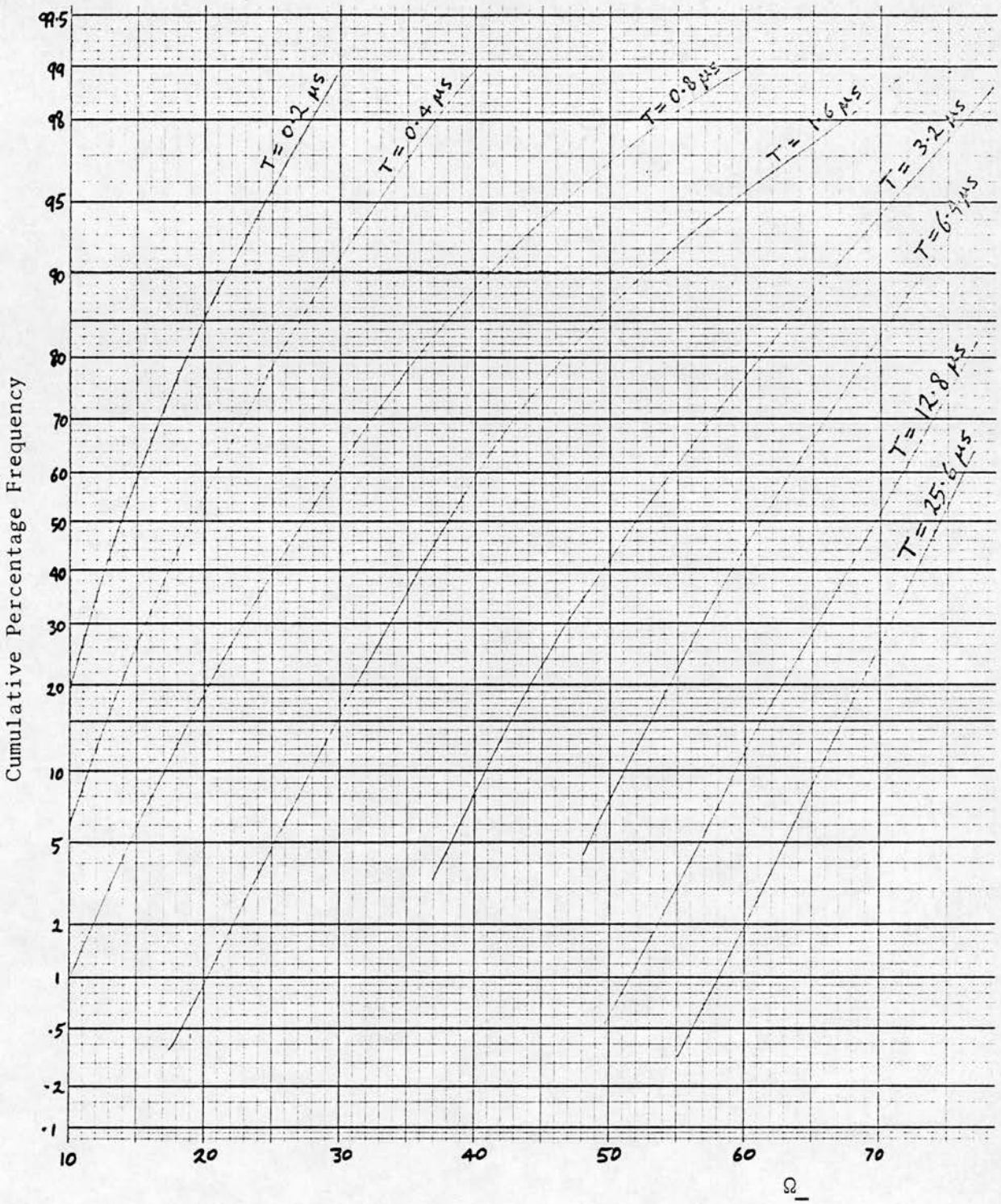

FIGURE 8.12 CUMULATIVE DISTRIBUTION OF Ω_- FOR NORMAL SIGNAL.

Ω_- is the minimum value of M(t,T) in a time t_w(=12 μs)
(See Equations 8.10 and 8.44)

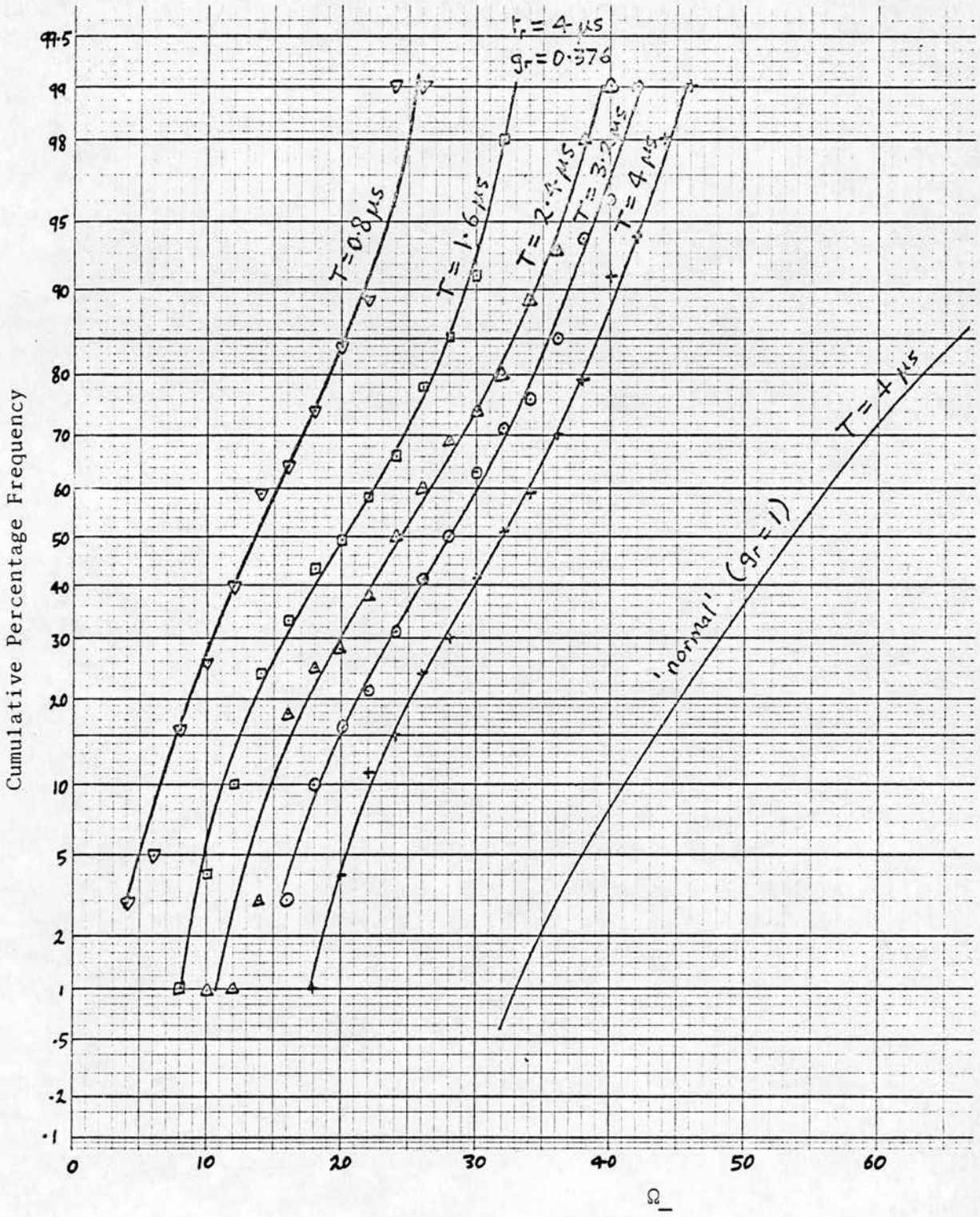

FIGURE 8.13 CUMULATIVE DISTRIBUTION OF Ω_- FOR ABNORMAL REGION WITH $g_r = 0.376$ AND $t_r = 4\ \mu s$.

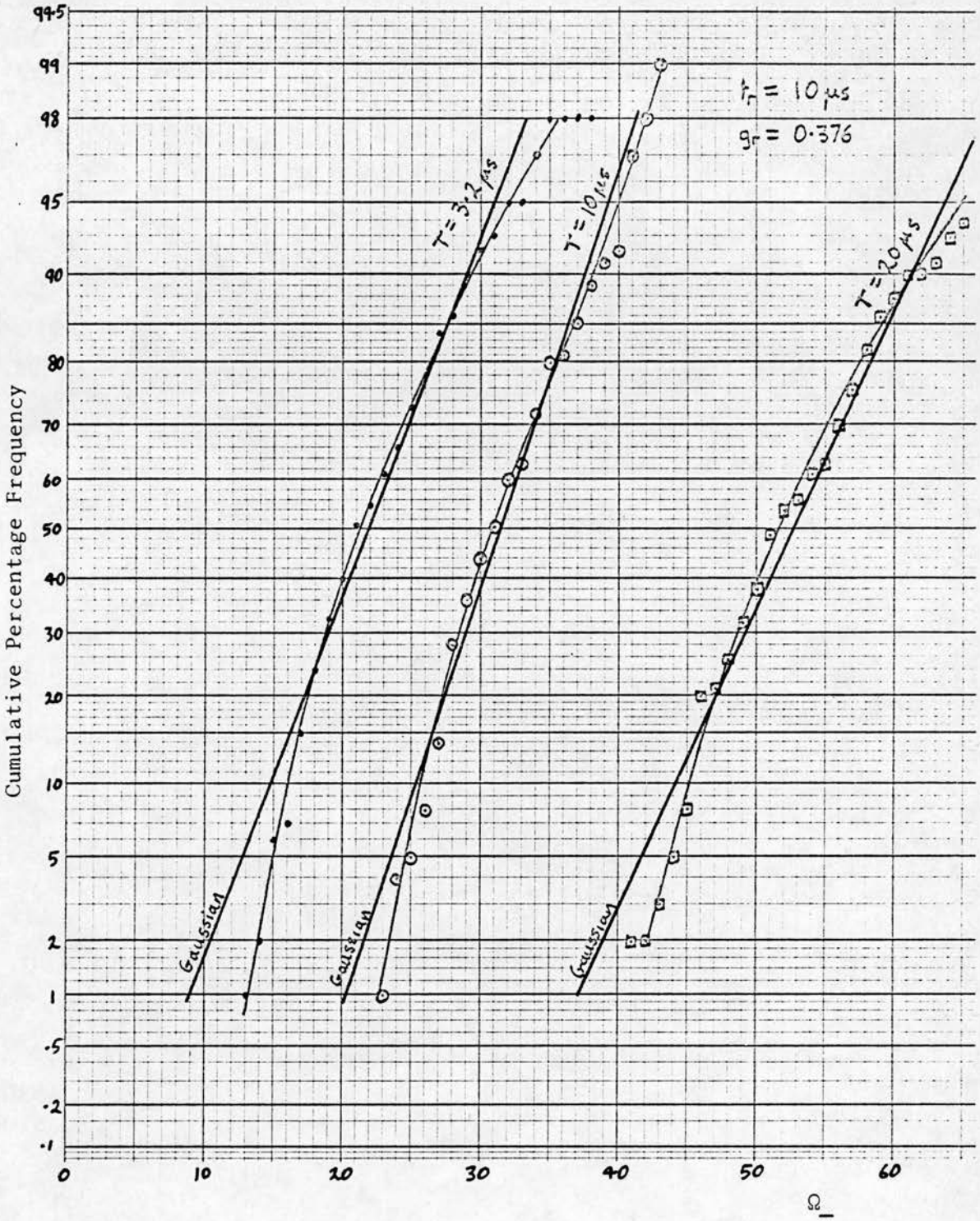

FIGURE 8.14 CUMULATIVE DISTRIBUTION OF Ω_- FOR ABNORMAL REGION WITH g_r = 0.376 AND t_r = 10 μs, COMPARED WITH CUMULATIVE GAUSSIAN DISTRIBUTION WITH SAME MEAN AND STANDARD DEVIATION.

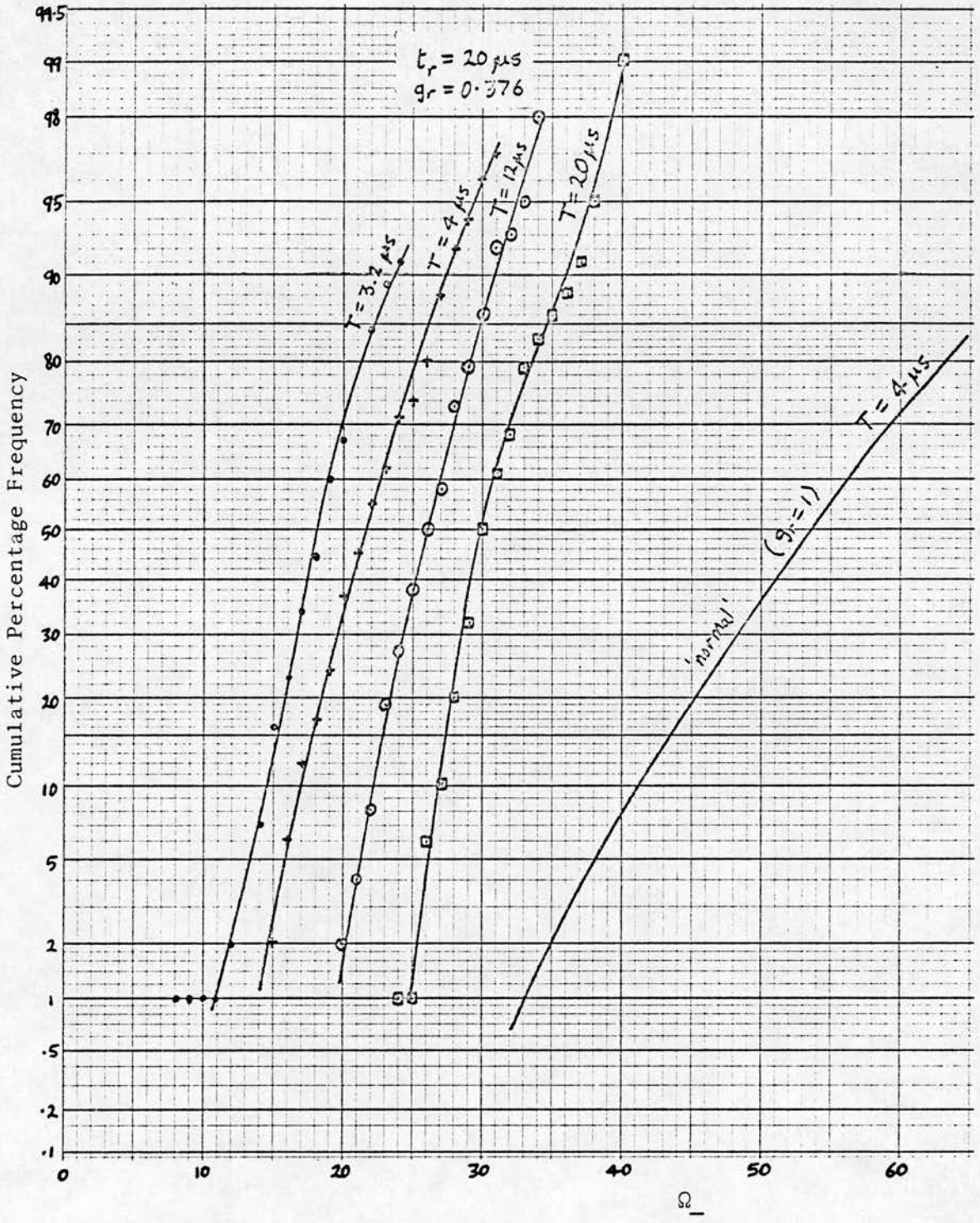

FIGURE 8.15 CUMULATIVE DISTRIBUTION OF Ω_- FOR ABNORMAL REGION WITH g_r = 0.376 AND t_r = 20 μs

A plot of the mean value and mean value plus or minus one standard deviation will give a useful guide to the dependence of the distribution on the independent variable. Such plots are shown in Figures 8.16-19. Figure 8.16 shows how the mean value of the distribution depends on the length of moving average for three abnormal signals and one normal signal. In Figures 8.17-19 the mean and mean plus one standard deviation for abnormal signals are compared with the mean and mean minus one standard deviation for a normal signal. In Figure 8.17 the two distributions have considerable overlap for short and long average lengths but with much less overlap for moving averages of around the same length as the abnormal region (t_r = 4 μs). For short moving averages the distributions are wide and this causes them to overlap. For longer averages the distributions are narrower but the presence of large amounts of normal signal within the length of the moving average of the abnormal signal raises the mean level and again causes the two distributions to overlap. The fairly rapid change in mean level when the length of moving average exceeds the length of the abnormality (see also Figures 8.18-19) indicates that, as we might expect, the optimum length of moving average will be around the length of the abnormal region. In practice the length of the abnormality will be unknown; Figures 8.16-19 indicate the effect of using different lengths of moving average.

The values of t_w used to obtain the distributions of Ω_- for the abnormal regions of length t_r = 4, 10 and 20 μs were t_w = 12, 14 and 16 μs respectively. The minima of moving averages of length $T \approx t_r$ will mainly occur when the centre of the moving average is close to

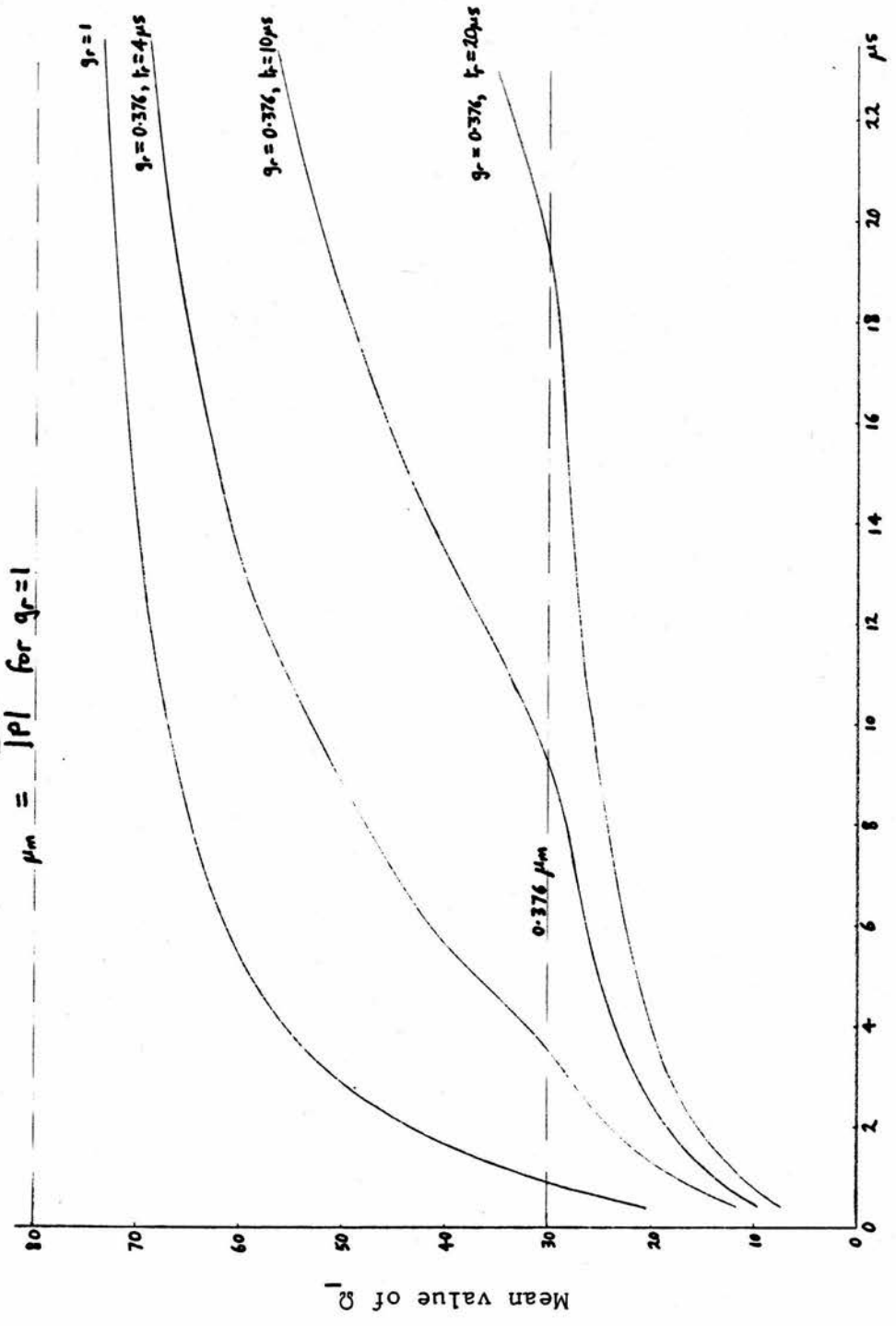

FIGURE 8.16 DEPENDENCE OF MEAN OF Ω_- ON LENGTH OF MOVING AVERAGE.

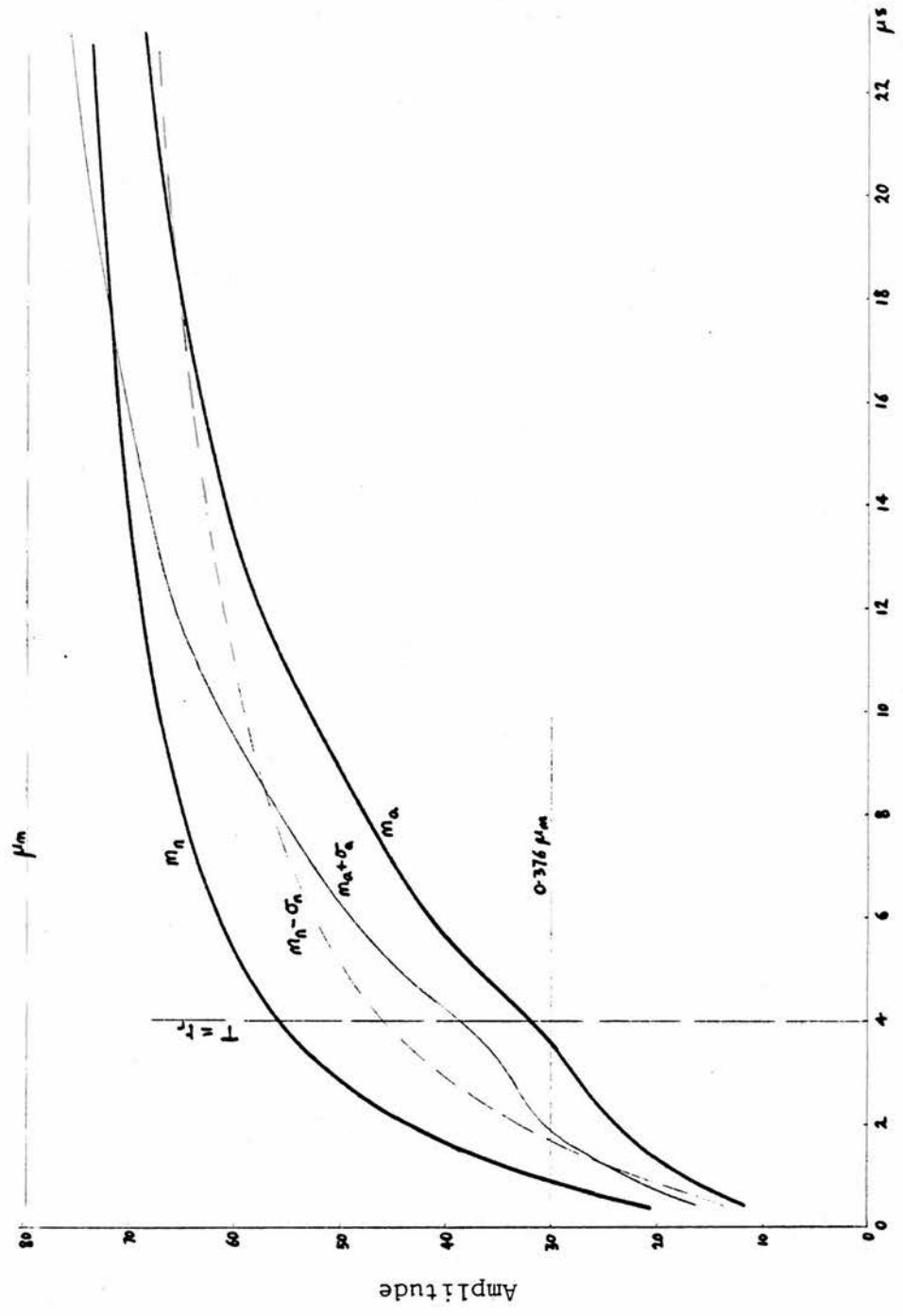

FIGURE 8.17 DEPENDENCE OF MEAN m_n AND MEAN MINUS ONE STANDARD DEVIATION ($m_n-\sigma_n$) OF Ω_- FOR NORMAL SIGNAL COMPARED WITH MEAN m_a AND MEAN PLUS ONE STANDARD DEVIATION ($m_a+\sigma_a$) OF Ω_- FOR ABNORMAL SIGNAL. g_r = 0.376, t_r = 4 μs

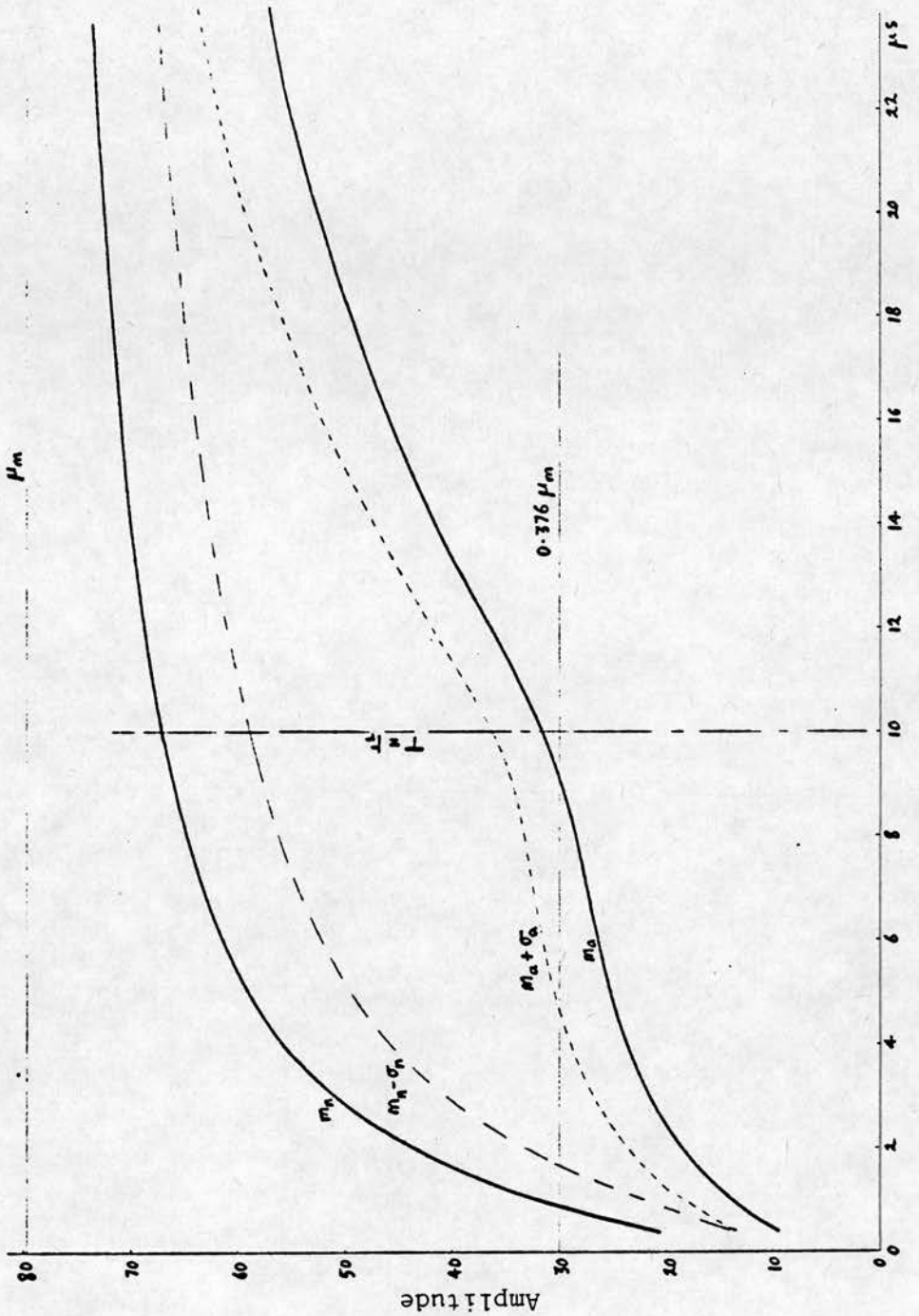

FIGURE 8.18 AS FOR FIGURE 8.17 BUT WITH t_r = 10 μs

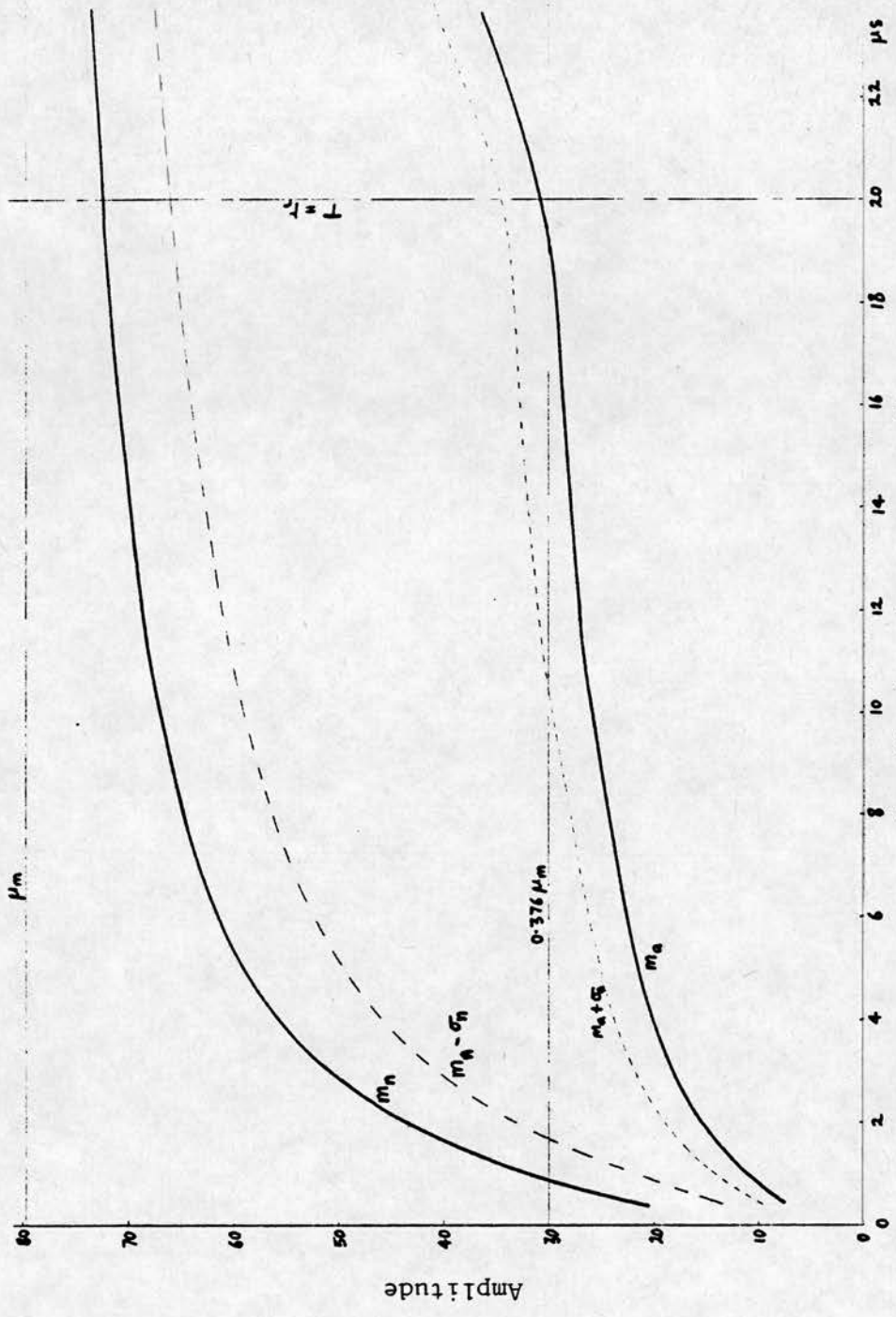

FIGURE 8.19 AS FOR FIGURE 8.17 BUT WITH t_r = 20 μs

the centre of the abnormal region. Provided t_w is large enough to include a large majority of the minima increasing t_w will make little difference to the observed distribution of Ω. For shorter moving averages the positions of the minima will have a wider distribution and a larger value of t_w will be required before further increases make little difference. This leads to a problem of appropriate choice of t_w when processing normal signals to make a comparison. The choice of t_w will depend on how the graph is to be used. The value of t_w = 12 μs used for processing the normal signal to produce Figures 8.16-19 should be suitable for giving a guide to the main features.

8.9.1.2 Cumulative distribution of Ω_+

Regions synthesised using $g_r > 1$ were processed to find the distribution of Ω_+ for normal signals and abnormal signals with g_r = 3, t_r = 4 μs are shown in Figure 8.20 and with g_r = 4, t_r = 4 μs in Figure 8.21. The cumulative distribution gives the fraction of values of Ω_+ that would be higher than the threshold level. The effect of changing the length of the moving average is seen. The plots are compared with cumulative Gaussian distributions with the same mean and standard deviation in Figures 8.22-23. Again we see that the cumulative Gaussian distribution gives a fair approximation to the actual distribution over a range within one standard deviation of the mean value. Again we conclude that a graph showing the mean and mean plus or minus one standard deviation will be a useful guide to how the distribution depends on the independent variable. The dependence of these parameters on the length of the moving average is shown in Figures 8.24-25. The large overlap between the distribution for

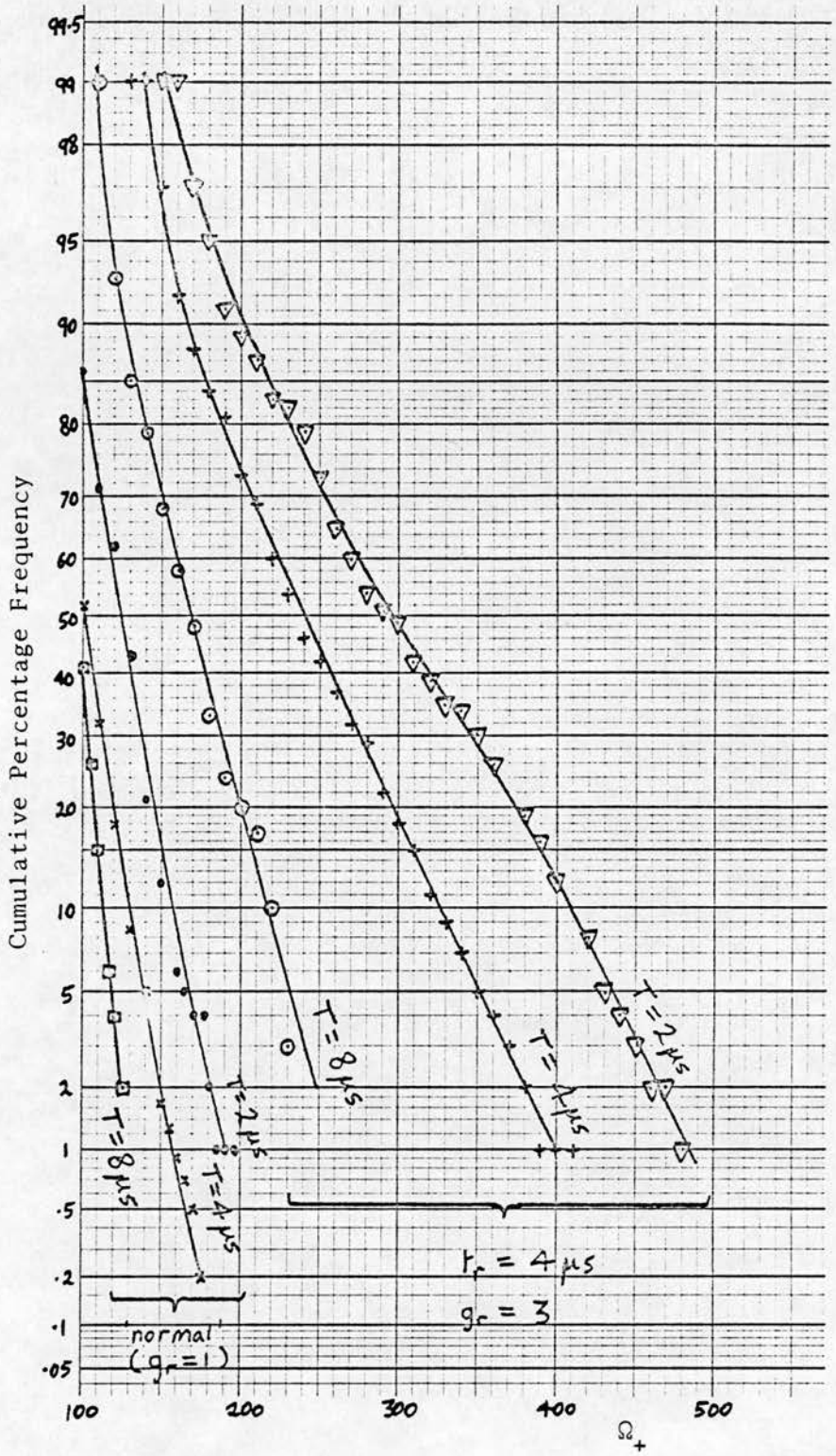

FIGURE 8.20 CUMULATIVE DISTRIBUTION OF Ω_+ FOR ABNORMAL REGION WITH $g_r = 3$ AND $t_r = 4$ μs.

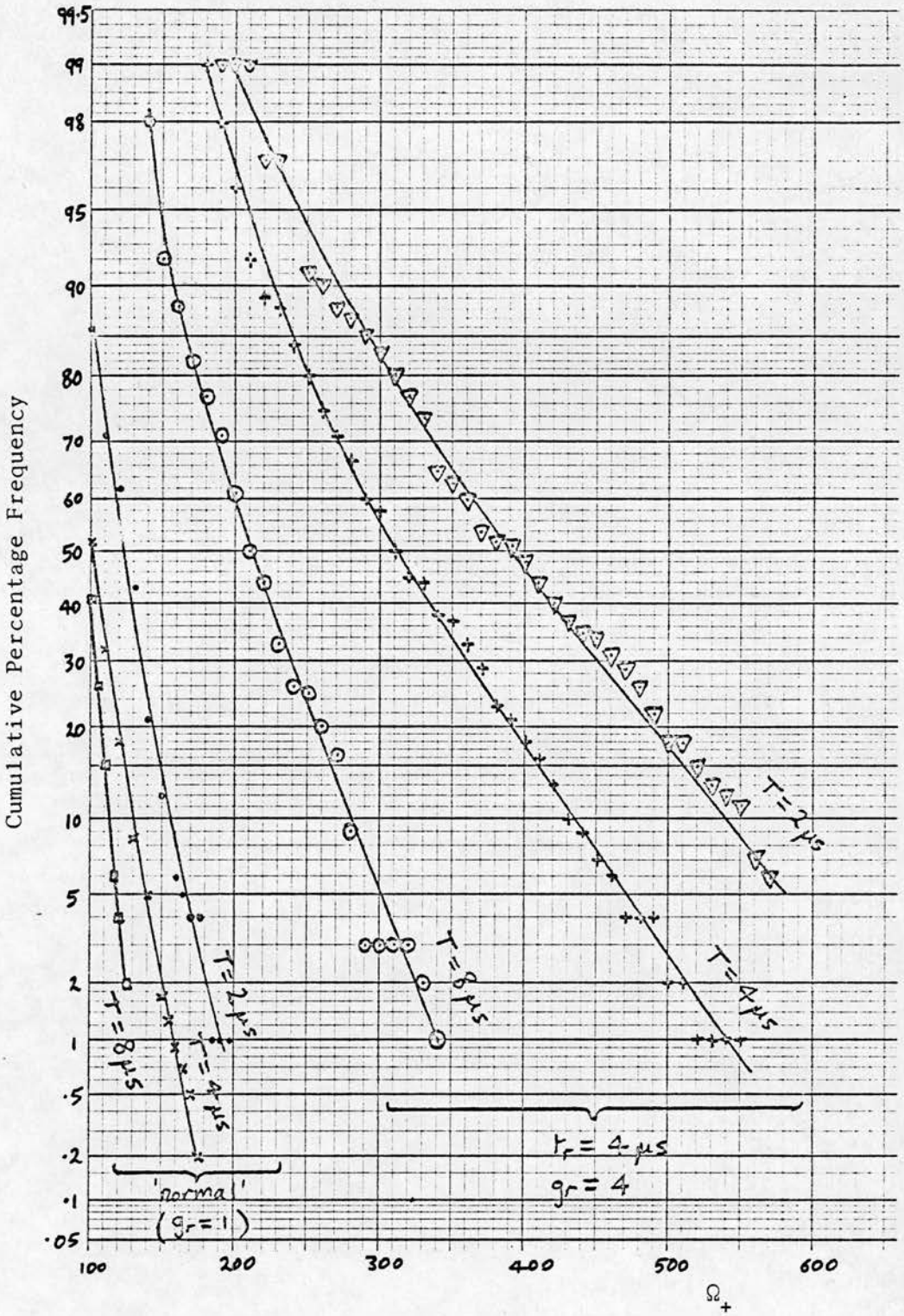

FIGURE 8.21 CUMULATIVE DISTRIBUTION OF Ω_+ FOR ABNORMAL REGION WITH g_r = 4 AND t_r = 4 μs.

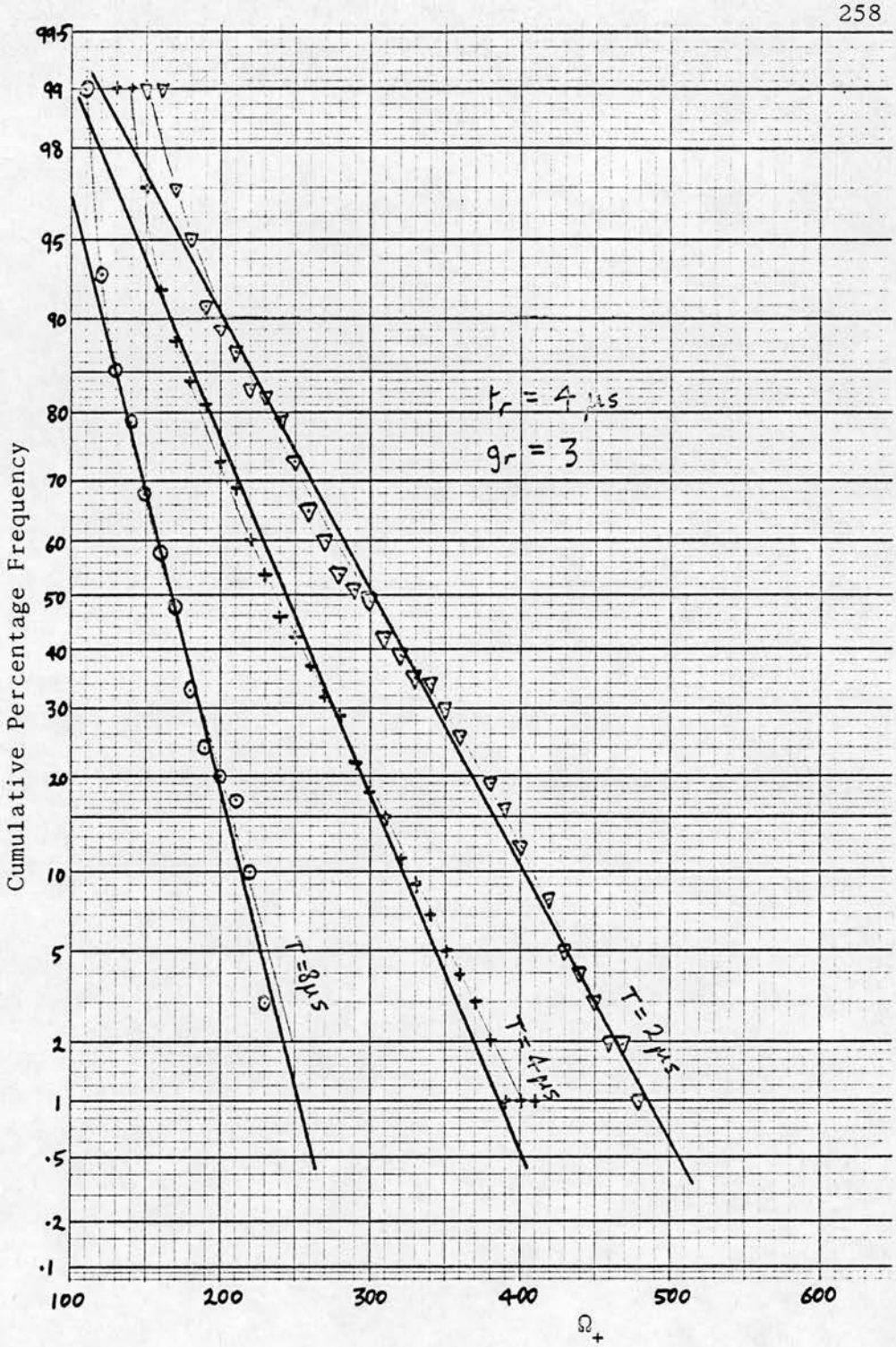

FIGURE 8.22 CUMULATIVE DISTRIBUTION OF Ω_+ FOR ABNORMAL REGION COMPARED WITH CUMULATIVE GAUSSIAN DISTRIBUTION WITH SAME MEAN AND STANDARD DEVIATION. $g_r = 3$, $t_r = 4\ \mu s$.

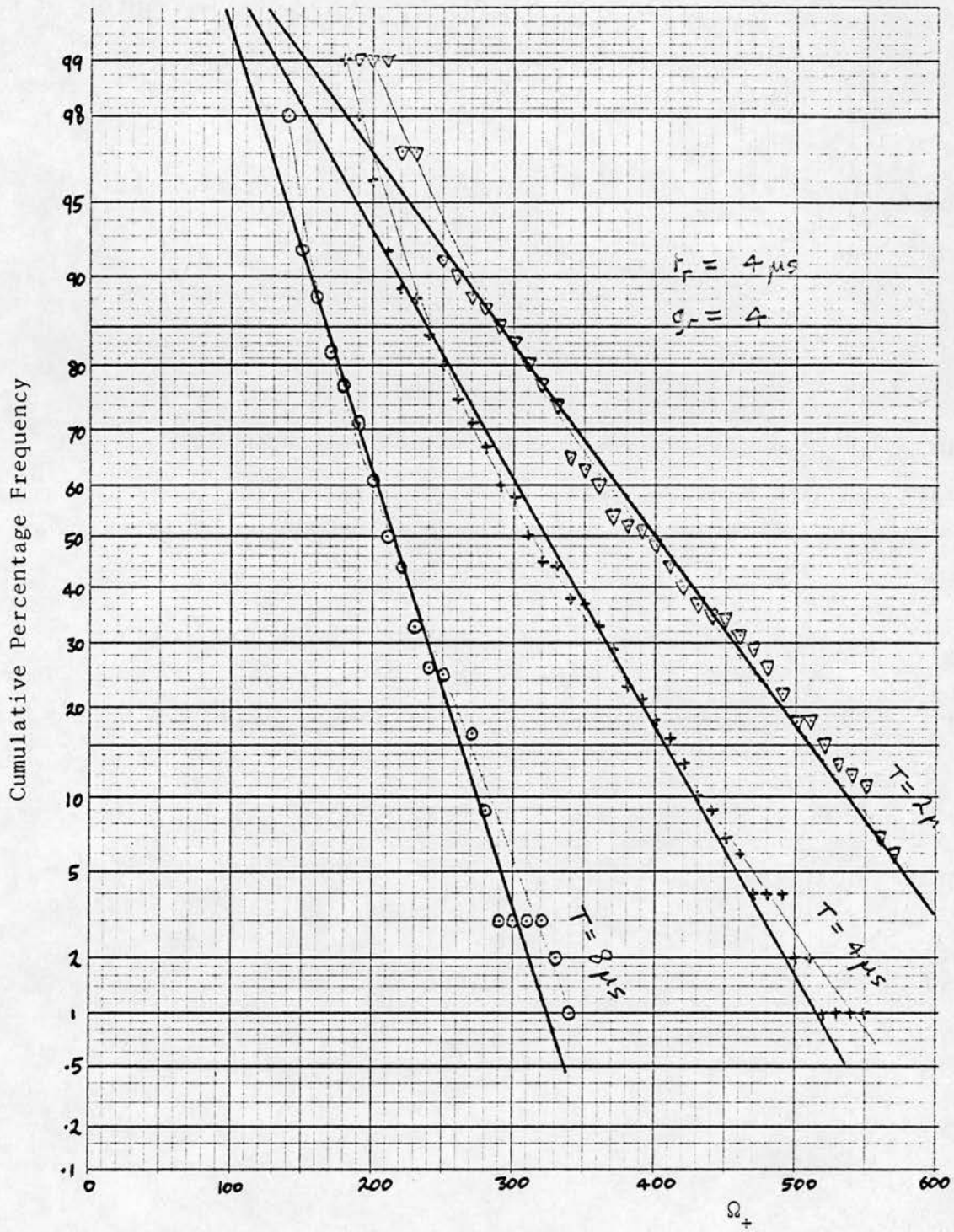

FIGURE 8.23 CUMULATIVE DISTRIBUTION OF Ω_+ FOR ABNORMAL REGION COMPARED WITH CUMULATIVE GAUSSIAN DISTRIBUTION WITH SAME MEAN AND STANDARD DEVIATION.
$g_r = 4$, $t_r = 4$ μs

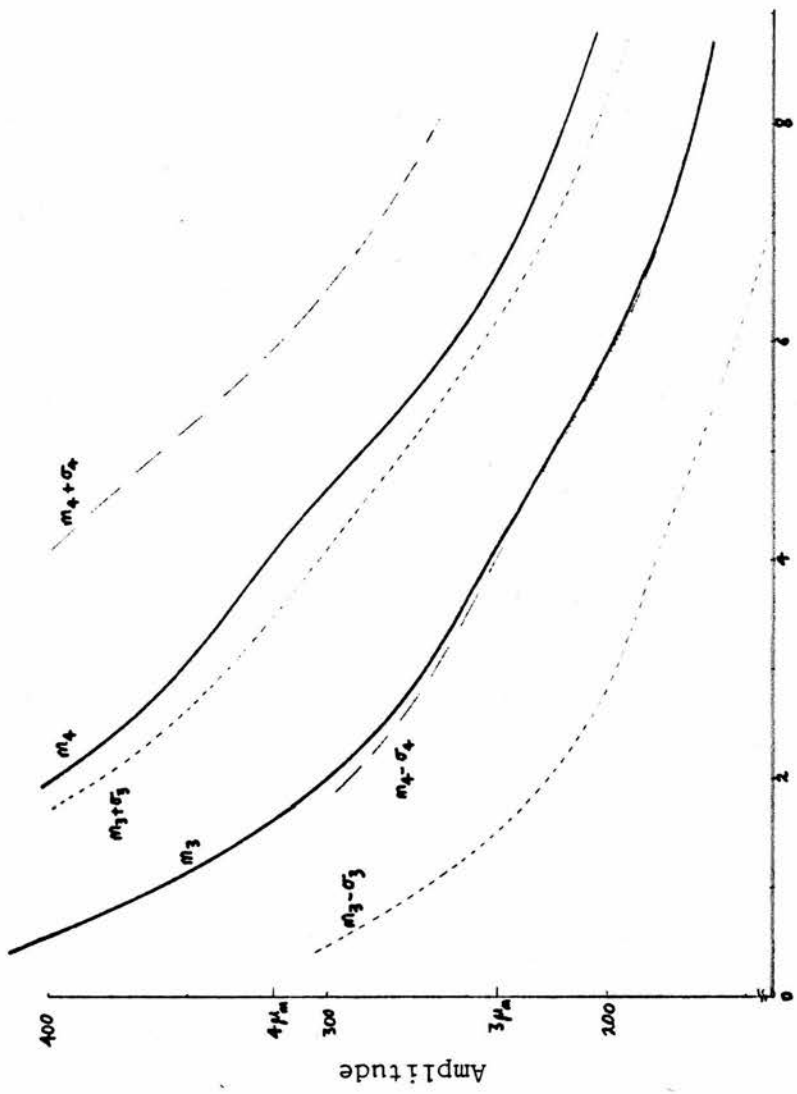

FIGURE 8.24 MEAN m_i AND MEAN PLUS OR MINUS ONE STANDARD DEVIATION ($m_i \pm \sigma_i$) OF Ω_+ FOR ABNORMAL REGIONS $g_r = i$, $t_r = 4$ μs.

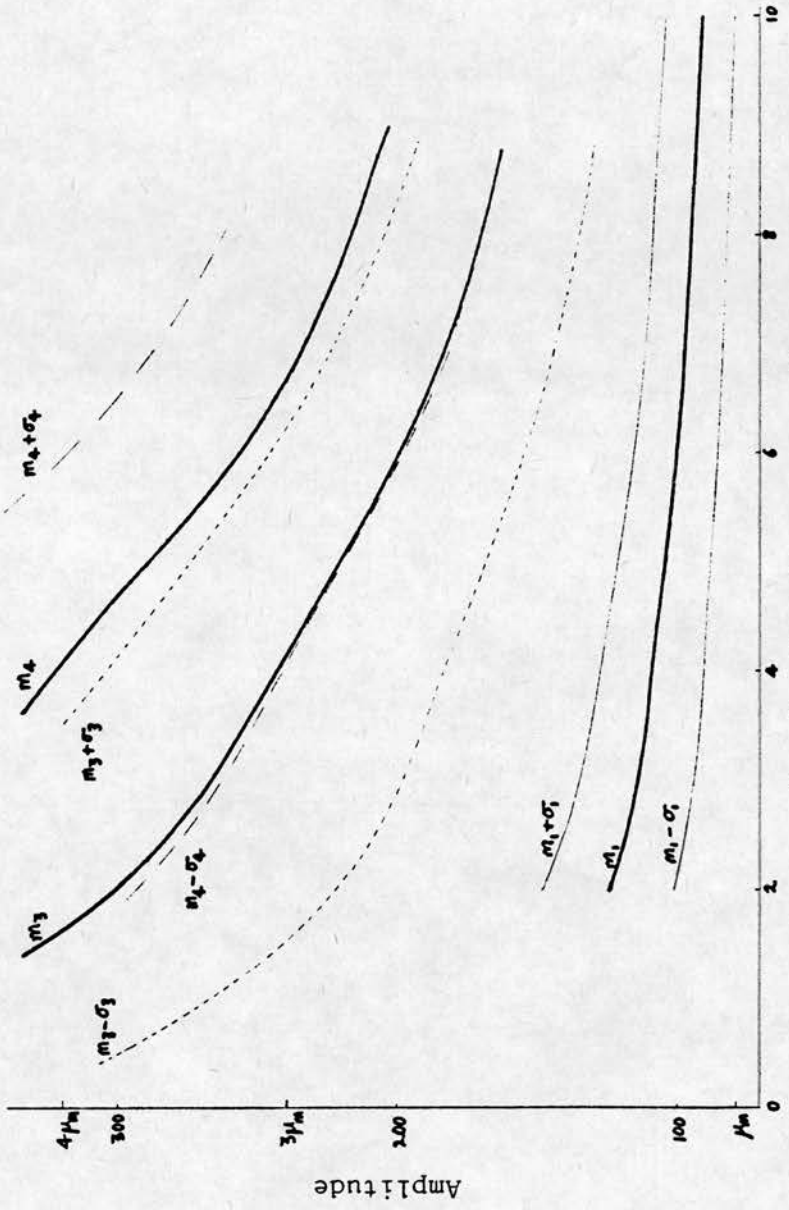

FIGURE 8.25 AS FOR FIGURE 8.24 BUT INCLUDING PLOTS FOR NORMAL SIGNAL ($g_r = i = 1$).

$g_r = 3$ and $g_r = 4$ indicates that one could not reliably distinguish between these abnormalities. In Figure 8.25 the results for the abnormal regions are compared with the results for normal signals. Again the fairly rapid change in mean value when the length of moving average exceeds the length of the abnormal region indicates that the optimum length of moving average will be around that length. There is little point in determining the optimum length precisely since in practice we will not know the length of the abnormality. Figures 8.24-25 indicate the effect of using lengths of moving average differing from the length of the abnormality.

8.10 EXPECTATION VALUES FOR SYNTHESISED SIGNALS

From the formula for the sum of the square of independent random variables (Hoel, 1971) we obtain for the expectation value of the rms amplitude of the signal at time t

$$E\left[\sqrt{P^2(t)}\right] = \frac{N}{\tau}\left\{\overline{w^2}\int_0^{\infty}\left[g(t')F(t-t')\right]^2 dt'\right\}^{\frac{1}{2}} \qquad (8.46)$$

assuming that $\bar{w} = 0$. This formula was solved numerically for a variety of functions for g(t') and some of the results are shown in Figures 8.26-27. The effect of changing t_r and g_r (Equation 8.43) can be seen.

The expectation value of the modulus of the signal is obtained by noting that for high reflector densities the amplitude distribution of $|P(t)|$ is semi-normal and the expectation value of $|P(t)|$ is simply $\sqrt{2/\pi}$ times the expectation value of the rms of P(t) given in Equation 8.46.

To obtain the expectation value of the moving average M(t,T) we can

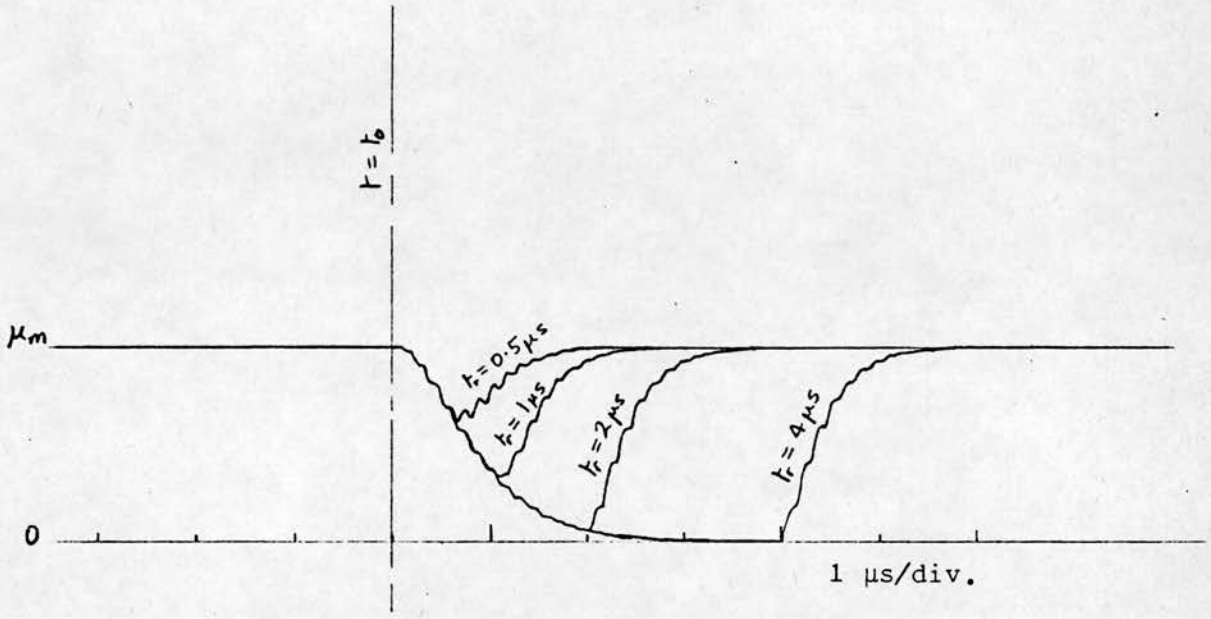

FIGURE 8.26 EXPECTATION VALUES FOR $|P(t)|$ FOR ABNORMAL REGIONS WITH $g_r = 0$ AND VARIOUS WIDTHS.

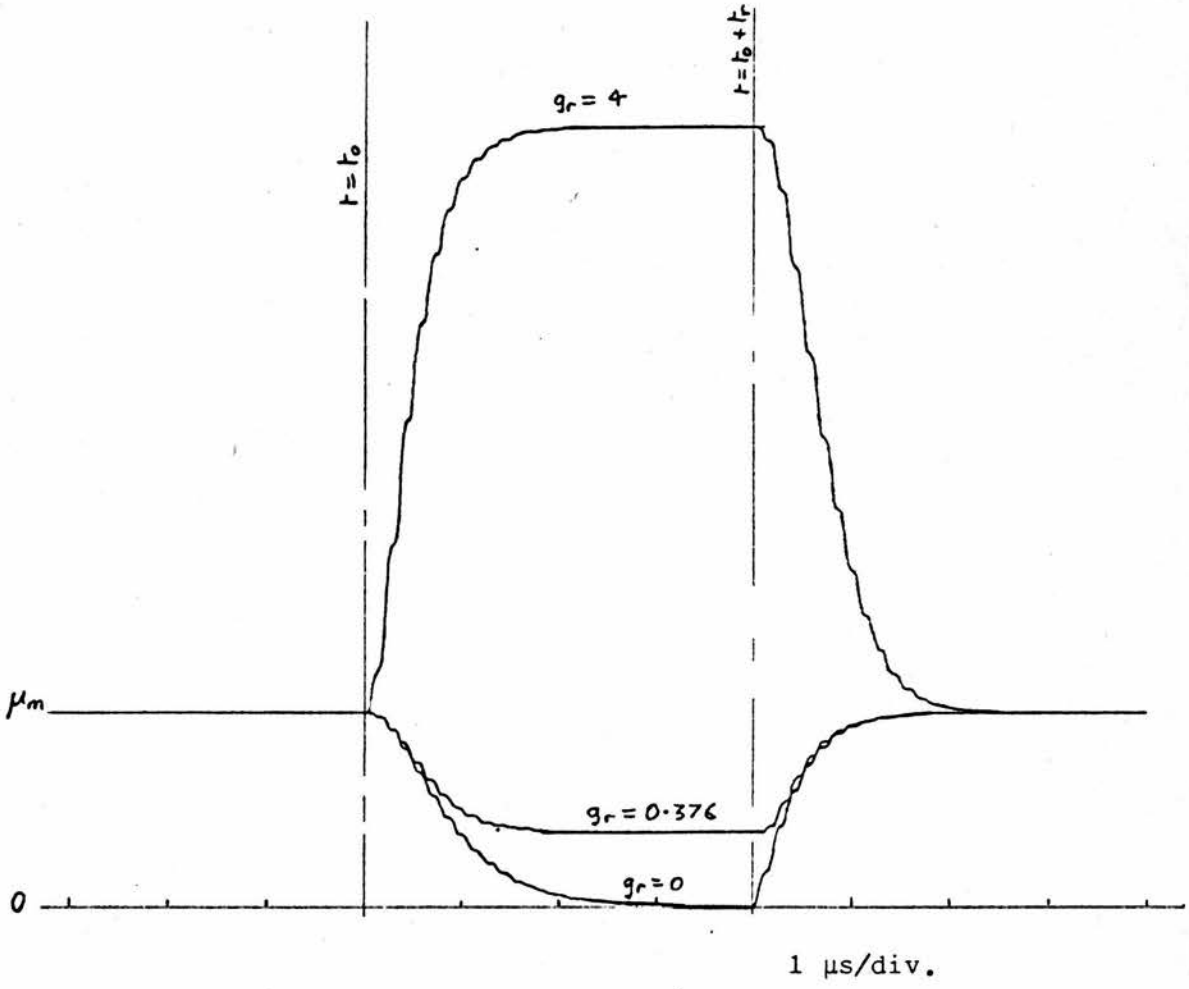

FIGURE 8.27 EXPECTATION VALUES FOR $|P(t)|$ FOR ABNORMAL REGIONS WITH t_r = 4 μs AND g_r = 0, 0.376 and 4.

use the fact that the expectation value of the integral of a function is equal to the integral of the expectation value of the function (Hoel, 1971). Thus we obtain

$$E\left[\frac{1}{T}\int_{t}^{t+T} |P(t')|\,dt'\right] = \frac{1}{T}\int_{t}^{t+T} E\left[|P(t')|\right] dt' \qquad (8.47)$$

That is, the expectation value of M(t,T) can be obtained by taking the moving average of the expectation value of the modulus of the signal. Since the expectation value of $|P(t)|$ can be found as described above we can process it to obtain the expectation value for the moving average. We can also find the maximum (or minimum) value of the expectation value of M(t,T) as t varies.

The dependence of the maximum value on T for an abnormal region (g_r = 4, t_r = 4 μs) is shown in Figure 8.28. It is compared with the mean value of Ω_+ found for synthesised signals using the same function g(t). It is expected that the mean value of Ω_+ will be higher than the maximum value of the expectation value of $|P(t)|$ because statistical fluctuations will raise the mean value of Ω_+. Comparison of the two lines allows us to estimate the importance of the effect of statistical fluctuations in raising the maximum value reached by the moving average. Figure 8.29 shows the minimum value of the expectation value of M(t,T) compared with the mean of Ω_- for an abnormal region with g_r = 0.376 and t_r = 4 μs.

8.11 DEPENDENCE OF Ω_+ ON LENGTH OF TIME WINDOW t_w

The dependence of the distribution of Ω_+ on length of time window t_w was determined for several lengths of moving average T. A normal signal was used for the determination. The dependence of the mean

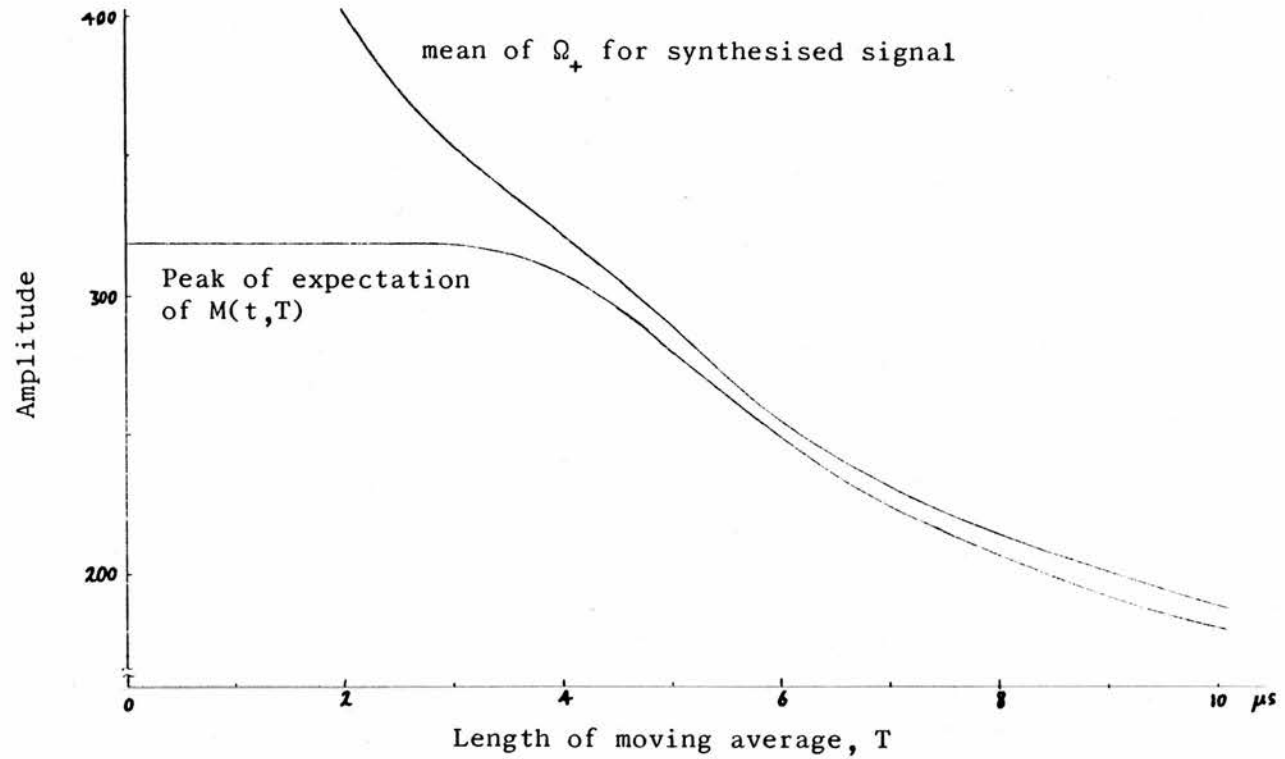

FIGURE 8.28 PEAK OF EXPECTATION VALUE OF MOVING AVERAGE M(t,T) COMPARED WITH MEAN OF Ω_+ FOR ABNORMAL REGION WITH g_r = 4 AND t_r = 4 μs.

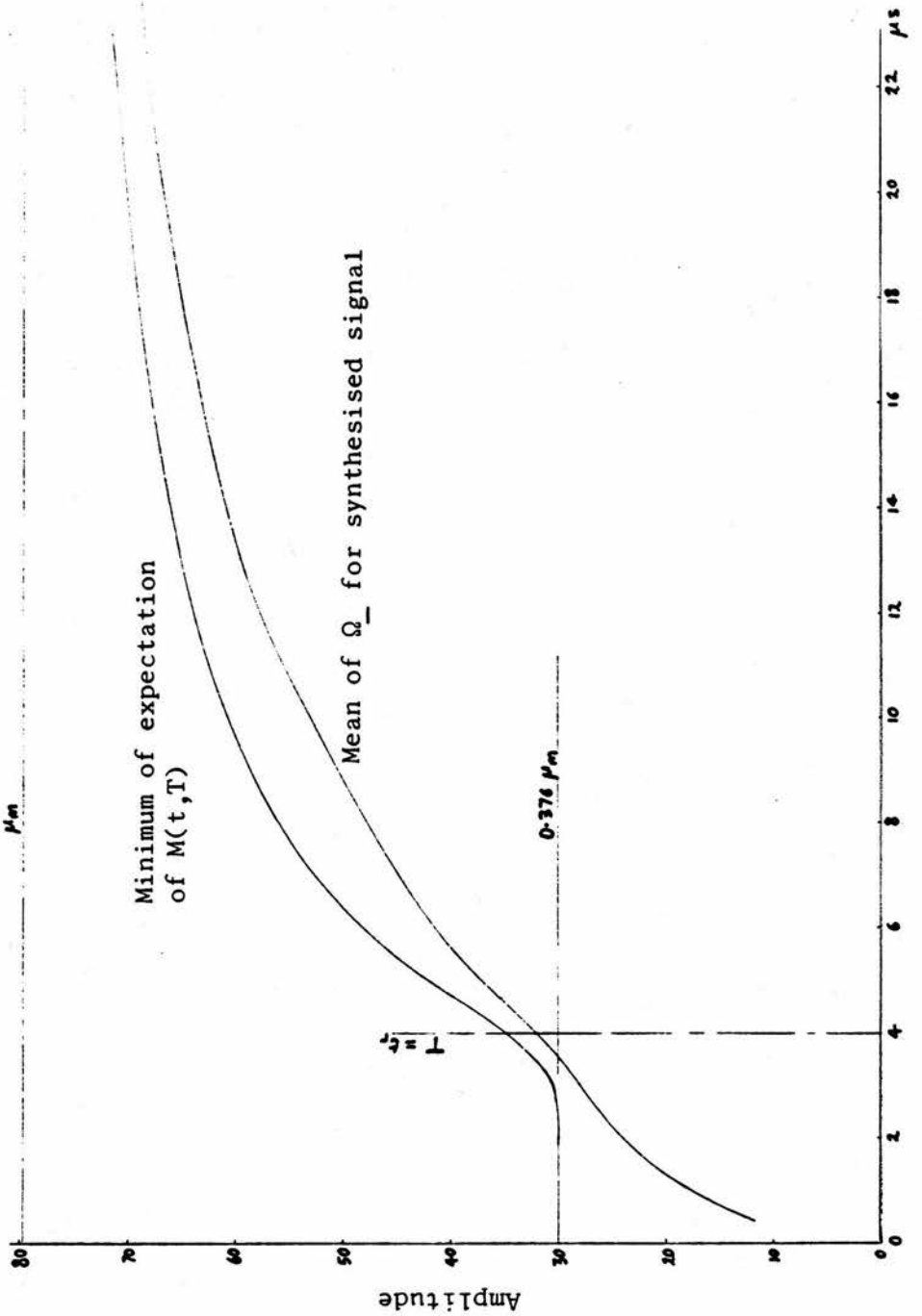

FIGURE 8.29 MINIMUM OF EXPECTATION VALUE OF MOVING AVERAGE M(t,T) COMPARED WITH MEAN OF Ω_- FOR ABNORMAL REGION WITH $g_r = 0.376$ AND $t_r = 4$ μs

value of Ω_+ on the length of time window is plotted in Figure 8.30.

As the length of the time window t_w is increased the mean value of Ω_+ increases, although slope of the curve reduces. As we would expect, the greatest increases are for low values of T. The mean of Ω_+ is determined from an ensemble of 100 signals and the error bars indicate $\sigma/10$ where σ is the standard deviation of a single sample of Ω_+. Figure 8.31 shows the dependence of the mean and mean plus or minus one standard deviation on the length of the time window.

Let $A(t_w,T)$ be the mean value of Ω_+ for a normal signal. This function may be used to estimate the mean value of Ω_+ for signals from long abnormal regions with $g_r \rangle 1$. In Section 8.10 we saw that the mean value of Ω_+ was greater than the maximum value of the expectation values of the moving average. The increase is due to random fluctuations in the moving average $M(t,T)$. The mean value of moving averages totally within the abnormal region will be $g_r\mu_m$, where μ_m is the mean of $|P(t)|$ for normal signals. If we ignore end effects the moving average will be totally within the abnormal region for a time t_r-T. Fluctuations within this time will raise the mean value of Ω_+. Although the maximum value of $M(t,T)$ is likely to occur during this time it could occur outside so we can set a lower limit for the mean value of Ω_+

$$\bar{\Omega}_+ \gg g_r A(t_r-T,T) \tag{8.48}$$

Provided g_r is not too small it is unlikely that the maximum value will occur when more than half the moving average is outside the

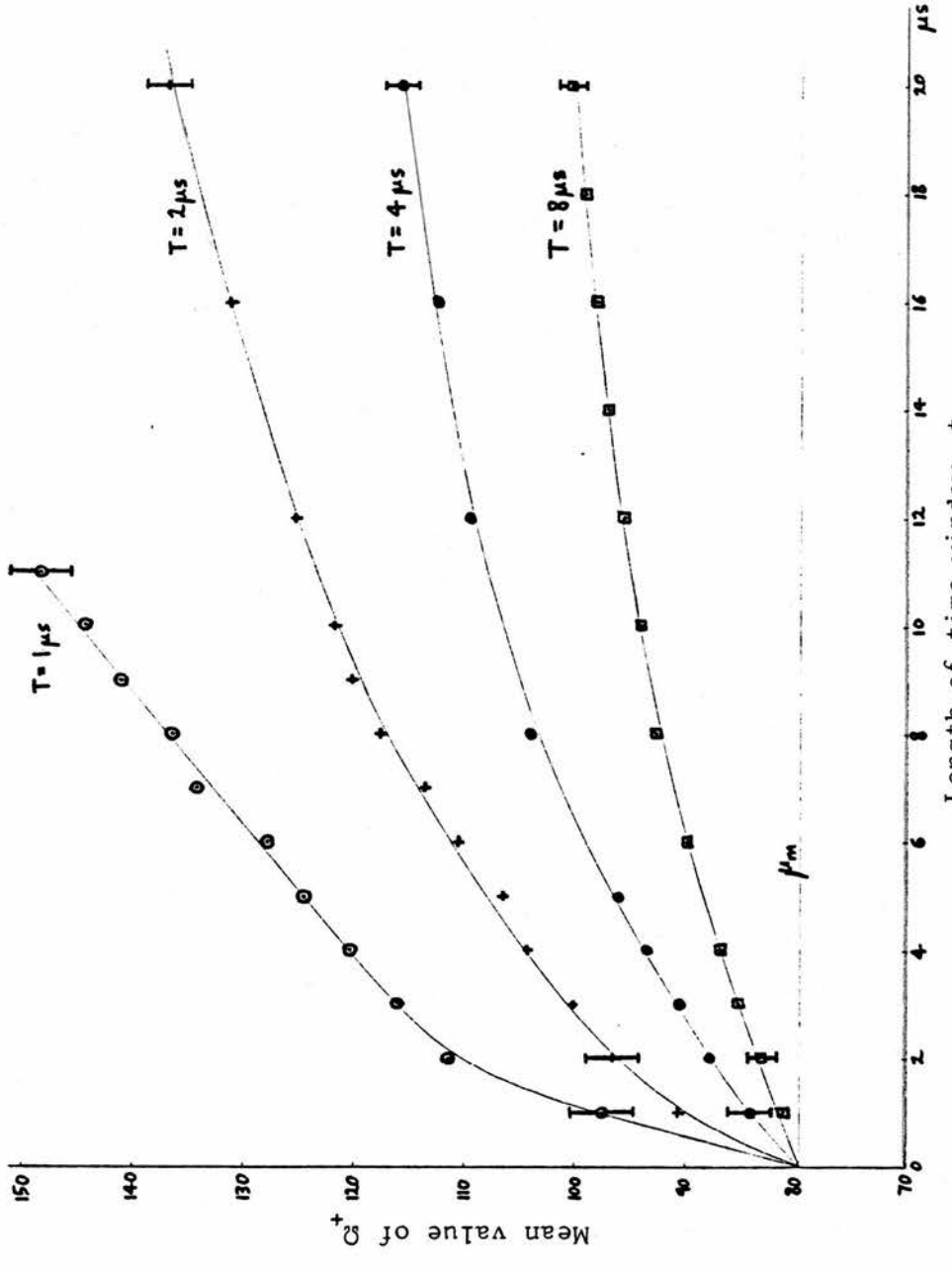

FIGURE 8.30 DEPENDENCE OF MEAN VALUE OF Ω_+ FOR NORMAL SIGNAL ON LENGTH OF TIME WINDOW t_w

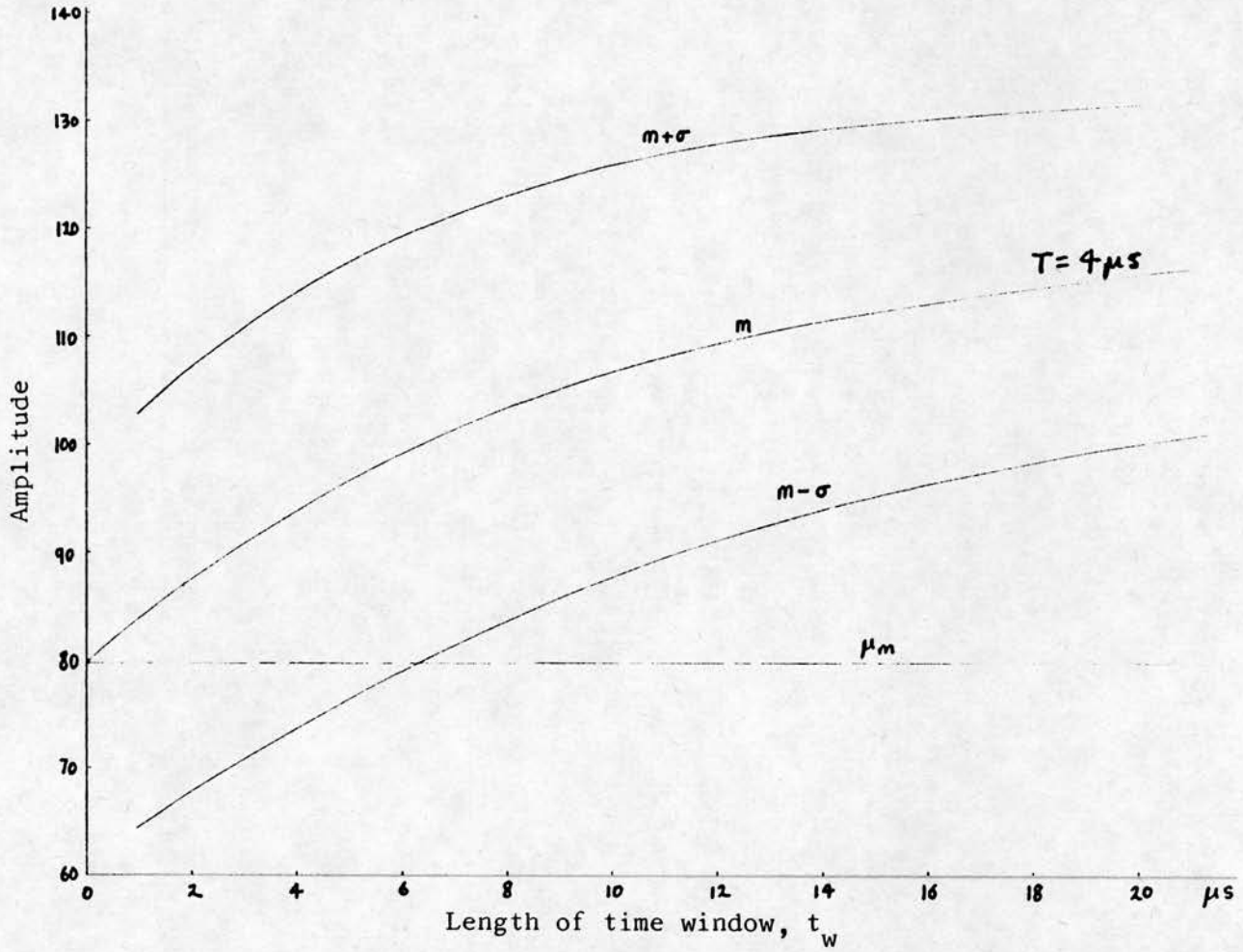

FIGURE 8.31 DEPENDENCE OF MEAN m AND MEAN PLUS OR MINUS ONE STANDARD DEVIATION ($m \pm \sigma$) OF Ω_+ FOR NORMAL SIGNAL, ON LENGTH OF TIME WINDOW t_w

abnormal region so we can estimate an upper limit for the mean value of Ω_+

$$\bar{\Omega}_+ \lesssim g_r A(t_r,T) \qquad (8.49)$$

Table 8.1 shows the results of using Equations 8.48 and 8.49 and data from Figure 8.30 to predict the lower and upper bounds on the mean value of Ω_+ for an abnormal region with $g_r = 3$, $t_r = 16$ μs. Since the range between the upper and lower bounds is small any estimate within this range is likely to be accurate enough for many purposes. The errors quoted are based on the standard deviations of the mean values of Ω_+ used to produce Figure 8.30.

Table 8.1 also shows the mean values of Ω_+ obtained for an ensemble of 100 signals synthesised with $g_r = 3$, $t_r = 16$ μs. The observed values all lie within one standard deviation of the upper and lower bounds estimated using Equations 8.48 and 8.49.

Although the estimates are fairly rough the comparison does lend some quantitative support to the qualitative statement that the random fluctuations in the value of M(t,T) increase the mean value of Ω_+. It is hoped that an understanding of the most significant factors affecting the distribution of Ω_+ will aid the design of an efficient detector.

8.12 RELATING LEVEL CROSSING FREQUENCY TO FALSE WARNING RATE

For convenience we will consider excursions of M(t,T) above a high threshold level but similar arguments may be applied to excursions below a low threshold level.

TABLE 8.1

ESTIMATES FOR UPPER AND LOWER BOUNDS ON THE MEAN VALUE OF Ω_+ COMPARED WITH VALUES FOUND FOR SYNTHESISED SIGNAL WITH $g_r = 3$, $t_r = 16$ μs.

Estimates are based on Equations 8.48 and 8.49 and data from Figure 8.30.

T	Lower bound for mean of Ω_+	Upper bound for mean of Ω_+	Mean of Ω_+ for synthesised signal
2	384 ± 7	395 ± 7	397 ± 8
4	327 ± 5	339 ± 5	322 ± 5
8	276 ± 4	294 ± 4	276 ± 4

If upcrossings of a threshold level are widely separated each upcrossing could be considered to be due to an abnormality. If clustering effects (Section 8.8.1) are significant the distance between clusters is more important than the distance between individual upcrossings because each cluster will be seen to be a manifestation of a single large excursion of the echo amplitude from its mean value.

Theoretical analysis of the distribution of time intervals between upcrossings is difficult (Blake and Lindsey, 1973). Experimental work on the distribution of level crossing intervals for filtered white noise has been reported by O'Neill et al. (1976). At present the level crossing program does not include facilities for determining the distribution of level crossing intervals for synthesised data.

If we can ignore the effect of clustering the mean distance between false warnings will be given by

$$\text{mean false warning separation} = \frac{2}{N_t} \cdot \frac{v}{2} = \frac{v}{N_t} \qquad (8.50)$$

where v is the group velocity of ultrasound in tissue and N_t is the level crossing frequency of M(t,T). The determination of the level crossing frequency N_t was described in Section 8.6.

8.12.1 Relating level crossing frequency to distribution of Ω

To calculate the cumulative distribution of Ω_+ for normal signals from the level crossing frequency of the moving average M(t,T) a number of simplifying assumptions will be made. Upcrossings that are far apart are independent and it will be assumed that all up-

crossings can be taken to be randomly distributed in time. If a threshold level Φ is crossed in the upwards direction during the time window t_w then Ω_+, the maximum value reached by $M(t,T)$, is certainly greater than Φ. If the level is not crossed in the upwards direction then either the threshold level is not exceeded at all or the level is exceeded due to an upward crossing before the start of the time window. If we assume that the excursion above the threshold level is short (on average) compared with the duration of the time window then we can neglect the small number of occasions on which the threshold level is exceeded due to an upcrossing before the start of the time window. Making this assumption we can equate the probability of an upcrossing to the probability that the level is exceeded during the interval. The latter probability is given by the cumulative probability distribution of Ω_+. Assuming that the times of the upcrossings are independent the probability of one or more upcrossings of the level Φ during interval t_w is given by

$$\Pr(\text{upward crossing}) = 1 - \exp(-t_w N_t/2) \qquad (8.51)$$

Substituting values of N_t found for the level crossing frequency of $M(t,T)$ and multiplying by 100 we obtain the percentage of sections of length t_w containing a value higher than the threshold. The values obtained in this way for t_w = 12 μs and T = 4 μs are compared with the cumulative distribution of Ω_+ in Figure 8.32.

Similar arguments apply to downward crossings of levels below the mean level and the same formula can be used to predict the cumulative distribution of Ω_-. Figure 8.33 compares the prediction based on

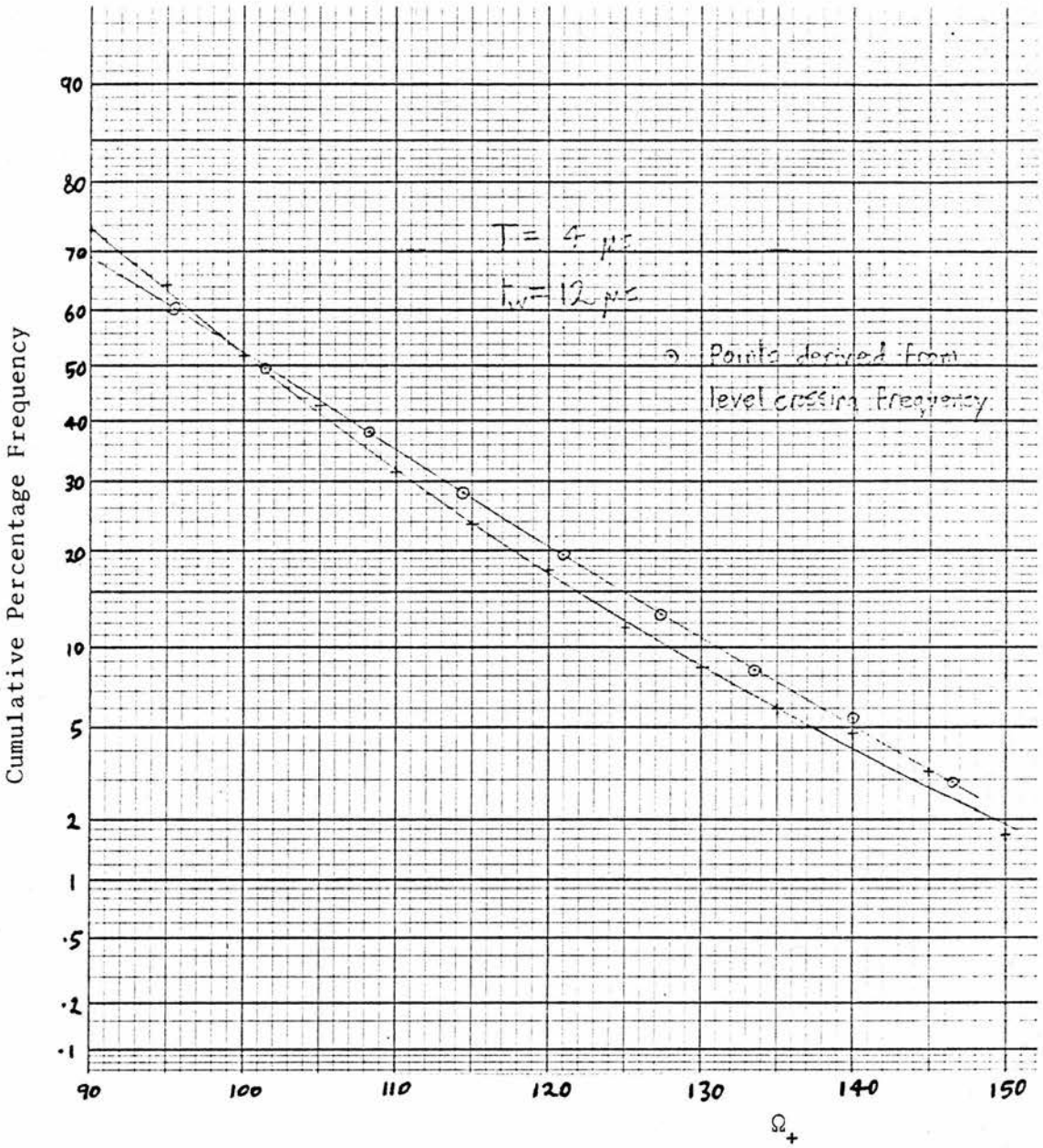

FIGURE 8.32 CUMULATIVE DISTRIBUTION OF Ω_+ FOR NORMAL SIGNAL COMPARED WITH PREDICTION DERIVED FROM LEVEL CROSSING FREQUENCY.

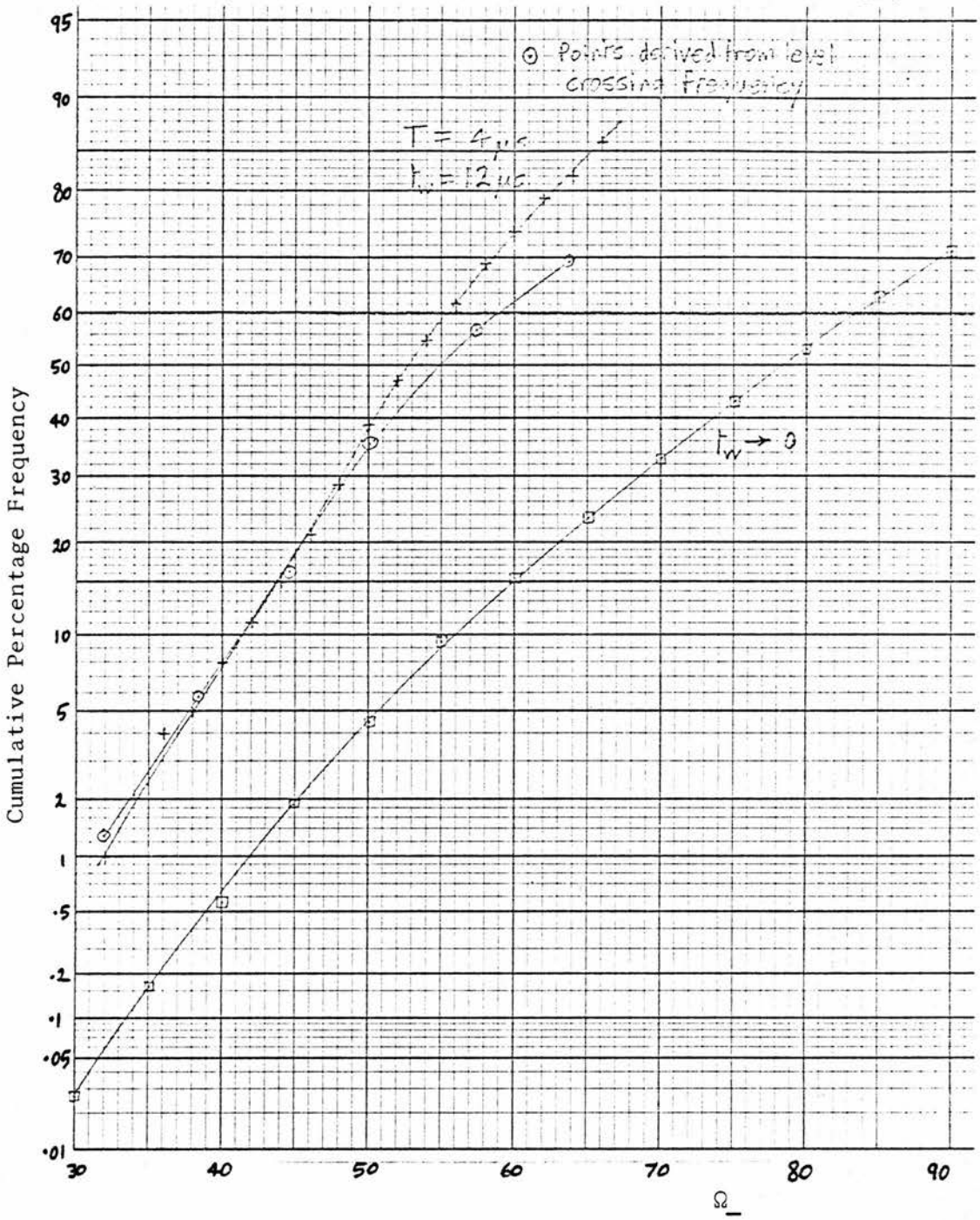

FIGURE 8.33 CUMULATIVE DISTRIBUTION OF Ω_{-} FOR NORMAL SIGNAL COMPARED WITH PREDICTION DERIVED FROM LEVEL CROSSING FREQUENCY.

the level crossing data with the cumulative distribution of Ω_-. Also shown on Figure 8.33 is the cumulative distribution of Ω_- for $t_w \rightarrow 0$.

In view of the simplifying assumptions the agreement between the predictions and the cumulative distributions is good. To make a better estimate it would be necessary to consider in more detail the trajectory of the moving average M(t,T) following a level crossing.

8.12.2 Extending the theory

Because very low false warning rates are desirable we wish to know the cumulative distributions for Ω_+ and Ω_- down to very low levels of probability. To synthesise enough signal to contain a significant number of rare events takes a long time; the simulation to obtain the line for a 4 μs moving average of the modulus of a normal signal in Figure 8.21 involved synthesising one thousand 12 μs segments and took approximately 3 hours. To obtain ten events that have a probability of 0.01 would require (on average) 100,000 sections to be simulated taking 300 hours. The long processing time makes this rather impractical. Possible solutions would be to optimise the simulation and analysis program or use a more powerful processor. Perhaps a more satisfactory solution would be to predict the probabilities by mathematical analysis. In practice the processing function is likely to be more complicated than the moving average so the mathematical analysis could be difficult. The most successful approach could be to combine the results of simulation and theory, using the simulation to check the validity of simplifying assumptions.

If several parallel A-scans are used to detect an abnormality the error rates for individual scans can be higher whilse still maintaining acceptable error rates for the combined scans. The program used to synthesise echo data would need to be modified to simulate the echo signals for different probe positions relative to the array of scatters. The optimum combination of signals from different probe positions is an important problem still to be tackled.

8.13 MODIFICATIONS TO THE DETECTOR FOR USE ON TISSUE DATA

The moving mean modulus M(t,T) was studied as a first step towards designing a better estimator. The simulations and calculations allow the importance of various factors to be determined and so provide useful information on which to base future designs. The process of designing a more suitable estimator is in its initial stages.

Since the error rate for the moving average threshold detector is rather dependent on the threshold level, variations in attenuation in overlying tissues could seriously lower the performance of the detector. One improvement could be to use one long moving average to establish the mean echo amplitude and use a second (and shorter) moving average to detect changes from that mean caused by abnormalities. Work has begun using the processing function $R_m(t,T_1,T_2)$ defined by

$$R_m(t,T_1,T_2) = \frac{M(t+T_2,T_1)}{M(t,T_2)+1} \qquad (8.52)$$

where T_1 and T_2 are the lengths of the moving averages. The ratio is compared with a fixed threshold. One of the problems is that there are now more parameters to vary, making it harder to establish the effect of the variations.

The form of processing defined in Equation 8.52 is only one of many possibilities that could be tried. The wide variety indicates that some theoretical framework will be required to direct the choice. The combination of theory and simulations should be useful in this respect.

8.13.1 Staging of bladder tumours

The detection of extended abnormal regions is only one example of a statistical decision problem in diagnostic ultrasound. Another statistical decision problem that was considered was the problem of determining whether a bladder tumour has penetrated the bladder wall. The staging of bladder tumours is an important clinical problem (Riddle, 1976; Morley, 1978). Of particular importance is to determine whether the tumour has penetrated the bladder wall. This is sometimes possible using standard ultrasound B-scanning (Morley, 1978) but quantitative analysis of the echoes may be able to improve the technique.

It seemed possible that if the tumour penetrated the bladder wall there would no longer be any large echoes from the wall; failure to find large echoes could indicate that the tumour had penetrated the wall. However, initial results indicate that it would be difficult to reliably detect penetration by this means. A primary problem

is that the echo amplitude from the bladder wall is highly dependent on the orientation of the wall relative to the ultrasound beam, which can reduce the amplitude to the level of echoes from the tumour. This problem is enhanced by the fact that the presence of the tumour can distort the wall so it is not easy to predict the position of the wall.

Another problem in bladder scanning is caused by the large difference in attenuation between tumour and urine. The attenuation in urine is very small. It may be possible to devise an automatic gain control which would not sweep the gain during echo-free periods (corresponding to urine). Normal automatic gain control (agc) will decrease the gain if the echo amplitude is large, but the proposed bladder agc will increase the gain when echoes are detected. Such an arrangement is potentially unstable and could create design problems. Using the data acquisition system to establish the range of echo signals that the agc system would have to process could help in its design. A proposed design could be simulated on the computer and tested with echo data from tumours and with synthesised data with known characteristics.

8.14 IMPLICATIONS FOR INTERPRETATION OF GREY SCALE IMAGES

Due to the random nature of the ultrasonic echoes it is necessary to be wary of relying on small details within the image; the fact that a detail is visible does not mean that it is significant.

In low light intensities statistical variations in the number of photons reaching the eye will limit the resolution of the visual system (Rose, 1973). In a similar way quantum mottle can limit

the resolution in X-ray images (Sturm and Morgan, 1949; Ter-Pogossian, 1967). In these cases the resolution will depend on the contrast in the image. To appreciate subtle changes the image must be averaged over larger areas before the change is significant. The speckled appearance of normal liver parenchyma limits the size of the smallest lesion that can be reliably detected (Cosgrove, 1978; Morrison et al., 1978). Again the resolution obtainable will depend on the degree of contrast in the image. The more similar the echogenicity of a lesion is to that of the surrounding normal tissue the larger it will have to be before it can be reliably detected. An additional problem is to distinguish between small ducts and small lesions giving low level echoes.

Whilst the analysis of echo signals for single directions is relevant to the problem of predicting the best resolution obtainable it is necessary to extend the theory to two dimensions. However, the problem is not purely technical, because the physiology of the visual system will also affect the achieved resolution (Gregory, 1966; Ter-Pogossian, 1967; Stockham, 1972; Rose, 1973; Goodenough, 1976; Hay and Chesters, 1976; Metz et al., 1976). Such considerations are beyond the scope of this thesis.

Even without going into the details of the visual system we can anticipate that if we can improve the statistics we will be able to improve the achieved resolution. In isotope and X-ray imaging it is sometimes possible to improve the statistics by increasing the intensity of the radiation or by increasing the scan time. Since the interference noise is inherent in the signal increasing the

transmitter power will increase the noise in proportion and we are no better off. If the object is stationary the echo signal will (apart from a small amount of noise added by the receiver) be identical from pulse to pulse so we cannot remove the inherent noise by averaging successive echo signals. In practice there will be some patient movement and there may be some advantage in averaging successive echo signals.

One way of improving statistics is to combine independent samples. One method of achieving this is to scan the same tissue from different angles. Scanning from a different angle changes the phase relationships of the echoes from the scatterers and changes the resulting echo amplitude. When bistable displays were in widespread use the main features of interest were major interfaces. Compound scanning was popular, since by scanning from several directions the beam could be brought closer to normal incidence at the interfaces. Scattering is less dependent on angle than specular reflections from large interfaces and satisfactory grey scale images are often made with a single sweep. However, scanning from more than one angle can improve the image if the statistics are limiting the resolution. Scanning from more than one direction can degrade the image due to patient movement and other registration errors so there is a compromise involved. If the lesion is small the degradation due to registration errors may outweigh the advantages of signal-to-noise ratio improvements, but for larger lesions only slightly different from the normal tissue the improvement in signal-to-noise ratio can outweigh the effects of poorer registration.

To minimise the registration errors due to patient movement the scan should be performed fairly rapidly during restricted respiration. One way to achieve a smooth action is to sweep the probe along the skin in one direction and then change the angulation of the probe before the return sweep. Several factors, including the build of the patient, will affect the choice of scan action and experience will be required to select the optimum. The choice of scan converter update algorithm can also affect the image quality and this is considered in the following section.

8.15 DIGITAL SCAN CONVERTER SIMULATION

8.15.1 Introduction

Digital scan converters store echo information in a digital store and output the image in a TV raster format. If the same pixel (picture element) is written to more than once the new value will depend on the form of update algorithm used. In the search mode the old value is simply replaced by the new echo amplitude. There is no need to erase the image between scans which, as the name suggests, is ideal for searching through the body. In the peak writing mode the old value is replaced by the new echo amplitude only if the new value exceeds the old value. In the pseudo-integration mode a fraction f_u of the difference between the old stored value and the new echo amplitude is added to the old stored value if the new echo amplitude exceeds the old stored value.

8.15.2 Method of simulation

The increase in signal-to-noise ratio due to combining two or more signal values can be expected to depend on the update algorithm.

To investigate this simulations were performed to compare the different update algorithms.

The simulations were performed to achieve an insight into some of the factors involved and so a number of simplifying assumptions were made. Only a single pixel was considered; the result of combining N_u signal values was found. It was assumed that samples (from different directions) were statistically independent and that all samples came from the same distribution. The distribution used was derived from liver echo data by the method described in Section 7.3.2. It was assumed that the scan converter uses the peak echo amplitude occurring within a 0.5 μs period as the signal value to be combined with the old stored value for the appropriate part of the image. This is a commonly used form of processing, although other forms are used. Quantisation effects are assumed to be negligible, although for a scan converter using only sixteen levels these effects could be significant.

The independent random numbers were combined using the various update algorithms described above. The distribution of the final values, after combining N_u random signal values, was analysed to determine the mean and the coefficient of variation. The simulations were repeated for different values of N_u. The pseudo-integration mode was simulated using different values for f_u.

Two modes not normally found on scan converters were also included for comparison; the mean of the N_u values, and the sum of the N_u values. The mean mode can be expensive to implement if the number N_u has to be stored for each pixel (there can be around 256K pixels).

8.15.3 Simulation results

Figure 8.34 shows how the coefficient of variation depends on N_u for various update algorithms. The biggest decrease in coefficient of variation is for the mean mode (or the sum mode). For very small values of f_u the pseudo-integration mode is similar to the sum mode. For higher values of f_u the coefficient of variation is higher and as f_u approaches unity the processing becomes equivalent to peak writing mode. The search mode gives no reduction in coefficient of variation because the old value is always replaced by the new value.

Figure 8.35 shows how the coefficient of variation depends on f_u for pseudo-integration mode. Again we can see that the biggest reduction in coefficient of variation is for low values of f_u.

Because some parts of the image may get scanned from more directions than other parts it is desirable that the mean of the final values is independent of N_u. The dependence of the mean value on N_u is shown in Figure 8.36. All the values are normalised to make the mean value equal unity when $N_u = 1$. The mean mode and the search mode will give a mean final value independent of N_u. The other modes give a performance in between these extremes. Pseudo-integration mode gives the greatest change in mean value for small values of f_u. As f_u is increased the change is reduced and as f_u approaches unity the pseudo-integration mode approaches the performance of the peak writing mode.

If the probe and object remain stationary several identical values will be used to update the stored value. To make the final stored

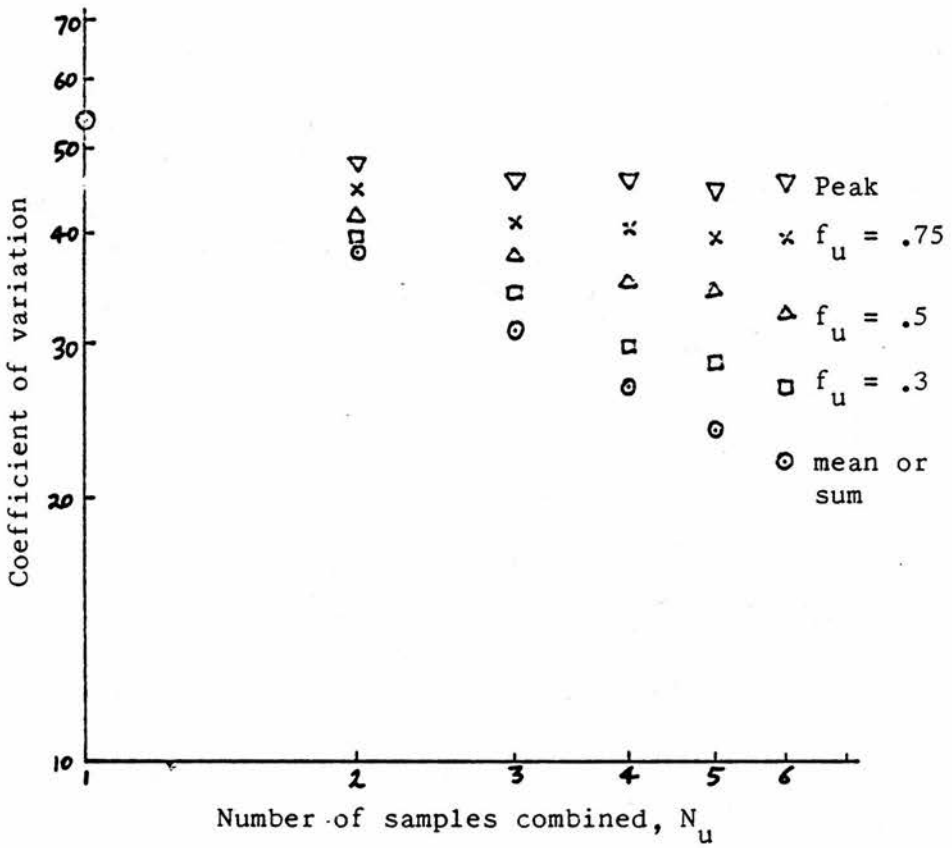

FIGURE 8.34 DIGITAL SCAN CONVERTER SIMULATION. DEPENDENCE OF COEFFICIENT OF VARIATION ON NUMBER OF SAMPLES COMBINED N_u FOR VARIOUS UPDATE ALGORITHMS. PSEUDO-INTEGRATION MODE IDENTIFIED BY VALUE OF f_u.

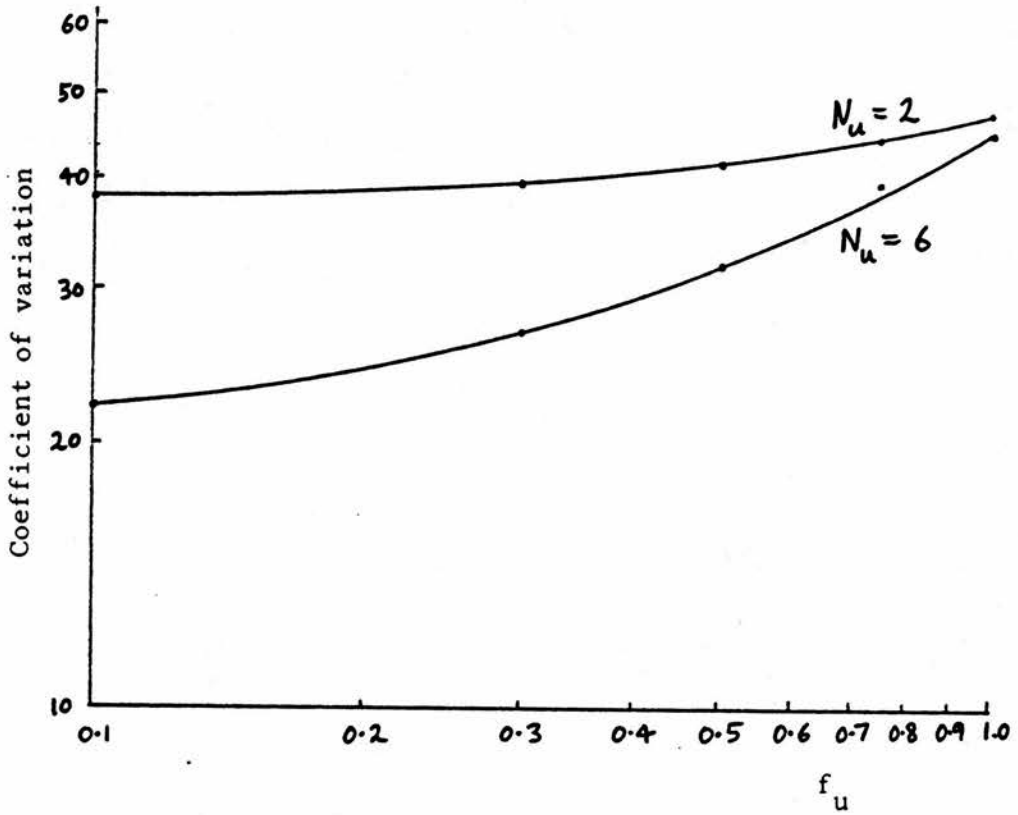

FIGURE 8.35 DIGITAL SCAN CONVERTER SIMULATION. DEPENDENCE OF COEFFICIENT OF VARIATION ON f_u FOR PSEUDO-INTEGRATION MODE UPDATE ALGORITHM.

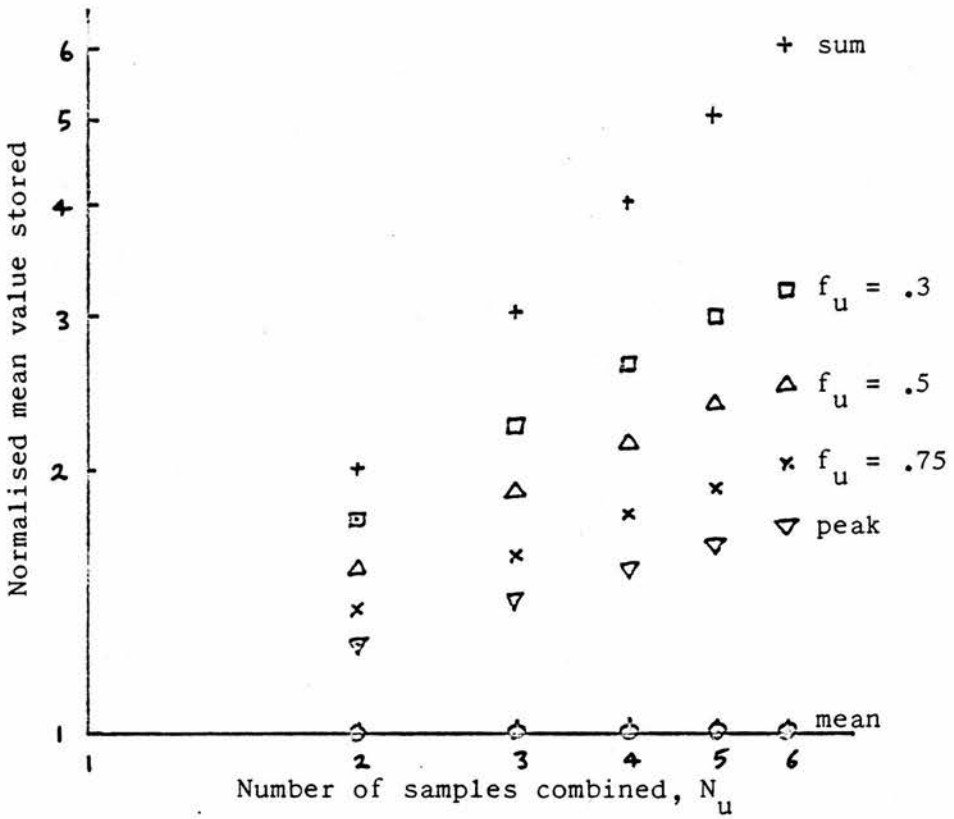

FIGURE 8.36 DIGITAL SCAN CONVERTER SIMULATION. DEPENDENCE OF MEAN VALUE STORED ON NUMBER OF SAMPLES COMBINED, FOR VARIOUS UPDATE ALGORITHMS. VALUES NORMALISED TO GIVE UNIT AMPLITUDE FOR SINGLE SAMPLE. PSEUDO-INTEGRATION MODE IDENTIFIED BY VALUE OF f_u.

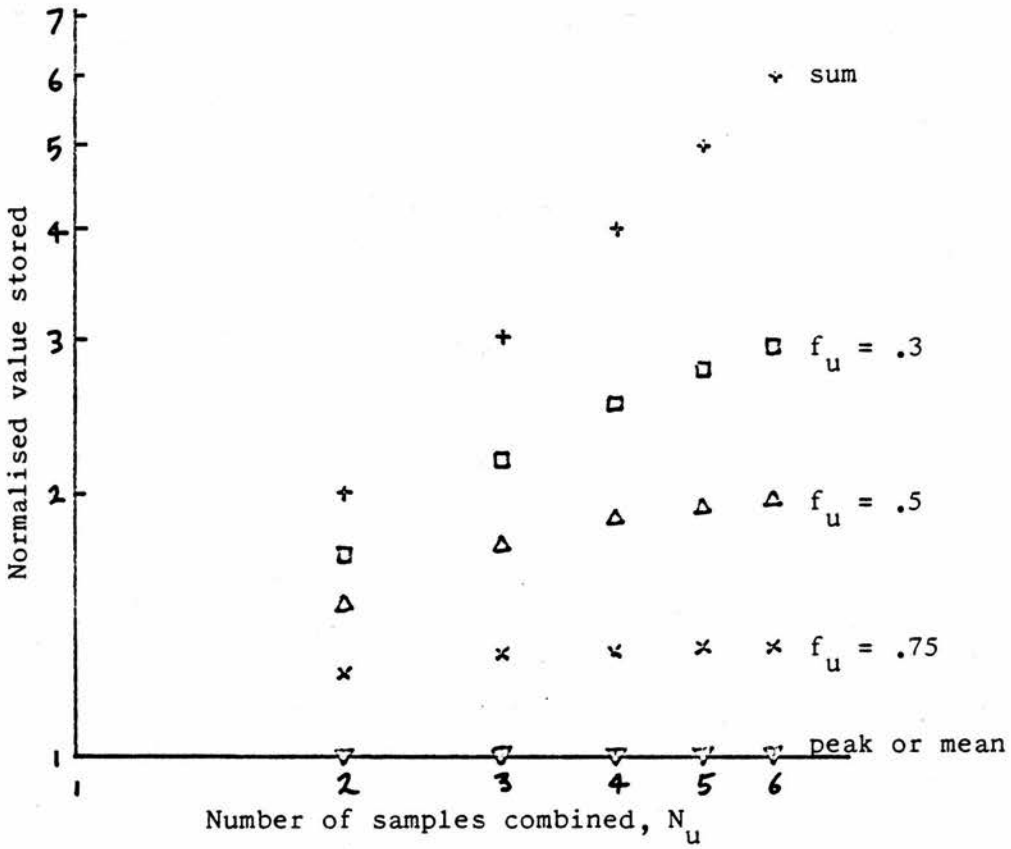

FIGURE 8.37 DIGITAL SCAN CONVERTER SIMULATION. FINAL STORED VALUE WHEN N_u IDENTICAL VALUES ARE COMBINED BY VARIOUS UPDATE ALGORITHMS. VALUES ARE NORMALISED TO GIVE UNIT AMPLITUDE FOR A SINGLE SAMPLE.

value independent of the scanning speed the final value should remain the same when several identical values are combined. The dependence of the final value on N_u when identical signal values are combined is shown in Figure 8.37. The mean mode, search mode and peak writing mode all give a final value independent of N_u. The final value for pseudo-integration mode increases as f_u decreases. For the sum mode the final value is proportional to N_u.

Both the change in coefficient of variation and the change in mean value should be taken into account when comparing different update algorithms. The change in mean should be considered for combining independent samples and for combining several identical samples. On all these counts the mean mode gives the best performance. The performance of the pseudo-integration mode approaches that of the sum mode for low values of f_u and as f_u is increased the performance approaches that of the peak writing mode. The reduction of coefficient of variation is greatest for small values of f_u but the change in mean value is least for high values of f_u. Thus the choice of f_u involves a compromise. A figure of merit combining all the factors could be devised but it could be hard to apply in practice since the choice will depend on several factors.

Further simulations could be performed to take into account more factors. In some update algorithms the stored value depends on how the write vector passes through the pixel, higher values being stored if the vector passes through the centre than if it only passes through a corner. The effects of non-linear processing and quantisation could be included. Various scan actions could be analysed. However, the large variety of effects involved could make it hard to

present the results in a useful form. Hopefully, a greater understanding of the various effects could help in the design of scan converters.

8.16 SUMMARY

The detection of abnormal regions was discussed within the framework of statistical decision theory. The difficulty of specifying a priori probabilities is seen to be a fundamental limitation.

Detection of abnormal regions by finding a change in the mean echo amplitude can be likened to the problem of detecting a change in mean in a sequence of random variables. To derive the ideal estimator analytically would be difficult so the simple moving average of synthesised echo data was studied as a first step towards designing a more efficient estimator.

Echo data was synthesised for arrays of scatterers containing regions with different scattering cross sections. The distribution of the maximum (or minimum) value of the moving average as it moves through the abnormal region was determined. The resulting distributions were compared with the distributions obtained for normal signals.

Expressions for the expectation values of the modulus and the moving mean modulus of the echo amplitude for abnormal regions were obtained. The expressions were evaluated numerically. The maximum (or minimum) expectation value for the moving average as it moves through the abnormal region was obtained. This could be compared with the distribution of maximum (or minimum) values of the moving average for synthesised echo data. We can use such comparisons to estimate the

importance of different factors affecting the distribution of maximum (or minimum) values.

The level crossing frequencies of long moving averages of the modulus of normal echo signals were determined. The level crossing frequencies were related to the false warning rates for a moving-agerage threshold detector.

Level crossing frequencies of the envelope of the synthesised echo waveform were measured to investigate a discrepancy between the theoretical and experimental results of Atkinson and Berry (1974). The experimental arrangement filtered the rectified echo waveform to obtain the envelope waveform. Because this filtering removes high frequency components of the envelope waveform the observed level crossing frequency is lower than that predicted by the theory. The ideal envelope was derived from a complex synthesised echo waveform. The level crossing frequencies of this synthesised envelope confirmed the theory.

Variations in attenuation in overlying tissues will degrade the performance of the simple moving-average threshold detector. Work on detectors better suited to in vivo detection is in its initial stages. Further work is required to determine the best way to combine echo information from A-scans for several probe positions.

The random nature of the echo amplitudes can limit the achievable resolution in standard grey-scale images. Detailed consideration of this requires a knowledge of the physiology of the visual system.

The performance of various digital scan converter update algorithms

were considered from a statistical viewpoint. Simulations were performed to determine the mean and standard deviation of the final stored value when several independent random variables are combined according to various update algorithms. The choice of update algorithm may involve a compromise; reducing the standard deviation can make the mean value more dependent on the number of values combined.

The problems caused by the interference of echoes from closely spaced scatterers are fundamental to many aspects of diagnostic ultrasound. In order to concentrate on these problems a number of simplifications were made. The problem of detecting a lesion in tissue was reduced to that of detecting an array of scatterers having a different scattering cross section from the surrounding array of scatterers. Even this simplified version of the problem presents formidable difficulties.

The use of simulations allowed many results to be obtained that would have been hard to obtain in any other way. By determining the most significant factors, simplified theories may be developed. In view of the random nature of the echo amplitudes approximate theories are likely to be adequate in many cases. Predictions based on simulations and theory may be tested on echo signals obtained with the data acquisition system.

Because lesions can be detected by studying grey scale images we know that there is enough information in the echo data to allow automatic detection of these lesions to be achieved. Ultrasonic examinations offer advantages of being convenient and non-invasive, making further development of the technique well worthwhile.

ACKNOWLEDGEMENTS

It is a pleasure to express my gratitude to my supervisor, Dr. Norman McDicken, for his guidance and friendship and for the freedom to pursue my own ideas.

My thanks are also due to:

Professor J. R. Greening for support and for making the facilities of the department available to me.

Dr. A. K. Boardman for advice on various aspects of computing.

Members of the Department of Medical Physics and Medical Engineering and especially my fellow research students for their company, interest and stimulating discussions.

The radiologists - Dr. W. A. Copeland, Dr. C. McArdle, Dr. D. Sinclair, Dr. S. R. Wild and Dr. G. B. Young - for their co-operation and valued discussions.

The Medical Faculty of the University of Edinburgh for the financial support of the Fullerton Scholarship.

The Medical Research Council for funding the data acquisition system.

I would also like to thank my family and friends for their interest and support. I offer my sincere apologies to those who suffered as a result of my preoccupation with the thesis.

I am very grateful to Dorothy McKinna for her conscientious and expert typing of the script. Her appetite for more text is unlikely to be matched by any other reader.

REFERENCES

ATKINSON, P., 1974. On the measurement of bloodflow by ultrasound. Ph.D. Dissertation. University of Bristol.

ATKINSON, P. and BERRY, M. V., 1974. Random noise in ultrasonic echoes diffracted by blood. J. Phys. A: Math., Nucl. Gen., Vol. 7, No. 11, pp. 1293-1302.

BARBÉ, A., 1976. A measure for the mean level-crossing activity of stationary normal processes. IEEE Trans. on Information Theory, Vol. IT-22, pp. 96-102.

BARHAM, P. M. and HUMPHRIES, D. E., 1969. Derivation of the Kalman filtering equations from elementary statistical principles. Royal Aircraft Establishment technical report 69095.

BECKMANN, P. and SPIZZICHINO, A., 1963. The scattering of electromagnetic waves from rough surfaces. Pergamon Press.

BERKOWITZ, R. S., (ed.) 1965. Modern radar: analysis, evaluation and system design. John Wiley & Sons, New York, London, Sydney.

BERRY, M. V., 1973. The statistical properties of echoes diffracted from rough surfaces. Phil. Trans. A 273, pp. 611-658.

BLAKE, I. F. and LINDSEY, W. C., 1973. Level-crossing problems for random processes. IEEE Trans. on Information Theory, Vol. IT-19, No. 3, pp. 295-315. (133 refs.).

BRIGNELL, J. E., and RHODES, G. M., 1975. Laboratory on-line computing. Intertext books.

CHERNOFF, H. and ZACKS, S., 1964. Estimating the current mean of a normal distribution which is subjected to changes in time. Annals of Math. Statistics, Vol. 35, pp. 999-1018.

CHERNOV, L. A., 1960. Wave propagation in a random medium. McGraw-Hill.

CHIVERS, R. C., 1973. The scattering of ultrasound by human tissues. Ph.D. thesis. University of London.

CHIVERS, R. C. 1977. The scattering of ultrasound by human tissues - some theoretical models. Ultrasound in Med. & Biol., Vol. 3, pp. 1-13. (37 refs.)

CHIVERS, R. C., 1978. Phase and amplitude fluctuations in the propagation of acoustic waves in lossless inhomogeneous continua with velocity, density and bulk modulus variations. Ultrasound in Med. & Biol., Vol. 4, pp. 353-361.

CHIVERS, R. C. and HILL, C. R., 1975. A spectral approach to ultrasonic scattering from human tissue: methods, objectives and backscattering methods. Phys. Med. Biol., Vol. 20, No. 5, pp. 799-815

CLULEY, J. C., 1975. Computer interfacing and on-line operation. Arnold-London.

CONNOR, F. R., 1973. Noise. Arnold.

COSGROVE, D. O., 1978. Evaluation of liver tumours. In "Ultrasound in tumour diagnosis" (ed. C. R. Hill, V. R. McCready and D. O. Cosgrove), pp. 104-127. Pitman Medical.

CRAMER, H. and LEADBETTER, M. R., 1967. Stationary and related stochastic processes. Wiley, New York - London - Sydney.

DAVENPORT, W. B. and ROOT, W. L., 1958. Random signals and noise. McGraw-Hill.

DEC, 1972. Introduction to programming. Vols. 1-2. Digital Equipment Corporation.

DEC, 1973. Small computer handbook. Digital Equipment Corporation.

DECKER, D., EPPLE, E., LEISS, W. and NAGEL, M., 1973. Digital computer analysis of time-amplitude ultrasonograms from the human eye. J. of Clinical Ultrasound, Vol. 1, No. 2, pp. 156-159.

DONOVAN, J. J., 1972. Systems programming. McGraw-Hill, Kogakusha.

FAIRCHILD, 1973. The TTL applications handbook. Fairchild Semiconductor.

FEUCHT, D., 1977. Pattern recognition: basic concepts and implementations. Computer Design, December 1977, pp. 57-68.

GEAR, C. W., 1969. Computer organization and programming. McGraw-Hill.

GILBERT, E. N. and POLLAK, H. O., 1960. Amplitude distribution of shot noise. Bell System Technical Journal, Vol. 39, pp. 333-350.

GLOVER, G. H., 1977. Computerised time-of-flight ultrasonic tomography for breast examination. Ult. in Med. & Biol. Vol. 3 Nos. 2/3 pp. 117-127.

GOODENOUGH, D. J., 1976. Assessment of image quality of diagnostic imaging systems. In "Medical images: formation, perception and measurement" (ed. G. A. Hay), pp. 263-277. The Institute of Physics, John Wiley & Sons.

GOODYEAR, C. C., 1971. Signals and information. London Butterworths.

GORE, J. C. and LEEMAN, S., 1977. Ultrasonic backscattering from human tissue: a realistic model. Phys. Med. Biol., Vol. 22, No. 2, pp. 317-326.

GREENLEAF, J. F. and JOHNSON, S. A., 1975. Algebraic reconstruction of spatial distributions of refractive index and attenuation in tissues from time-of-flight and amplitude profiles. (See NBS, 1975, pp. 109-119).

GREENLEAF, J. F., JOHNSON, S. A. and LENT, A. H., 1978. Measurement of spatial distribution of refractive index in tissues by ultrasonic computer assisted tomography. Ultrasound in Med. & Biol., 3/4 pp. 327-339.

GREGORY, R. L., 1966. Eye and brain: the psychology of seeing. World University Library.

HALLIWELL, B. J., (ed.) 1974. Advanced communication systems. Newnes-Butterworths.

HAY, G. A. and CHESTERS, M. S., 1976. Threshold mechanisms in the presence of visible noise. In "Medical images: formation, perception and measurement" (ed. G. A. Hay), pp. 208-219. The Institute of Physics, John Wiley & Sons.

HEALEY, M., 1976. Minicomputers and microporcessors. Hodder & Stoughton.

HILL, C. R., 1975. Frequency and angular dependence of ultrasonic scattering from tissue. (See NBS, 1975, pp. 197-206).

HILL, C. R., McCREADY, V. R. and COSGROVE, D. O., (ed.), 1978. Ultrasound in tumour diagnosis. Pitman Medical.

HINES, W. G. S., 1976a. A simple monitor of a system with sudden parameter changes. IEEE Trans. on Information Theory, Vol. IT-22, No. 2, pp. 210-216.

HINES, W. G. S., 1976b. Improving a simple monitor of a system with sudden parameter changes. IEEE Trans. on Information Theory, Vol. IT-22, pp. 496-499.

HINKLEY, D. V., 1970. Inference about the change-point in a sequence of random variables. Biometrika, Vol. 57, No. 1, pp. 1-17.

HOEL, P. G., 1971. Introduction to mathematical statistics. Wiley.

HUSSEY, M., 1975. Diagnostic ultrasound: an introduction to the interactions between ultrasound and biological tissues. Blackie.

KAILATH, T., 1974. A view of three decades of linear filtering theory. IEEE Trans. on Information Theory, Vol. IT-20 pp. 146-181. (390 refs.)

KAK, A. C. and FRY, F. C., 1975. Acoustic impedance profiling: An analytical and physical model study. (See NBS, 1975, pp. 231-251).

KOSSOF, G., 1975. Reflection techniques for measurement of attenuation and velocity. (See NBS, 1975, pp. 135-139).

KUK, R. B., 1979. Application of Kalman filtering techniques to diagnostic ultrasound. Ultrasonic Imaging, Vol. 1, No. 2, pp. 105-120.

LAWSON, J. L. and UHLENBECK, G. E., 1950. Threshold signals. Radiation Laboratory Series. McGraw-Hill.

LELE, P. P., MANSFIELD, A. B., MURPHY, A. I., NAMERY, J. and SENAPATI, N., 1975. Tissue characterization by ultrasonic frequency-dependent attenuation and scattering. (See NBS, 1975, pp. 167-196).

LERSKI, R. A., 1978. On-line digital analysis of clinical ultrasonic data. Proceedings of the British Medical Ultrasound Society tenth annual meeting (Newcastle); abstract in British Journal of Radiology, 1979, Vol. 52, p. 518.

LEWIS, J. L., 1973. An approximation for the distribution of shot noise. IEEE Trans. on Information Theory, IT-19, pp. 235-237.

LISTER, A. M., 1975. Fundamentals of operating systems. Macmillan.

LYNN, P. A., 1973. An introduction to the analysis and processing of signals. Macmillan.

McDICKEN, W. N., 1976. Diagnostic ultrasonics: principles and use of instruments. Wiley, New York.

MACY, J., 1965. Analogue-digital conversion systems. In "Computers in biomedical research" (ed. R. W. Stacy and B. D. Waxman), Vol. 2, Chapter 1, pp. 3-34. Academic Press, New York and London.

MAUS, A. and ENDERSON, J., 1979. Misuse of computer-generated results. Med. & Biol. Eng. & Comput., 17, pp. 126-129.

METZ, C. E., STARR, S. J. and LUSTED, L. B., 1976. Quantitative evaluation of visual detection performance in medicine: ROC analysis and determination of diagnostic benefit. In "Medical images: formation, perception and measurement" (ed. G. A. Hay), pp. 220-241. The Institute of Physics, John Wiley & Sons.

MORLEY, P., 1978. Clinical staging of epithelial bladder ltumours by echo-tomography. In "Ultrasound in tumour diagnosis" (ed. C. R. Hill, V. R. McCready and D. O. Cosgrove), pp. 145-161. Pitman Medical.

MORRISON, D. C., 1978. Fast data acquisition system for ultrasonic tissue categorisation. Proceedings of the joint Hospital Physicists' Association and Biological Engineering Society eighth computing conference (Bristol).

MORRISON, D. C., McDICKEN, W. N., WILD, S. R. and COPELAND, W. A., 1978. Statistical variation in echo amplitudes and their effect on interpretation of grey scale images. Proceedings of the British Medical Ultrasound Society tenth annual meeting (Newcastle); abstract in British Journal of Radiology, 1979, Vol. 52, pp. 518-519.

MOUNTFORD, R. A., HALLIWELL, M. and ATKINSON, P., 1973. Ultrasonic liver scanning: automated A-scan analysis. Phys. Med. Biol. Vol. 18, pp. 559-569.

MOUNTFORD, R. A. and WELLS, P. N. T., 1972a. Ultrasonic liver scanning: the quantitative analysis of the normal A-scan. Phys. Med. Biol. Vol. 17, pp. 14-25.

MOUNTFORD, R. A. and WELLS, P. N. T., 1972b. Ultrasonic liver scanning: the A-scan in the normal and cirrhosis. Phys. Med. Biol. Vol. 17, pp. 261-269.

NAYLOR, T. H., (ed.) 1969. The design of computer simulation experiments. Duke University Press.

NBS, 1975. Ultrasonic tissue characterisation. Proceedings of seminar held at the National Bureau of Standards, 1975. (ed. M. Linzer.) NBS Special Publication 453.

NICHOLAS, D., 1975. Ultrasonic scattering and the structure of human tissues. Ph.D. thesis. University of London.

NICHOLAS, D., 1978. Tissue characterisation in vivo by ultrasonic backscattering analysis. In "Ultrasound and tumour diagnosis" (ed. C. R. Hill, V. R. McCready and D. O. Cosgrove), pp. 258-272, Pitman Medical.

O'NEILL, E. L.. LEE, E. E. and CZEKANSKI, D. R., 1976. Some experimental results on the zero-crossing intervals of random processes. IEEE Trans. on Information Theory, Vol. IT-22, pp 230-231.

PEATMAN, J. B., 1972. The design of digital systems. McGraw-Hill.

PIERCE, J. R., 1973. The early days of information theory. IEEE Trans. on Information Theory, Vol. IT-19 pp. 3-8.

PRESTON, K., 1975. Use of pattern recognition for signal processing in ultrasonic histopathology. (See NBS, 1975, pp. 51-59.

PRICE, R., 1960. Detection theory. J. of Research of the National Bureau of Standards, Vol. 64D, No. 6, pp. 678-680.

REID, J. M., 1975. The scattering of ultrasound by tissues. (See NBS, 1975, pp. 29-47).

RICE, S. O., 1944, 1945. Mathematical analysis of random noise. Bell System Technical Journal Vol. 23, pp. 282-332 and Vol. 24, pp. 46-156. Reprinted in "Selected papers on noise and stochastic processes" (ed. N. Wax), 1954, pp. 133-294. Dover Publications.

RIDDLE, P., 1976. Carcinoma of the bladder. Brit. J. of Hospital Medicine, November, pp. 468-478.

ROSE, A., 1973. Vision: human and electronic. Plenum Press, New York - London.

SAGE, A. P. and MELSA, J. L., 1971. System identification. Academic Press.

SCARLETT, J. A., 1972. Transistor-Transistor Logic and its interconnections. Van Nostrand Reinhold MARCONI SERIES.

SCHWARTZ, M., 1970. Information transmission, modulation, and noise. McGraw-Hill.

SEN, A. and SRIVASTAVA, M. S., 1975. On tests for detecting change in mean when variance is unknown. Annals of Inst. of Statistical Math., Vol. 27, pp. 479-486.

SHANNON, C. E. and WEAVER, W., 1949. The mathematical theory of communication. University of Illinois Press, Urbana, Chicago, London.

SKOLNIK, M. I., 1962. Introduction to radar systems. McGraw-Hill, Kogakusha.

SLEPIAN, D., 1958. Fluctuations of random noise power. Bell System Technical Journal, Vol. 39, pp. 163-184.

STOCKHAM, T. G., 1972. Image processing in the context of a visual model. Proceedings of the IEEE, Vol. 60, No. 7, pp. 828-842.

STURM, R. E., and MORGAN, R. H., 1949. Screen intensification systems and their limitations. Amer. J. Roentgen, Vol. 62, pp. 617-634.

TAYLOR, K. J. W. and MILAN, J., 1975. Digital A-scan analysis in the diagnosis of chronic splenic enlargement. (See NBS, 1975, pp. 71-78).

TER-POGOSSIAN, M. M., 1967. The physical aspects of diagnostic radiology. Hoeber Medical Division.

TOCHER, K. D., 1963. The art of simulation. The English Universities Press Ltd.

TWERSKY, V., 1960. On multiple scattering of waves. Journal of Research of the National Bureau of Standards. Vol. 64D No. 6, pp. 715-730 (over 250 refs.) (See also Twersky, 1964).

TWERSKY, V., 1964. Acoustic bulk parameters of random volume distribution of small scatterers. J. Acoust. Soc. Amer., 36 No. 7, pp. 1314-1329.

VAN TREES, H. L., 1968. Detection, estimation, and modulation theory. Part I. Wiley.

WAAG, R. C., LERNER, R. M. and GRAMIAK, R., 1975. Swept-frequency ultrasonic determination of tissue macrostructure. (See NBS, 1975, pp. 213-228).

WELLS, P. N. T., 1977. Biomedical ultrasonics. Academic Press.

WELLS, P. N. T., MOUNTFORD, R. A., HALLIWELL, M. and ATKINSON, P., 1975. Quantitative A-scan analysis of normal and cirrhotic liver. (See NBS, 1975, pp. 61-70).

WELLS, P. N. T. and WOODCOCK, J. P., 1977. Computers in ultrasonic diagnosis. Research Studies Press.

WHITE, D. and LYONS, E. A., (ed.) 1978. Ultrasound in Medicine Vol. 4. Plenum Press, New York and London.

WHITTLE, P., 1970. Probability. Chivers-Penguin.

WILDE, D. J. and BEIGHTLER, C. S., 1967. Foundations of optimization. Prentice-Hall.

WOODWARD, P. M., 1953. Probability and information theory with applications to radar. Pergamon Press.

WOOLLONS, D. J., 1972. Introduction to digital computer design. McGraw-Hill.

ZADEH, L. A., 1960. Prediction and filtering. J. of Research of the National Bureau of Standards, Vol. 64D, No. 6, pp. 681-685.

SYMBOL INDEX

The descriptions provided in the following list are for guidance only: more detailed descriptions are on the indicated pages. Symbols occurring only in restricted parts of the thesis have been omitted from the list.

		Equation	Page
$a(t)$	shape of pulse envelope	7.10 7.11 8.17	145 145 218
$b(h)$	Transverse beam profile	7.1 7.25	143 196
$F(t)$	echo signal from point reflector	7.1 7.2 7.10	143 143 145
$F_s(t)$	standard form of $F(t)$	7.12	145
f_u	fraction added in pseudo-integration mode		283
$g(t)$	scaling factor to allow for regions with differing echogenicity	7.2 8.43	143 242
g_r	value taken by $g(t)$ in abnormal region	8.43	242
h	transverse displacement of point reflector	7.1	143
L_r	likelihood ratio	8.1	206
$M(t,T)$	moving mean modulus of length T	8.10	215
N	number of reflectors in each segment	7.13	145
$N_t(\Phi)$	level crossing frequency of level Φ	8.13 8.15	216 218
N_u	number of signals combined in scan converter		284
$P(t)$	pressure waveform	7.2	143
$p(\Phi,\beta)$	joint probability distribution of Φ and β	8.11	216
$P_{env}(t)$	envelope of complex signal	8.27	224
s	polarity of echo waveform	7.1 7.6 7.7	143 144 144
T	length of moving average	 8.10	160 215
t_k	time of arrival of echo from k^{th} reflector	7.4	143
T_p	constant defining width of Gaussian pulse envelope	8.17	218
t_r	width of abnormal region	8.43	242
t_s	start of time window for Ω_- and Ω_+	8.44 8.45	244 244

		Equation	Page
t_w	width of time window for Ω_- and Ω_+	8.44 8.45	242 244
u_k	random number giving magnitude of echo from point reflector	7.5 7.8 7.9	144 144 144
v	mean group velocity of ultrasound in soft tissue	7.4	143
w_k	random number giving magnitude and polarity of echo from point reflector	7.2 7.3 7.5	143 143 144
z	depth of point reflector	7.1	143
α	parameter defining width of pulse envelope	7.11	145
β	first time differential of random signal	8.11	216
θ	phase parameter in definition of F(t)	7.10	145
μ	mean of modulus of echo signal	7.19 7.22	161 161
μ_e	mean of signal envelope		227
μ_m	mean of modulus of echo signal		268
σ	standard deviation	7.16 7.17	158 158 165
τ	segment length for synthesis	7.13	145
Φ	signal level		216
Ψ	parameter defining Rayleigh distribution	7.21	161
ω	angular frequency in definition of F(t)	7.10	145
Ω_-	minimum value of M(t,T) in time window of length t_w starting at time t_s	8.44	242
Ω_+	maximum value of M(t,T) in time window of length t_w starting at time t_s	8.45	244